Technical Report GL-95-2
February 1995

US Army Corps
of Engineers
Waterways Experiment
Station

HEMTT Dynamic Sensitivity to Small Obstacles at Low Velocities

Report 2
Validation Study Using VEHDYN 3.0

by Daniel C. Creighton, Randolph A. Jones

DTIC
ELECTE
APR 2 0 1995
S D
G

Approved For Public Release; Distribution Is Unlimited

19950419 014

Prepared for Defense Nuclear Agency

The contents of this report are not to be used for advertising, publication, or promotional purposes. Citation of trade names does not constitute an official endorsement or approval of the use of such commercial products.

PRINTED ON RECYCLED PAPER

Technical Report GL-95-2
February 1995

HEMTT Dynamic Sensitivity to Small Obstacles at Low Velocities

Report 2
Validation Study Using VEHDYN 3.0

by Daniel C. Creighton, Randolph A. Jones

U.S. Army Corps of Engineers
Waterways Experiment Station
3909 Halls Ferry Road
Vicksburg, MS 39180-6199

Accesion For	
NTIS CRA&I	☒
DTIC TAB	☐
Unannounced	☐
Justification	
By	
Distribution /	
Availability Codes	
Dist	Avail and / or Special
A-1	

Report 2 of a series

Approved for public release; distribution is unlimited

Prepared for Defense Nuclear Agency
6801 Telegraph Road
Alexandria, VA 22310-3398

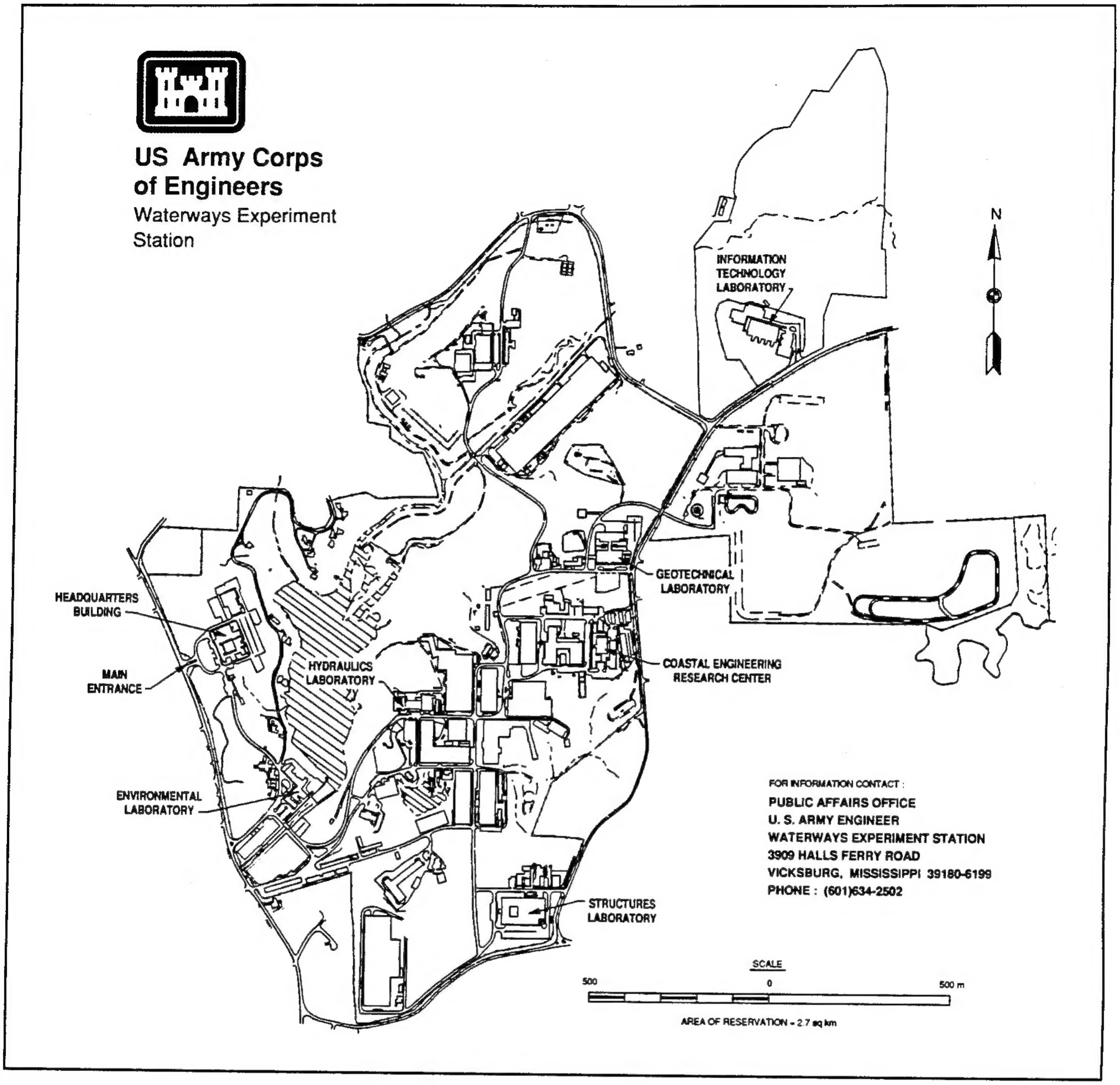

Waterways Experiment Station Cataloging-in-Publication Data

Creighton, Daniel C.
HEMTT dynamic sensitivity to small obstacles at low velocities. Report 2, Validation study using VEHDYN 3.0 / by Daniel C. Creighton, Randolph A. Jones ; prepared for Defense Nuclear Agency.
151 p. : ill. ; 28 cm. -- (Technical report ; GL-95-2)
Includes bibliographic references.
Report 2 of a series.
1. Military trucks -- Computer programs -- Validation. 2. Obstacles -- Computer simulation. 3. Vehicles, Military -- Computer simulation. I. Jones, Randolph A. II. United States. Army. Corps of Engineers. III. U.S. Army Engineer Waterways Experiment Station. IV. Geotechnical Laboratory (U.S.) V. United States. Defense Nuclear Agency. VI. Title. VII. Title: Validation study using VEHDYN 3.0. VIII. Series: Technical report (U.S. Army Engineer Waterways Experiment Station) ; GL-95-2.
TA7 W34 no.GL-95-2

PREFACE

The work reported herein was sponsored by the Defense Nuclear Agency and was conducted during the period from May, 1992 to February, 1993. This effort was performed in support of the Weigh-In-Motion program to examine the feasibility of using an existing vehicle dynamics model VEHDYN 3.0 in such a study.

The study was conducted at the U.S. Army Engineer Waterways Experiment Station (WES) under the general supervision of Dr. W. F. Marcuson III, Chief, Geotechnical Laboratory (GL), and Mr. N. R. Murphy, Jr., Chief, Mobility Systems Division (MSD). The work was performed by personnel of the staff of the MSD for Al Bush and Richard Bradley of the Pavement Systems Division (PSD) who were the Principal Investigators. The programming and simulation effort, including making appropriate modifications to VEHDYN 3.0 and plotting the simulation results was acccomplished by Mr. Daniel C. Creighton, MSD. Technical guidance and support was provided by Mr. Randolph A. Jones, MSD, who was responsible for the field testing aspect of this project. This report was prepared by Mr. Creighton and Mr. Jones.

Dr. Robert W. Whalin was Director of WES during preparation of this report. COL Bruce K. Howard, EN, was Commander.

The contents of this report are not to be used for advertising, publication, or promotional purposes. Citation of trade names does not constitute an official endorsement or approval for the use of such commercial products.

Conversion Factors, Non-SI to SI Units of Measurement

Non-SI units of measurement used in this report can be converted to SI units as follows:

Multiply	By	To Obtain
g's (acceleration of gravity)	9.80665	meters per second squared
feet	0.3048	meters
hertz	6.283185	radians per second
inches	2.54	centimeters
miles (U.S. statute)	1.609347	kilometers
pounds (force)	4.448222	newtons
pounds (force)-seconds squared-inches	0.112986	kilogram-meters squared
pounds (force) per inch	175.1268	newtons per meter
pounds (force)-seconds per inch	175.1268	newtons-seconds per meter

TABLE OF CONTENTS

FIGURES

TABLES

SECTION 1
INTRODUCTION

1.1 BACKGROUND.

The problem of interest in this study is that of weighing a vehicle while it is slowly moving over some type of pressure-sensitive mat or strips. The funding for this project was provided by the Defense Nuclear Agency (DNA) and is referred to as the Weighing-In-Motion (WIM) problem. Because the vehicle to be weighed is moving, it is possible that dynamic vibration modes of the vehicle's sprung mass may be excited when it encounters the sensing mat/strips, or that the sprung mass is still responding to an excitation that occurred shortly before encountering the weigh station. This would cause the weight under each road wheel to continually change as the sprung mass accelerates up and down or pitches fore and aft resulting in an erroneous vehicle weight.

In the initial phase of this study, the Vehicle Dynamics Model VEHDYN 3.0, developed in the Mobility Systems Division (MSD) of the Geotechnical Laboratory (GL) at the US Army Engineer Waterways Experiment Station (WES), will be used to examine the dynamic sensitivity of the M977 Heavy Expanded Mobility Tactical Truck (HEMTT) when it rolls at low speed (about 1.8 mph) over small square-edged bumps having heights ranging from 0.25 - 3.00 inches. Model simulation results, in the form of displacements, velocities, and accelerations, will be compared to field test data to determine if the VEHDYN 3.0 model is a reasonable tool to be used in the low-speed small-obstacle environment. This report only documents the results of this initial phase without actually using VEHDYN 3.0 to evaluate various types of weighing strips/mats. A subsequent phase of this study is expected to address such evaluations.

1.2 SCOPE.

Section 2 of this report describes the relevant aspects of the Vehicle Dynamics Model VEHDYN 3.0. Included in the section is a discussion of a special version of VEHDYN 3.0 that can provide force output (due to wheel-terrain interaction) for multiple strips arbitrarily layed out over a particular terrain profile. Section 2 also discusses the use of drop tests to obtain simple linear spring and damper relationships for a vehicle using damped free oscillation theory.

Section 3 provides a comparison of VEHDYN 3.0 simulated data with field data for the HEMTT, collected as it was driven at about 1.8 mph over small two-foot-long squared-edged bumps. Pitch rate of the sprung mass, vertical acceleration of the center of gravity (CG), vertical acceleration of an axle, and displacement of a forward-mounted string pot are the kinds of data comparisons that are made.

Section 4 presents some conclusions and recommendations regarding the use of VEHDYN 3.0 in this type of environment.

Finally, there are two appendices included at the end of this report. Appendix A contains all of the time history and Fast Fourier Transform frequency comparisons of the field test data to the VEHDYN 3.0 simulations. Appendix B is a list of the notation used in this report.

SECTION 2

DESCRIPTION OF THE VEHICLE DYNAMICS MODEL VEHDYN 3.0

2.1 GENERAL.

The VEHDYN 3.0 Vehicle Dynamics Model (Creighton, 1993) is the latest version of WES' VEHDYN computer model series that predicts ride and shock performance for vehicles negotiating a rigid terrain profile at a constant velocity. VEHDYN 3.0 allows the modeling of a vehicle as a sprung mass mounted on a number of spring and damping elements, beam elements, and tires. A VEHDYN 3.0 vehicle is a two-dimensional (2D) model which moves forward at a constant speed to negotiate a rigid user-inputted section of terrain.

Until now, VEHDYN has normally been used to predict motion and ride characteristics over long (eg., 500-foot) courses or over half-round obstacles ranging from 4 to 16 inches in height. Vehicle speeds range normally from 3-4 mph for rough courses and large obstacles to 40 or 50 mph over smoother terrain and small obstacles. The study herein investigates VEHDYN 3.0's ability to simulate low-speed (about 1.8 mph) motion of an M977 HEMTT over very small (0.25-3.00 inches in height) square-edged 2-foot-long obstacles. A full description of the test series can be found in Report 1 of this study (Jones, 1993).

Two models of the M977 were put together for this study. The first is that of an empty M977 which is the vehicle with no payload. Figure 2-1 is a drawing of the M977. The empty HEMTT weighs 38,000 lbs, has a pitch mass moment of inertia of 1,668,000 lb-sec^2-in, and its

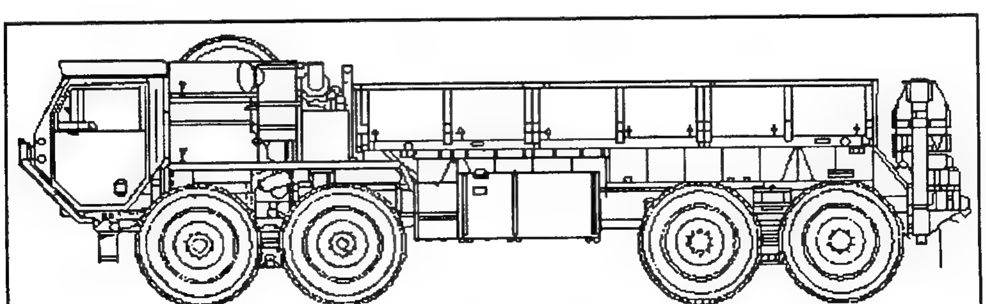

Figure 2-1. Drawing of M977 Heavy Expanded Mobility Tactical Truck.

CG is located 45.0 inches above the ground surface at equilibrium. The fully loaded HEMTT, which is an empty M977 with a 22,400-lb full payload in its cargo bay, weighs 60,400 lbs, has a pitch mass moment of inertia of 1,717,000 lb-sec^2-in, and its CG is located 62.0 inches above the ground surface at rest.

The suspension system of the M977 HEMTT consists of two walking beams. Each walking beam consists of a beam mounted under a set of leaf springs, with 26.5-inch wheels mounted at each end of the beam about 30 inches out from the beam's pivot point. Each wheel assembly weighs 1,406 lbs. Each beam was modeled as having a moment of inertia of 6,168 lb-sec^2-in and a rotational damping coefficient of 500 lb-in. Each beam also had outboard dampers mounted at each end of the beam connecting from the beam (about 7-8 inches out from the corresponding wheel axle) up to the frame in a slightly tipped mounting configuration. Figure 2-2 is a drawing of the M977 model used in the VEHDYN 3.0 simulations in this report.

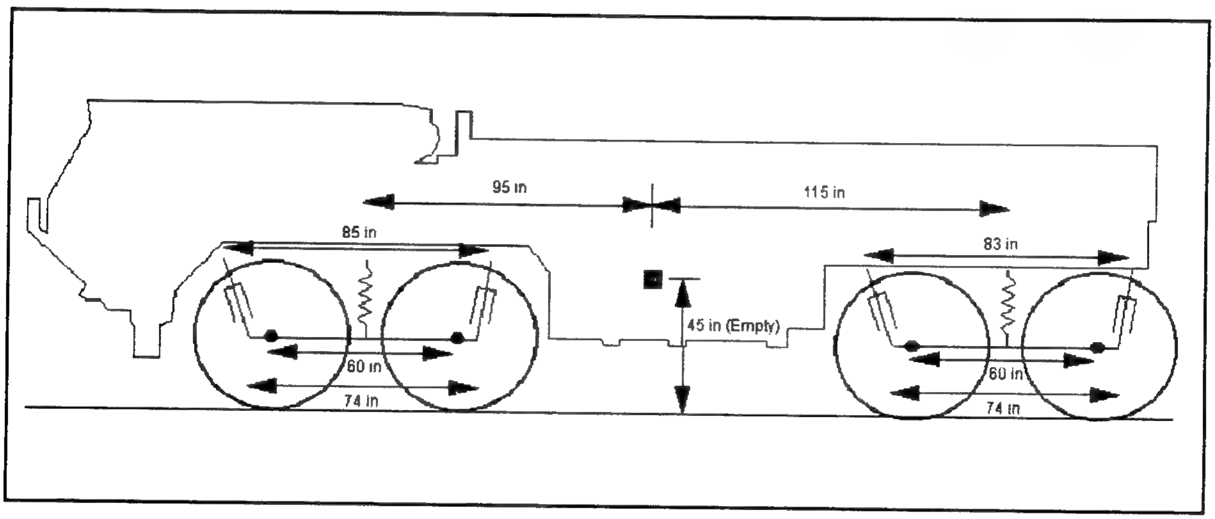

Figure 2-2. VEHDYN 3.0 Model of M977 HEMTT.

2.2 MODIFICATIONS TO VEHDYN 3.0 FOR THE WEIGHING-IN-MOTION PROBLEM.

It was necessary to modify VEHDYN 3.0 such that a user could specify one or more strips or

mats on the terrain profile. Each strip or mat would then record a history of normal force as the vehicle rolled over that section of the terrain. The modifications to VEHDYN 3.0 require the user to specify one or more locations on the profile to collect force histories as the vehicle passes over. The user inputs start and stop locations for each strip to be modeled.

The tire used on the M977 HEMTT is 16 inches wide with a diameter of 53 inches. At full payload inflated with the on-road tire pressure, the tire has an oblong footprint (somewhere between a rectangle and an ellipse) with a length of 16.0 inches, a width of 13.6 inches, and an area of 178.3 square inches (Michelin Tire Corporation, 1986).

One WIM field implementation involves a series of thin (0.50-1.00 inch thick) pressure-sensitive "piezo" strips. Typically, each of these strips is 1.0-2.0 inches long (only a fraction of the tire's diameter) and is wider than the vehicle's width. Several of them are layed down on the pavement with 1.0-5.0 inch gaps between them. The pattern of strips is designed to be long enough to include several wavelengths of the natural frequency of the vehicle chassis (about 3 Hz). The necessary electronics and software are used to convert the pressure-time output from the strips as a vehicle rolls slowly over them to give a dynamically measured vehicle weight. A sample of the kind of output that can be obtained relating to this implementation is seen in Figure 2-3. This shows the forces experienced by two 2.0-inch-long strips placed on the terrain 1.0 inch apart as a fully loaded M977 HEMTT rolls over a half-inch-high square-edged bump at 3.3 mph. This picture is merely a demonstration of the kind of output generated by the modified VEHDYN 3.0, not a validation.

Another WIM implementation uses a mat containing a Cartesian grid of wires overlaid by a thin piece of rubber for protection. This mat is large enough so that the entire tire footprint can be contained on the mat at a single instant of time. The software provided with the mat graphically portrays the stress distribution of the tire's entire footprint and gives the total force acting on the mat by the tire. Figure 2-4 shows some sample output using the modified VEHDYN 3.0 where a 2-foot-long mat has been selected for force output. As with the previous example, this is only a demonstration of the code's capability, not a validation.

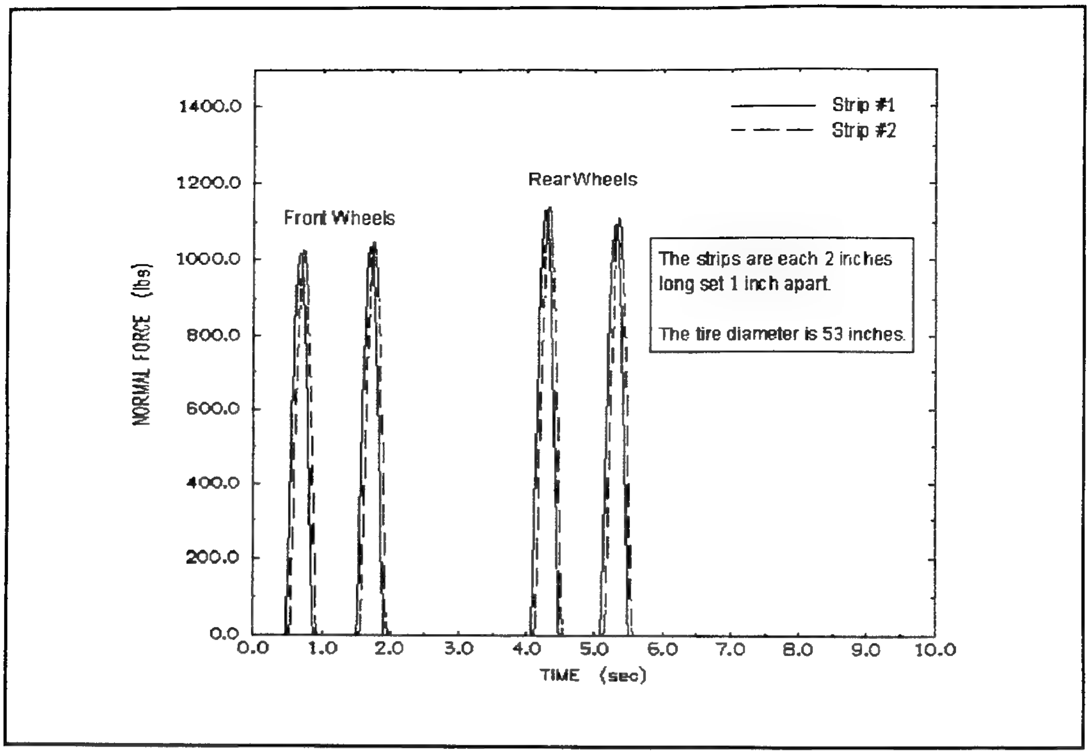

Figure 2-3. Modified VEHDYN 3.0 force output from two strips for a HEMTT at 3.3 mph over a 0.25-inch-high bump.

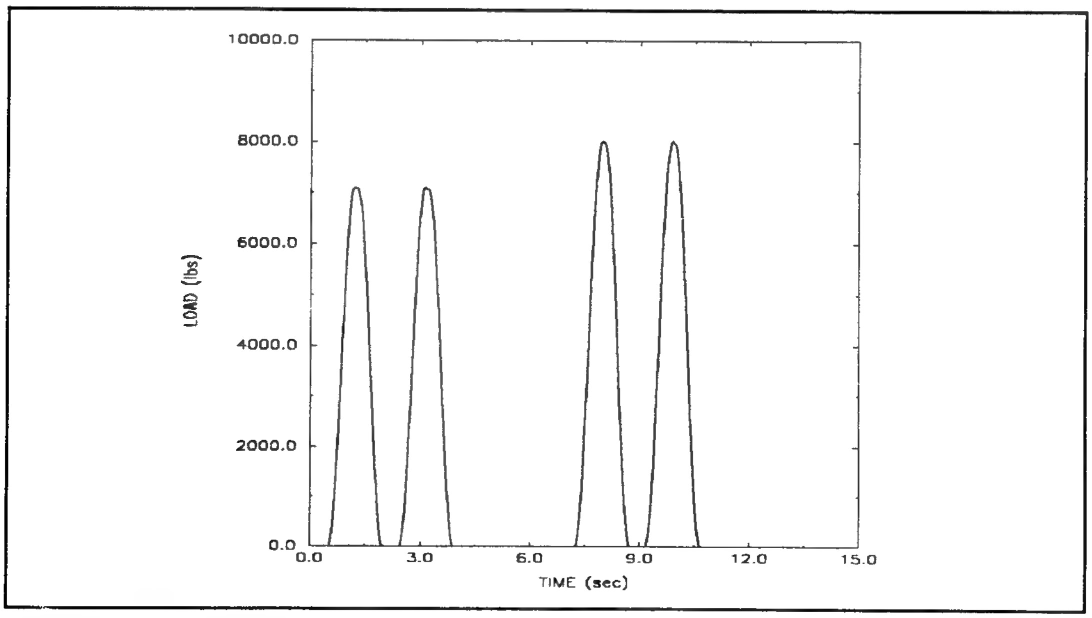

Figure 2-4. Modified VEHDYN 3.0 output for a loaded HEMTT at 1.8 mph over a 0.25-in-high 2-ft-long WIM mat.

2.3 DEVELOPMENT OF M977 HEMTT SUSPENSION DATA.

Some of the most difficult data to determine when modeling any vehicle are the spring and damping relationships for the undercarriage suspensions. In this section, a process will be outlined that gives simple linear spring and damping coefficients based on acceleration data gathered by performing front and rear drop tests on a given vehicle. Even though a manufacturer may provide these relationships, the characteristics change as the vehicle is driven and begins to age. It should become standard operating procedure to perform these drop tests on any vehicle at the time it is tested. The tests are easy to perform and only require about 1-2 hours additional time if the vehicle is already instrumented with a vertical accelerometer mounted anywhere on its chassis (sprung mass).

2.3.1 Application of Damped Free Oscillation Theory to Drop Test Data.

The first drop test that needs to be performed involves lifting the front end of the vehicle just high enough so that the front wheels come up off the ground. The vehicle is then dropped and acceleration data are gathered from a vertical accelerometer mounted somewhere on the vehicle chassis, like at the CG or in the cargo bay. The same procedure is then repeated for the rear end of the vehicle. A complete description of these tests as performed on the M977 HEMTT is given in Volume 1 of this study (Jones, 1993).

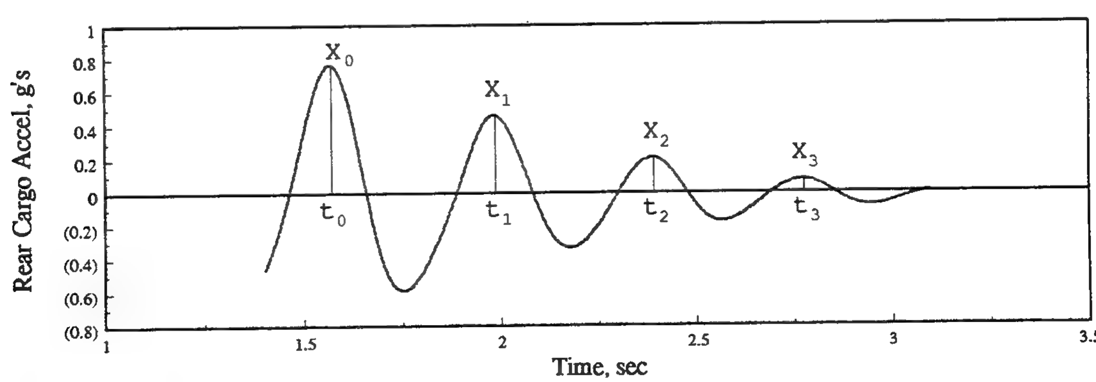

Figure 2-5. Sample acceleration trace from a drop test on the M977 HEMTT.

Figure 2-5 shows a sample of the acceleration data gathered from an accelerometer mounted in the rear area of the cargo bay for the HEMTT as one of these drop tests was performed.

The character of this curve is that it is a decaying periodic function that can be used in conjunction with damped free oscillation theory to provide a linear spring constant k and a linear damping constant c for a simple model of a mass m mounted on the spring and damper as shown in Figure 2-6.

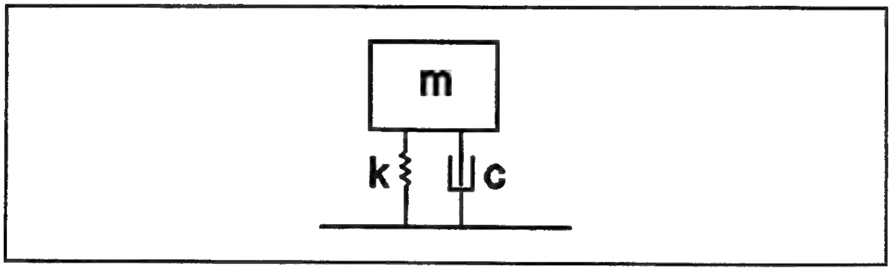

Figure 2-6. Mass m mounted on spring k and damper c.

The approach to the analysis is to first examine the results of a drop test on the front end of the HEMTT. An assumption is made that lifting up the front end and dropping it primarily excites only the front end suspension elements while lifting up the rear end and dropping it only excites the rear suspension elements. The justification for this assumption is the fact that these drop tests are performed in such a way that the front or rear portion of the vehicle is only lifted up a small distance before dropping. If the vehicle was lifted up several feet before dropping, the vehicle's entire suspension system would likely be excited. Separate low-amplitude front and rear drop tests allow the modeler to determine different values of k and c respectively for the front and rear suspensions.

The damped free oscillation theory (Durham and Murphy, 1976) proceeds by first calculating the log decrement δ using the following equation

$$\delta = \frac{1}{n} \ln \frac{x_o}{x_n} \tag{2.1}$$

where

δ = the log decrement

n = the number of cycles to consider

x_o = initial amplitude (Figure 2-5)

x_n = amplitude after n cycles (Figure 2-5)

The log decrement expresses how rapidly the acceleration history decays. The analysis herein considers three cycles; thus n equals 3. Next, the damping factor ζ is computed as

$$\zeta = \sqrt{\frac{\delta^2}{\delta^2 + 4\pi^2}} \tag{2.2}$$

where

ζ = the damping factor

π = 3.14159265 (approx.)

Now, the spring constant k can be calculated as

$$k = \frac{4\pi^2 m f_d^2}{1 - \zeta^2} \tag{2.3}$$

where

k = spring constant

m = mass

f_d = damped frequency

The damped frequency f_d is given by

$$f_d = \frac{1}{t_1 - t_o} \tag{2.4}$$

where

t_o , t_1 = the times associated with the corresponding amplitudes x_o and x_1 from Figure 2-5.

Finally, the damping coefficient c is calculated as

$$c = 2\zeta\sqrt{km} \tag{2.5}$$

2.3.2 Front Suspension Properties.

The first step in analyzing the front end drop tests is to determine the sprung mass m to be used. Because of the assumption that only the front end is being excited, the sprung mass to be considered is that which is acting on the forward suspensions only. The distribution of weight of the empty M977 HEMTT is 21,000 lbs under the front wheels and 17,000 lbs under the rear wheels. To obtain the sprung weight of the front w_f , the four front wheel assembly weights must be subtracted as follows

$$w_f = 21{,}000 - (4)(1406) = 15{,}376 \text{ lbs} \tag{2.6}$$

Three tests were performed on the front end. The results of the computations are shown in Table 2-1 on the next page.

Table 2-1. Front end drop test results.

Test No.	δ (log decr.)	ζ (damp fact)	k (lb/in)	c (lb-sec/in)
3	0.655	0.1037	10275	133
4	0.611	0.0968	10089	123
5	0.721	0.1140	9843	143
Ave. Front	0.662	0.1048	10069	133

Given these values for c and k, they must be distributed over all the relevant components on the front end. There are 2 springs and 4 dampers on the front end; therefore, application of Equations 2.1 through 2.5 yields a spring constant k_f for each spring given by

$$k_f = \frac{10069}{2} = 5035 \text{ lb/in} \tag{2.7}$$

and a damping coefficient c_f for each damper given by

$$c_f = \frac{133}{4} = 33 \text{ lb-sec/in} \tag{2.8}$$

These values were combined with the manufacturer's spring bump stops and damper blow-off values to obtain the curves used to produce the VEHDYN 3.0 simulations in Section 3.

2.3.3 Rear Suspension Properties.

The rear drop test data was handled the same way as the front end data. The sprung weight of the rear section w_r was computed subtracting four wheel assembly weights from the weight under the section yielding

$$w_r = 17{,}000 - (4)(1406) = 11{,}376 \text{ lbs} \tag{2.9}$$

Table 2-2 on the next page provides the results of the three rear end drop tests.

Table 2-2. Rear end drop test results.

Test No.	δ (log decr.)	ζ (damp fact)	k (lb/in)	c (lb-sec/in)
6	0.967	0.152	8134	149
7	1.034	0.162	8319	161
8	0.999	0.157	8682	159
Ave. Rear	1.000	0.157	8378	156

Given these values for c and k, they were distributed over all the relevant components on the rear end. As with the front end, there are 2 springs and 4 dampers on the rear end; therefore, application of Equations 2.1 through 2.5 yields a spring constant k_r for each spring given by

$$k_r = \frac{8378}{2} = 4189 \text{ lb/in} \tag{2.10}$$

and a damping coefficient c_r for each damper given by

$$c_r = \frac{156}{4} = 39 \text{ lb-sec/in} \tag{2.11}$$

As with the front end values, manufacturer specifications for spring bump stops and damper blow-off were used to generate the data used in the VEHDYN 3.0 simulations in the next section.

SECTION 3

COMPARISON OF VEHDYN 3.0 SIMULATIONS WITH FIELD DATA

3.1 INTRODUCTION.

In this section, several comparisons of VEHDYN 3.0 simulations will be made with field data gathered by WES personnel (Jones, 1993) while driving both an empty and a fully loaded M977 HEMTT over several small obstacles at a nominal velocity of about 1.8 mph. The test obstacles were 2-foot-long by 10-foot-wide sections of plywood at varying heights ranging from 0.25 inches to 3.00 inches.

The simulations were made for obstacles having heights of 0.25, 0.50, 1.00, 2.00, and 3.00 inches. Both empty and fully loaded M977 HEMTT models were developed and used. Table 3-1 is the VEHDYN 3.0 vehicle file (see format of file in Creighton, 1993) for the empty HEMTT, making use of the parameters described in Section 2, while Table 3-2 is the vehicle file for the fully loaded HEMTT.

Table 3-1. VEHDYN 3.0 vehicle data file for empty M977 HEMTT.

```
M977CURB
OTC HEMTT M977 ... EMPTY ... WES SPG/DMP TABLES (9/92)
1,2,2,0,0,1
4,0,0,0,4.35
-1.,0.,4.35,5.35
-25000.,0.,21902.,46902.
4,0,0,0,4.35
-1.,0.,4.35,5.35
-25000.,0.,18222.,43222.
4,0,0
-100.,-45.45,45.45,100.
-1500.,-1500.,1500.,1500.
4,0,0
-100.,-38.46,38.46,100.
-1500.,-1500.,1500.,1500.
4,0,0,1.4486,1.6930
.4486,1.4486,1.6930,2.6930
-3.65E6,0.,0.,3.65E6
0,0,2,0,0,0,1
132.,45.
0,0,0,0
38000.,1.668E6,45.,5.,62.,168.,169.,0.
26.5,1406.,125.,24.67,2.11,6325,5250,1
26.5,1406.,65.,24.68,2.11,6325,5250,1
26.5,1406.,-85.,24.79,2.28,6825,4250,1
26.5,1406.,-145.,24.80,2.28,6825,4250,1
1,0,0,0,1
95.,6168.,500.
1,1,0,0,139.,132.
2,1,0,0,54.,58.
2,0,0,0,1
-115.,6168.,500.
3,2,0,0,-74.,-78.
4,2,0,0,-157.,-152.
```

Table 3-2. VEHDYN 3.0 vehicle data file for fully loaded M977 HEMTT.

```
M977LOAD
OTC HEMTT M977 ... FULL PAYLOAD ... WES SPG/DMP TABLES (9/92)
1,2,2,0,0,1
4,0,0,0,4.35
-1.,0.,4.35,5.35
-25000.,0.,21902.,46902.
4,0,0,0,4.35
-1.,0.,4.35,5.35
-25000.,0.,18222.,43222.
4,0,0
-100.,-45.45,45.45,100.
-1500.,-1500.,1500.,1500.
4,0,0
-100.,-38.46,38.46,100.
-1500.,-1500.,1500.,1500.
4,0,0,1.4486,1.6930
.4486,1.4486,1.6930,2.6930
-3.65E6,0.,0.,3.65E6
0,0,2,0,0,0,1
150.,28.
0,0,0,0
60400.,1.717E6,62.,22.,45.,150.,187.,0.
26.5,1406,143.,24.23,2.11,6325,7045.,1
26.5,1406,83.,24.22,2.11,6325,7129.,1
26.5,1406,-67.,23.96,2.28,6825,8013.,1
26.5,1406,-127.,23.96,2.28,6825,8013.,1
1,0,0,0,1
113.,6168.,500
1,1,0,0,157.0,150.0
2,1,0,0,72.0,76.0
2,0,0,0,1
-97.,6168.,500
3,2,0,0,-56.0,-60.0
4,2,0,0,-139.0,-134.0
```

Using these data as input, the state variable plotting post-processor for VEHDYN 3.0 was used to generate comparison plots of sprung mass pitch rate $\dot{\theta}$, CG vertical acceleration $\ddot{Z}_{CG}$, forward-most axle vertical acceleration $\ddot{Z}_1$, and displacement δ_1 of a forward mounted string pot (measuring the relative displacement of the forward-most axle with respect to the M977's frame) as functions of time and frequency. All of the time-history field data plots were filtered with a 5-Hz low-pass filter to minimize the noise. The frequency field data plots, however, were produced using the raw unfiltered data.

All of the comparison plots are located in Appendix A of this report. Table 3-3 gives the organizational scheme to the appendix. The first 16 figures are of the same type in that each figure contains four plots of a single quantity (eg., $\dot{\theta}$) for either the fully loaded or empty HEMTT at a single nominal velocity of about 1.8 mph negotiating four different obstacles (0.25, 0.50, 1.00, and 3.00 inches high). The remainder of the appendix contains a single plot on each figure. Each figure is a plot of one of the above-mentioned four state variables for either the fully loaded or empty HEMTT at about 1.8 mph over a single obstacle of one of the heights from 0.25, 0.50, 1.00, 2.00, or 3.00 inches.

The output step chosen from VEHDYN 3.0 was 0.02 sec. Assuming one requires at least 5-6 data points to resolve a given frequency sine wave, the highest frequency this sampling rate would allow the simulation output to show would be about 8-10 Hz when applying a Fast Fourier Transform (FFT) to a given time history. Indeed, 8 Hz is about the highest frequency any of the simulation FFTs show.

Table 3-3. Appendix A organization.

Figure Number	Description
A-1 - A-4	4 time history plots (obs. hts. = 0.25, 0.50, 1.0, 3.0 inches) on each figure for loaded HEMTT ($\dot{\theta}$, $\ddot{Z}_{CG}$, $\ddot{Z}_1$, and δ_1)
A-5 - A-8	4 frequency plots on each figure (same quantities as Figures A-1 - A-4) for loaded HEMTT
A-9 - A-12	Same series as Figures A-1 - A-4 for empty HEMTT
A-13 - A-16	Same series as Figures A-5 - A-8 for empty HEMTT
A-17	$\dot{\theta}$ vs. time for loaded HEMTT over 0.25-in. obs.
A-18	$\dot{\theta}$ vs. freq for loaded HEMTT over 0.25-in. obs.
A-19	$\ddot{Z}_{CG}$ vs. time for loaded HEMTT over 0.25-in. obs.
A-20 - A-21	$\ddot{Z}_{CG}$ vs. freq (2 scales) for loaded HEMTT over 0.25-in obs.
A-22	$\ddot{Z}_1$ vs. time for loaded HEMTT over 0.25-in. obs.
A-23 - A-24	$\ddot{Z}_1$ vs. freq (2 scales) for loaded HEMTT over 0.25-in. obs.
A-25	δ_1 vs. time for loaded HEMTT over 0.25-in. obs.
A-26 - A-27	δ_1 vs. freq (2 scales) for loaded HEMTT over 0.25-in. obs.
A-28 - A-38	Same series as Figures A-17 - A-27 for loaded HEMTT over 0.50-in. obs.
A-39 - A-49	Same series as Figures A-17 - A-27 for loaded HEMTT over 1.00-in. obs.
A-50 - A-60	Same series as Figures A-17 - A-27 for loaded HEMTT over 2.00-in. obs.
A-61 - A-71	Same series as Figures A-17 - A-27 for loaded HEMTT over 3.00-in. obs.
A-72 - A-126	Same series as Figures A-17 - A-71 for empty HEMTT

The FFT algorithm used herein allows input of an even number of points from the time history and uses an algorithm developed at the University of Michigan at Ann Arbor, Michigan (Univ. of Mich., 1979). FORTRAN-callable subroutines employing this algorithm were provided by Dr. Nabih Alem from the U.S. Army Aeromedical Research Laboratory at Fort Rucker, Alabama.

3.2 PITCH RATE OF THE SPRUNG MASS.

The first comparison that will be examined is that of the rate of fore-aft pitching of the sprung mass represented by the variable $\dot{\theta}$. Figure A-1 shows time-history comparison plots of the field data to simulation for the fully loaded HEMTT at about 1.80 mph (±0.03 mph) for obstacle heights of 0.25, 0.50, 1.00, and 3.00 inches. Individual comparison graphs are also displayed on Figures A-17 (0.25 inch), A-28 (0.50 inch), A-39 (1.00 inch), A-50 (2.00 inches), and A-61 (3.00 inches).

The magnitude of the simulation compares favorably with the magnitude of the test results and the low-frequency character of the oscillations is preserved. As already stated above, the data in the figures (as all the time-history data presented herein) has been filtered at 5 Hz to minimize the noise for these displays. The FFT frequency spectra of the unfiltered data for these same cases appears in Figures A-5 (four-obstacle-height comparison), A-18 (0.25 inch), A-29 (0.50 inch), A-40 (1.00 inch), A-51 (2.00 inches), and A-62 (3.00 inches). Table 3-4 shows the frequencies where significant activity occurs in both the field test data and the simulations at various obstacle heights.

The group of peaks at 0.4-0.7 Hz is evident throughout the comparisons and is the reason that the general qualitative character of the simulations is similar to the field data. The simulations, however, almost always show activity at 1.0 and 1.7 Hz, while the field data's major activity is at about 2.2 and 3.1 Hz, although the data shows some minor activity at 1.0 Hz throughout. There is a more in-depth discussion of the probable sources for the different frequencies in the field data in Volume 1 of this series (Jones, 1993). The VEHDYN 3.0 model is not able to capture some of the intricate 3D modeling details, like tire tread pattern,

Table 3-4. Frequencies of significant activity for pitch rate of the fully loaded HEMTT.

Obstacle Height	Significant Activity at These Frequencies (Hz)	
(inches)	VEHDYN 3.0	Test Data
0.25	.4-.7, 1.0, 1.7	.4-.7, 2.1-2.5, 3.1, 6.2
0.50	.4-.7, 1.0, 1.7	.4-.7, 2.6, 3.1
1.00	.4-.7, 1.0, 1.2, 1.7	.5, 2.2-2.6
2.00	.4-.7, 1.0, 1.7	.5, 2.0-2.5, 3.0-3.3
3.00	.4-.7, 1.0, 1.6	.4-.6, 1.0-1.2, 2.0-2.7

various suspension joints, etc. that cause some of the vibrations observed at certain frequencies in the data and yet not produced in the simulation. On the other hand, the general low-frequency character of the data is reproduced by VEHDYN 3.0.

Turning to the empty HEMTT, Figure A-9 shows time-history comparison plots of the field data to simulation at about 1.80 mph (±0.06 mph) for obstacle heights of 0.25, 0.50, 1.00, and 3.00 inches. Individual comparison graphs are also displayed on Figures A-72 (0.25 inch), A-83 (0.50 inch), A-94 (1.00 inch), A-105 (2.00 inches), and A-116 (3.00 inches).

The magnitude of the simulation is generally higher than for the data at the beginning of each event, particularly for the smaller obstacles. In general, the magnitude becomes much more comparable during the second half of the event. The character of the first part of the two smallest-obstacle simulations does not seem to match the test data, but the latter part of the events for all four obstacle heights appears reasonably well matched. The FFT frequency spectra of the unfiltered data for these same cases appear in Figures A-13 (four-obstacle-height comparison), A-73 (0.25 inch), A-84 (0.50 inch), A-95 (1.00 inch), A-106 (2.00 inches), and A-117 (3.00 inches). Table 3-5 shows the frequencies where significant activity occurs in both the field test data and the simulations at various obstacle heights.

As with the fully loaded HEMTT, the group of peaks at 0.4-0.7 Hz is evident throughout the comparisons (field data and simulations) and is the reason that the general qualitative

Table 3-5. Frequencies of significant activity for pitch rate of the empty HEMTT.

Obstacle Height	Significant Activity at These Frequencies (Hz)	
(inches)	VEHDYN 3.0	Test Data
0.25	.3-.6, 1.0, 1.4	.3-.6, 2.5, 2.9-3.1, 6.1
0.50	.4-.7, 1.0, 1.4	.4-.7, .9, 1.6, 2.2-2.7, 3.0, 6.2
1.00	.4-.7, 1.0, 1.2, 1.4, 1.6	.4-.7, 1.5-1.7, 2.4-2.7, 3.0
2.00	.4-.7, 1.0, 1.2, 1.4, 1.6	.4-.6, 1.2, 1.4-1.7, 2.1, 2.6, 3.0, 4.9
3.00	.4-.7, 1.0, 1.3-1.4, 1.6	.4-.6, 1.1, 2.1, 2.5

character of the simulations is similar to the field data. The simulations, however, almost always show activity in the 1.0-1.6 Hz range, but usually not much higher. While the data shows activity in these same areas, the presence of higher frequency activity, particularly at 2.1-2.7 and 3.0 Hz, is also obvious.

3.3 CG VERTICAL ACCELERATION.

The second quantity to be compared is the vertical acceleration of the CG of the sprung mass $\ddot{Z}_{CG}$. Figure A-2 shows time-history comparison plots of the field data to simulation for the fully loaded HEMTT at about 1.80 mph (±0.03 mph) for obstacle heights of 0.25, 0.50, 1.00, and 3.00 inches. Individual comparison graphs are also displayed on Figures A-19 (0.25 inch), A-30 (0.50 inch), A-41 (1.00 inch), A-52 (2.00 inches), and A-63 (3.00 inches).

The magnitude of the simulations is generally much smaller than the magnitude of the test results, especially for the smaller obstacles. The vertical motion of the sprung mass in the VEHDYN 3.0 model does not seem to be as sensitive as the test data evidence to the low-speed small-obstacle excitations entering at the tire-terrain interface until the obstacle height reaches about 3.00 inches. At the 3.00-inch height, however, the magnitude and the general character of the accelerations from field test and simulation are comparable. The FFT frequency spectra of the unfiltered field data for these same cases appear in Figures A-6

(four-obstacle-height comparison), A-20 and A-21 (0.25 inch at two frequency scales), A-31 and A-32 (0.50 inch at two frequency scales), A-42 and A-43 (1.00 inch at two frequency scales), A-53 and A-54 (2.00 inche at two frequency scales), and A-64 and A-65 (3.00 inches at two frequency scales). Table 3-6 shows frequencies where significant activity occurs in both the field test data and the simulations at various obstacle heights.

Table 3-6. Frequencies of significant activity for CG vertical acceleration of the fully loaded HEMTT.

Obstacle Height	Significant Activity at These Frequencies (Hz)	
(inches)	VEHDYN 3.0	Test Data
0.25	.4-.7, .9-1.1, 1.6, 1.9-2.1	.4-.7, 2.1, 2.3, 2.7, 2.9-3.2, 5.0-5.5, 6.2, 11.1, 12.3, 18.4-18.8
0.50	.4-.7, .9-1.1, 1.7, 1.9-2.1	.4-.7, .9-1.1, 2.3-2.7, 3.0, 3.2-3.3, 5.0-5.3, 6.2, 11.2, 12.4-12.7
1.00	.4-.7, .9-1.1, 1.7, 2.0-2.2	.4-.7, 2.3-2.7, 3.2, 4.9-5.3, 6.2-6.5, 11.2, 12.8-13.4
2.00	.4-.7, .9-1.1, 1.7	.4-.6, 1.2, 1.5, 2.0-2.6, 3.2
3.00	.4-.7, .9-1.1, 1.6, 2.1, 2.6	.4-.6, 1.1, 2.1, 2.5

As with the pitch rate comparisons, there is a common 0.4-0.7 Hz mode throughout both the field data and simulations. Another common mode is at about 1.0 Hz for both the field data and the simulations, although it becomes more obvious in the larger obstacles. The major difference is that the simulations don't ever show a mode above 2.6 Hz, but the field data has several modes between 5.0 and 19.0 Hz in the smallest obstacles. As we've previously discussed, a more in-depth discussion of possible sources of these higher-frequency modes is found in Volume 1 of this series (Jones, 1993) and are likely from real-vehicle components not able to be modeled with the simplicity of VEHDYN 3.0.

The main concern with these CG acceleration comparisons is that the acceleration magnitudes of the simulations are much smaller than the test data for the smaller obstacles.

The sensitivity of the VEHDYN 3.0 model does not seem to be adequate to pick up these small-magnitude accelerations.

Turning to the empty HEMTT, Figure A-10 shows time-history comparison plots of the field data to simulation at about 1.80 mph (±0.06 mph) for obstacle heights of 0.25, 0.50, 1.00, and 3.00 inches. Individual comparison graphs are also displayed on Figures A-74 (0.25 inch), A-85 (0.50 inch), A-96 (1.00 inch), A-107 (2.00 inches), and A-118 (3.00 inches).

The magnitude of the simulation is much closer to the test results in all cases except the smallest obstacle (0.25 inch) where the test data is still about twice as large in general magnitude. Otherwise, the VEHDYN 3.0 model seems sensitive enough to be able to detect the small vertical accelerations even for very small bumps. The VEHDYN 3.0 empty-vehicle model does seem somewhat "bouncier" than the test vehicle in that a buildup of accelerations does not seem to decay as fast (see Figure A-118 for 3.00-inch results) as the test data indicates. It must be remembered that very simple spring and damper models were employed and it may be necessary to develop a more sophisticated nonlinear damper model in future work. The FFT frequency spectra of the unfiltered field test data for these same cases appear in Figures A-14 (four-obstacle-height comparison), A-75 and A-76 (0.25 inch at two frequency scales), A-86 and A-87 (0.50 inch at two frequency scales), A-97 and A-98 (1.00 inch at two frequency scales), A-108 and A-109 (2.00 inches at two frequency scales), and A-119 and A-120 (3.00 inches at two frequency scales). Table 3-7 lists those frequencies where significant activity occurs in both the field test data and the simulations at various obstacle heights.

For the smaller bumps, VEHDYN 3.0 always shows predominant activity at about 2.0 Hz, a frequency that does not show up in the field data until the bigger bumps. The predominant activity in the small-obstacle test data is at about 3.0 Hz and is probably due to unmodeled components in the HEMTT vibrating and dominating the FFT spectrum. It must be realized that these magnitudes are extremely small and easily dominated by small vibrations. Again, review the comments in Volume 1 (Jones, 1993) for a more detailed explanation. For the larger bumps (2-3 inches), the .5 Hz and 2.0 Hz modes show up in both the data and the simulations.

Table 3-7. Frequencies of significant activity for CG vertical acceleration of the empty HEMTT.

Obstacle Height	Significant Activity at These Frequencies (Hz)	
(inches)	VEHDYN 3.0	Test Data
0.25	2.1	2.9-3.1, 6.1, 9.1, 11.0, 12.1, 17.9
0.50	1.9-2.1	2.5-3.2, 4.7-5.0, 6.2, 10.9, 12.2, 14.2, 16.8
1.00	.7, 2.0-2.2, 2.6-2.8, 6.5	.6, 1.5, 2.4-2.6, 3.0-3.2, 3.5, 4.3-4.5, 4.9-5.3, 5.8, 6.2-6.4, 11.0, 12.2, 16.4, 17.0
2.00	.4-.6, .9-1.1, 1.5-1.7, 1.9-2.3, 2.6-2.8	.4-.7, 1.0-1.5, 2.1, 2.3, 2.5, 2.7-3.1, 3.3, 3.6, 4.3-4.5, 4.9, 5.8, 6.2-6.9, 10.0, 11.1, 12.6, 13.6, 14.5, 15.0, 16.0
3.00	.4-.6, 1.5-1.7, 1.9-2.1	.5, 1.0-1.2, 1.9-2.1, 2.4-3.0, 4.2, 4.8-5.0

3.4 VERTICAL ACCELERATION OF FORWARD-MOST WHEEL AXLE.

The third comparison that will be examined is that of the vertical acceleration of the front wheel axle represented by the variable $\ddot{Z}_1$. Figure A-3 shows the time-history comparison plots of the field data to simulation for the fully loaded HEMTT at about 1.80 mph (±0.03 mph) for obstacle heights of 0.25, 0.50, 1.00, and 3.00 inches. Individual comparison graphs are also displayed on Figures A-22 (0.25 inch), A-33 (0.50 inch), A-44 (1.00 inch), A-55 (2.00 inches), and A-66 (3.00 inches).

The magnitude of the simulations is generally good at the beginning of the event (for all except the 0.25-inch obstacle where the simulation magnitude is too small). The test data show much higher acceleration magnitudes than the VEHDYN 3.0 simulations in the second half of the event in most cases, especially for the 0.25 and 0.50-inch obstacle tests. It must be pointed out again that the magnitudes of these accelerations are very small (on the order of 0.1 g and less) and the VEHDYN 3.0 fully loaded model does not seem as sensitive as the test data indicates in predicting these small accelerations. The FFT spectra of the unfiltered

field test data for these same cases appear in Figures A-7 (four-obstacle-height comparison), A-23 and A-24 (0.25 inch at two frequency scales), A-34 and A-35 (0.50 inch at two frequency scales), A-46 and A-47 (1.00 inch at two frequency scales), A-56 and A-57 (2.00 inches at two frequency scales), and A-67 and A-68 (3.00 inches at two frequency scales). Table 3-8 lists those frequencies where significant activity occurs in both the field test data and the simulations at various obstacle heights.

Table 3-8. Frequencies of significant activity for the foremost axle vertical acceleration of the fully loaded HEMTT.

Obstacle Height	Significant Activity at These Frequencies (Hz)	
(inches)	VEHDYN 3.0	Test Data
0.25	6.8	2.3, 3.2, 6.2, 8.0, 8.4-8.7, 9.2, 10.4, 12.2-12.6, 15.5
0.50	1.7, 5.4, 6.8	2.3, 3.1, 5.3, 5.7, 6.2-6.4, 8.2-9.2, 12.7
1.00	.6-.8, 1.7, 4.0, 5.5, 6.5, 7.0	.6-.8, 1.5-1.9, 2.6, 3.0, 3.4-3.7, 4.3, 4.7, 5.0-5.2, 5.6-5.9, 6.2-6.6, 6.9-7.1, 8.0-9.0, 9.4-10.2, 12.6-13.0
2.00	5.-.7, 1.7, 2.5-2.8, 3.9, 7.5	.6, 1.5, 2.4, 3.2, 6.0-6.6, 8.0-8.4, 8.9
3.00	.6, 1.6, 2.5, 2.9, 5.0-7.5	.6, 1.2, 2.5, 3.4, 5.2-7.4, 8.6, 9.1, 10.5-11.3, 11.7, 12.4, 16.8

It is difficult to comment on these frequency spectra because both the simulations and the test data have significant activity over broad ranges of frequencies. The test data, however, exhibits activity at many more frequencies and at higher frequencies than the simulations. As previously discussed, a more in-depth discussion of possible sources of these higher-frequency modes is found in Volume 1 of this series (Jones, 1993) and is likely from real-vehicle components not able to be modeled with the simplicity of VEHDYN 3.0.

As with the CG accelerations, the main concern with these acceleration comparisons is that the magnitudes from the simulations are much smaller than the test data for the smaller obstacles. The sensitivity of the VEHDYN 3.0 model does not seem to be adequate to pick up these small-magnitude accelerations.

Turning to the empty HEMTT, Figure A-11 shows time-history comparison plots of the field data to simulation at about 1.80 mph (±0.06 mph) for obstacle heights of 0.25, 0.50, 1.00, and 3.00 inches. Individual comparison graphs are also displayed on Figures A-77 (0.25 inch), A-88 (0.50 inch), A-99 (1.00 inch), A-110 (2.00 inches), and A-121 (3.00 inches).

As in the case of the CG accelerations, the magnitude of the simulation is much closer (than for the fully loaded HEMTT) to the test results in all cases except the latter half of the two smallest obstacles (0.25 and 0.50 inch) where the test data does not decay as much as the simulation does. Otherwise, the VEHDYN 3.0 model seems sensitive enough to be able to detect the small vertical axle accelerations even for very small bumps. The FFT frequency spectra of the unfiltered test data for these same cases appear in Figures A-15 (four-obstacle-height comparison), A-78 and A-79 (0.25 inch at two frequency scales), A-89 and A-90 (0.50 inch at two frequency scales), A-100 and A-101 (1.00 inch at two frequency scales), A-111 and A-112 (2.00 inches at two frequency scales), and A-122 and A-123 (3.00 inches at two frequency scales). Table 3-9 lists those frequencies where significant activity occurs in both the field test data and the simulations at various obstacle heights.

Table 3-9. Frequencies of significant activity for the foremost axle vertical acceleration of the empty HEMTT.

Obstacle Height	Significant Activity at These Frequencies (Hz)	
(inches)	VEHDYN 3.0	Test Data
0.25	1.4, 2.1, 7.1	2.5, 2.9-3.1, 5.6, 5.8, 6.2, 6.6, 9.0-9.2, 12.2, 15.3
0.50	.6, 1.0, 1.4, 2.0, 3.0, 4.0, 4.5, 5.5, 5.9, 7.0-7.4	.7, 1.5, 2.5, 3.0, 5.0, 5.5, 6.3, 6.8, 7.7, 8.8-9.3, 10.1, 12.5, 15.4-15.7, 18.9
1.00	.5-.7, 1.0, 1.4, 2.0, 3.0, 4.2, 4.5, 5.6, 6.8, 7.1, 7.6	.6, 1.6, 2.3, 3.2, 3.6, 4.5, 5.1, 6.0, 6.4, 7.0, 7.7, 8.4, 8.9, 9.5, 10.0, 12.0, 12.5, 13.2
2.00	.6, 1.0, 1.4, 1.7, 2.0-2.2, 2.4, 2.8, 4.0, 4.5-4.9, 5.5, 6.5-7.2, 8.0-8.4	.6, 1.1, 1.4, 2.5-3.0, 3.6, 4.4, 5.0, 5.7, 6.0-6.7, 7.2-7.4, 8.0-8.4, 8.9, 9.3, 9.9, 12.6-13.0, 17.9-18.1
3.00	.6, 1.4, 1.7, 2.0, 2.4, 3.4, 4.5, 4.9, 6.7-7.2	.5, 1.1, 2.1-2.5, 3.0, 4.3-4.5, 4.9, 5.4-7.2, 7.7, 8.4, 8.8-10.5

There again is activity at numerous frequencies in both the test data and the simulations and sometimes there is agreement, sometimes not. In dealing with the small-magnitude accelerations, vehicle component vibrations again can be attributed to much of the higher frequency activity in the test data (see Jones, 1993). However, the low-frequency mode at about 0.6 Hz is observed in both the simulations and field test data for all cases except the smallest obstacle. Modes at about 1.0 and 1.4 Hz are present in many of the cases as well; thus it can be concluded that the general low-frequency character of both the test data and the simulations is similar.

3.5 DISPLACEMENT OF THE FORWARD-MOUNTED STRING POT.

The final comparison to be examined is that of the displacement of a forward-mounted string pot represented by the variable δ_1 . The test vehicle actually had four string pots mounted on it. Each string pot measured the displacement of one axle relative to the underside of the frame directly above it. A more detailed description of the test setup for the string pots is found in Volume 1 of this series (Jones, 1993). Because the string pot connects the axle (which is near the end on a walking beam) to the frame, its displacement (ie., lengthening and shortening) measures a combination of vertical axle displacement, beam rotation, CG vertical displacement, and sprung mass rotation. Primarily, however, it provides an indicator of whether the "action" of the beam is realistic. Because the data from each of the string pots is similar to that of the other string pots, this section will only address the data from one of the them, namely, the forward-mounted string pot.

Figure A-4 shows time-history comparison plots of the field data to simulation for the fully loaded HEMTT at about 1.80 mph (±0.03 mph) for obstacle heights of 0.25, 0.50, 1.00, and 3.00 inches. Individual comparison graphs are also displayed on Figures A-25 (0.25 inch), A-36 (0.50 inch), A-47 (1.00 inch), A-58 (2.00 inches), and A-69 (3.00 inches).

The magnitude of the simulation matches the magnitude of the test results extremely well for all obstacle heights. The general character of the simulation time histories mimic those of the field tests quite closely. As with the previous time histories, the field data have been filtered

at 5 Hz for clearer presentation. The FFT frequency spectra of the unfiltered test data for these same cases appears in Figures A-8 (four-obstacle-height comparison), A-26 and A-27 (0.25 inch at two frequency scales), A-37 and A-38 (0.50 inch at two frequency scales), A-48 and A-49 (1.00 inch at two frequency scales), A-59 and A-60 (2.00 inches at two frequency scales), and A-70 and A-71 (3.00 inches at two frequency scales). Table 3-10 lists those frequencies where significant activity occurs in both the field test data and the VEHDYN 3.0 simulations at various obstacle heights.

Table 3-10. Frequencies of significant activity for the forward-mounted string pot displacement of the fully loaded HEMTT.

Obstacle Height	**Significant Activity at These Frequencies (Hz)**	
(inches)	**VEHDYN 3.0**	**Test Data**
0.25	0.2, 0.7, 1.6	0.1-0.2, 0.7, 2.4, 3.1, 6.2, 19.2
0.50	0.2, 0.7, 1.7	0.1-0.3, 0.8, 1.2, 1.9, 2.4-2.6, 3.1, 6.2, 19.4-19.8
1.00	0.2, 0.7, 1.7	0.3, 0.8, 3.2
2.00	0.2, 0.7, 1.7	0.2, 0.7, 1.3, 2.3
3.00	0.2, 0.7, 1.6	0.2, 0.5-0.7, 1.2

The two low-frequency modes at about 0.2 and 0.7 Hz are present at all obstacle heights for both the simulations and the test data. This is why the general character of the simulations match that of the test data throughout. The simulations, however, show activity at about 1.7 Hz, whereas the test data shows higher frequency activity at 1.2, 2.3, and 3.2 Hz. The two smallest obstacles also indicate activity at or near 6.2 and 19.4 Hz; these are frequencies which are probably the result of vehicle vibration from components VEHDYN 3.0 does not model (see Jones, 1993). Generally, the comparisons indicate excellent agreement between simulation and field test results.

Turning to the empty HEMTT, Figure A-12 shows time-history comparison plots of the field data to simulation at about 1.80 mph (±0.06 mph) for obstacle heights of 0.25, 0.50, 1.00, and

3.00 inches. Individual comparison graphs are displayed on Figures A-80 (0.25 inch), A-91 (0.50 inch), A-102 (1.00 inch), A-113 (2.00 inches), and A-124 (3.00 inches).

The magnitudes are again quite comparable between the test results and the simulations except for the first two major peaks for the two smallest obstacles. In these two cases, the peaks in the simulations overestimate the magnitude by as much as a factor of two. The general character of all of the comparisons is reasonable throughout, however.

One noticeable attribute in the simulation at the smallest obstacle is the higher frequency oscillations about the apparent steady state trace. This is a direct result of similar motion observed in the pitching motion of the sprung mass discussed earlier due to a bouncier-than-realistic phenomenon in the simulations. Note that the motion recorded by the string pots includes the fore-aft pitching of the sprung mass.

The FFT frequency spectra of the unfiltered field data for the empty HEMTT for these same cases appear in Figures A-16 (four-obstacle-height comparison), A-81 and A-82 (0.25 inch), A-92 and A-93 (0.50 inch), A-103 and A-104 (1.00 inch), A-114 and A-115 (2.00 inches), and A-125 and A-126 (3.00 inches). Table 3-11 lists those frequencies where significant activity occurs in both the field test data and the simulations at various obstacle heights.

Table 3-11. Frequencies of significant activity for the forward-mounted string pot displacement of the empty HEMTT.

Obstacle Height	Significant Activity at These Frequencies (Hz)	
(inches)	VEHDYN 3.0	Test Data
0.25	0.2, 0.7, 1.4, 2.1	0.3, 0.5, 0.7, 3.1, 6.1, 18.8-19.0
0.50	0.2, 0.7, 1.4, 2.1	0.3, 0.5, 0.7, 3.1, 19.3-19.7
1.00	0.2, 0.7, 1.4, 2.0	0.2, 0.7, 3.2
2.00	0.2, 0.7, 1.4	0.2, 0.6-0.7, 1.2
3.00	0.2, 0.7, 1.4, 2.0-2.1	0.2, 0.6, 1.2

The FFT spectra for both the field tests and the simulations are quite similar on the whole. Both sets exhibit activity at or near 0.2 and 0.7 Hz for all obstacle heights and 1.4 Hz for the larger obstacles. However, the smaller-obstacle results show activity at 2.0 Hz in the simulations and 3.1 Hz in the tests. Overall, the VEHDYN 3.0 simulations approximate the motion of the HEMTT walking beams quite well.

SECTION 4

CONCLUSIONS AND RECOMMENDATIONS

The following conclusions can be drawn after examining the comparisons between the field test data and the VEHDYN 3.0 simulations:

1- Concerning the sprung mass pitch rate comparisons, the fully loaded HEMTT model produced excellent magnitudes for all obstacle heights (0.25, 0.50, 1.00, 2.00, 3.00 inches). The empty HEMTT model produced high early-time magnitudes, but the late-time results converged toward the test data magnitudes. The FFT analyses for both the fully loaded and empty HEMTT models revealed excellent low-frequency comparisons, but the simulations did not pick up the higher frequency motion at 2.0 Hz and above exhibited in the test data.

2- Concerning the CG vertical acceleration comparisons, both the fully loaded and the empty models produced low magnitudes for all but the largest obstacle height (3.00 inches); the agreement between field test and simulation improved with increasing obstacle height. The FFT analyses for the fully loaded HEMTT showed good low-frequency agreement between field tests and simulations throughout, but the major simulation peak was at 1.7 Hz, while the major field test peak was somewhat higher at 2.5 Hz. The FFT analyses for the empty HEMTT gave good low-frequency agreement at all but the smallest obstacle. The dominant peak for the simulation was at 2.1 Hz, while major peaks in the tests were somewhat higher (3.0 and 6.1 Hz for the smallest obstacles, and 2.5, 3.0, and 5.0 Hz for the largest obstacles) and revealed higher-frequency harmonics.

3- Concerning the vertical acceleration of the forward-most wheel axle, both the fully loaded and the empty HEMTT models somewhat underpredicted the test magnitudes, particularly in the latter half of the event. Much of this can be explained by tire details not able to be modeled in a VEHDYN 3.0 vehicle representation. It's also possible that the vehicle properties derived from the simple mass-spring-damper representation did

not fully capture the true properties of the vehicle suspension system. The FFT analyses exhibit many low-frequency similarities between tests and simulation (eg., 0.6, 1.7, and 2.5 Hz). The field data shows activity at many frequencies, however, that are not present in the simulations. Again, the simple representation of the vehicle in VEHDYN 3.0 precludes detecting some of the higher-frequency modes that the testing instrumentation measured.

4- Concerning the displacement of the forward-mounted string pot, both the fully loaded and the empty HEMTT models produced magnitudes very close to the field test magnitudes, revealing that the action of the simulated walking beams was an accurate representation of the actual walking beams. The FFT analyses of the low-frequency activity compared very well, producing significant activity at 0.2 and 0.7 Hz in both the tests and simulations throughout. The tests, however, exhibited activity at higher frequencies (2.4 and 3.1 Hz) on the smallest obstacles that was not observed in the simulations. The simulations, on the other hand, showed activity throughout all cases at the slightly lower frequency of 1.7 Hz that was not observed in the tests.

The VEHDYN 3.0 HEMTT models do a reasonable job at predicting the motion (accelerations, pitch velocities, and displacements) and can be confidently used to perform parameter, feasibility, and optimization studies to examine the effects of varying different types of WIM configurations (strip patterns and mats of various sizes). Although the simple HEMTT models used herein used linear spring and damper relationships, they still were able to accurately reproduce the displacement magnitudes and lower frequencies measured by the string pots indicating an accurate duplication of the walking beam motion in the simulations. These two models were also sensitive enough to predict most of the lower-frequency motions in both pitch velocity and acceleration histories. Although the magnitudes were not always accurate in the acceleration histories, they were quite comparable in the pitch velocity histories.

It is recommended that some further refinements be made to the VEHDYN 3.0 HEMTT models that time and funding constraints precluded on this initial study. The two most difficult data to obtain for a vehicle are the pitch mass moment of inertia (in a 2D study) and the spring/damper relationships. The following improvements could be performed:

1- Measured values for the pitch mass moment of inertia were provided by two professional organizations for the HEMTT and they differed by a factor of two. The value that ultimately was used in the simulations was calculated by assuming the mass lumped over the suspensions. A sensitivity study was not done, but could be performed to see the overall effect of varying this parameter.

2- Linear spring and damper relationships were obtained from drop test results in this study. Better, nonlinear spring relationships could be produced by actually executing complete loading and unloading test cycling on each suspension. The funding constraints precluded this action in this study, but more accurate response relationships would be produced in this fashion.

SECTION 5
REFERENCES

Creighton, D. C. (1993). "Enhanced Vehicle Dynamics Module: User's Guide For Computer Program VEHDYN 3.0," Technical Report in Publication, unclassified, U.S. Army Engineer Waterways Experiment Station, Vicksburg, MS.

Durham, G. N., and Murphy, N. R., Jr. (1976). "Preliminary Evaluation of the Ability of the C-12A Aircraft to Operate Safely on Substandard Airstrips," Miscellaneous Paper M-76-18, unclassified, U.S. Army Engineer Waterways Experiment Station, Vicksburg, MS.

Jones, R. A. (1993). "HEMTT Dynamic Sensitivity to Small Obstacles at Low Velocities, Volume 1: Field Tests," Technical Report DNA-TR-93-116-V1, unclassified, U.S. Army Engineer Waterways Experiment Station, Vicksburg, MS.

Michelin Tire Corporation (1986). "Michelin Truck, Industrial & Off-The-Road Tire Data Book 1985-1986," unclassified, Greenville, SC.

University of Michigan Computing Center (1979). "The Discrete Fourier Transform," Computing Center Memo 327, unclassified, Ann Arbor, MI.

APPENDIX A

TIME HISTORY AND FFT COMPARISONS OF FIELD TEST DATA TO VEHDYN 3.0 SIMULATIONS

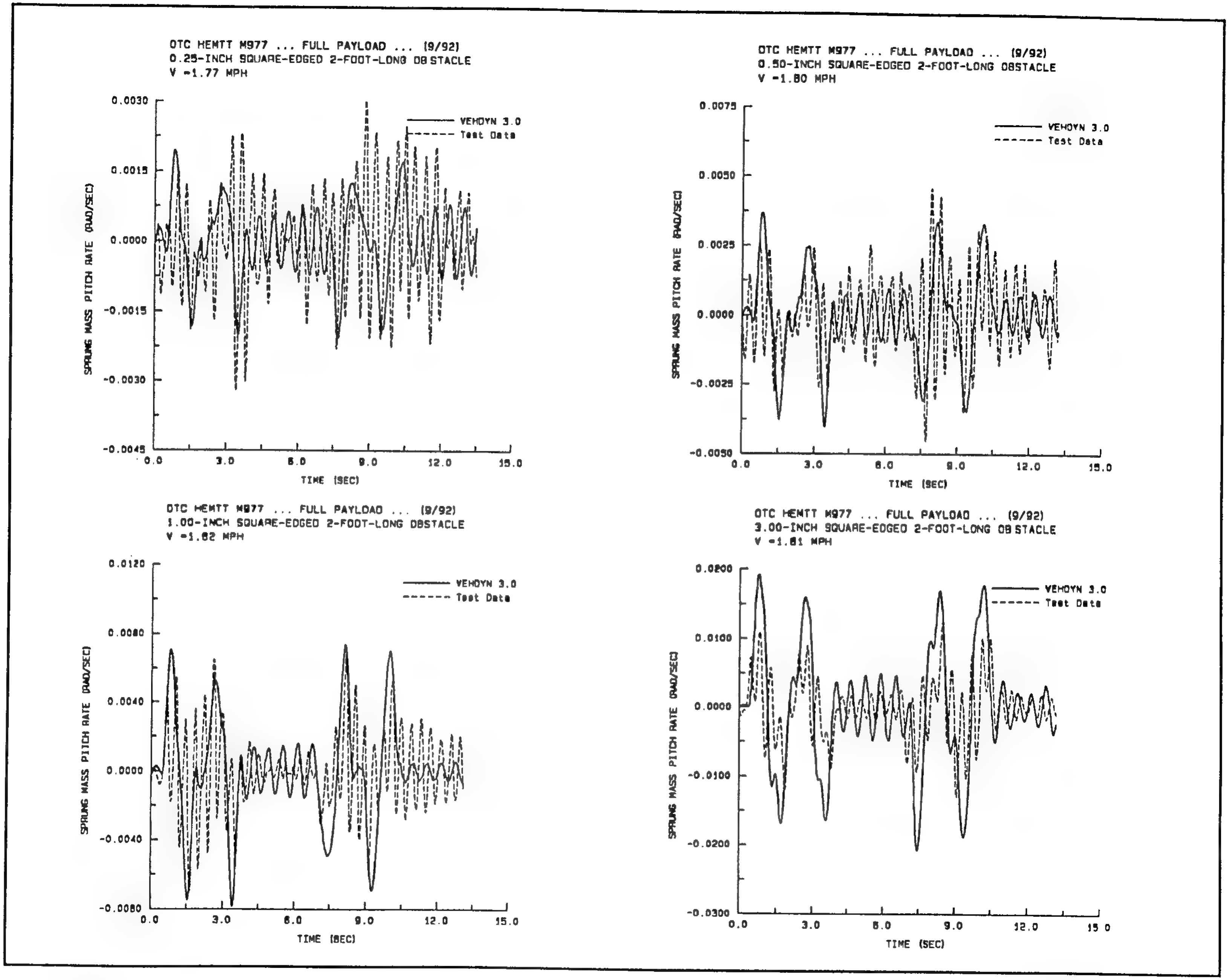

Figure A-1. Sprung mass pitch rate time histories for a fully loaded HEMTT traveling at about 1.80 miles per hour encountering obstacles of heights 0.25, 0.50, 1.00, and 3.00 inches.

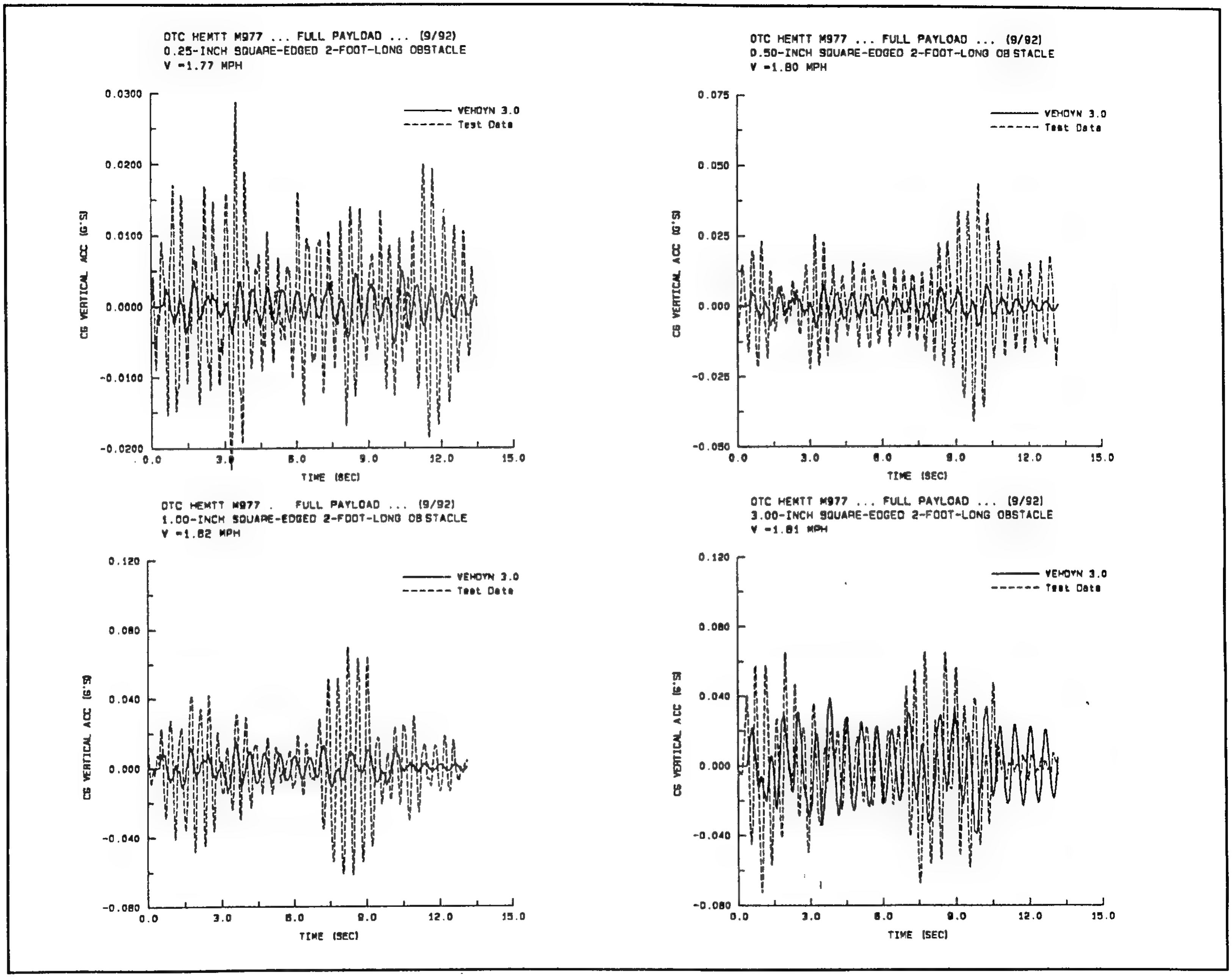

Figure A-2. CG vertical acceleration time histories for a fully loaded HEMTT traveling at about 1.80 miles per hour encountering obstacles of heights 0.25, 0.50, 1.00, and 3.00 inches.

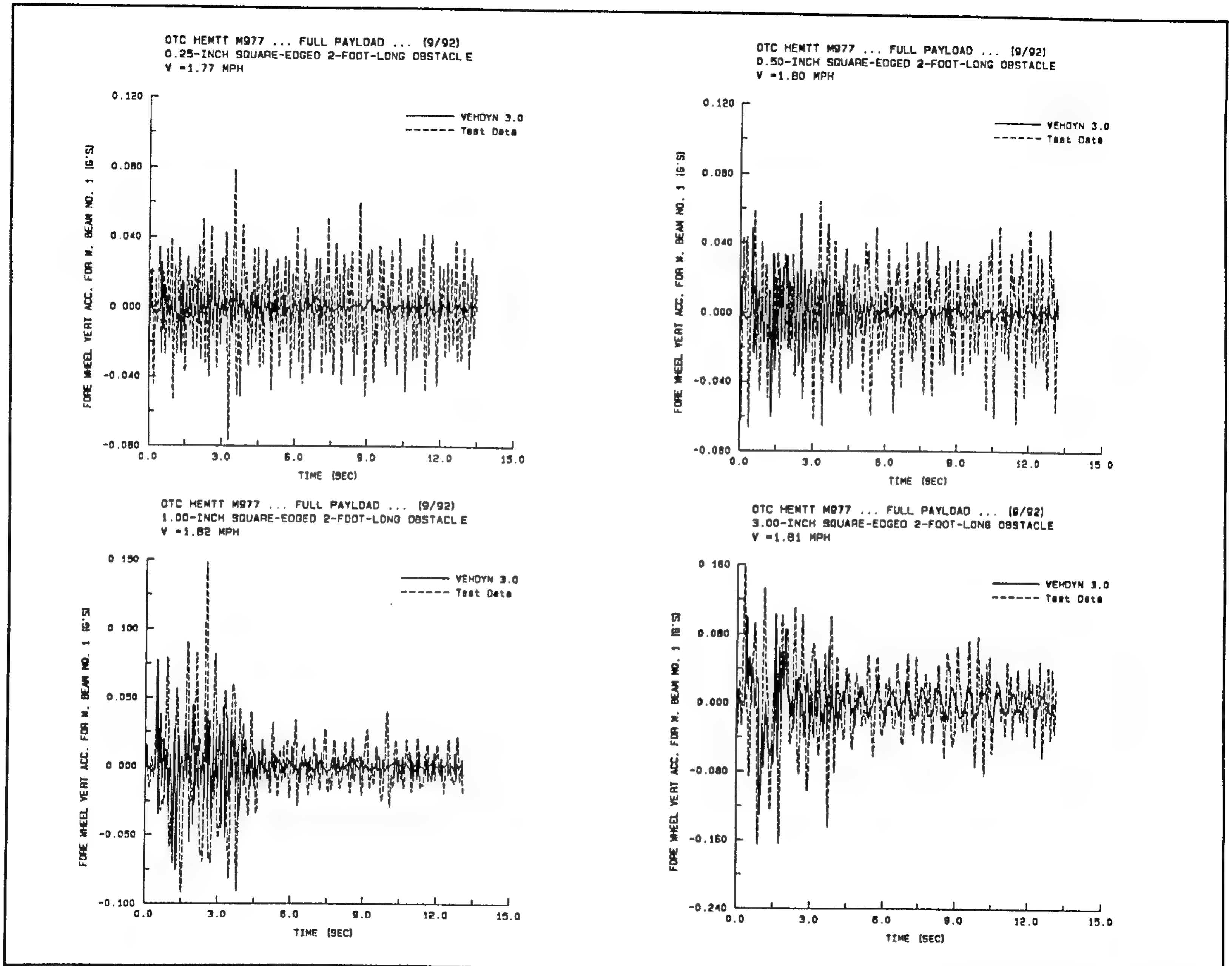

Figure A-3. Vertical acceleration of the forward-most axle time histories for a fully loaded HEMTT traveling at about 1.80 miles per hour encountering obstacles of heights 0.25, 0.50, 1.00, and 3.00 inches.

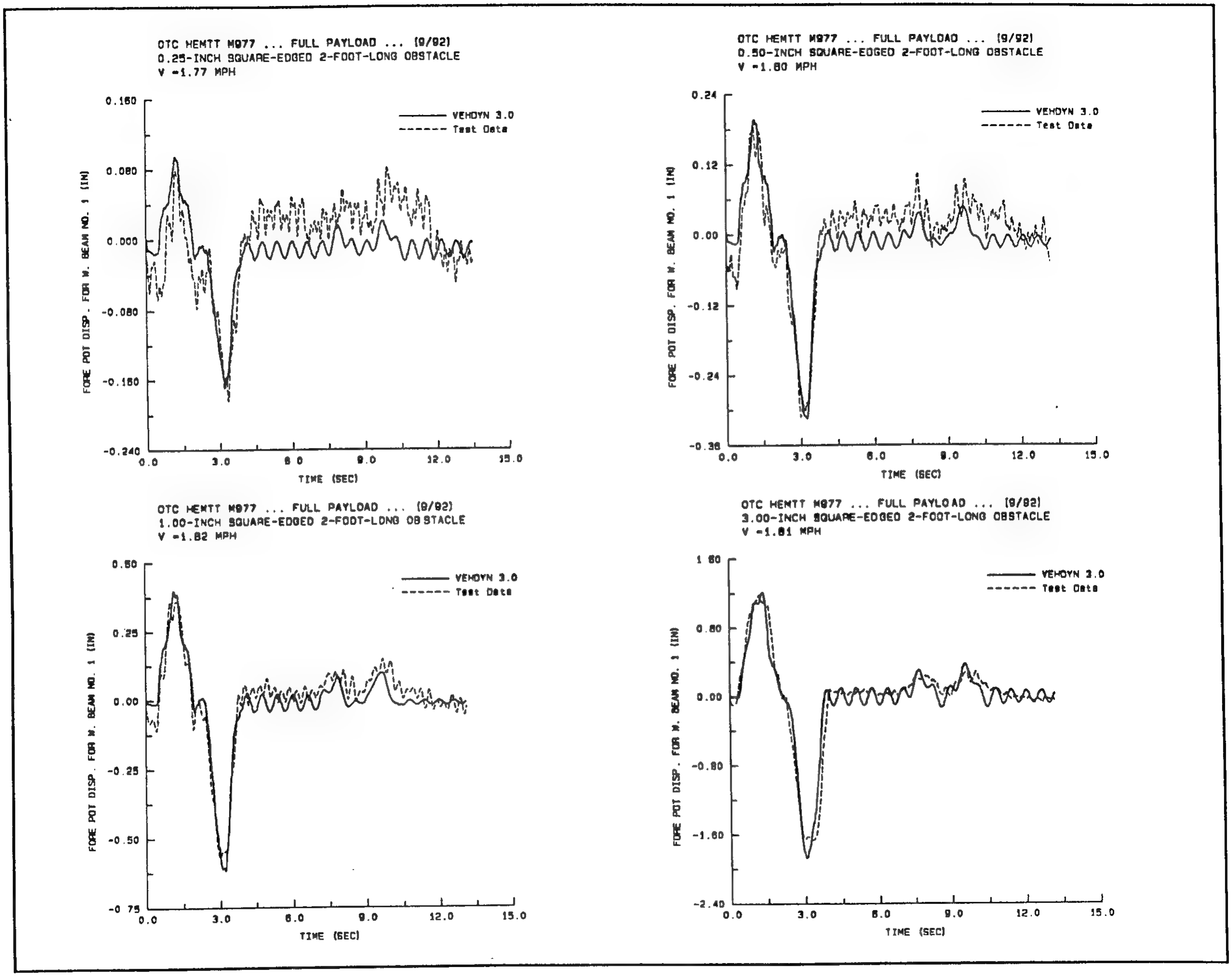

Figure A-4. Forward axle displacement relative to the frame time histories for a fully loaded HEMTT traveling at about 1.80 miles per hour encountering obstacles of heights 0.25, 0.50, 1.00, and 3.00 inches.

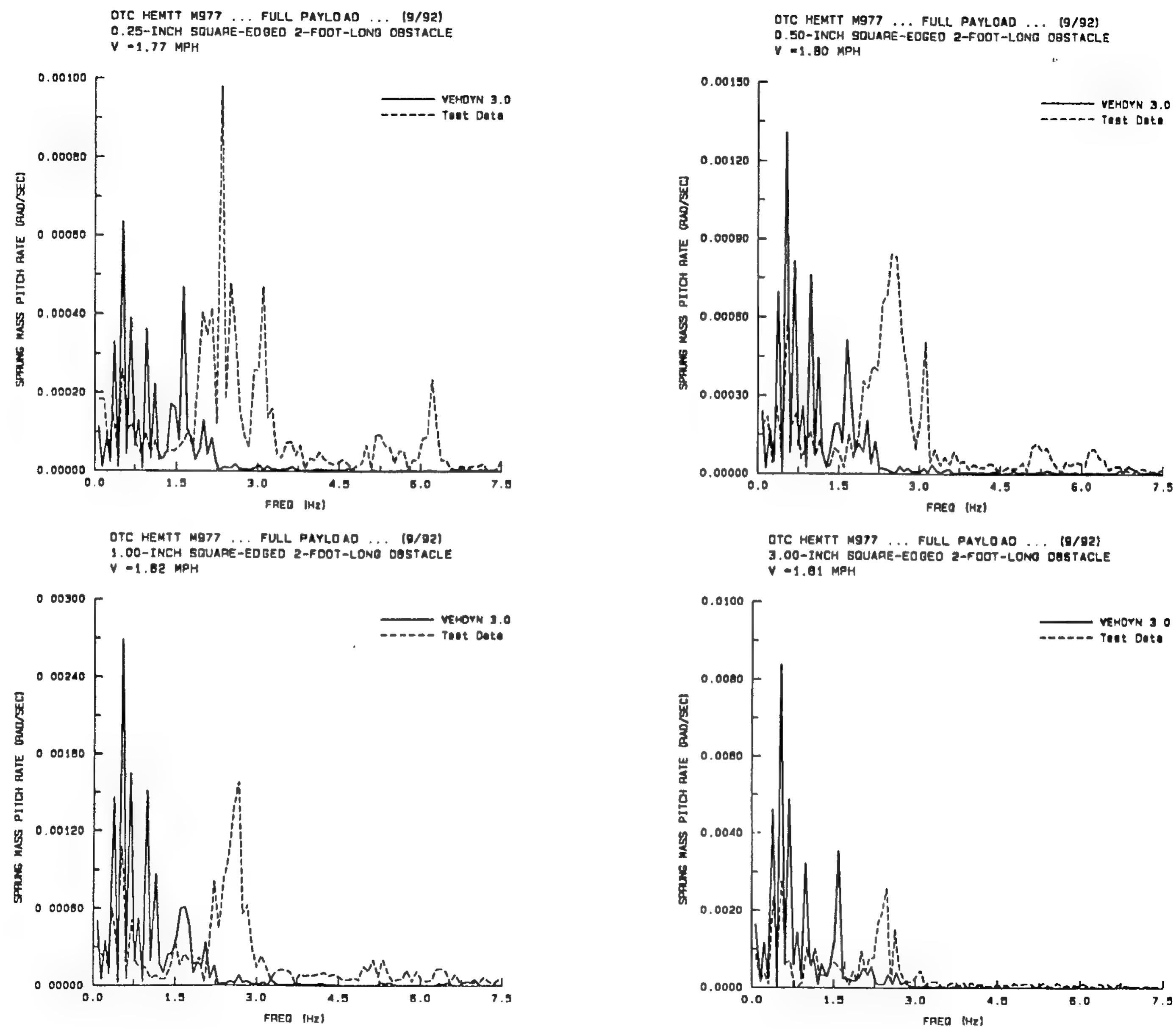

Figure A-5. Sprung mass pitch rate frequency plots for a fully loaded HEMTT traveling at about 1.80 miles per hour encountering obstacles of heights 0.25, 0.50, 1.00, and 3.00 inches.

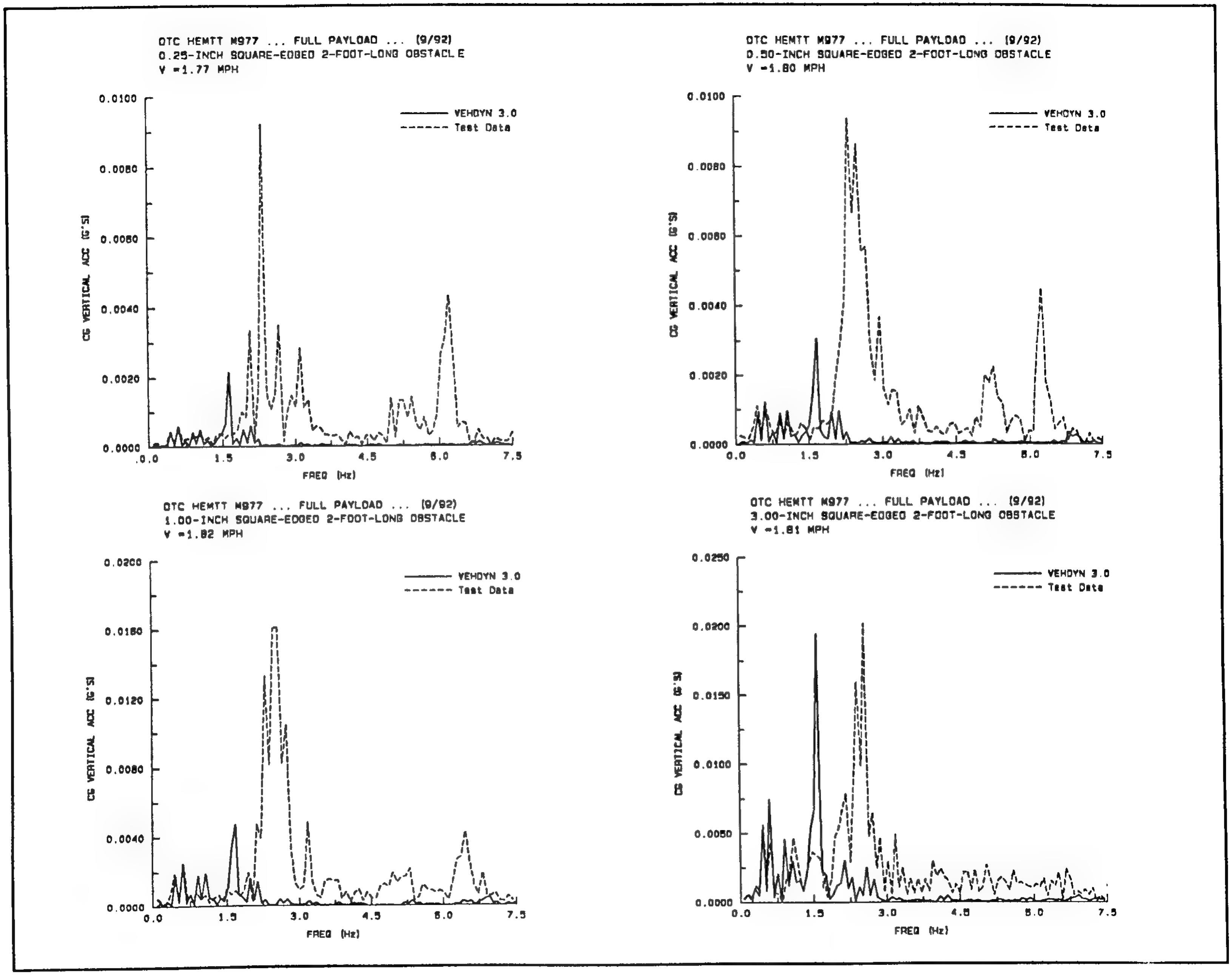

Figure A-6. CG vertical acceleration frequency plots for a fully loaded HEMTT traveling at about 1.80 miles per hour encountering obstacles of heights 0.25, 0.50, 1.00, and 3.00 inches.

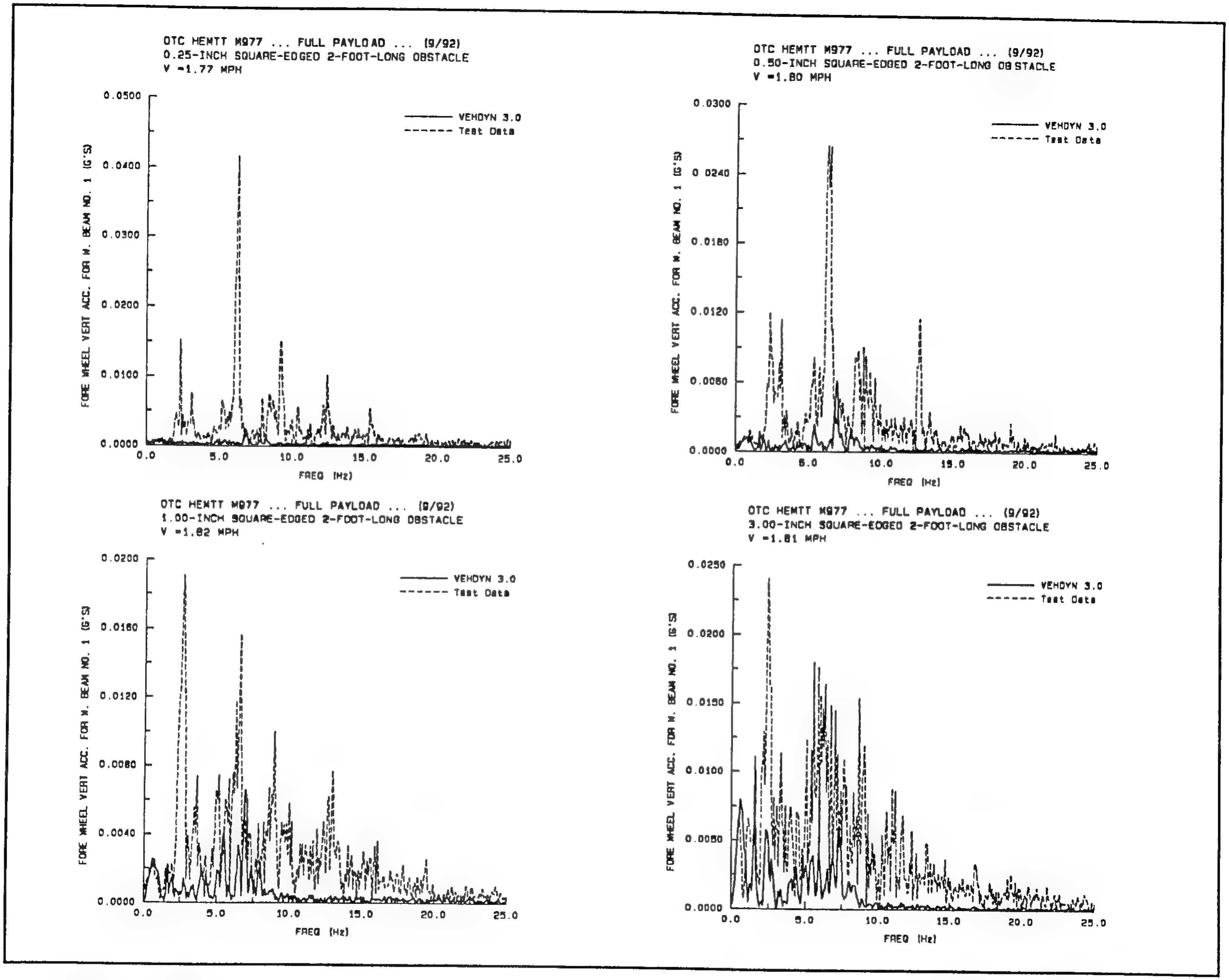

Figure A-7. Vertical acceleration of the forward-most axle frequency plots for a fully loaded HEMTT traveling at about 1.80 miles per hour encountering obstacles of heights 0.25, 0.50, 1.00, and 3.00 inches.

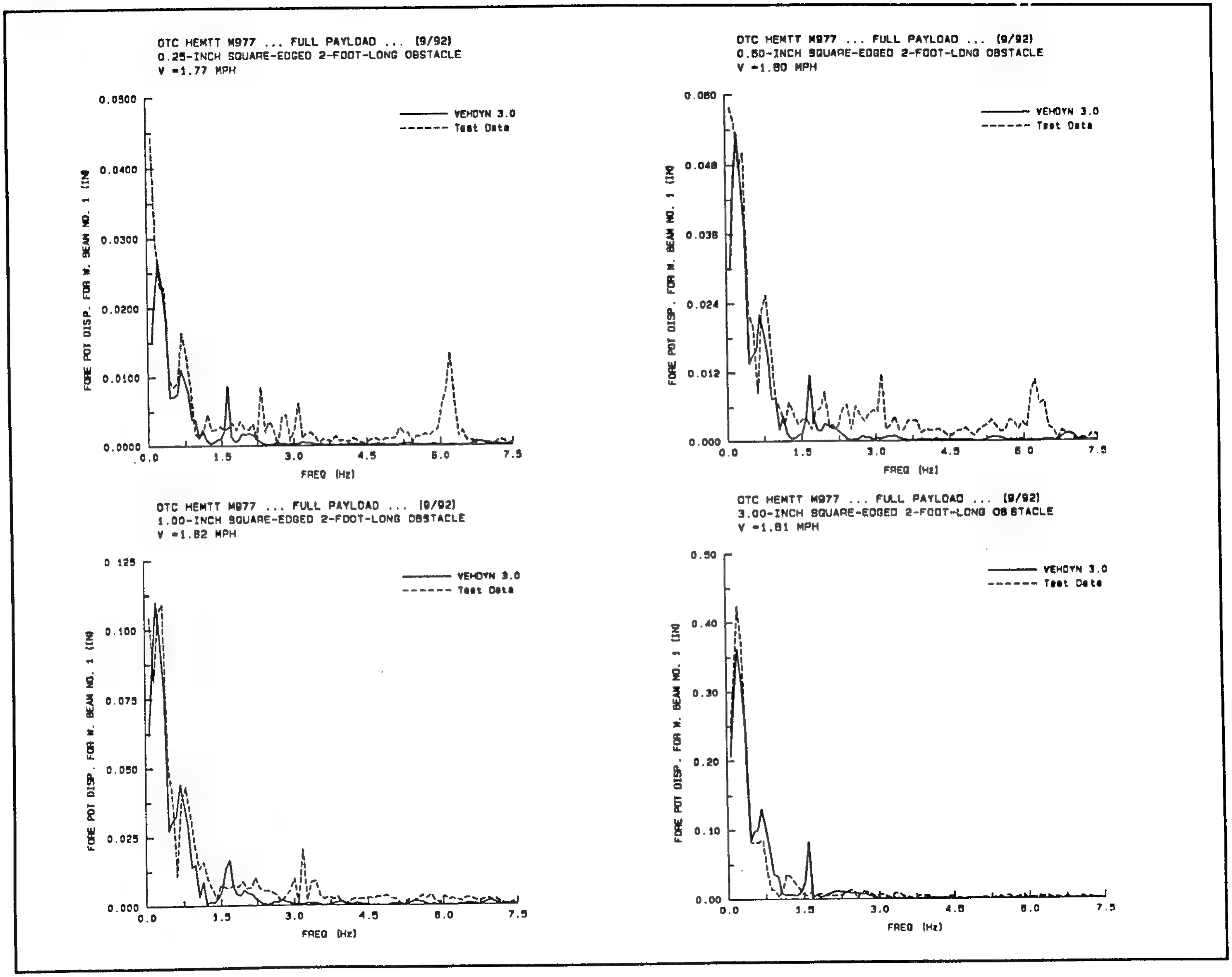

Figure A-8. Forward axle displacement relative to the frame frequency plots for a fully loaded HEMTT traveling at about 1.80 miles per hour encountering obstacles of heights 0.25, 0.50, 1.00, and 3.00 inches.

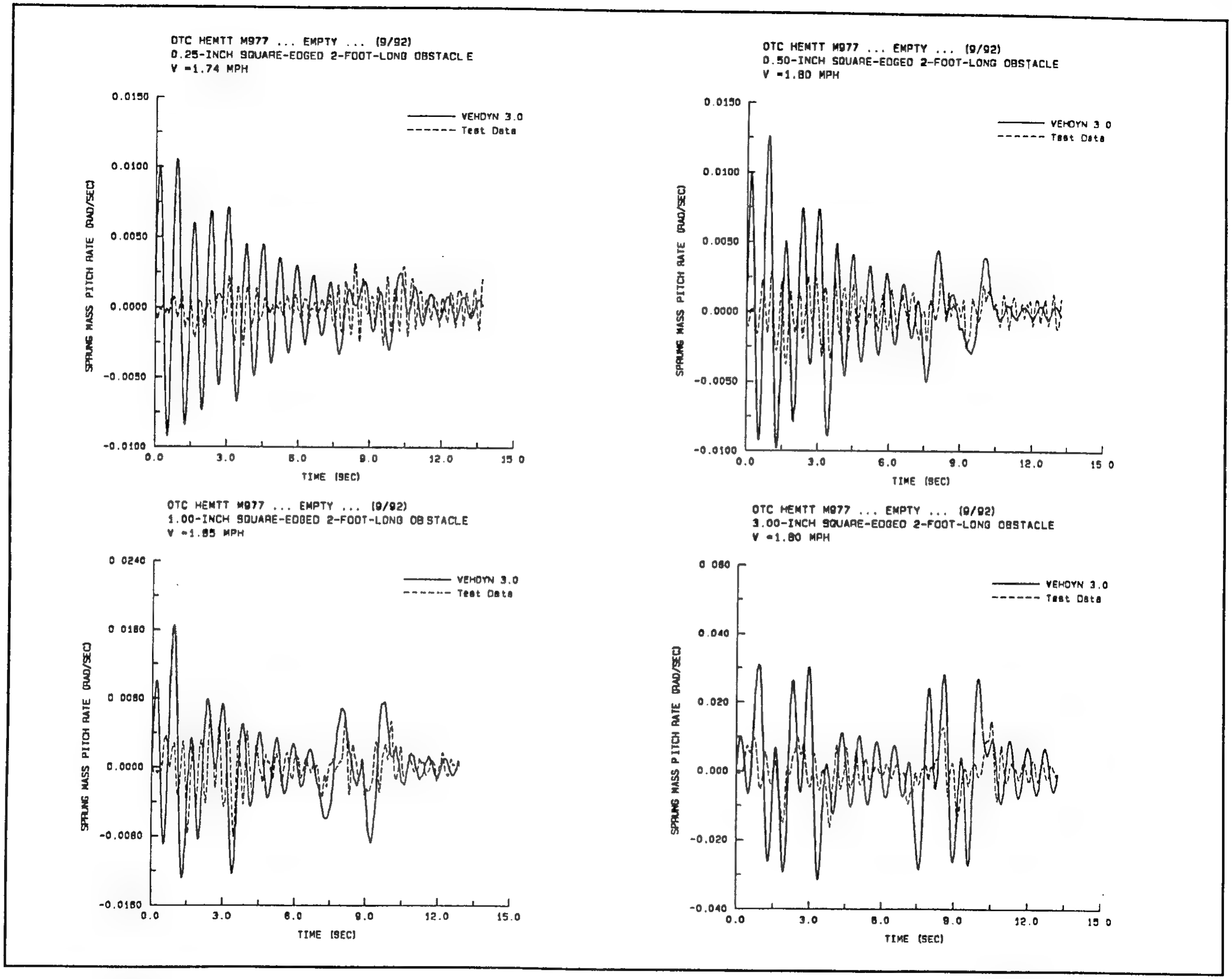

Figure A-9. Sprung mass pitch rate time histories for an empty HEMTT traveling at about 1.80 miles per hour encountering obstacles of heights 0.25, 0.50, 1.00, and 3.00 inches.

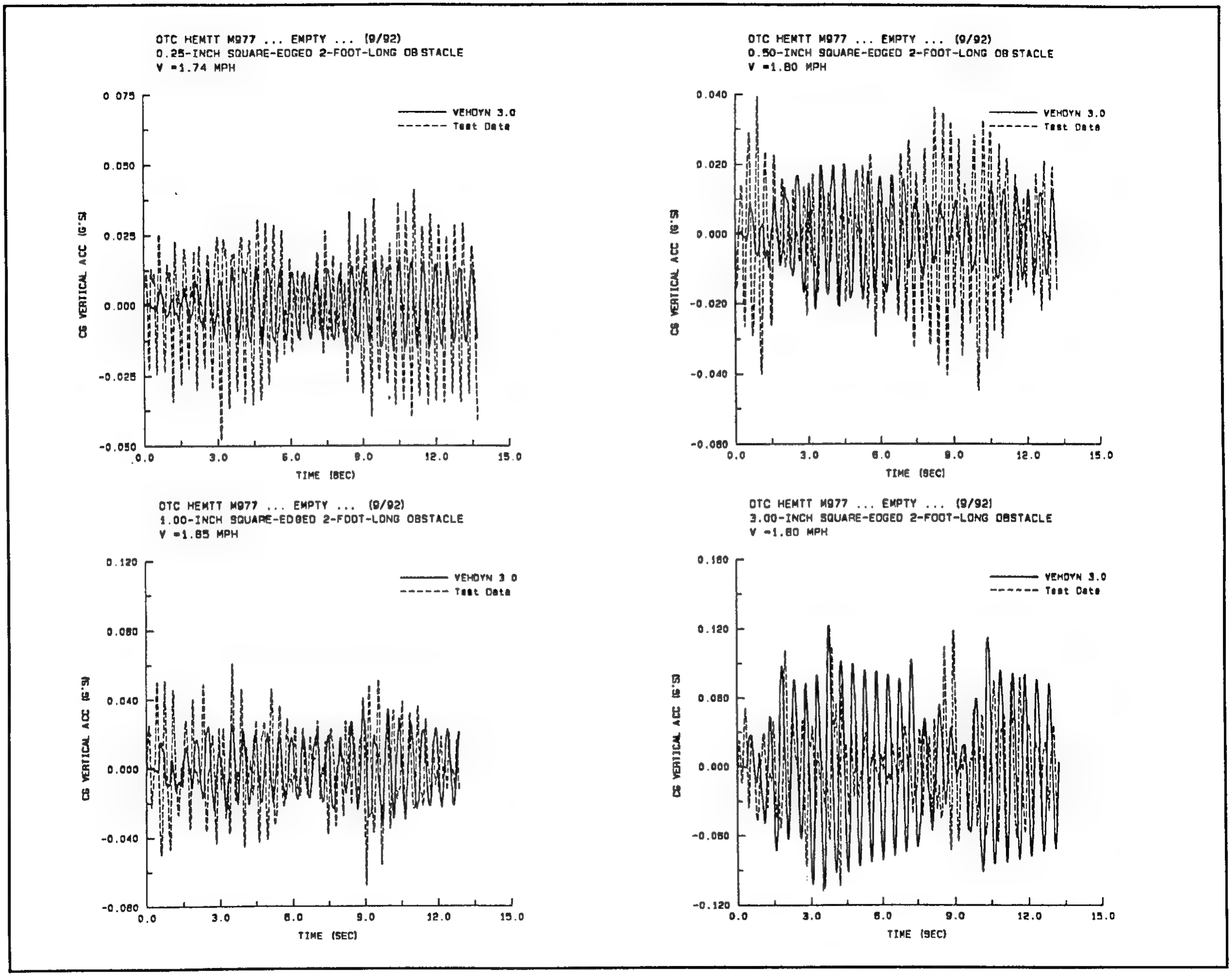

Figure A-10. CG vertical acceleration time histories for an empty HEMTT traveling at about 1.80 miles per hour encountering obstacles of heights 0.25, 0.50, 1.00, and 3.00 inches.

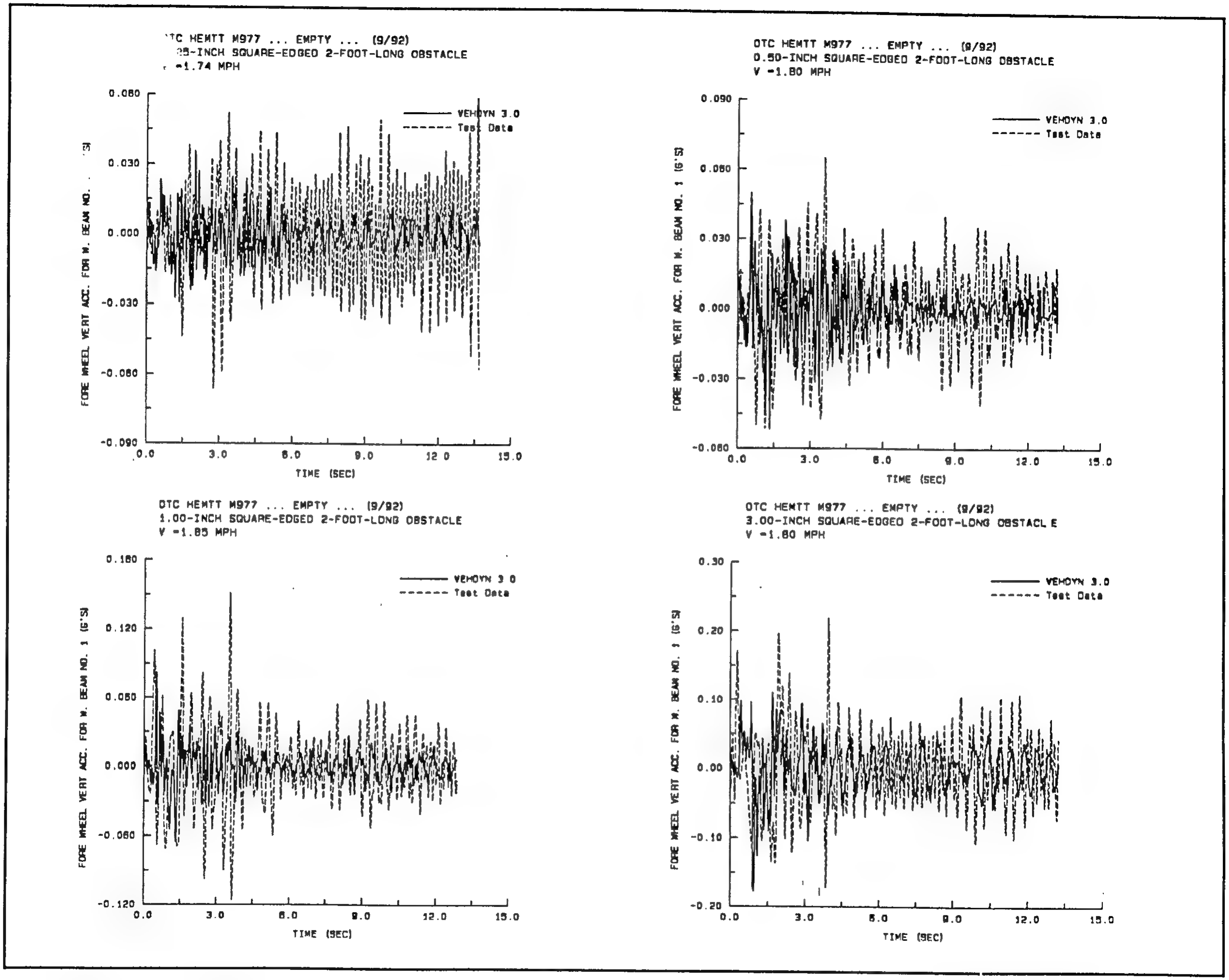

Figure A-11. Vertical acceleration of the forward-most axle time histories for an empty HEMTT traveling at about 1.80 miles per hour encountering obstacles of heights 0.25, 0.50, 1.00, and 3.00 inches.

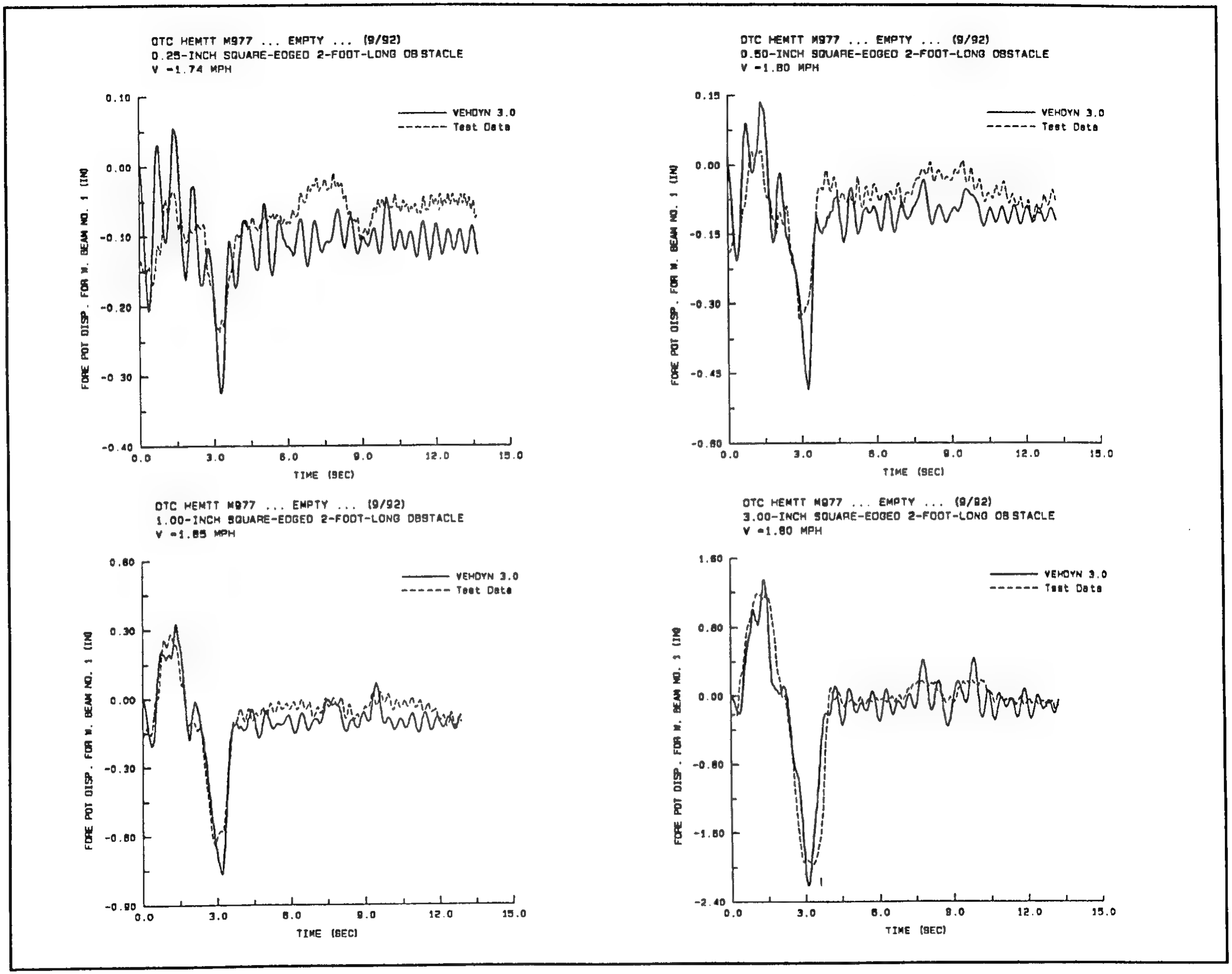

Figure A-12. Forward axle displacement relative to the frame time histories for an empty HEMTT traveling at about 1.80 miles per hour encountering obstacles of heights 0.25, 0.50, 1.00, and 3.00 inches.

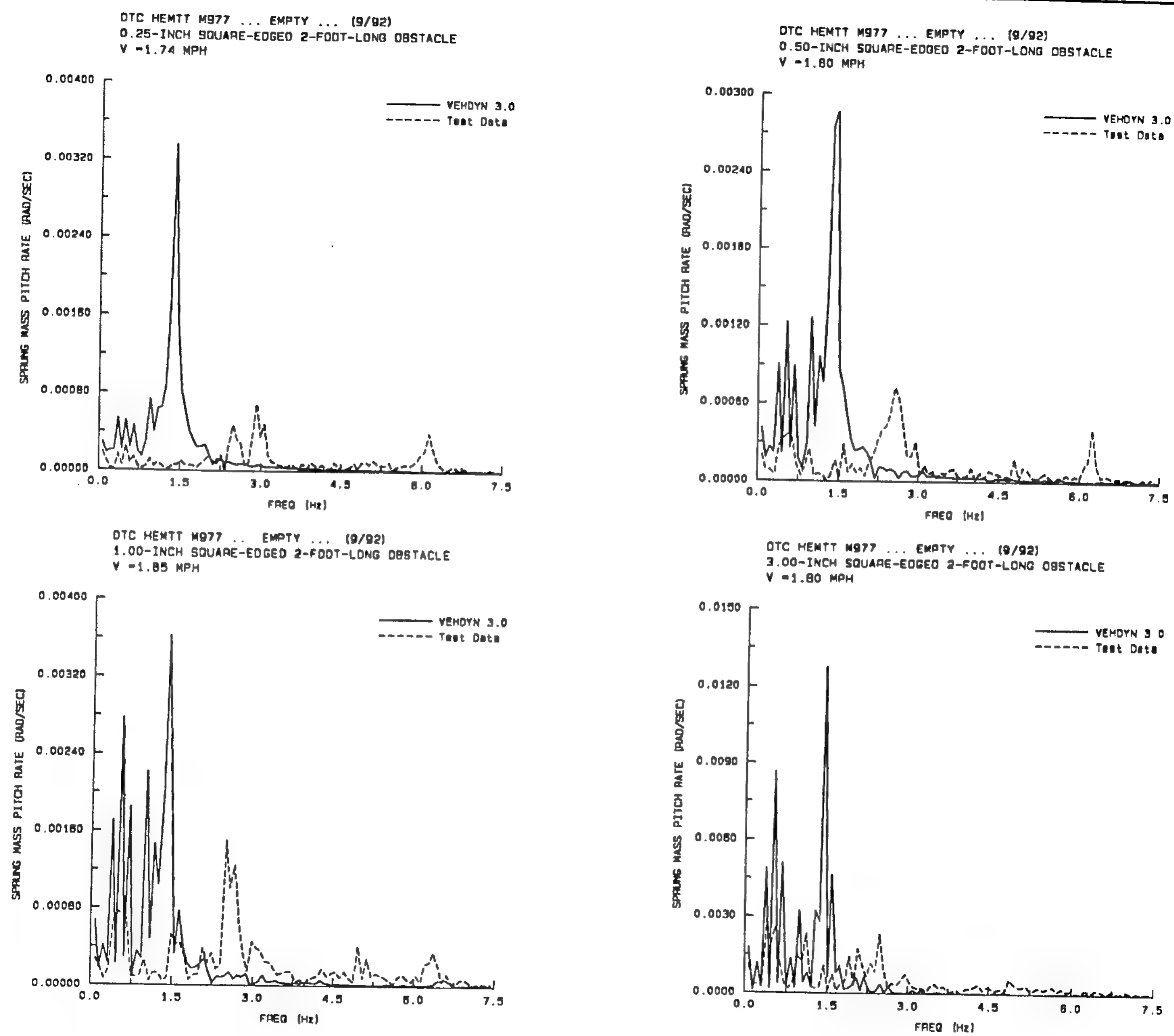

Figure A-13. Sprung mass pitch rate frequency plots for an empty HEMTT traveling at about 1.80 miles per hour encountering obstacles of heights 0.25, 0.50, 1.00, and 3.00 inches.

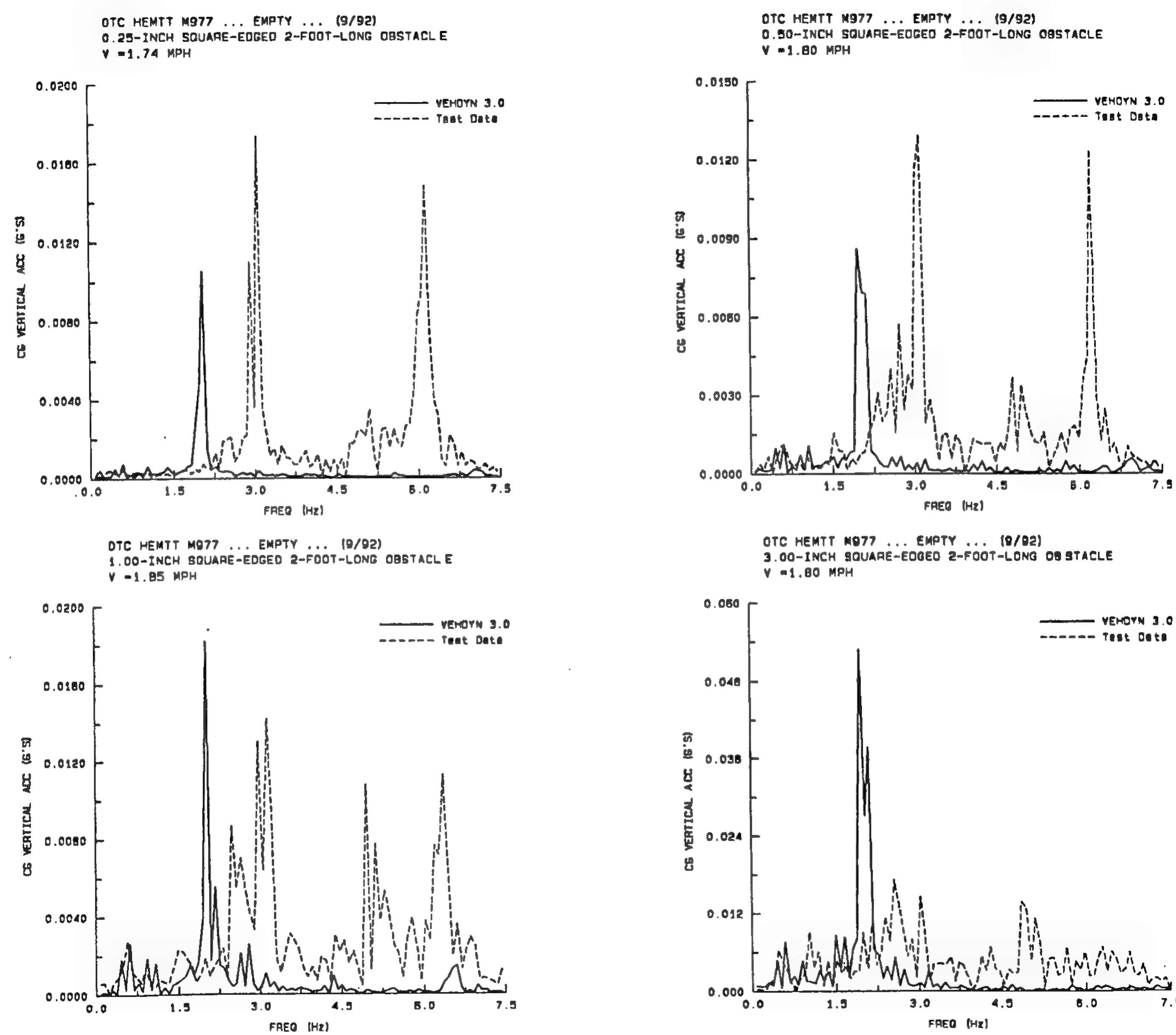

Figure A-14. CG vertical acceleration frequency plots for an empty HEMTT traveling at about 1.80 miles per hour encountering obstacles of heights 0.25, 0.50, 1.00, and 3.00 inches.

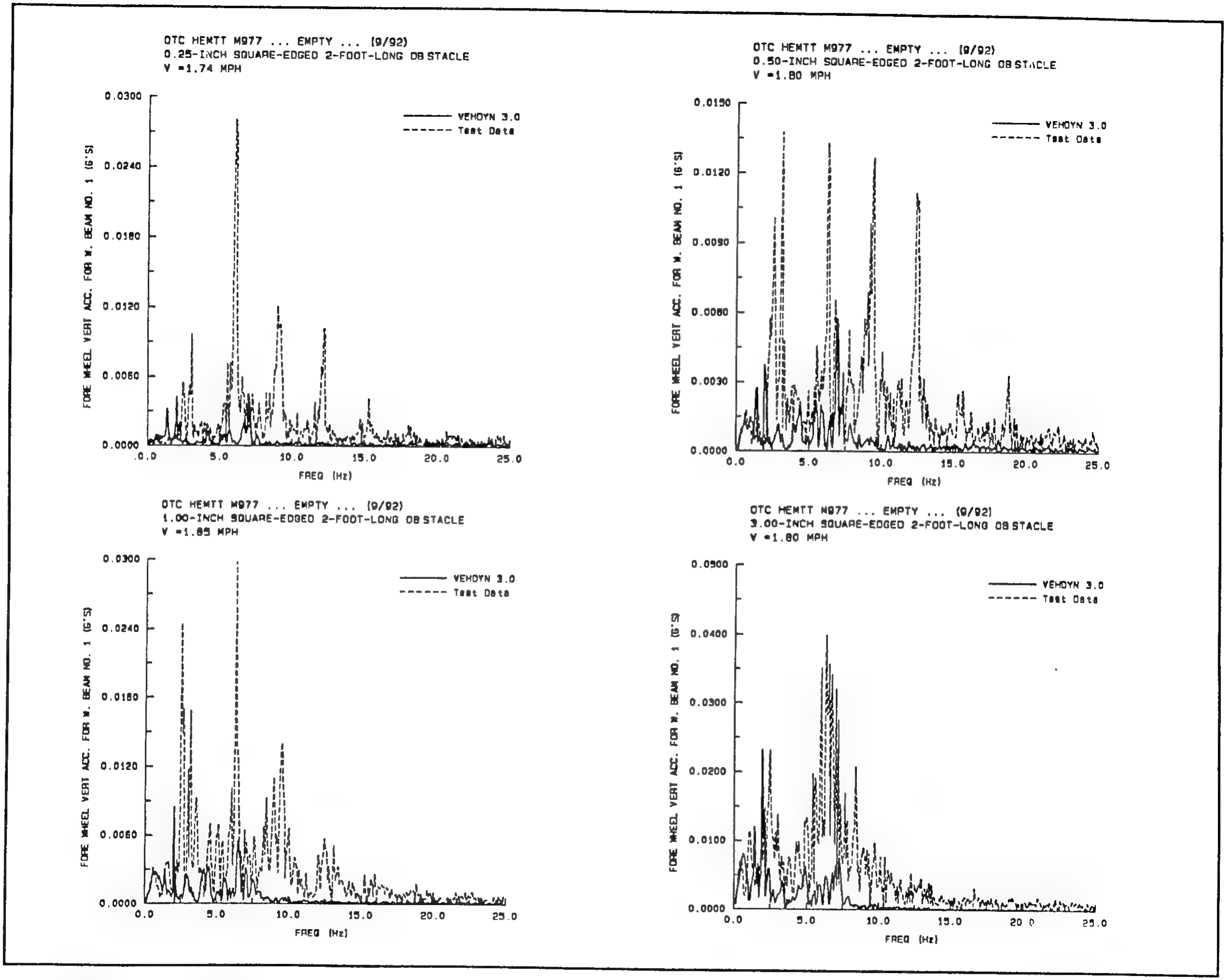

Figure A-15. Vertical acceleration of the forward-most axle frequency plots for an empty HEMTT traveling at about 1.80 miles per hour encountering obstacles of heights 0.25, 0.50, 1.00, and 3.00 inches.

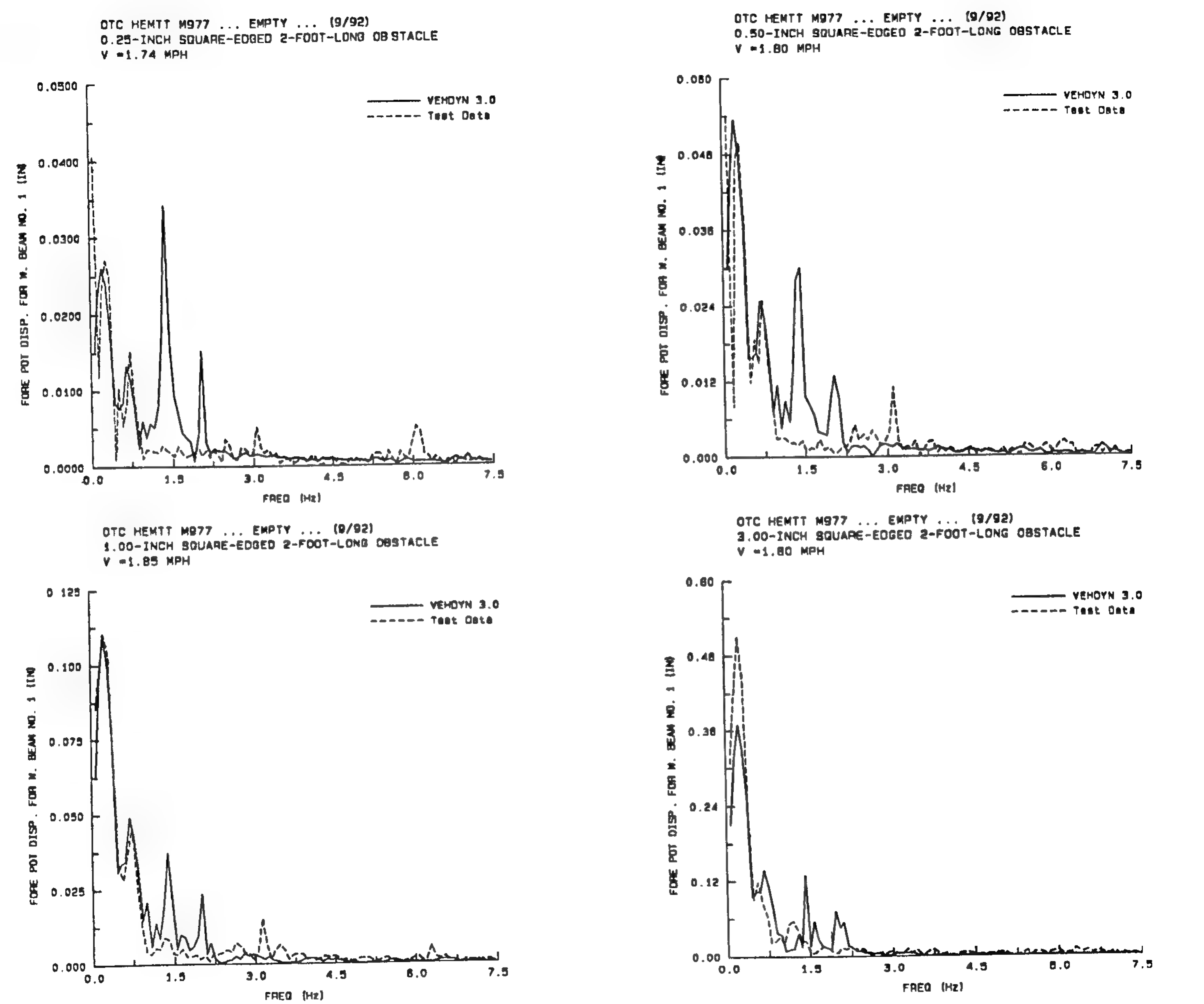

Figure A-16. Forward axle displacement relative to the frame frequency plots for an empty HEMTT traveling at about 1.80 miles per hour encountering obstacles of heights 0.25, 0.50, 1.00, and 3.00 inches.

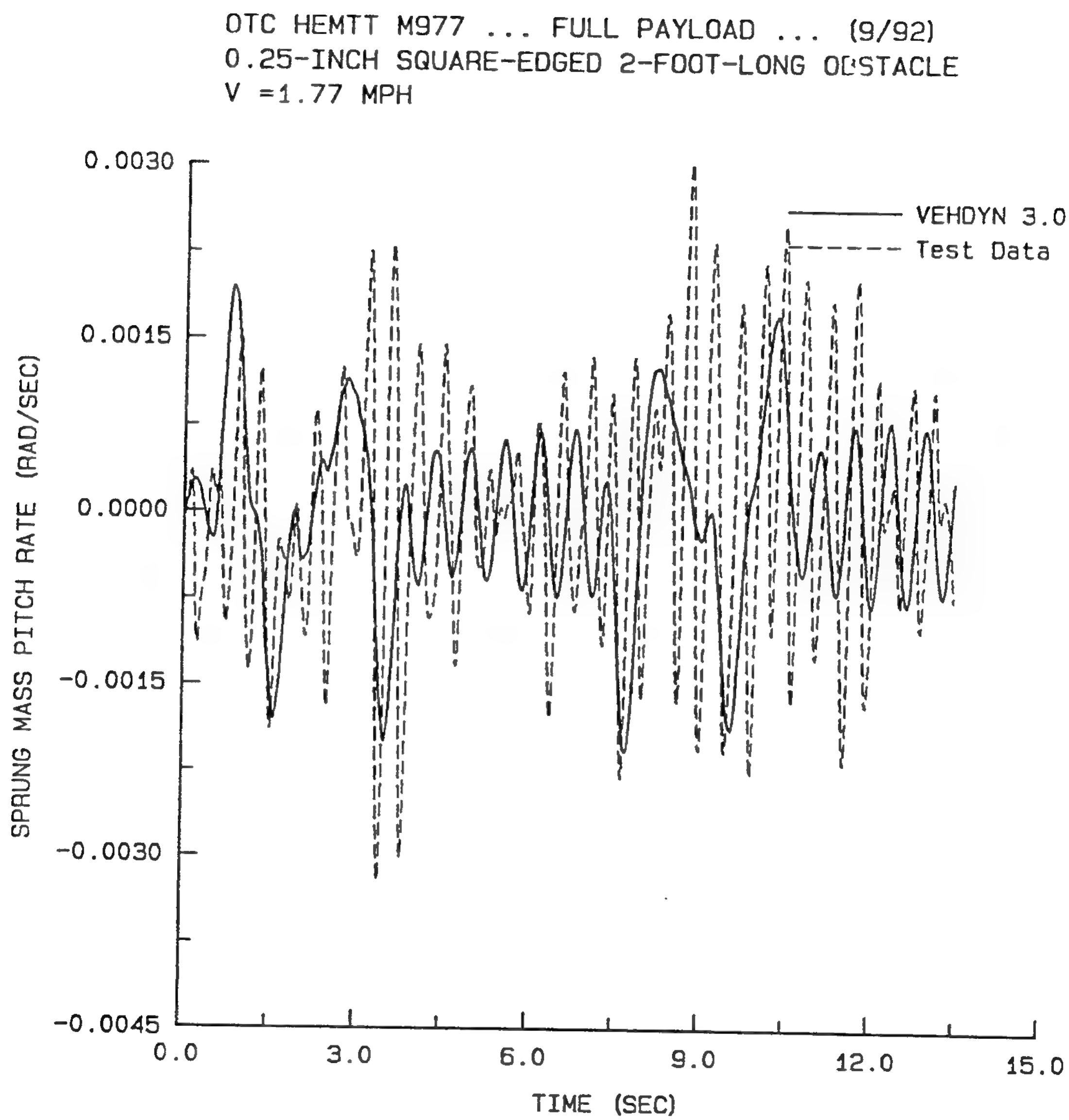

Figure A-17. Sprung mass pitch rate time history for a fully loaded HEMTT traveling at 1.77 miles per hour encountering a 0.25-inch-high obstacle.

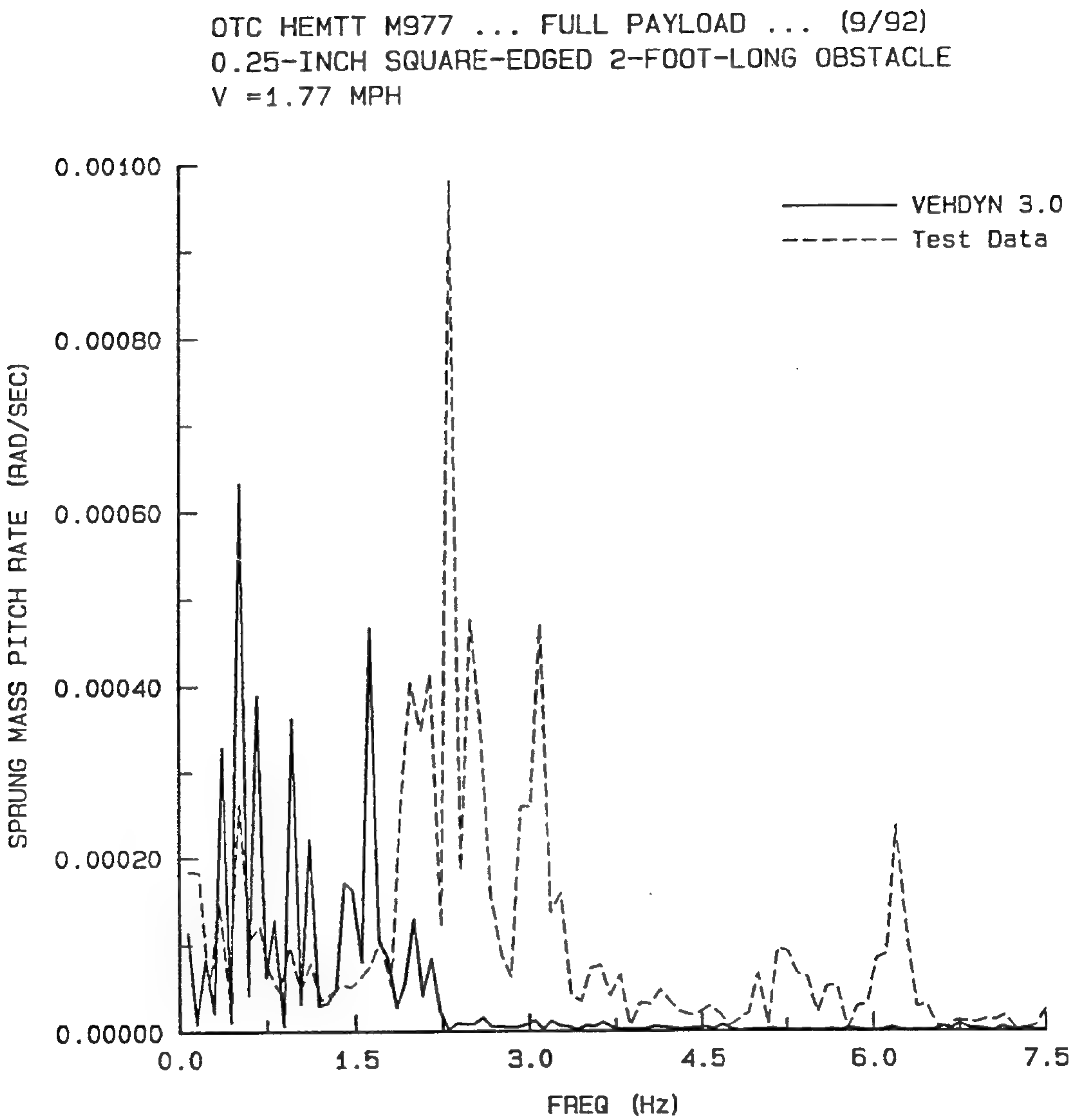

Figure A-18. Sprung mass pitch rate frequency plot for a fully loaded HEMTT traveling at 1.77 miles per hour encountering a 0.25-inch-high obstacle.

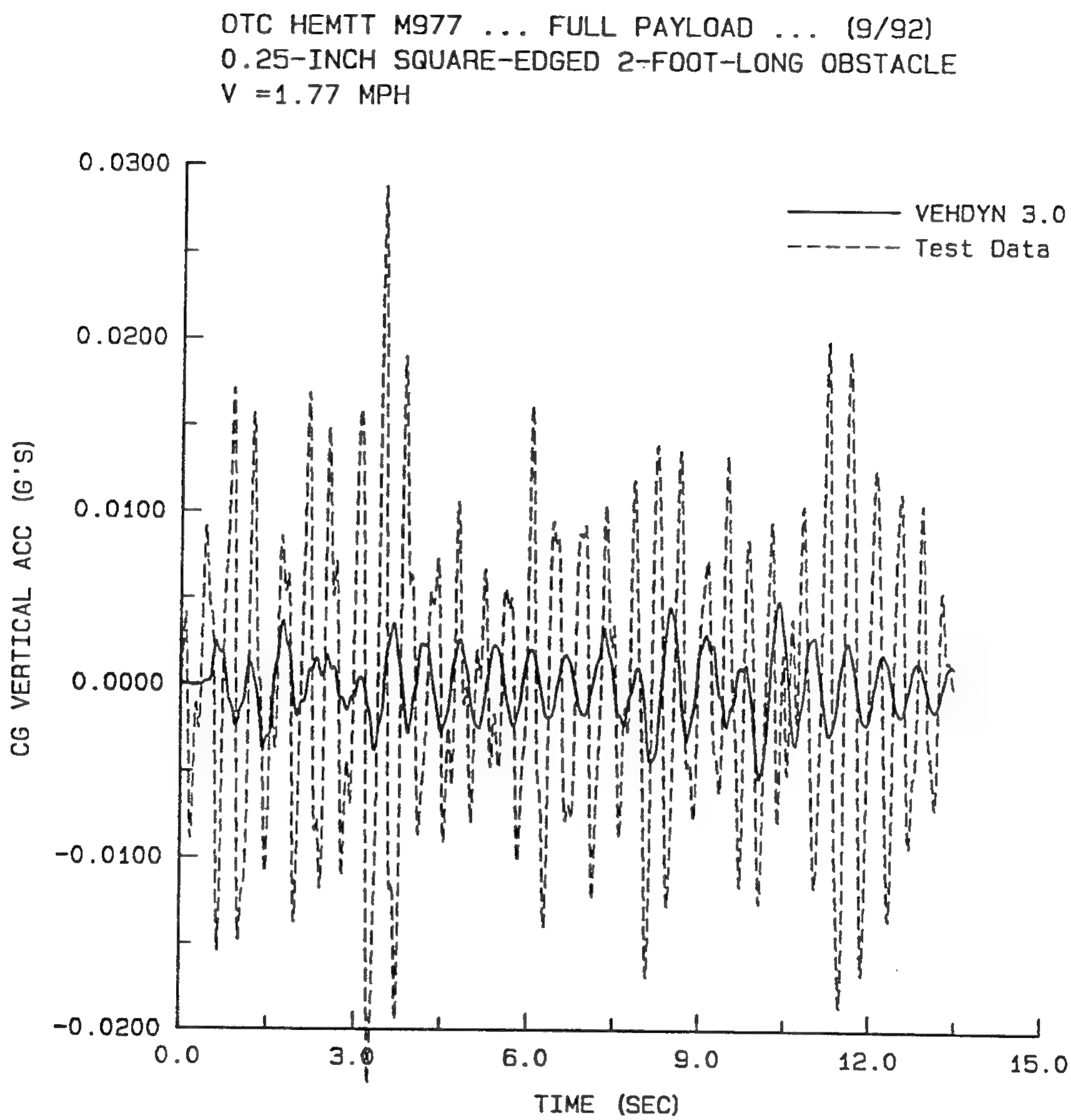

Figure A-19. CG vertical acceleration time history for a fully loaded HEMTT traveling at 1.77 miles per hour encountering a 0.25-inch-high obstacle.

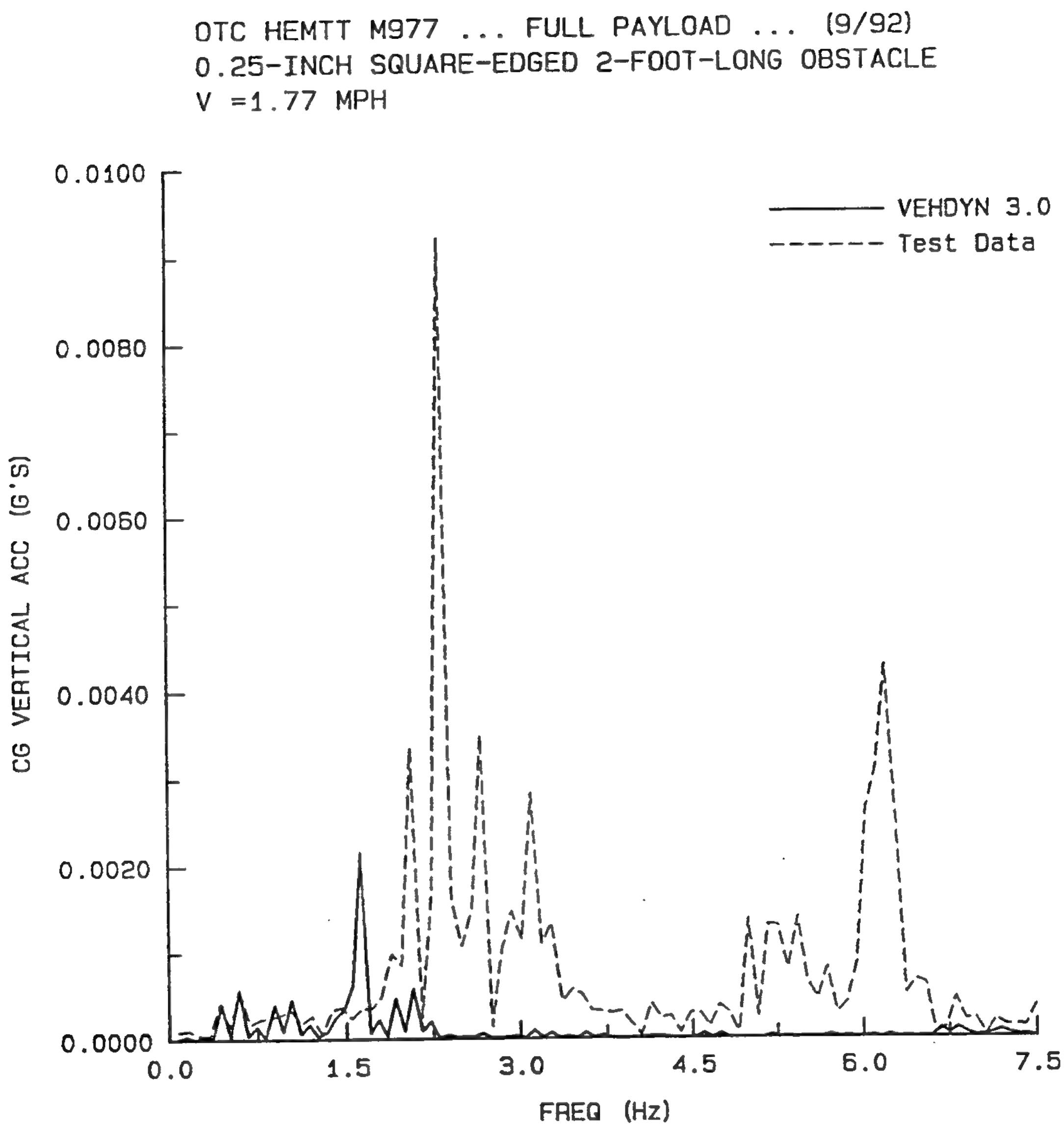

Figure A-20. CG vertical acceleration frequency plot (frequency scale = 1.5 Hz/inch) for a fully loaded HEMTT traveling at 1.77 miles per hour encountering a 0.25-inch-high obstacle.

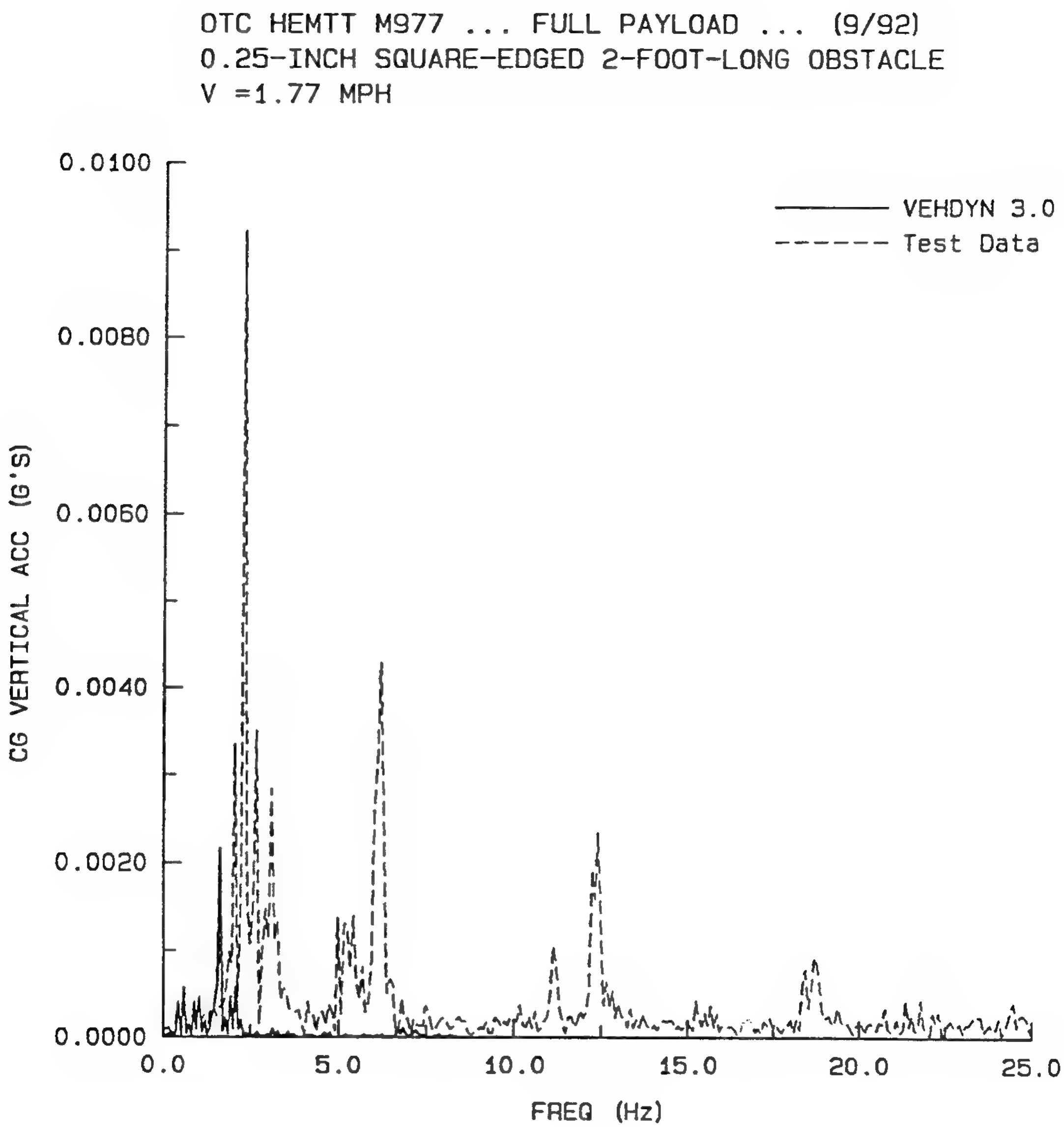

Figure A-21. CG vertical acceleration frequency plot (frequency scale = 5.0 Hz/inch) for a fully loaded HEMTT traveling at 1.77 miles per hour encountering a 0.25-inch-high obstacle.

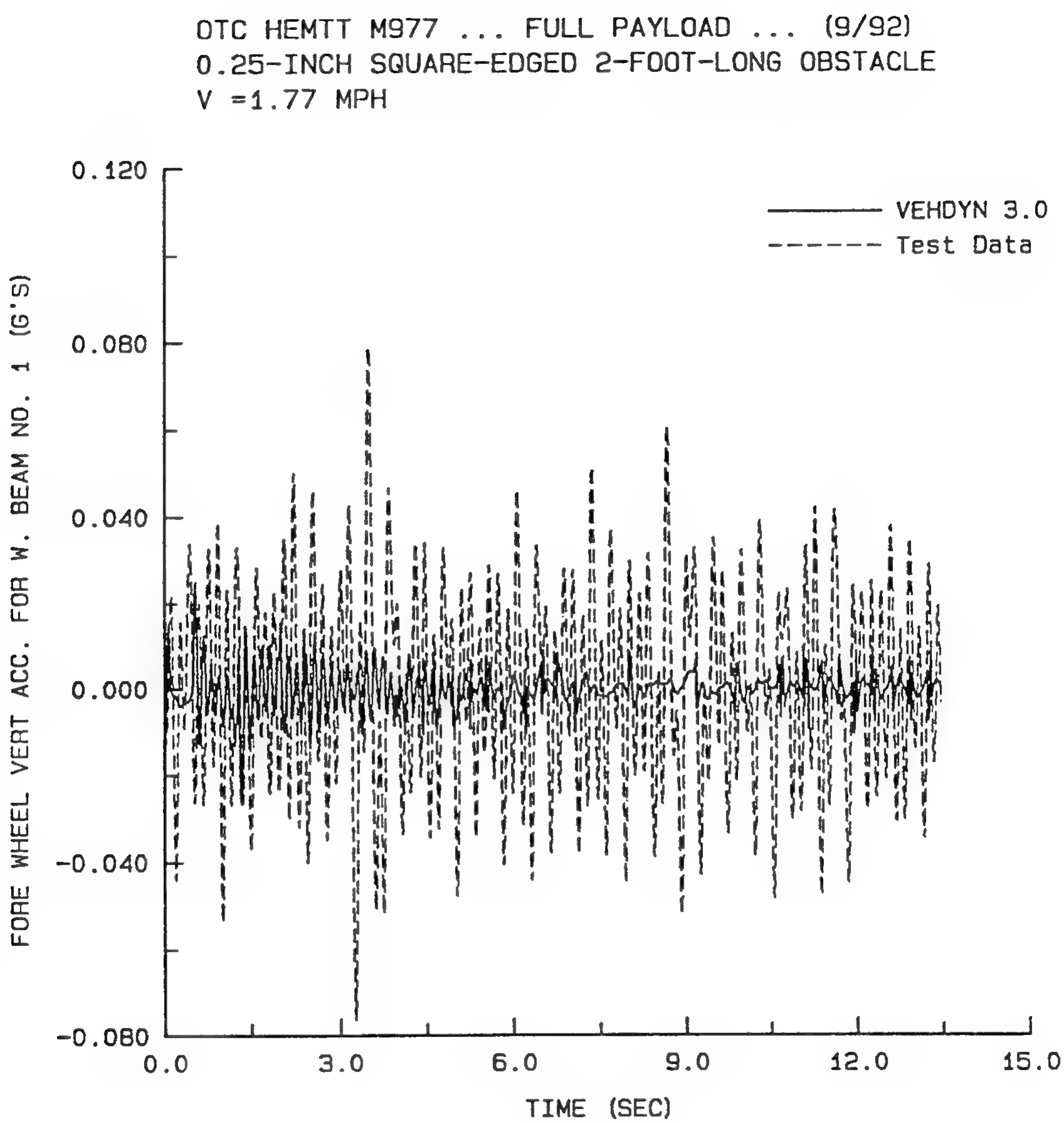

Figure A-22. Vertical acceleration time history of the forward-most axle for a fully loaded HEMTT traveling at 1.77 miles per hour encountering a 0.25-inch-high obstacle.

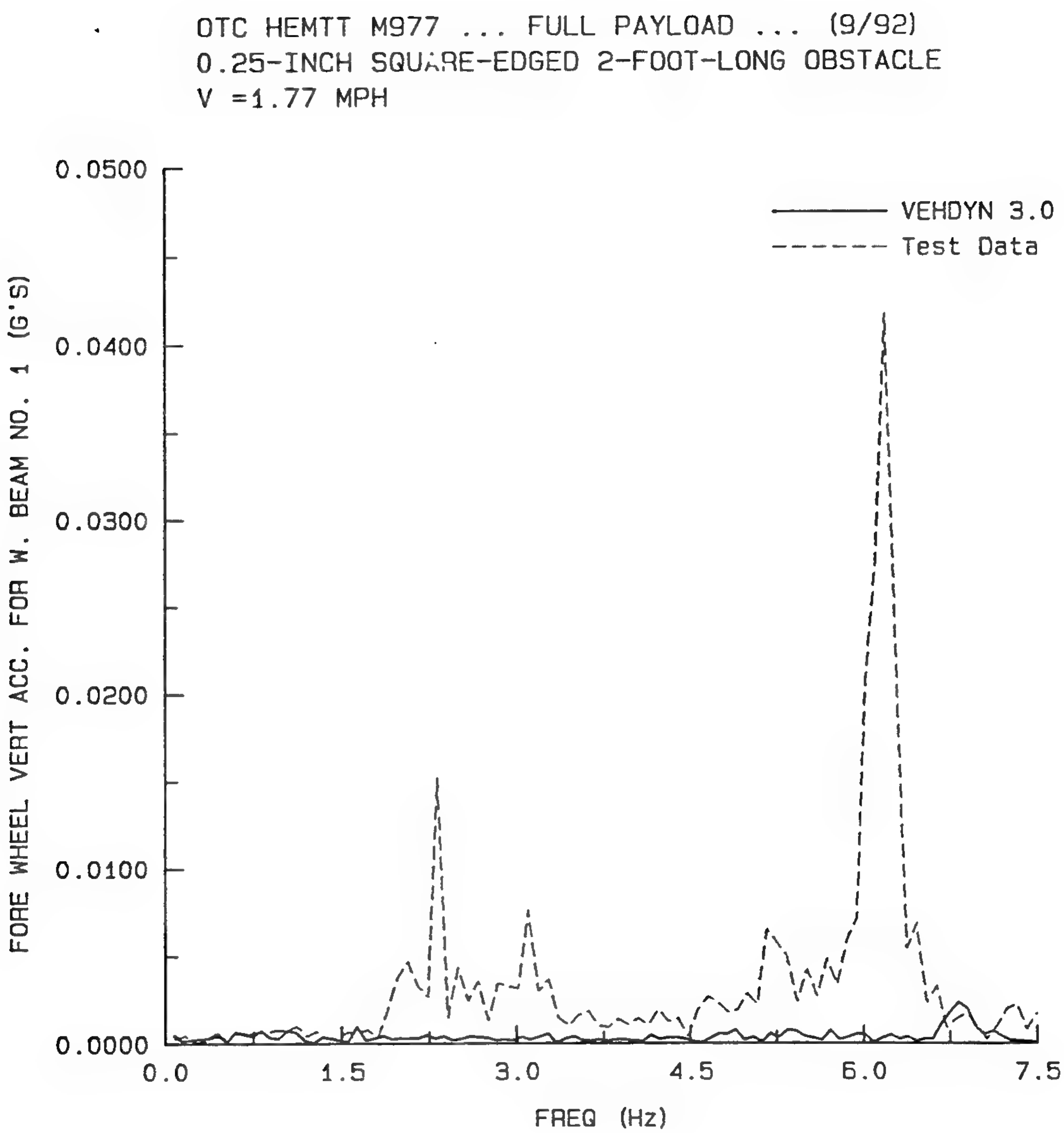

Figure A-23. Vertical acceleration frequency plot (frequency scale = 1.5 Hz/inch) of the forward-most axle for a fully loaded HEMTT traveling at 1.77 miles per hour encountering a 0.25-inch-high obstacle.

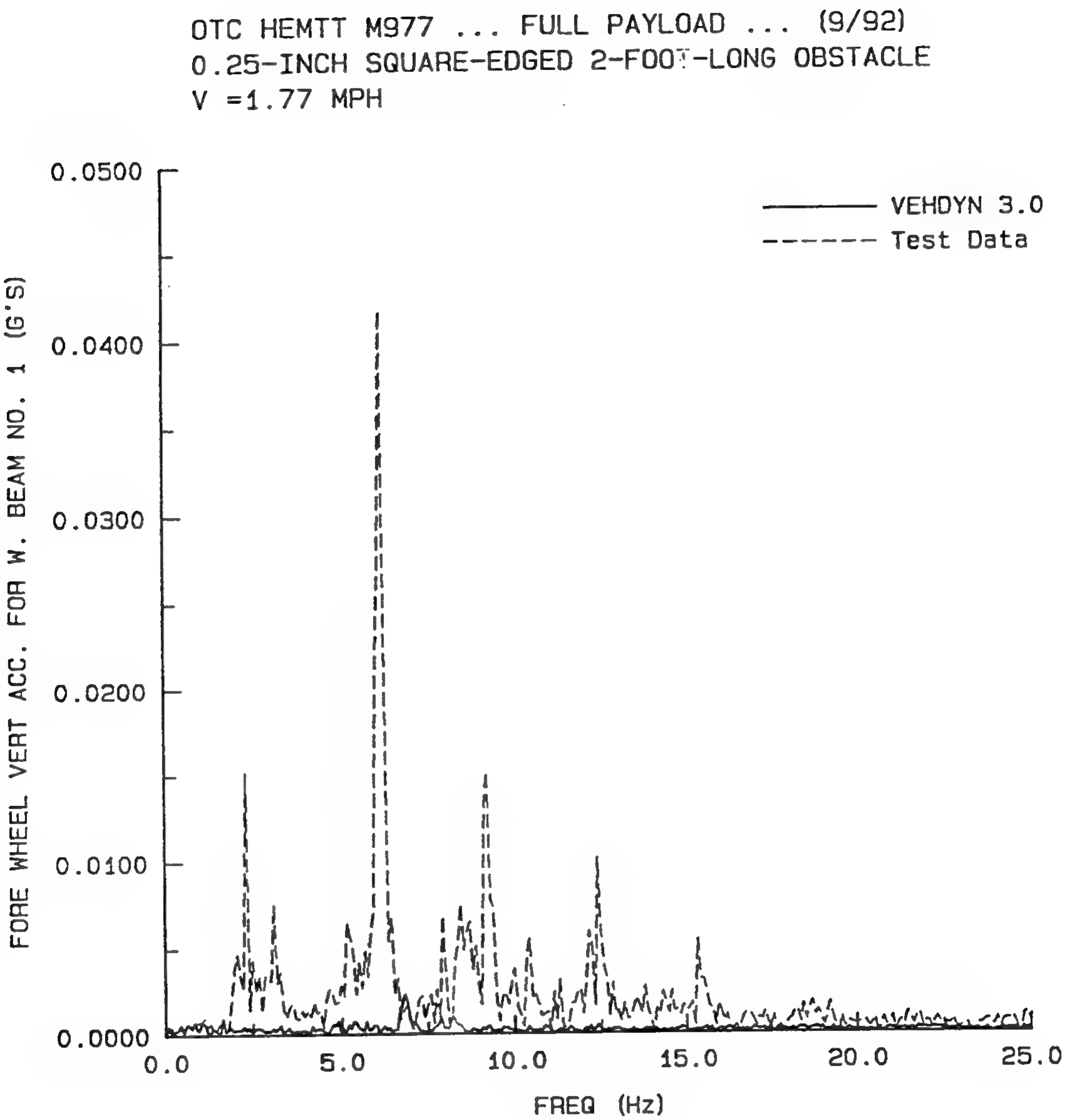

Figure A-24. Vertical acceleration frequency plot (frequency scale = 5.0 Hz/inch) of the forward-most axle for a fully loaded HEMTT traveling at 1.77 miles per hour encountering a 0.25-inch-high obstacle.

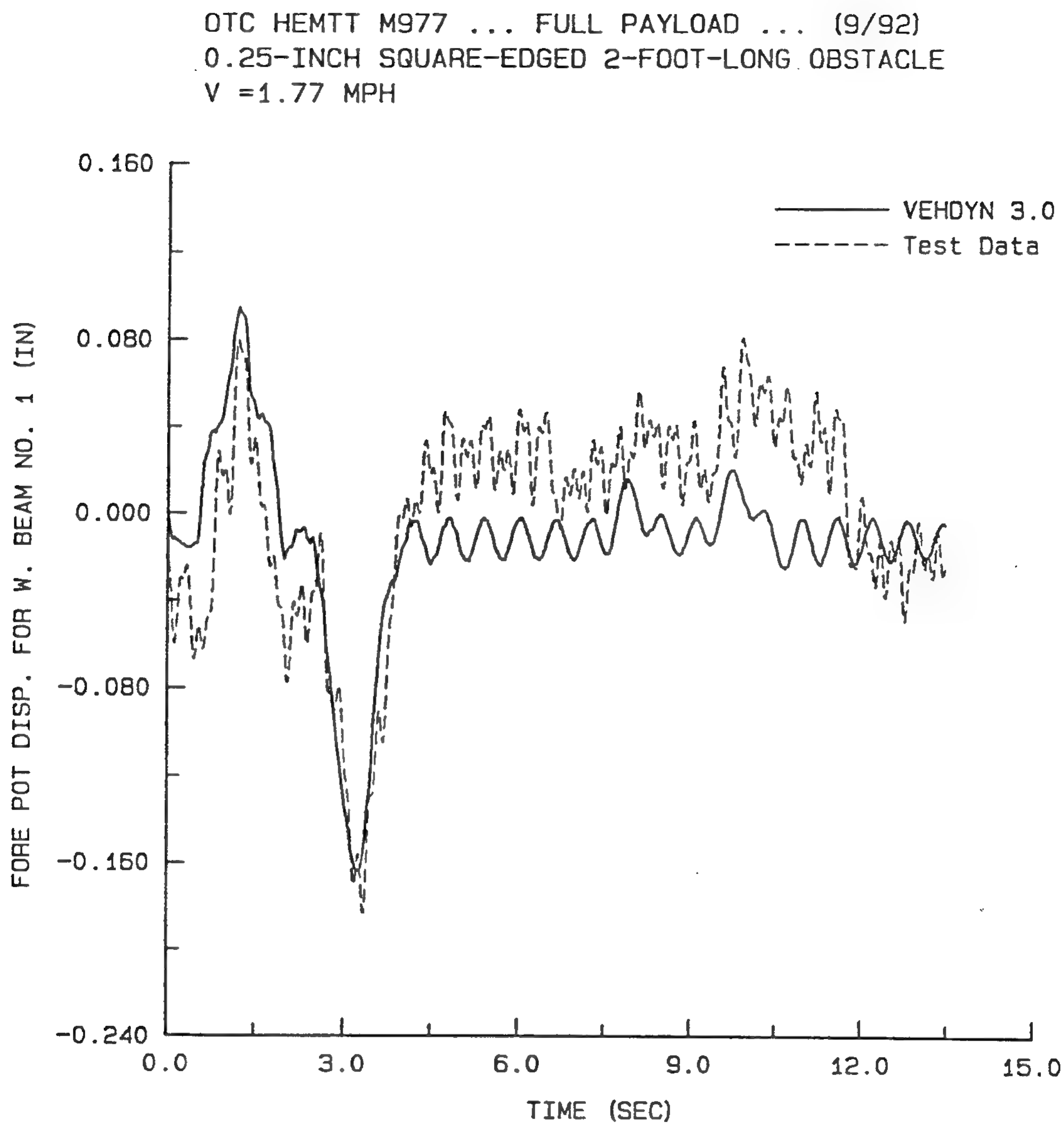

Figure A-25. Relative displacement time history of the forward-most axle with respect to the frame for a fully loaded HEMTT traveling at 1.77 miles per hour encountering a 0.25-inch-high obstacle.

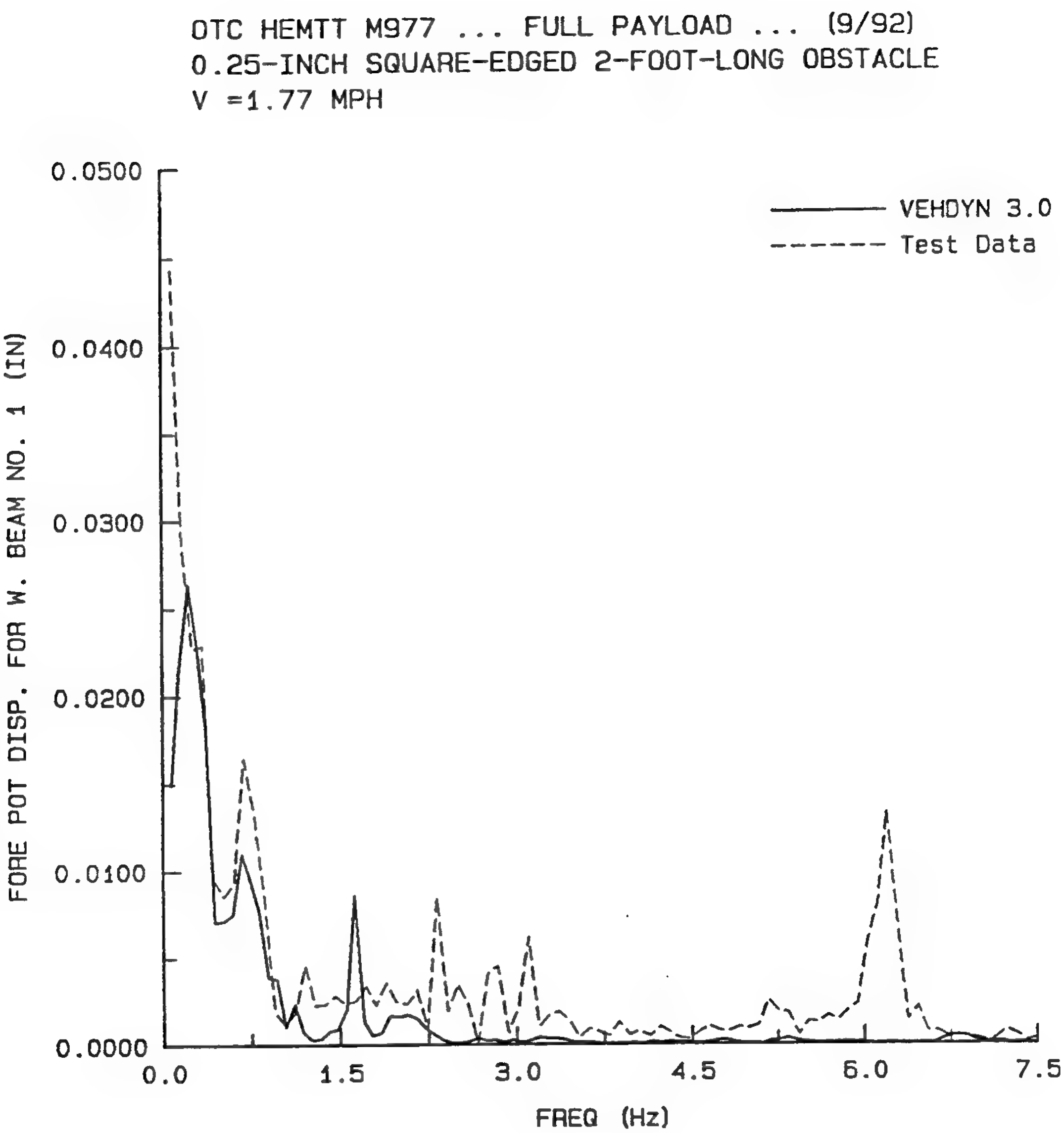

Figure A-26. Relative displacement frequency plot (frequency scale = 1.5 Hz/inch) of the forward-most axle with respect to the frame for a fully loaded HEMTT traveling at 1.77 miles per hour encountering a 0.25-inch-high obstacle.

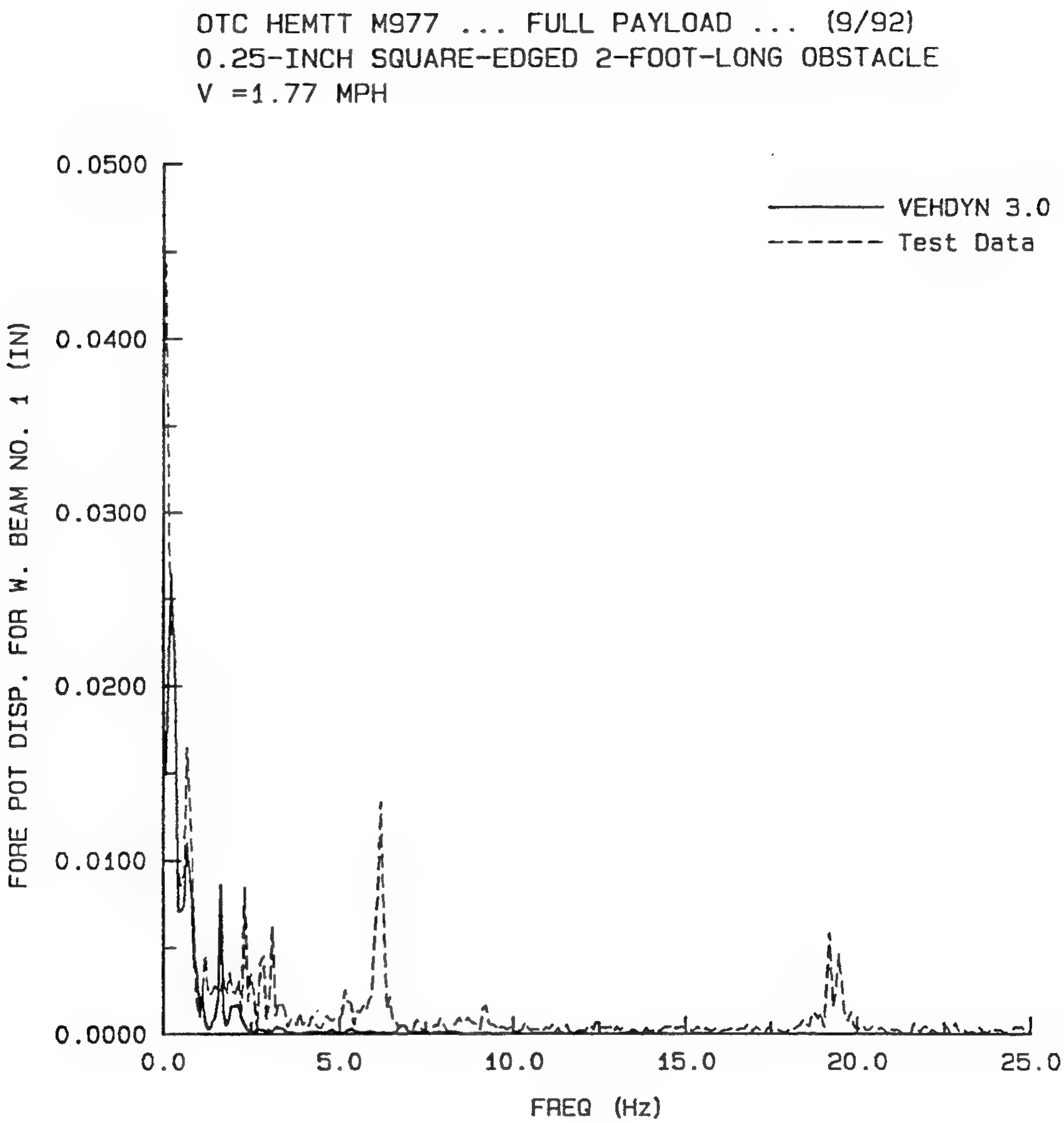

Figure A-27. Relative displacement frequency plot (frequency scale = 5.0 Hz/inch) of the forward-most axle with respect to the frame for a fully loaded HEMTT traveling at 1.77 miles per hour encountering a 0.25-inch-high obstacle.

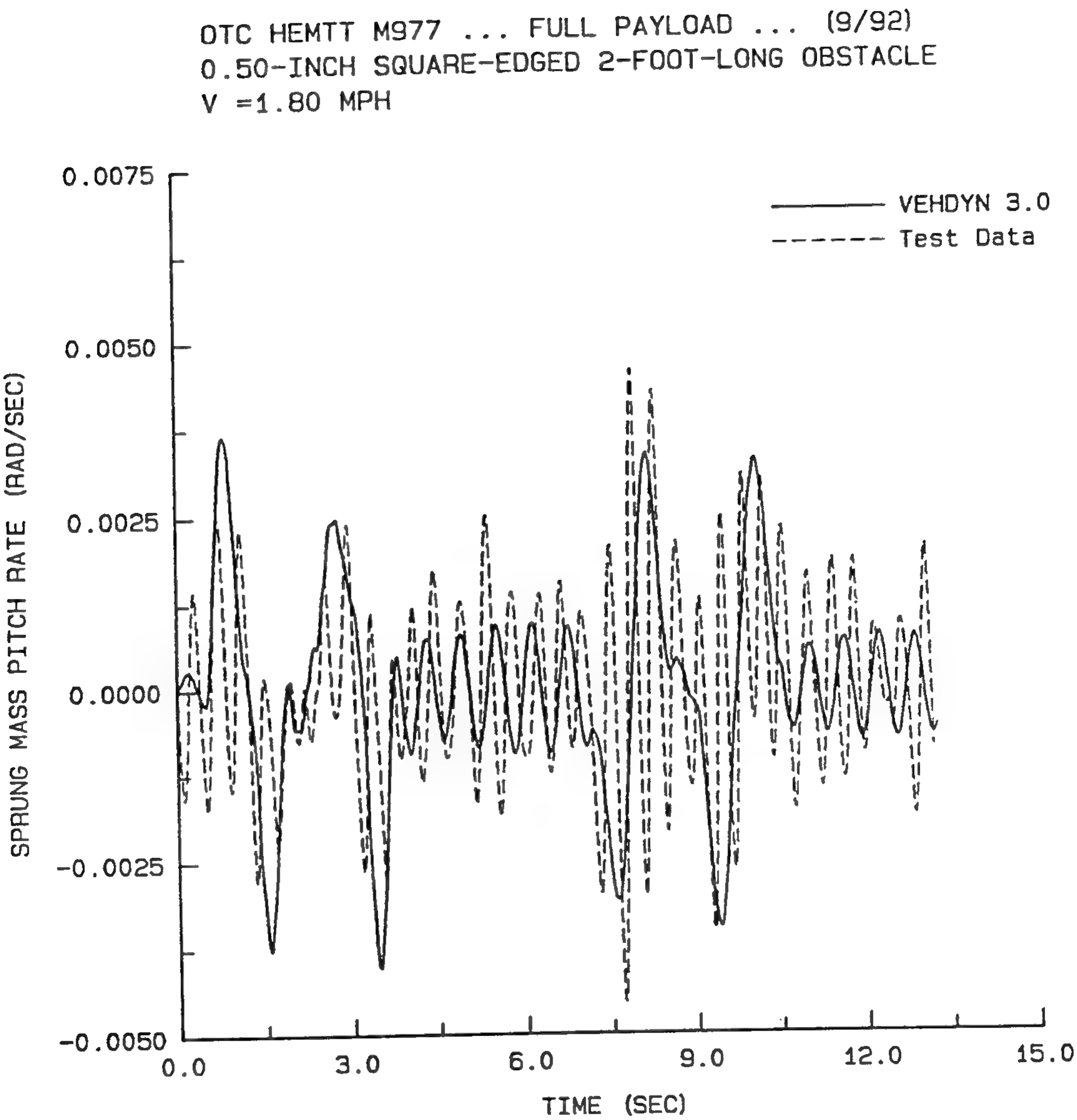

Figure A-28. Sprung mass pitch rate time history for a fully loaded HEMTT traveling at 1.80 miles per hour encountering a 0.50-inch-high obstacle.

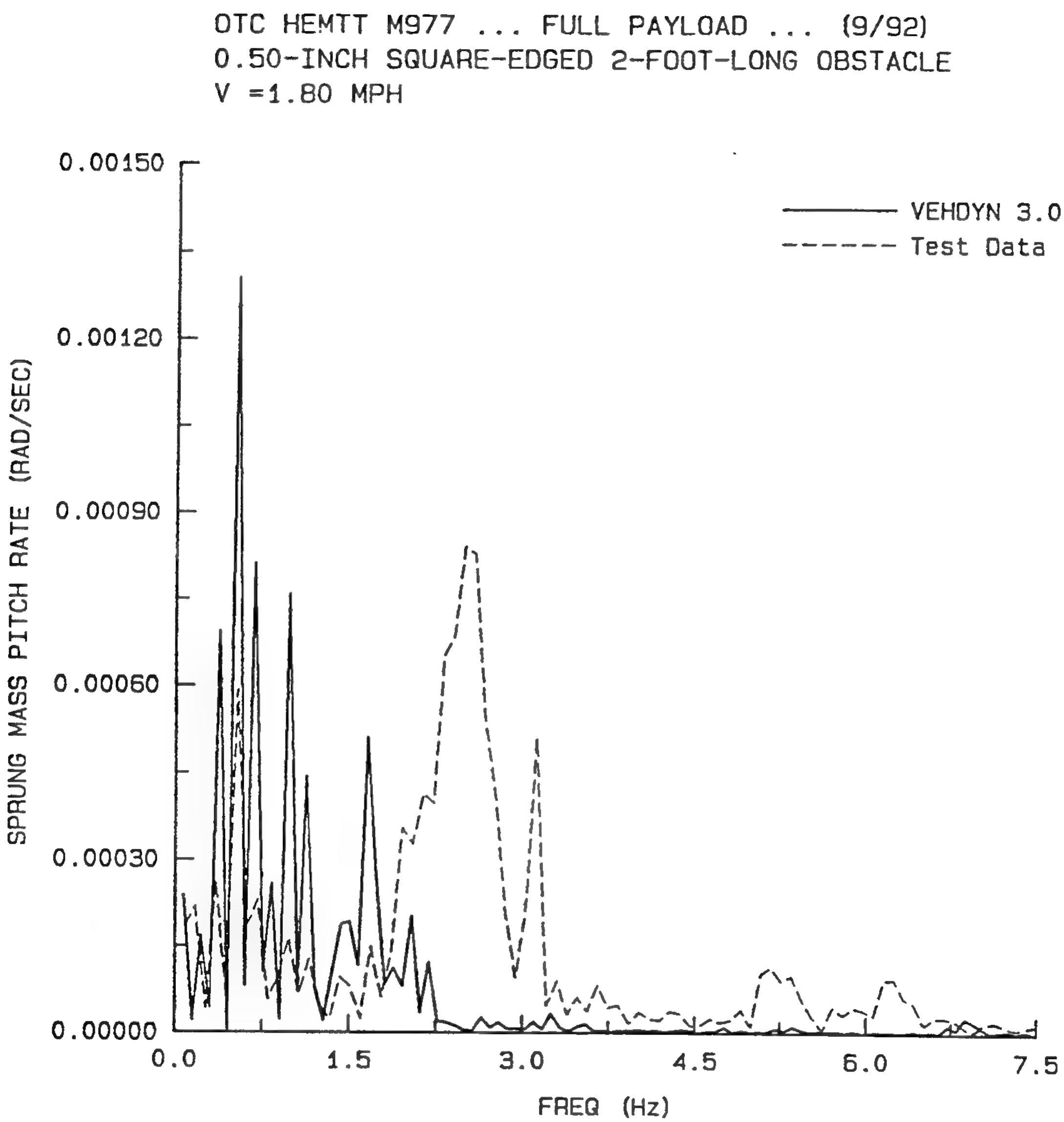

Figure A-29. Sprung mass pitch rate frequency plot for a fully loaded HEMTT traveling at 1.80 miles per hour encountering a 0.50-inch-high obstacle.

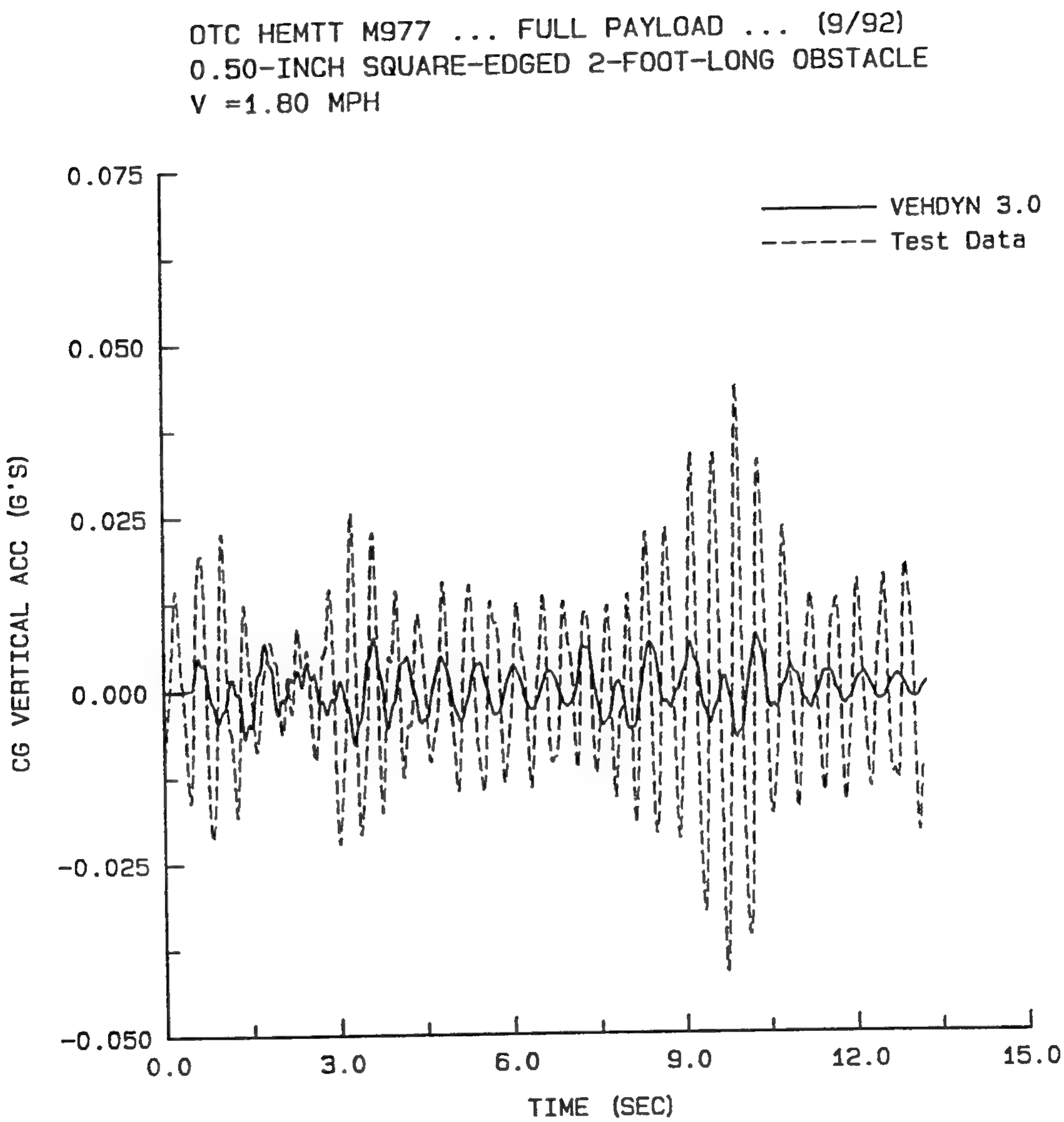

Figure A-30. CG vertical acceleration time history for a fully loaded HEMTT traveling at 1.80 miles per hour encountering a 0.50-inch-high obstacle.

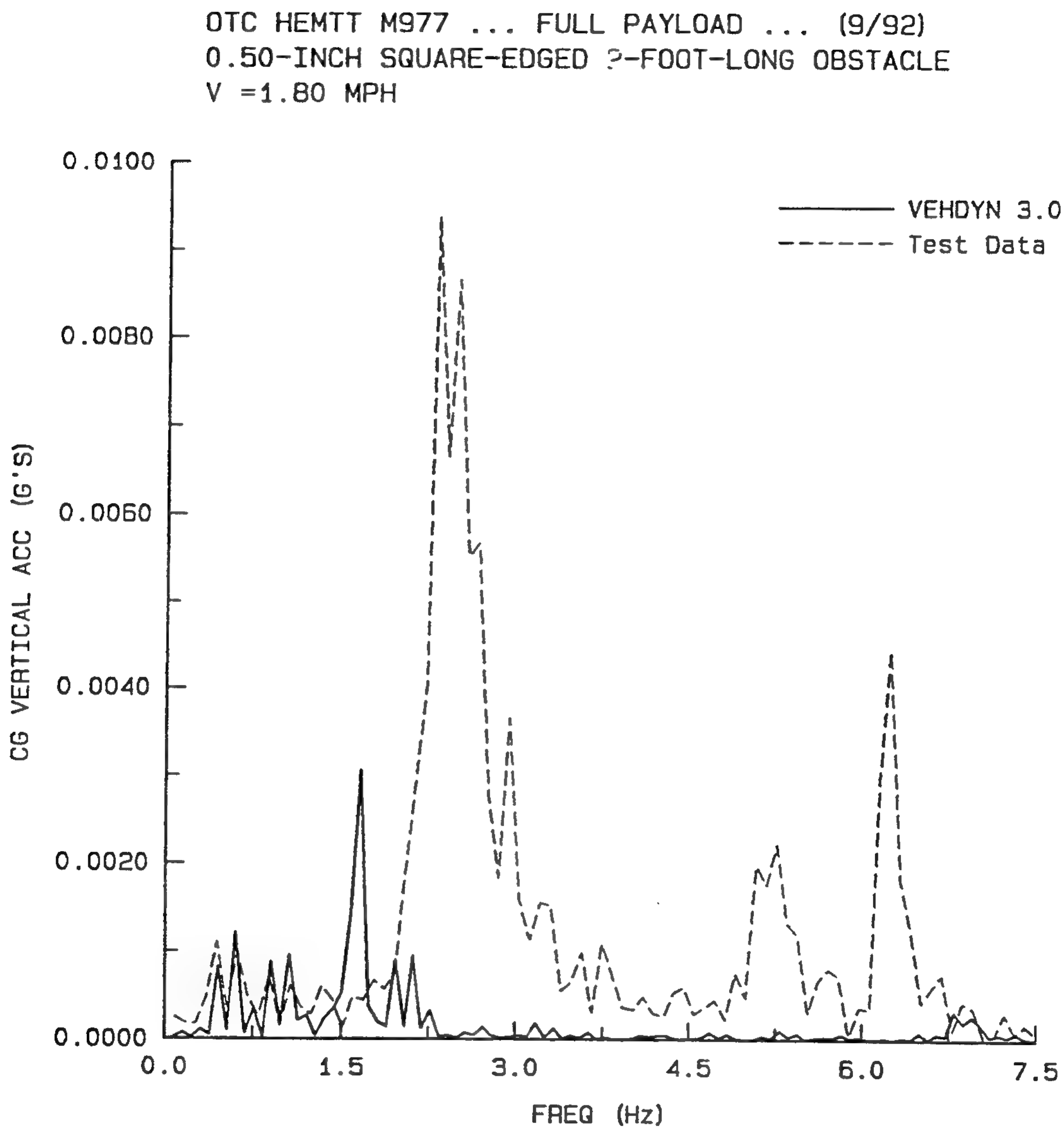

Figure A-31. CG vertical acceleration frequency plot (frequency scale = 1.5 Hz/inch) for a fully loaded HEMTT traveling at 1.80 miles per hour encountering a 0.50-inch-high obstacle.

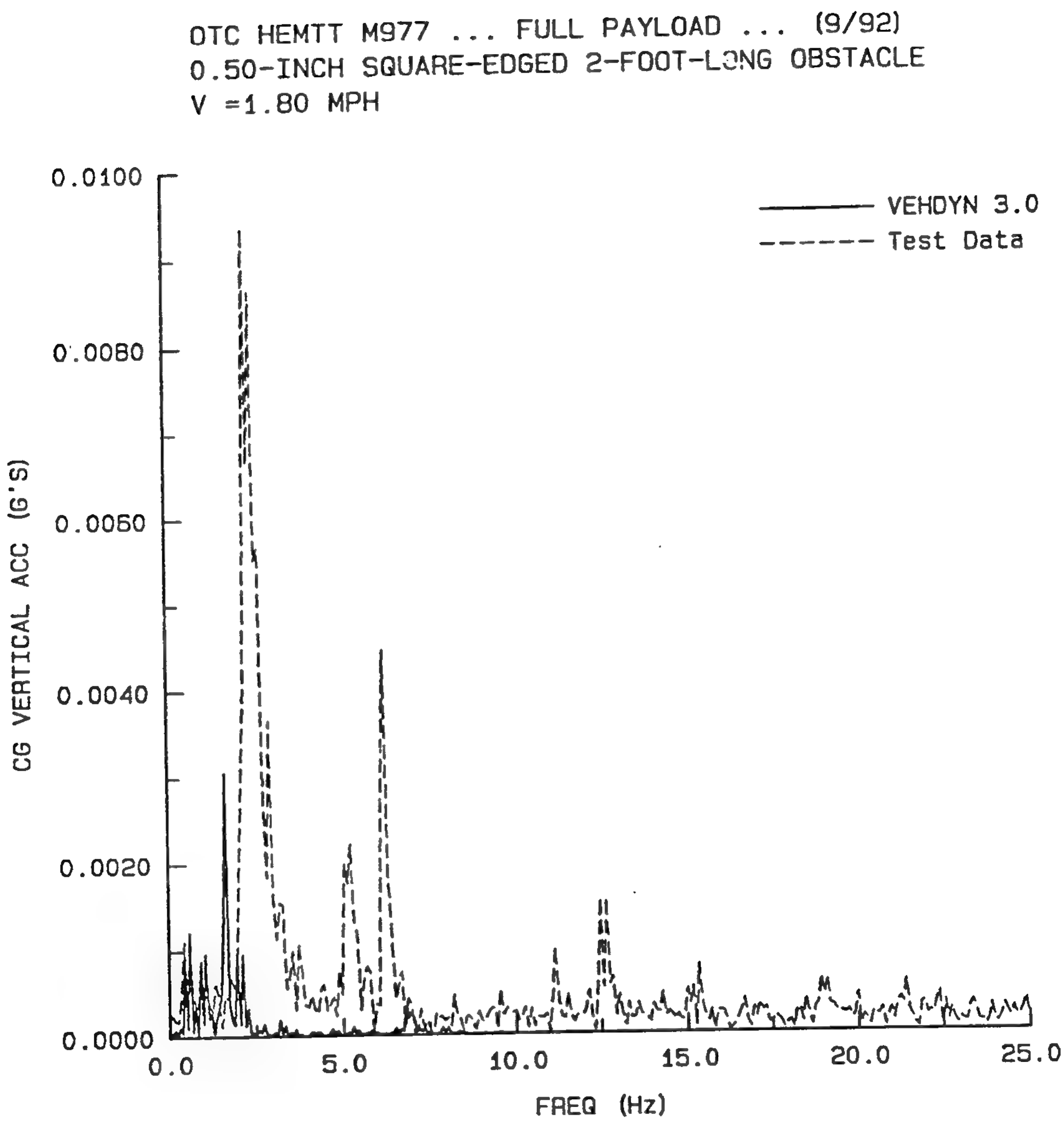

Figure A-32. CG vertical acceleration frequency plot (frequency scale = 5.0 Hz/inch) for a fully loaded HEMTT traveling at 1.80 miles per hour encountering a 0.50-inch-high obstacle.

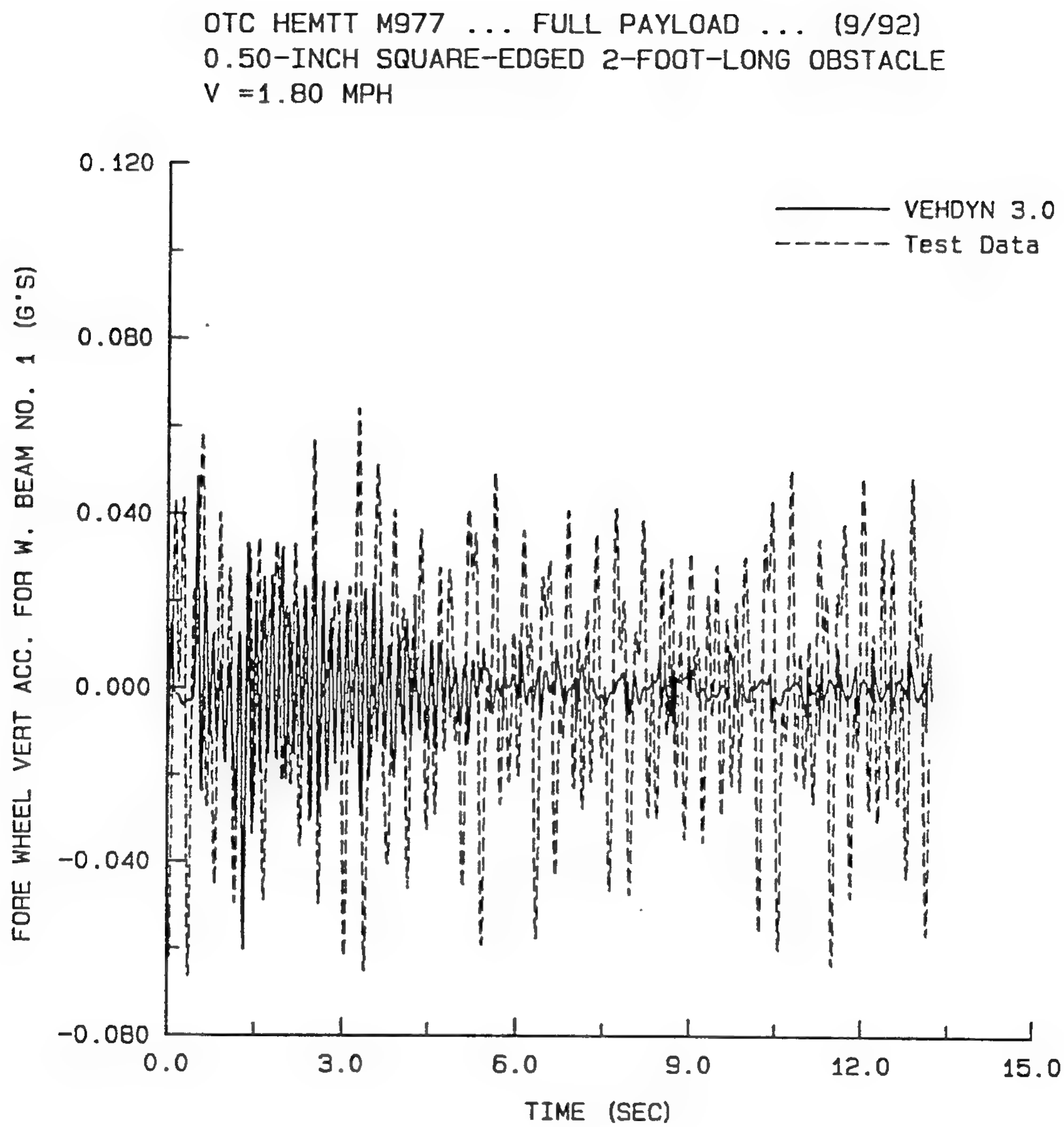

Figure A-33. Vertical acceleration time history of the forward-most axle for a fully loaded HEMTT traveling at 1.80 miles per hour encountering a 0.50-inch-high obstacle.

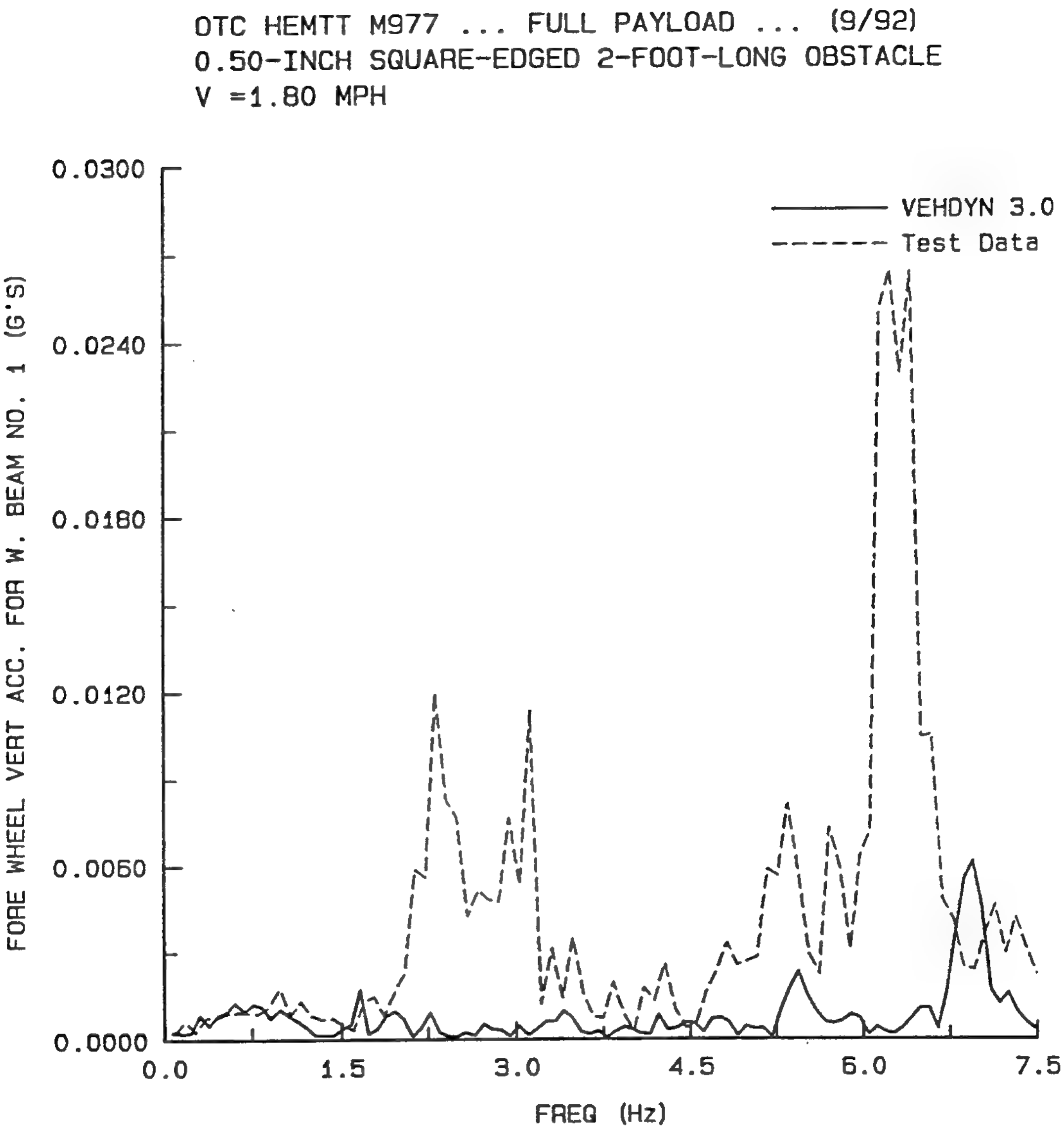

Figure A-34. Vertical acceleration frequency plot (frequency scale = 1.5 Hz/inch) of the forward-most axle for a fully loaded HEMTT traveling at 1.80 miles per hour encountering a 0.50-inch-high obstacle.

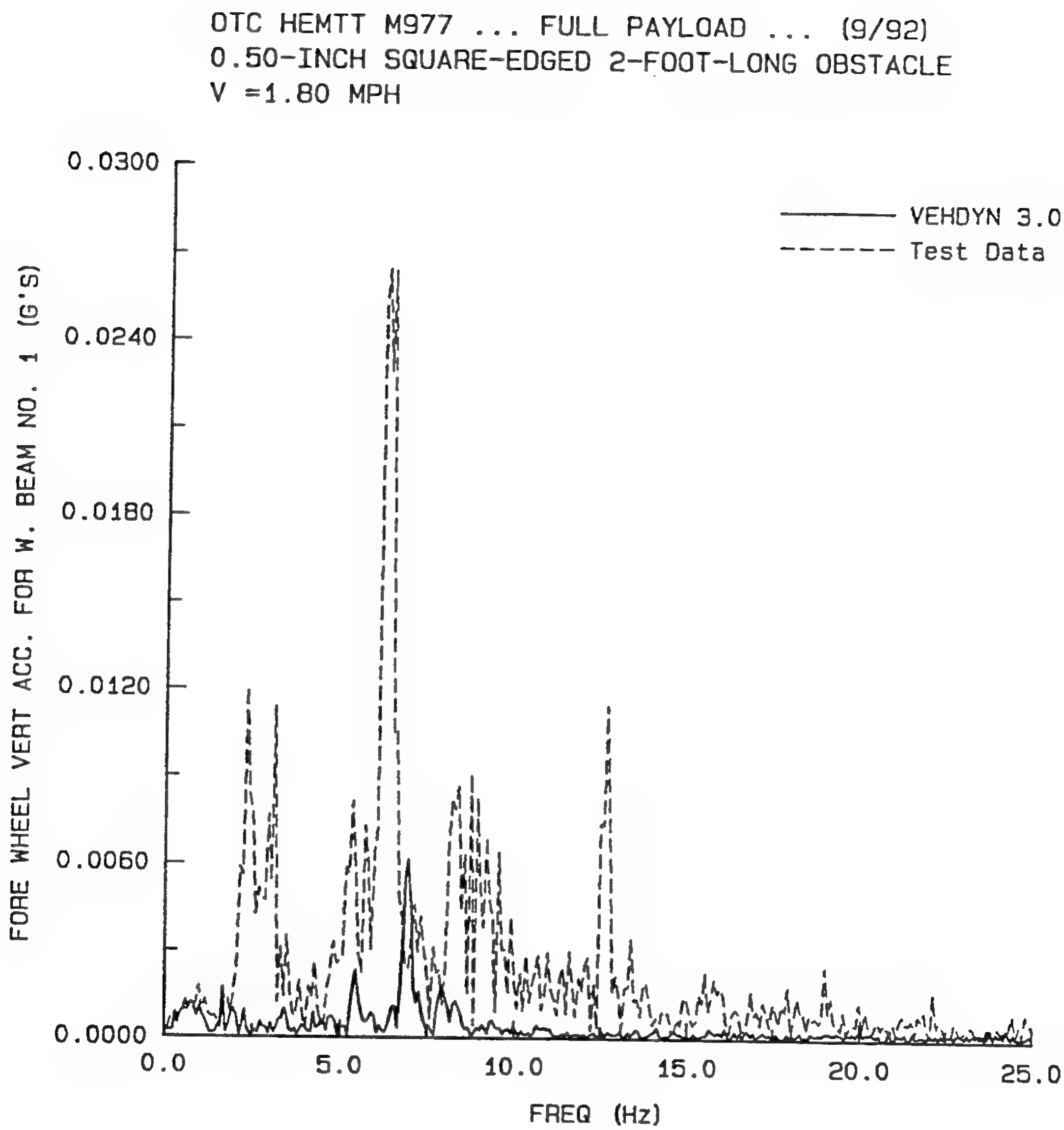

Figure A-35. Vertical acceleration frequency plot (frequency scale = 5.0 Hz/inch) of the forward-most axle for a fully loaded HEMTT traveling at 1.80 miles per hour encountering a 0.50-inch-high obstacle.

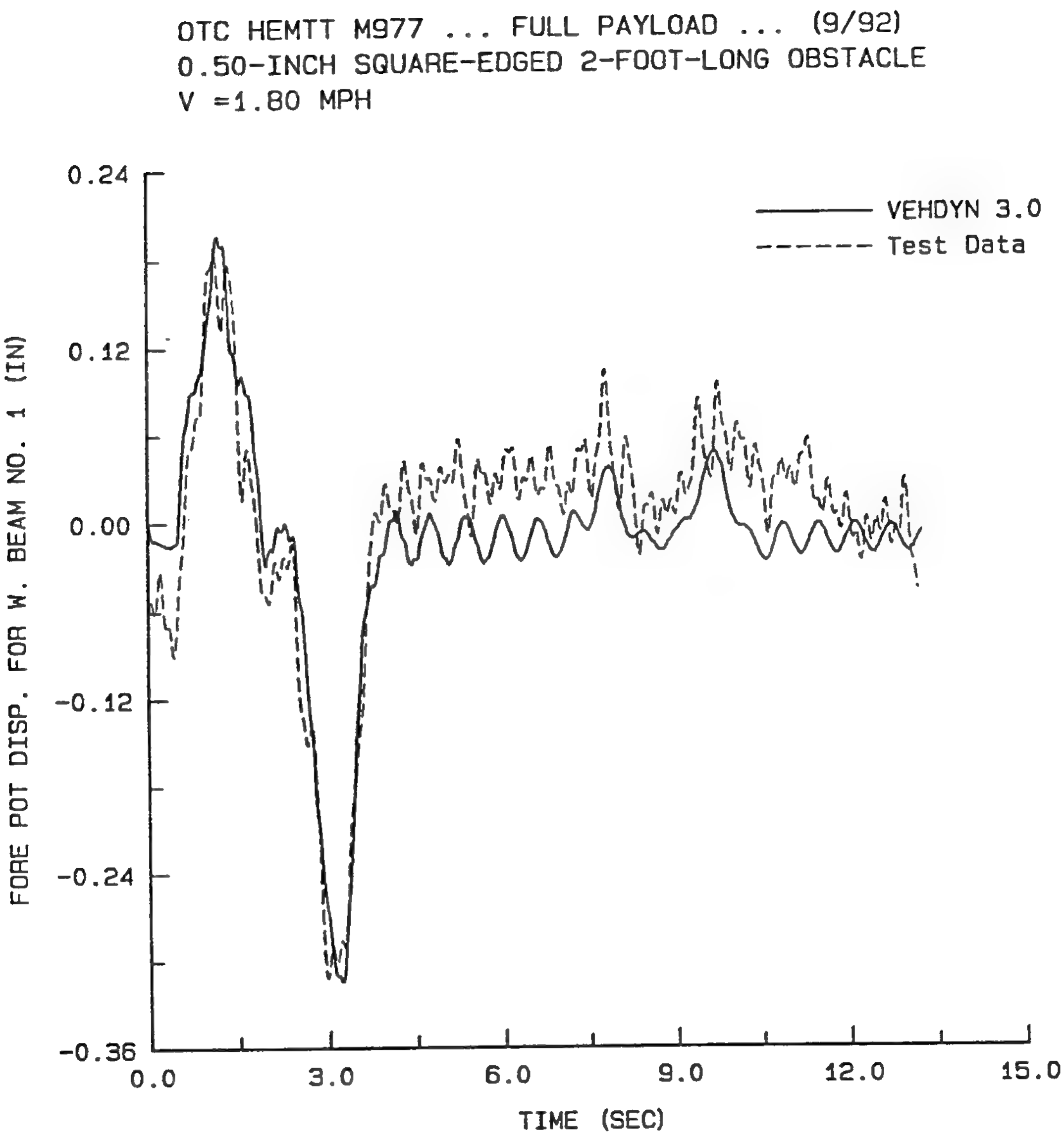

Figure A-36. Relative displacement time history of the forward-most axle with respect to the frame for a fully loaded HEMTT traveling at 1.80 miles per hour encountering a 0.50-inch-high obstacle.

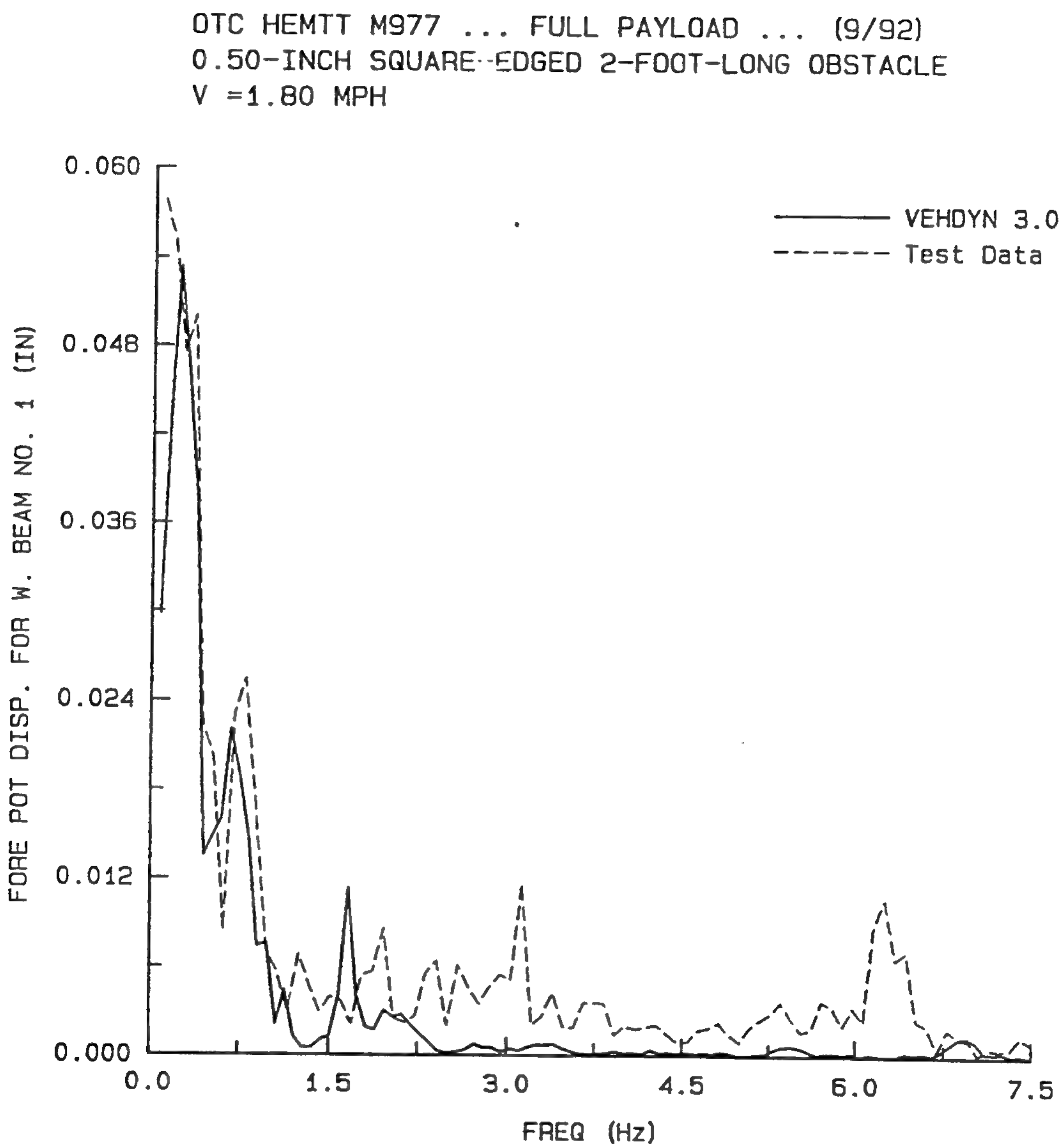

Figure A-37. Relative displacement frequency plot (frequency scale = 1.5 Hz/inch) of the forward-most axle with respect to the frame for a fully loaded HEMTT traveling at 1.80 miles per hour encountering a 0.50-inch-high obstacle.

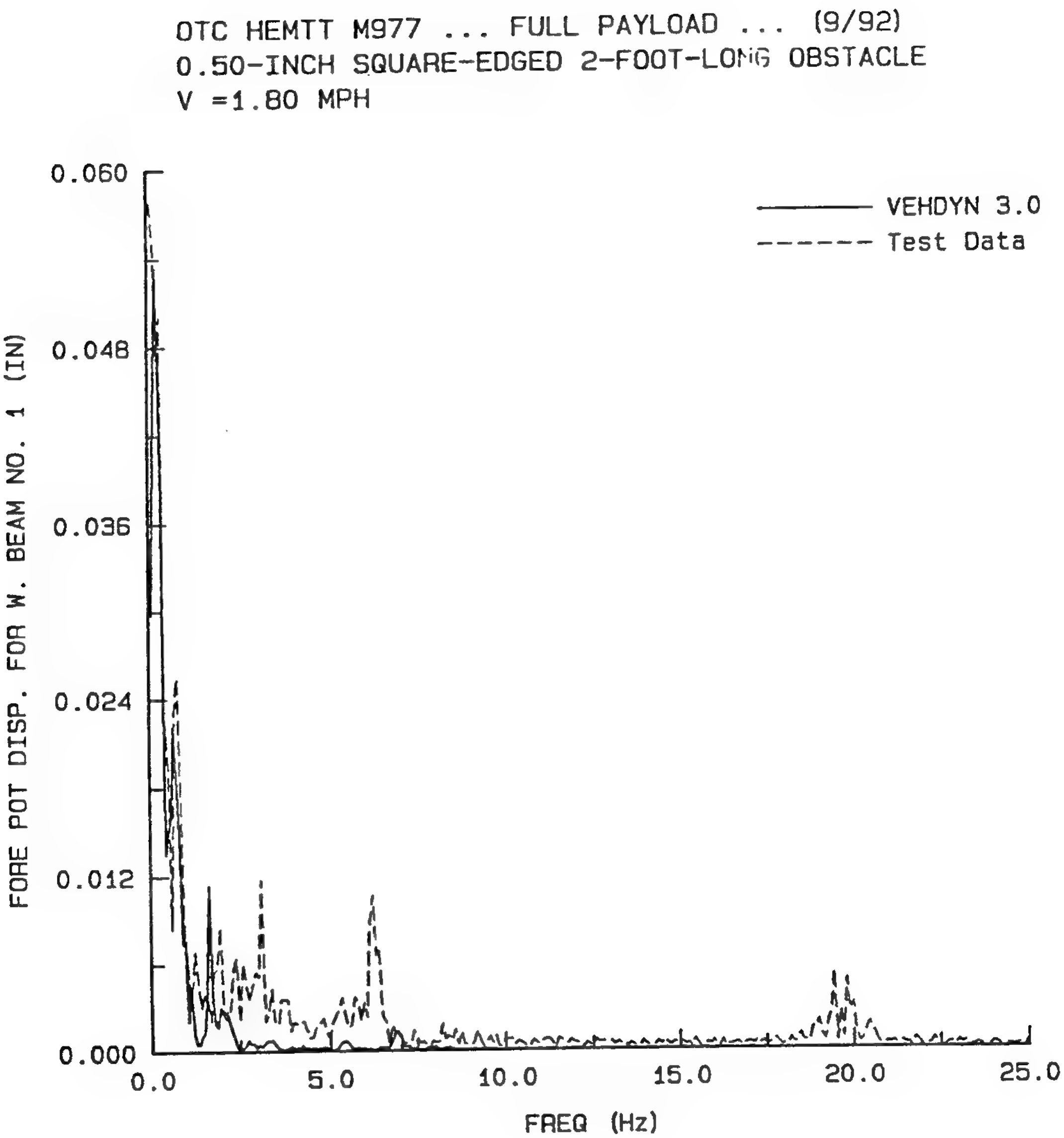

Figure A-38. Relative displacement frequency plot (frequency scale = 5.0 Hz/inch) of the forward-most axle with respect to the frame for a fully loaded HEMTT traveling at 1.80 miles per hour encountering a 0.50-inch-high obstacle.

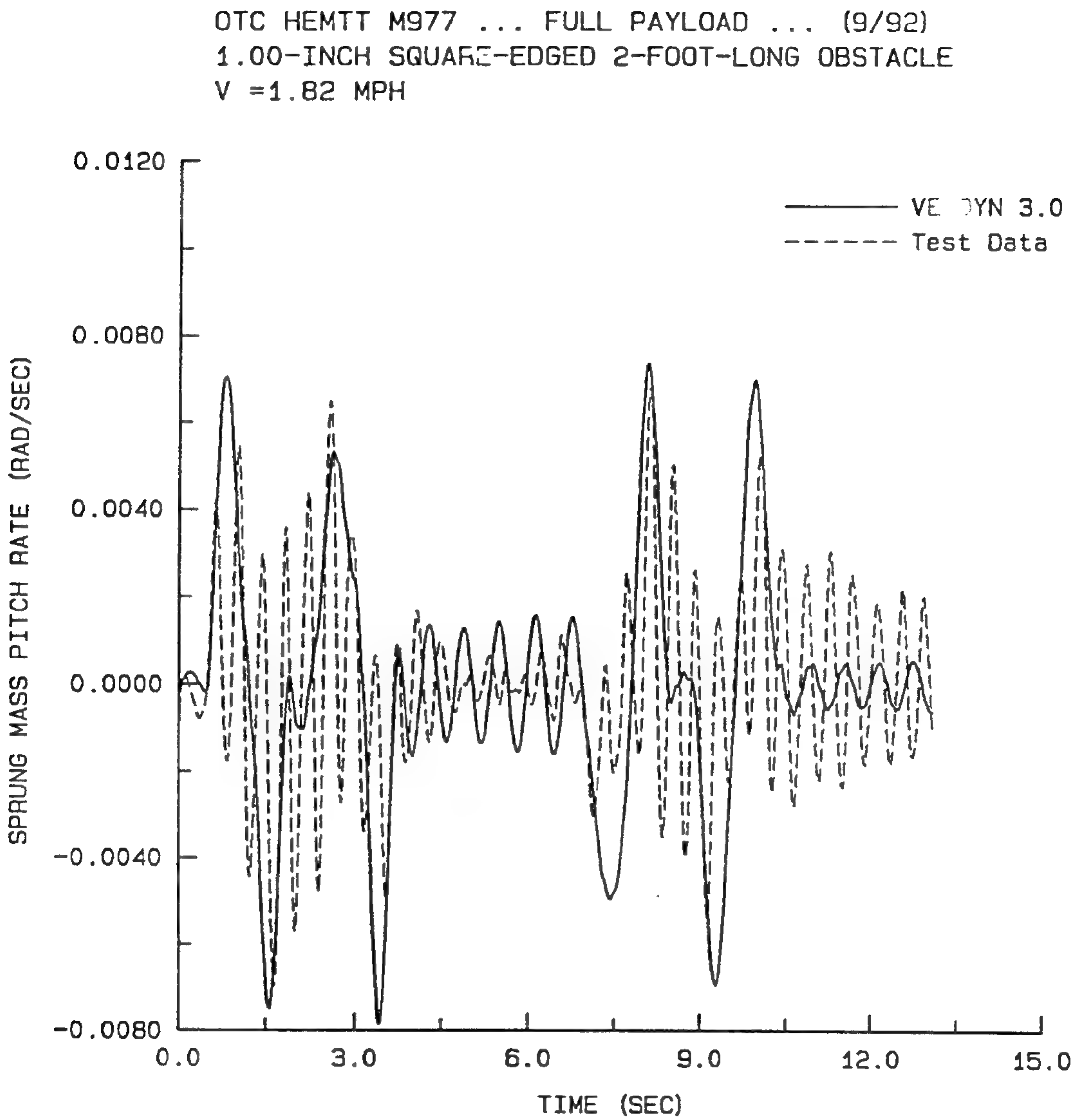

Figure A-39. Sprung mass pitch rate time history for a fully loaded HEMTT traveling at 1.82 miles per hour encountering a 1.00-inch-high obstacle.

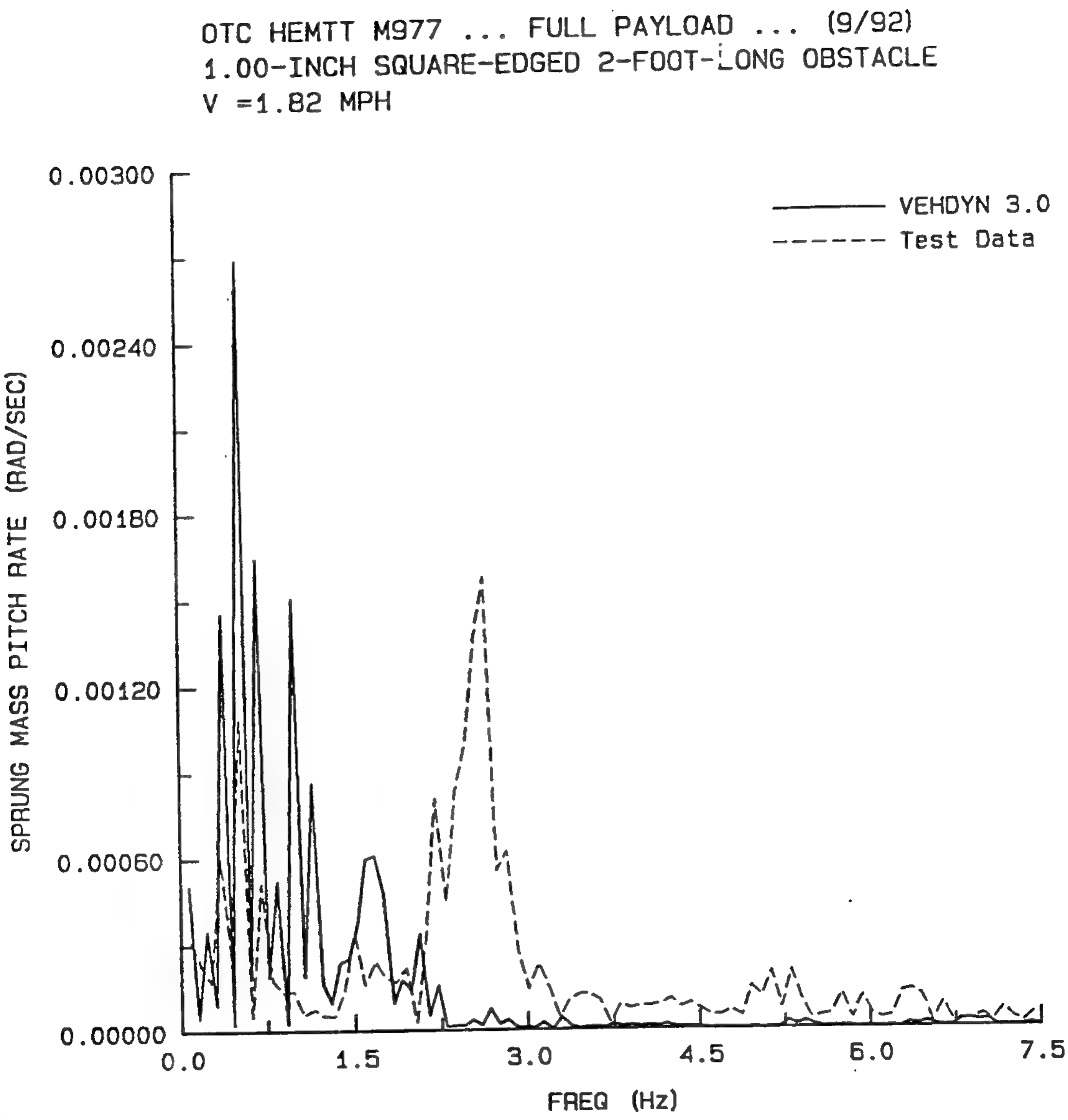

Figure A-40. Sprung mass pitch rate frequency plot for a fully loaded HEMTT traveling at 1.82 miles per hour encountering a 1.00-inch-high obstacle.

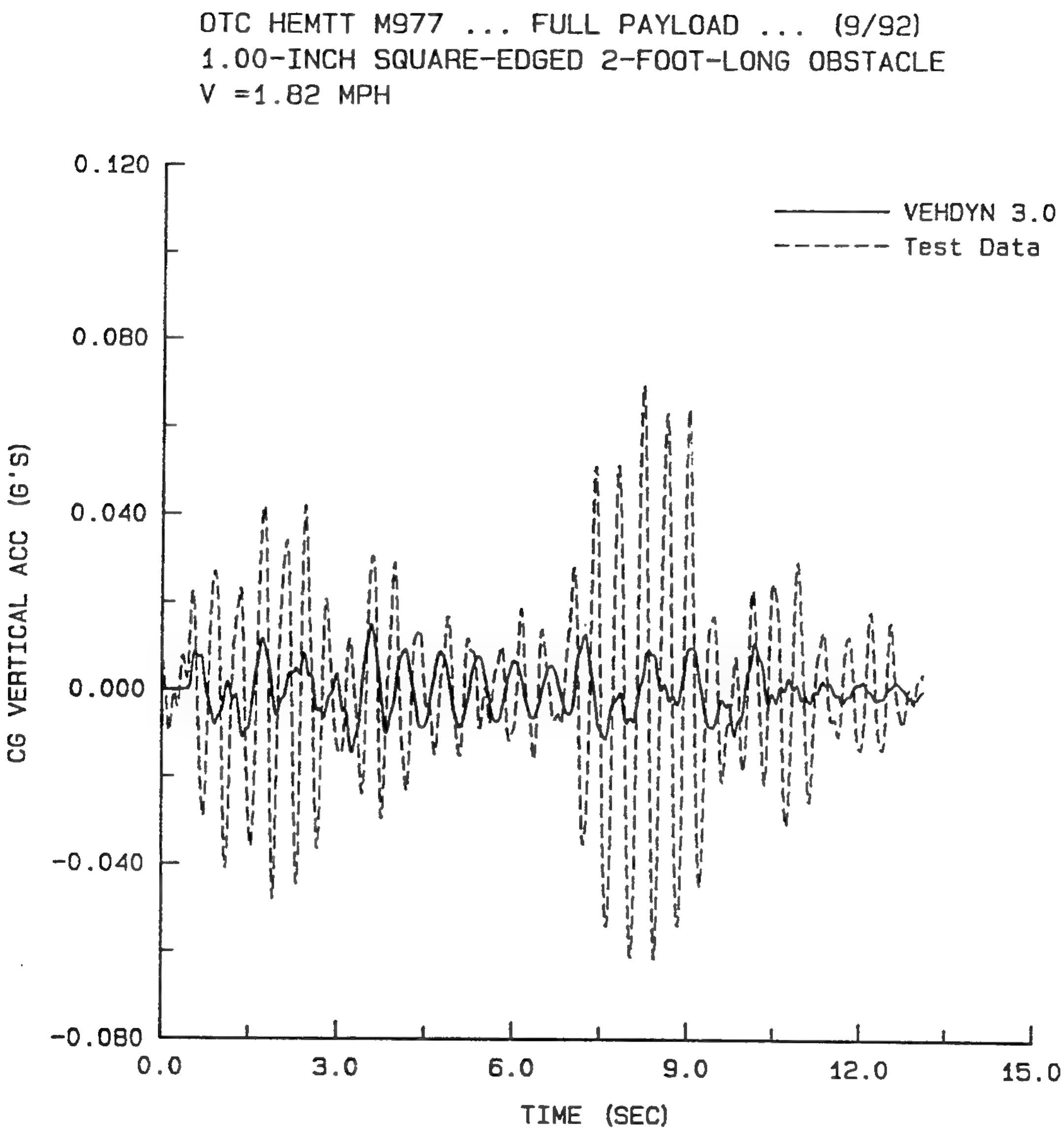

Figure A-41. CG vertical acceleration time history for a fully loaded HEMTT traveling at 1.82 miles per hour encountering a 1.00-inch-high obstacle.

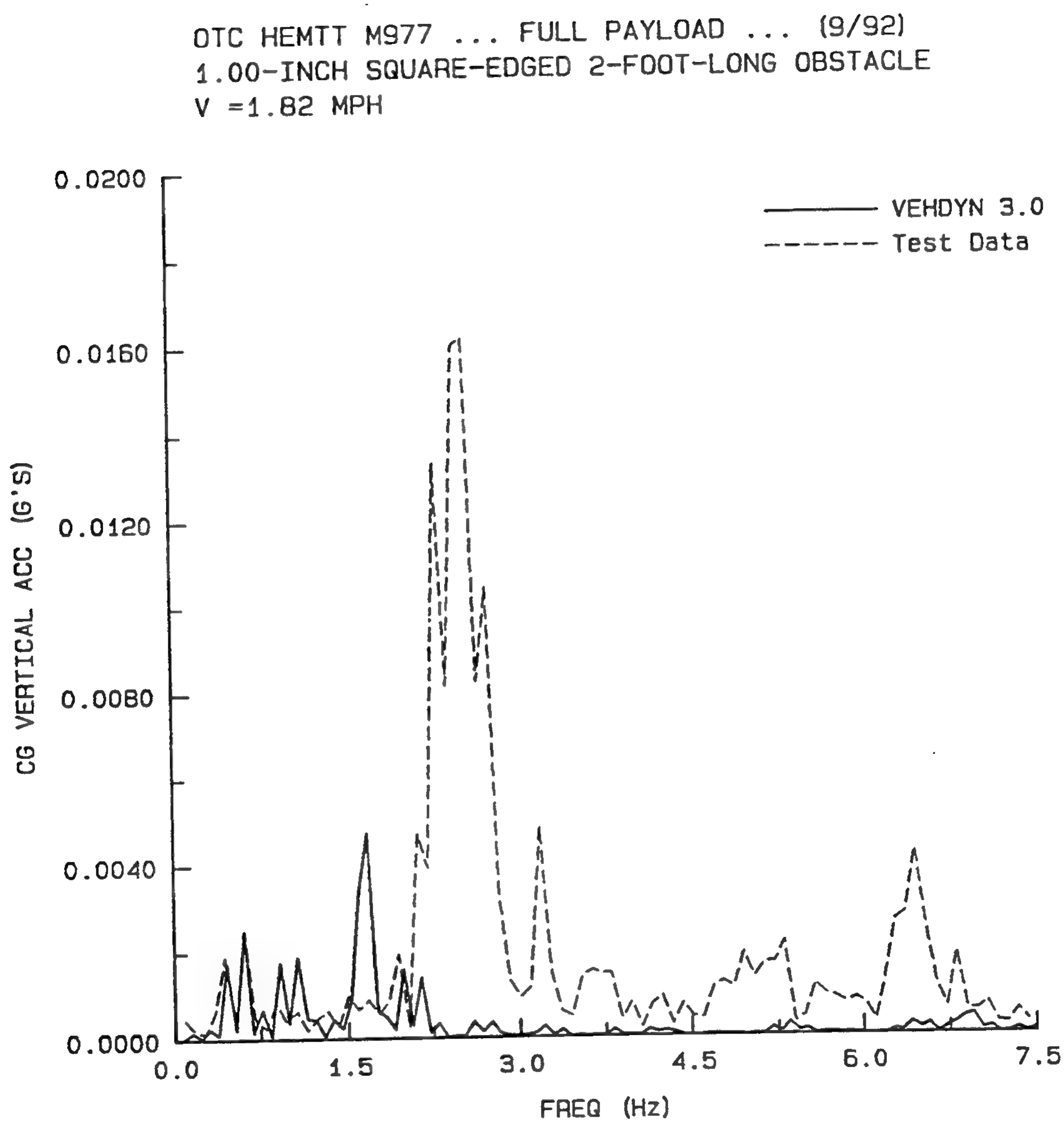

Figure A-42. CG vertical acceleration frequency plot (frequency scale = 1.5 Hz/inch) for a fully loaded HEMTT traveling at 1.82 miles per hour encountering a 1.00-inch-high obstacle.

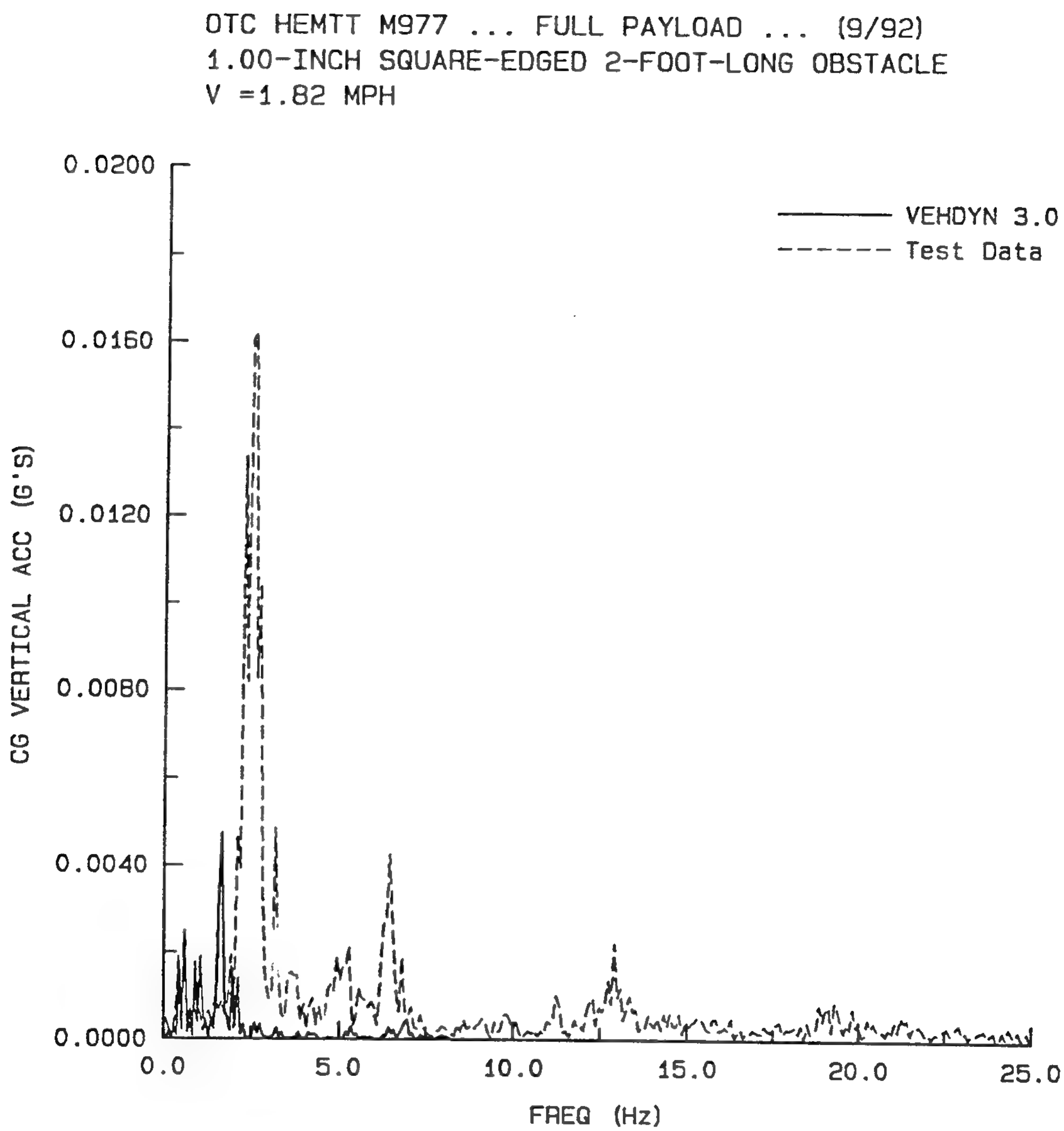

Figure A-43. CG vertical acceleration frequency plot (frequency scale = 5.0 Hz/inch) for a fully loaded HEMTT traveling at 1.82 miles per hour encountering a 1.00-inch-high obstacle.

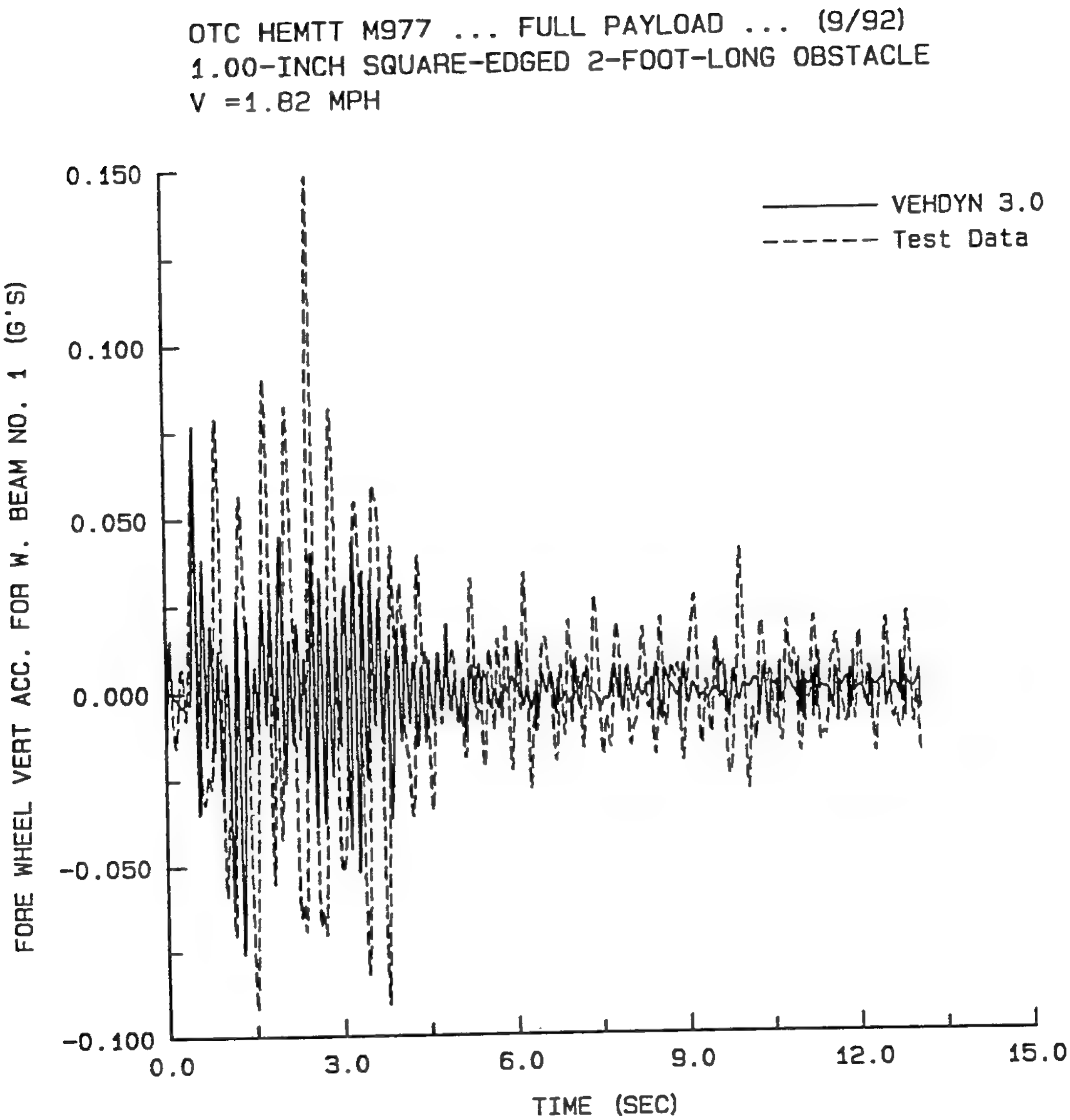

Figure A-44. Vertical acceleration time history of the forward-most axle for a fully loaded HEMTT traveling at 1.82 miles per hour encountering a 1.00-inch-high obstacle.

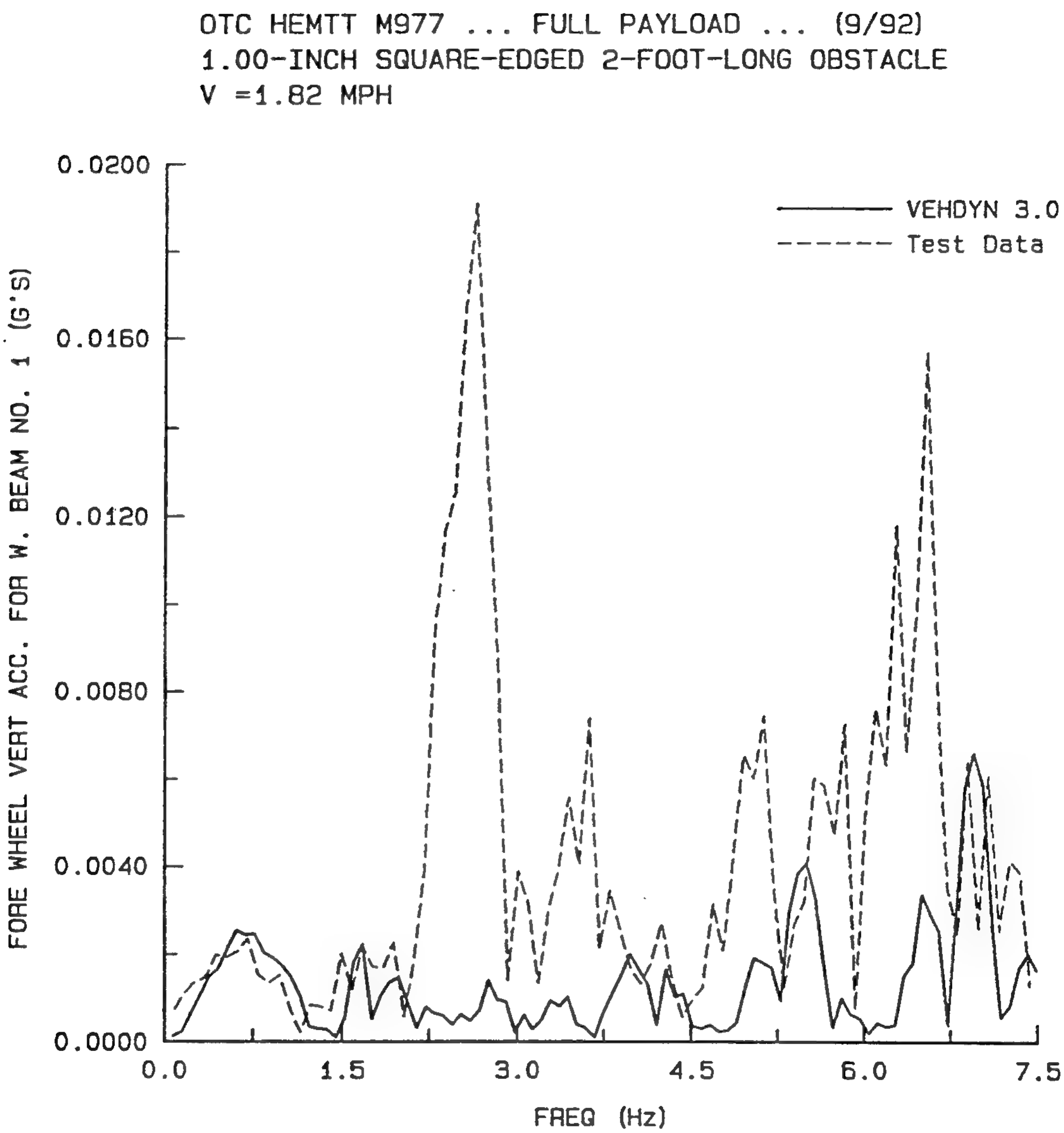

Figure A-45. Vertical acceleration frequency plot (frequency scale = 1.5 Hz/inch) of the forward-most axle for a fully loaded HEMTT traveling at 1.82 miles per hour encountering a 1.00-inch-high obstacle.

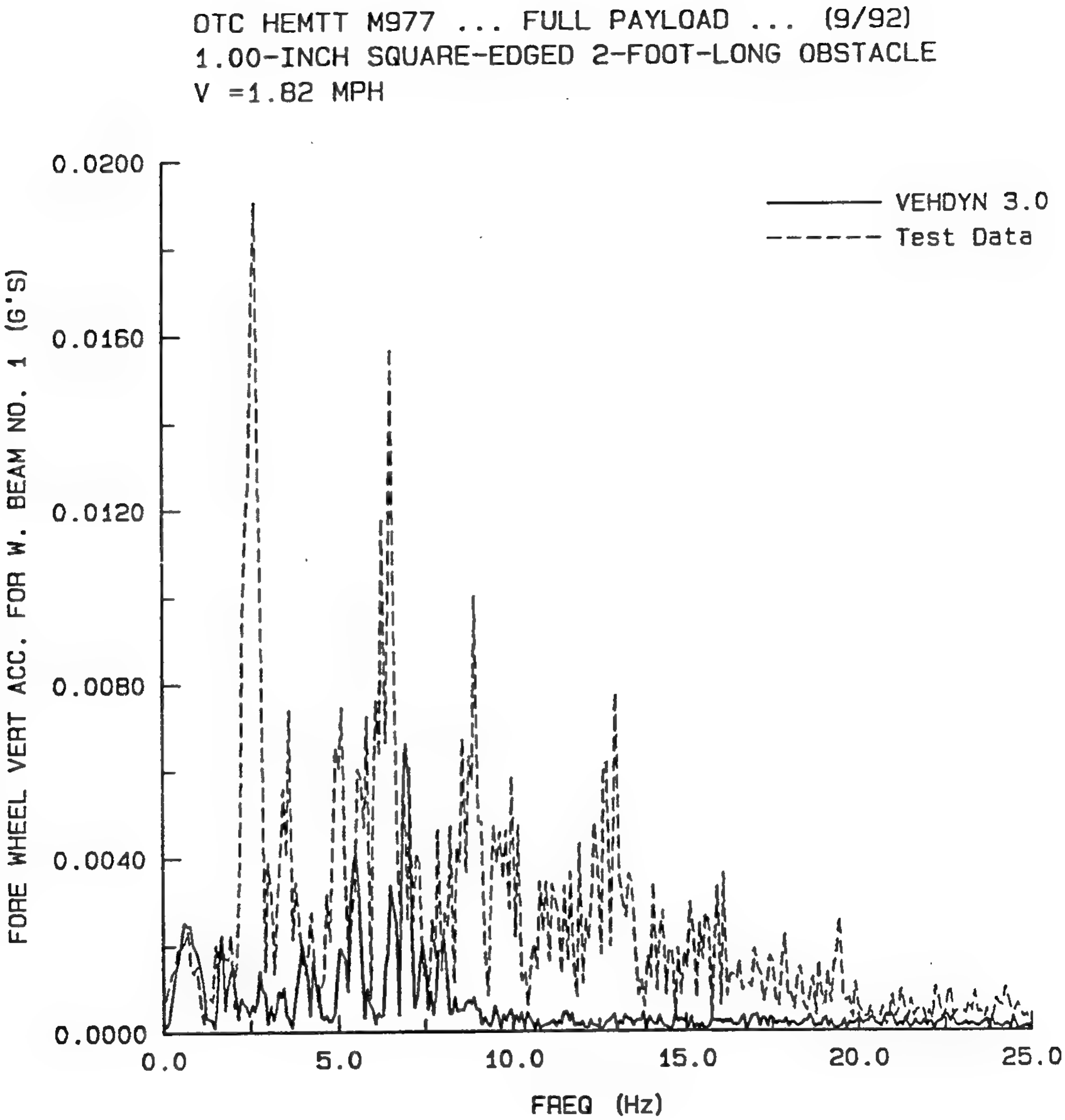

Figure A-46. Vertical acceleration frequency plot (frequency scale = 5.0 Hz/inch) of the forward-most axle for a fully loaded HEMTT traveling at 1.82 miles per hour encountering a 1.00-inch-high obstacle.

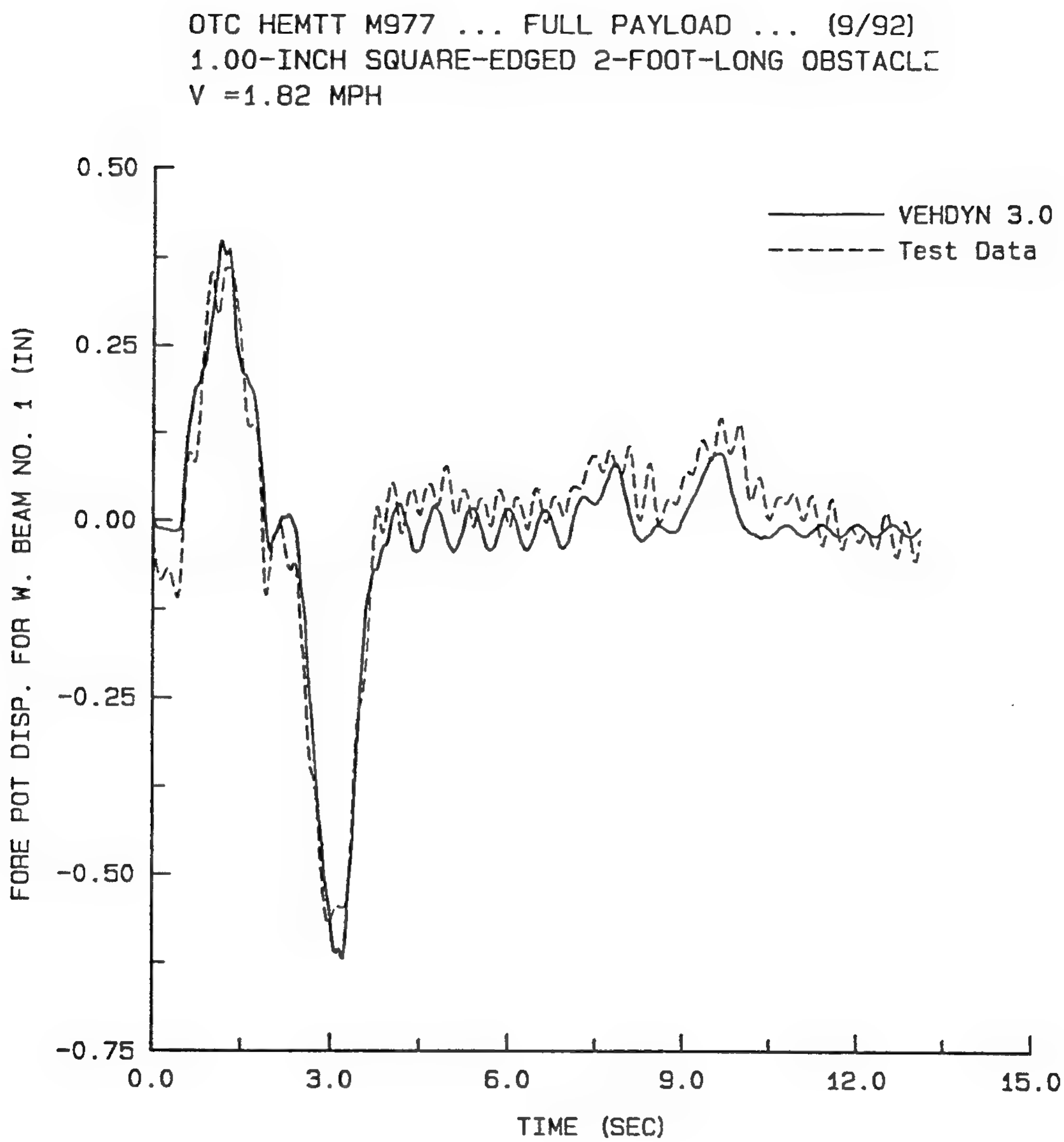

Figure A-47. Relative displacement time history of the forward-most axle with respect to the frame for a fully loaded HEMTT traveling at 1.82 miles per hour encountering a 1.00-inch-high obstacle.

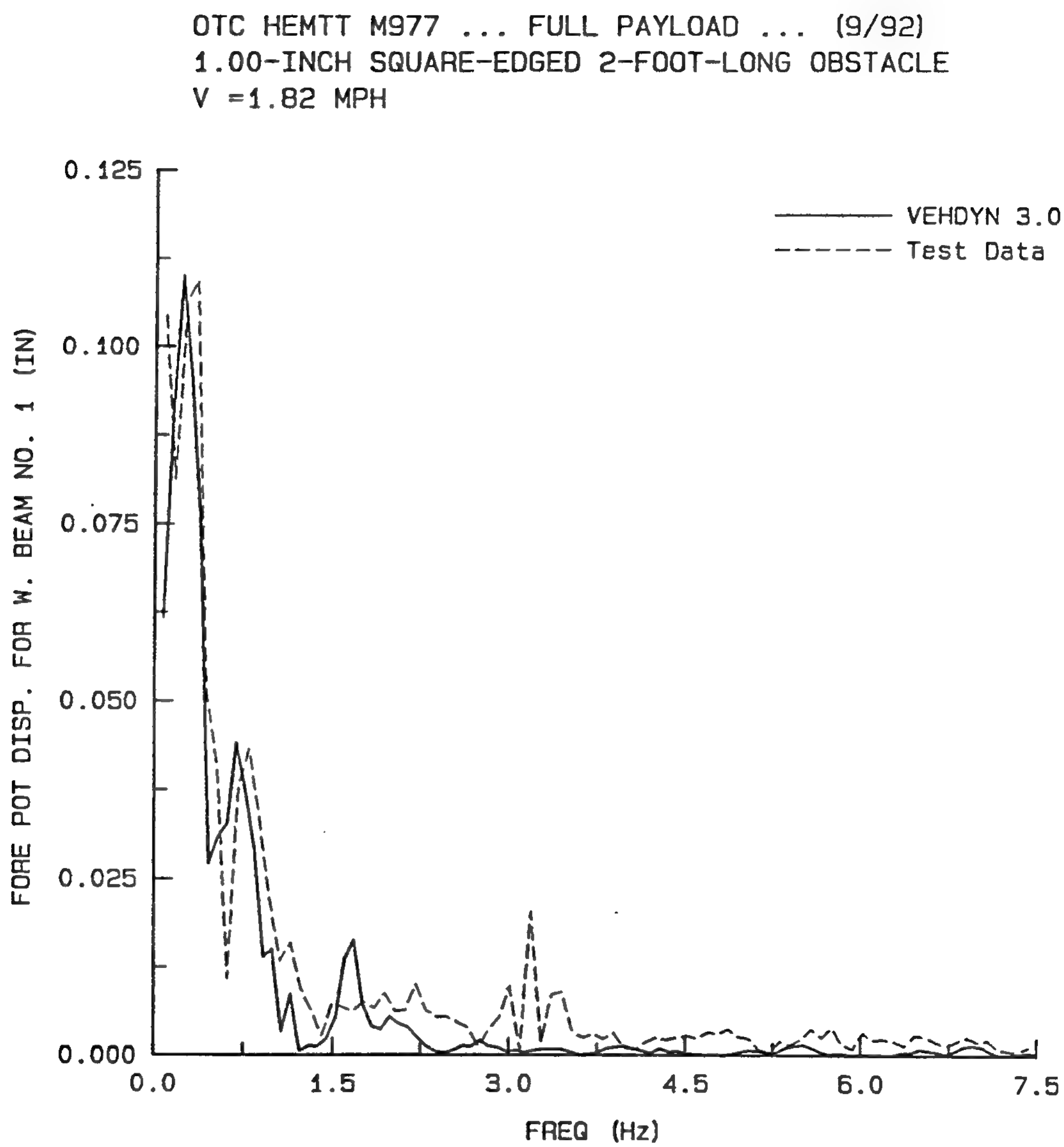

Figure A-48. Relative displacement frequency plot (frequency scale = 1.5 Hz/inch) of the forward-most axle with respect to the frame for a fully loaded HEMTT traveling at 1.82 miles per hour encountering a 1.00-inch-high obstacle.

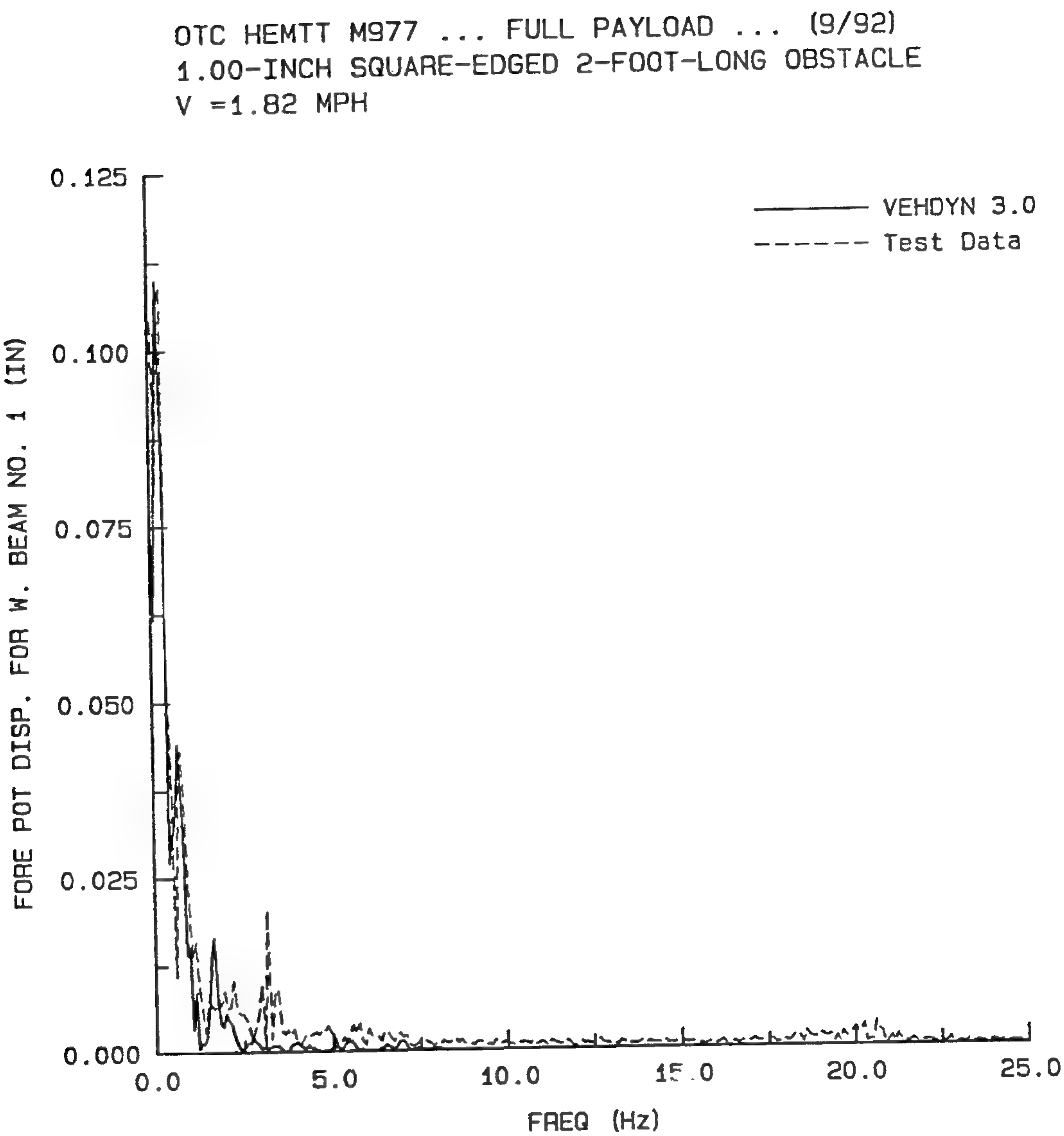

Figure A-49. Relative displacement frequency plot (frequency scale = 5.0 Hz/inch) of the forward-most axle with respect to the frame for a fully loaded HEMTT traveling at 1.82 miles per hour encountering a 1.00-inch-high obstacle.

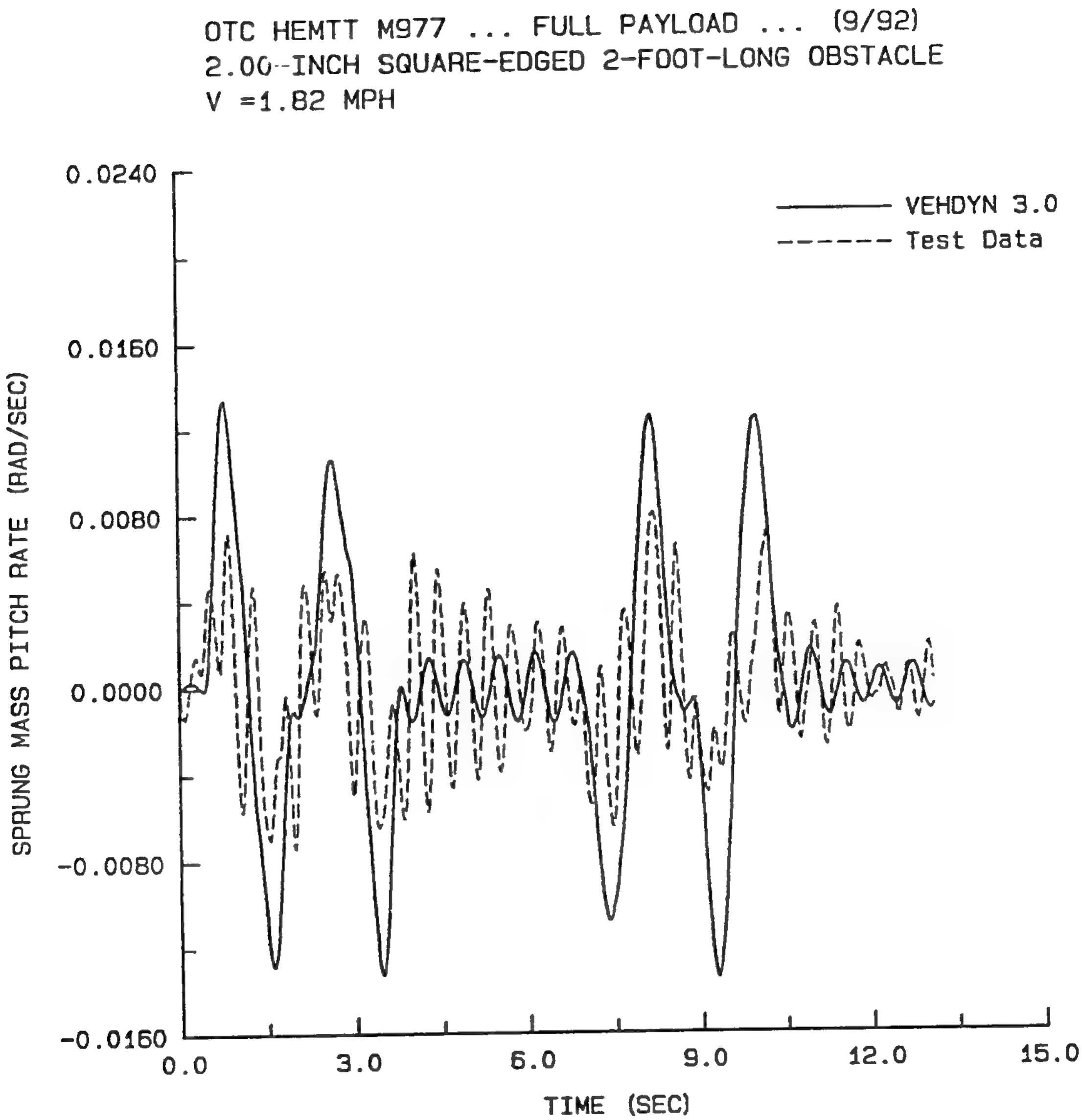

Figure A-50. Sprung mass pitch rate time history for a fully loaded HEMTT traveling at 1.82 miles per hour encountering a 2.00-inch-high obstacle.

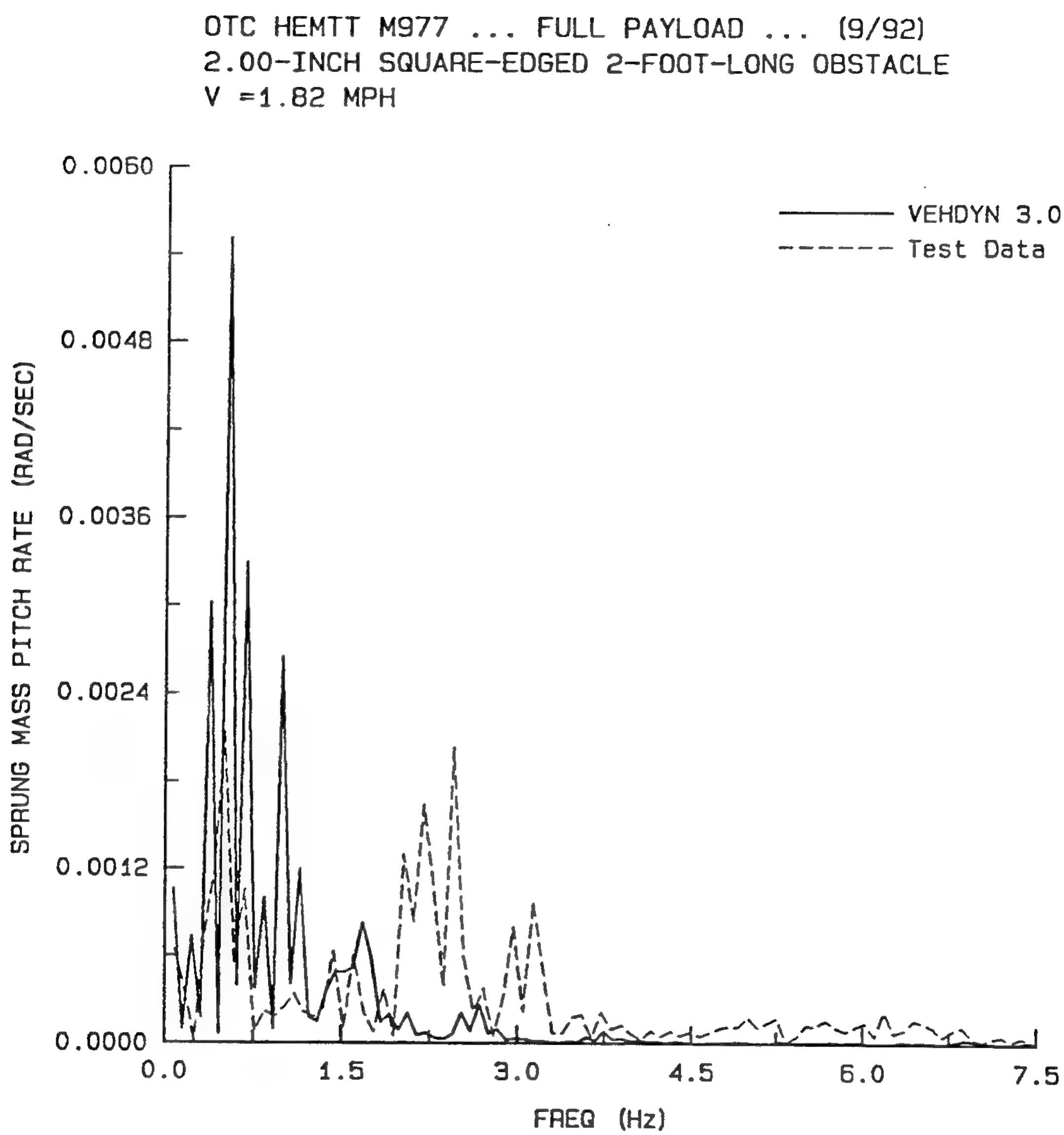

Figure A-51. Sprung mass pitch rate frequency plot for a fully loaded HEMTT traveling at 1.82 miles per hour encountering a 2.00-inch-high obstacle.

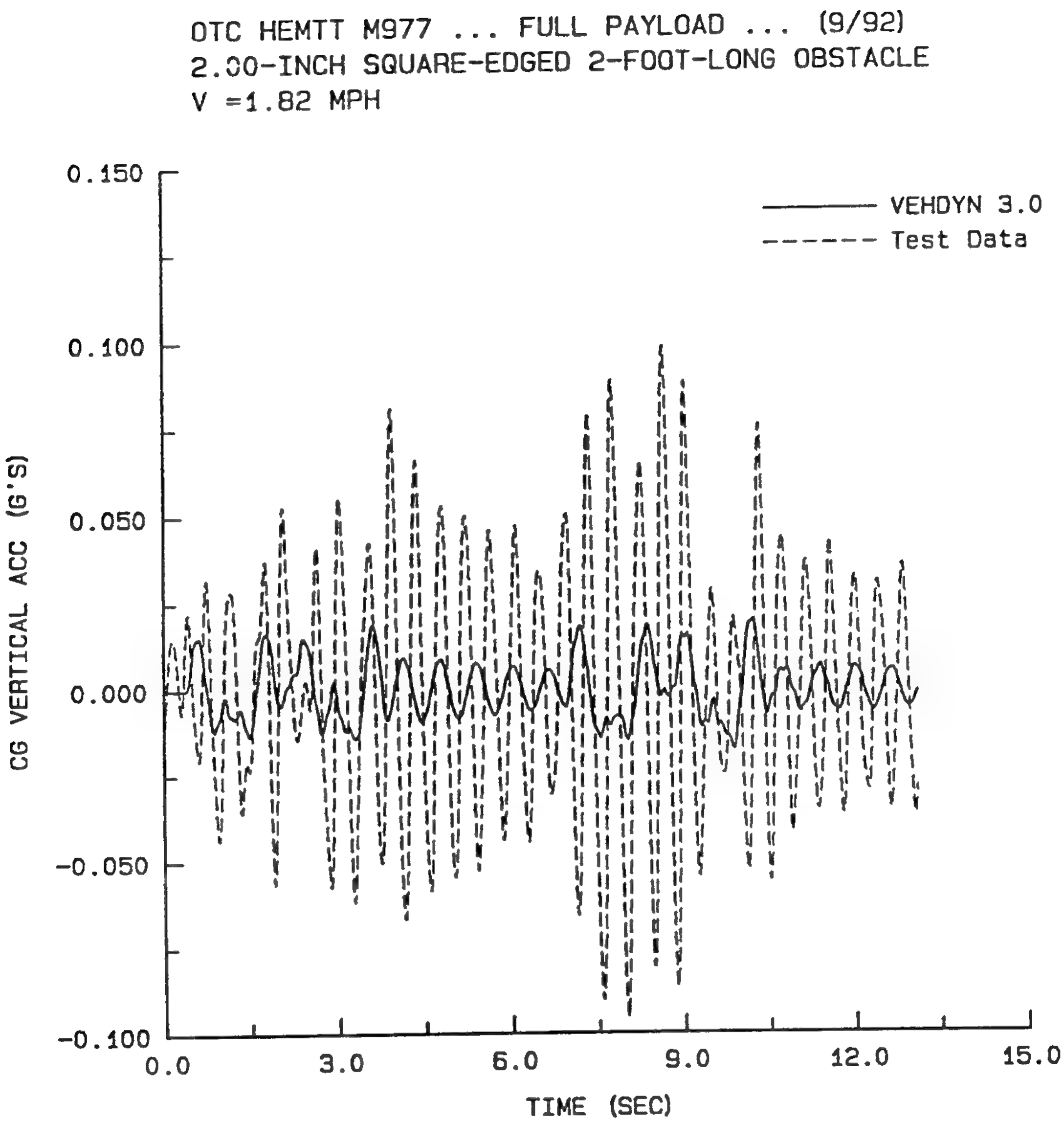

Figure A-52. CG vertical acceleration time history for a fully loaded HEMTT traveling at 1.82 miles per hour encountering a 2.00-inch-high obstacle.

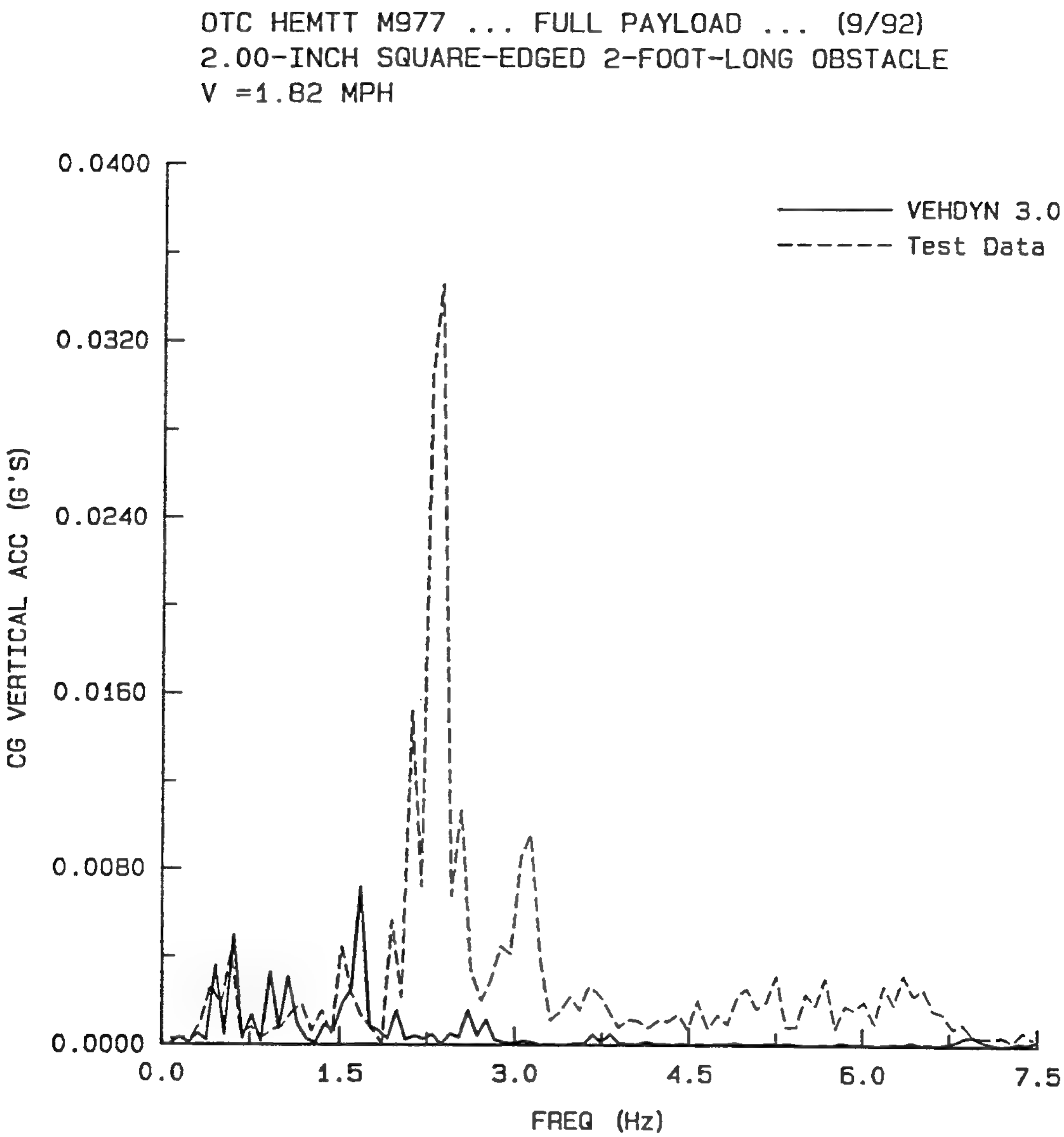

Figure A-53. CG vertical acceleration frequency plot (frequency scale = 1.5 Hz/inch) for a fully loaded HEMTT traveling at 1.82 miles per hour encountering a 2.00-inch-high obstacle.

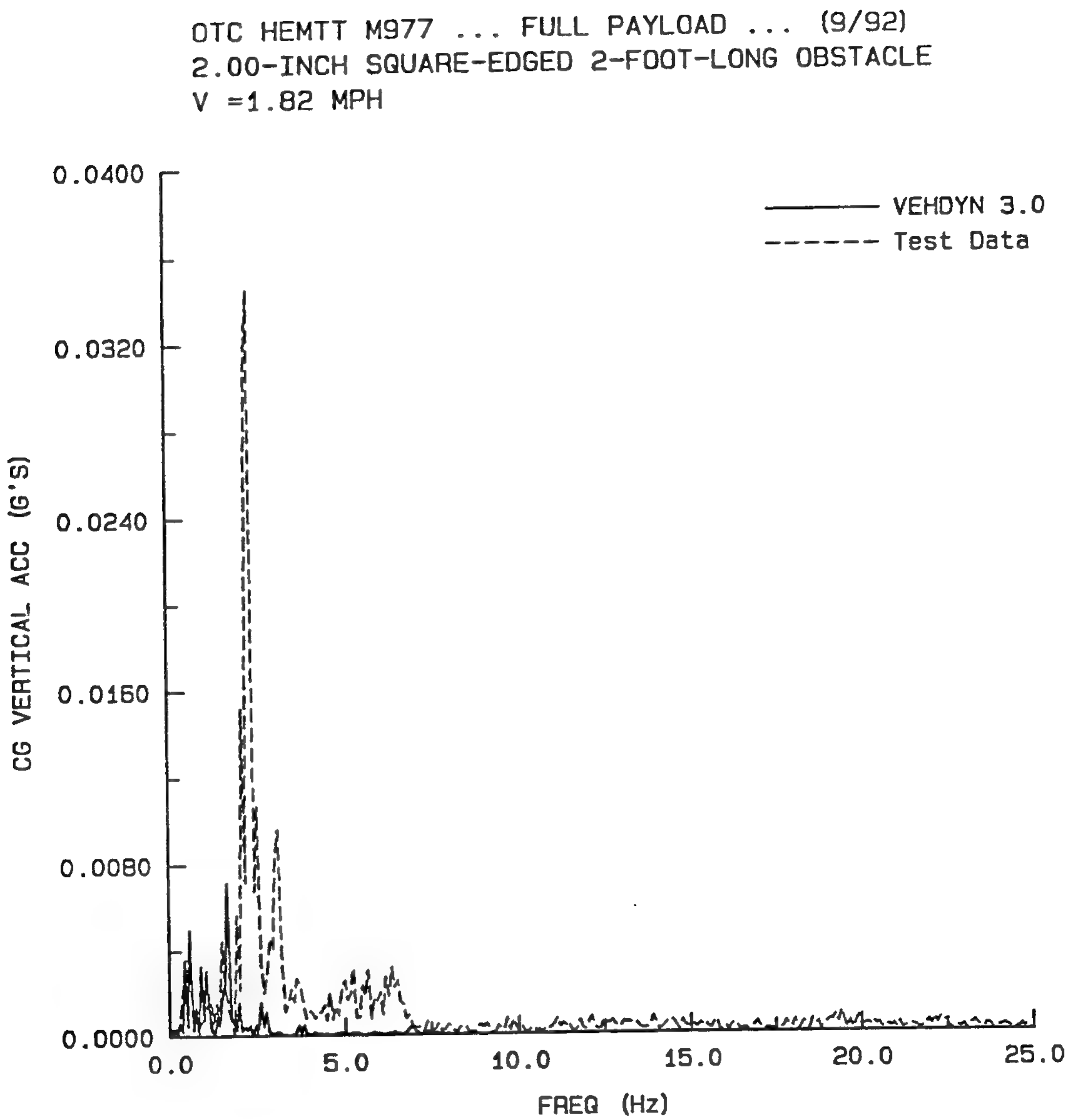

Figure A-54. CG vertical acceleration frequency plot (frequency scale = 5.0 Hz/inch) for a fully loaded HEMTT traveling at 1.82 miles per hour encountering a 2.00-inch-high obstacle.

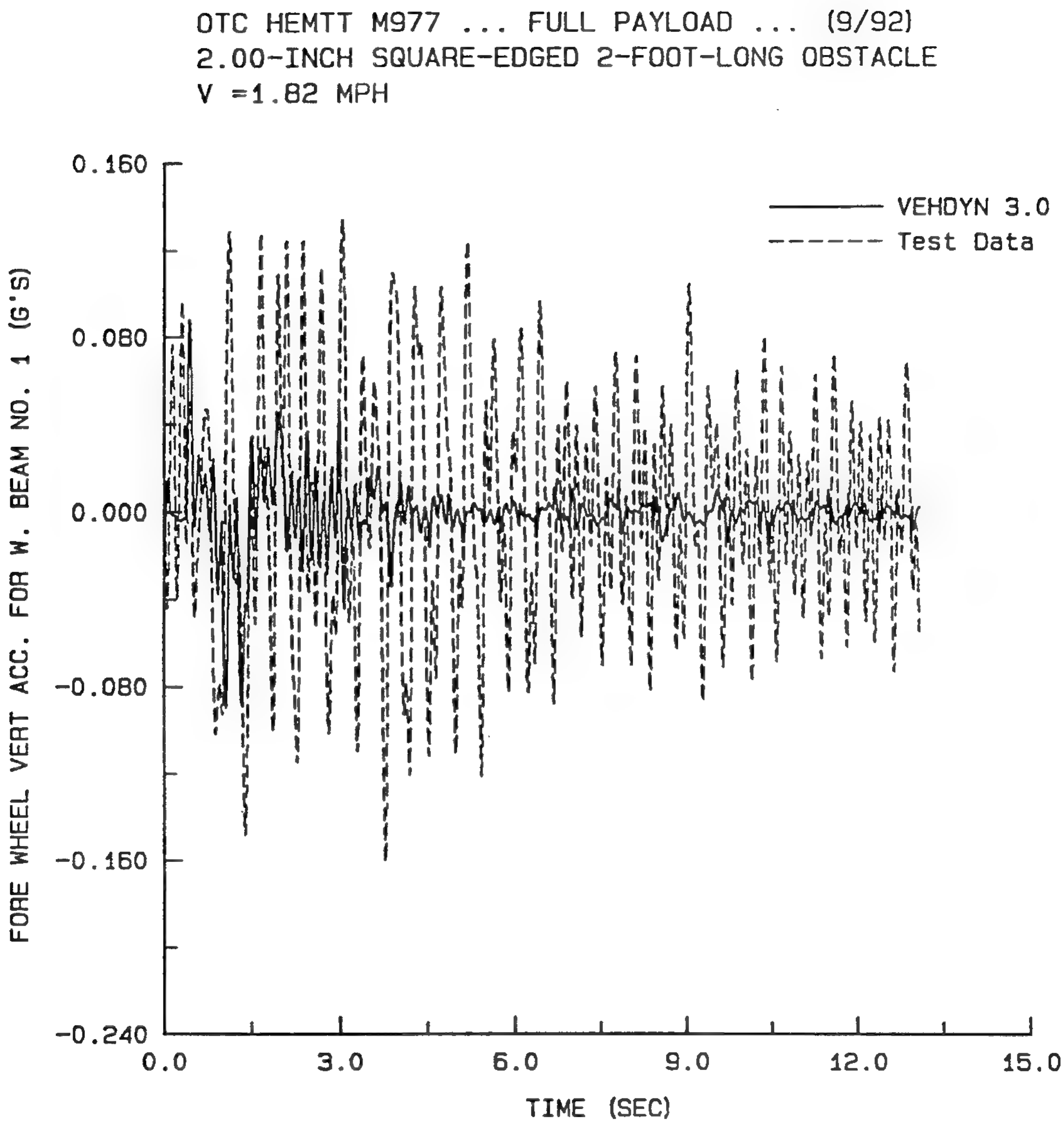

Figure A-55. Vertical acceleration time history of the forward-most axle for a fully loaded HEMTT traveling at 1.82 miles per hour encountering a 2.00-inch-high obstacle.

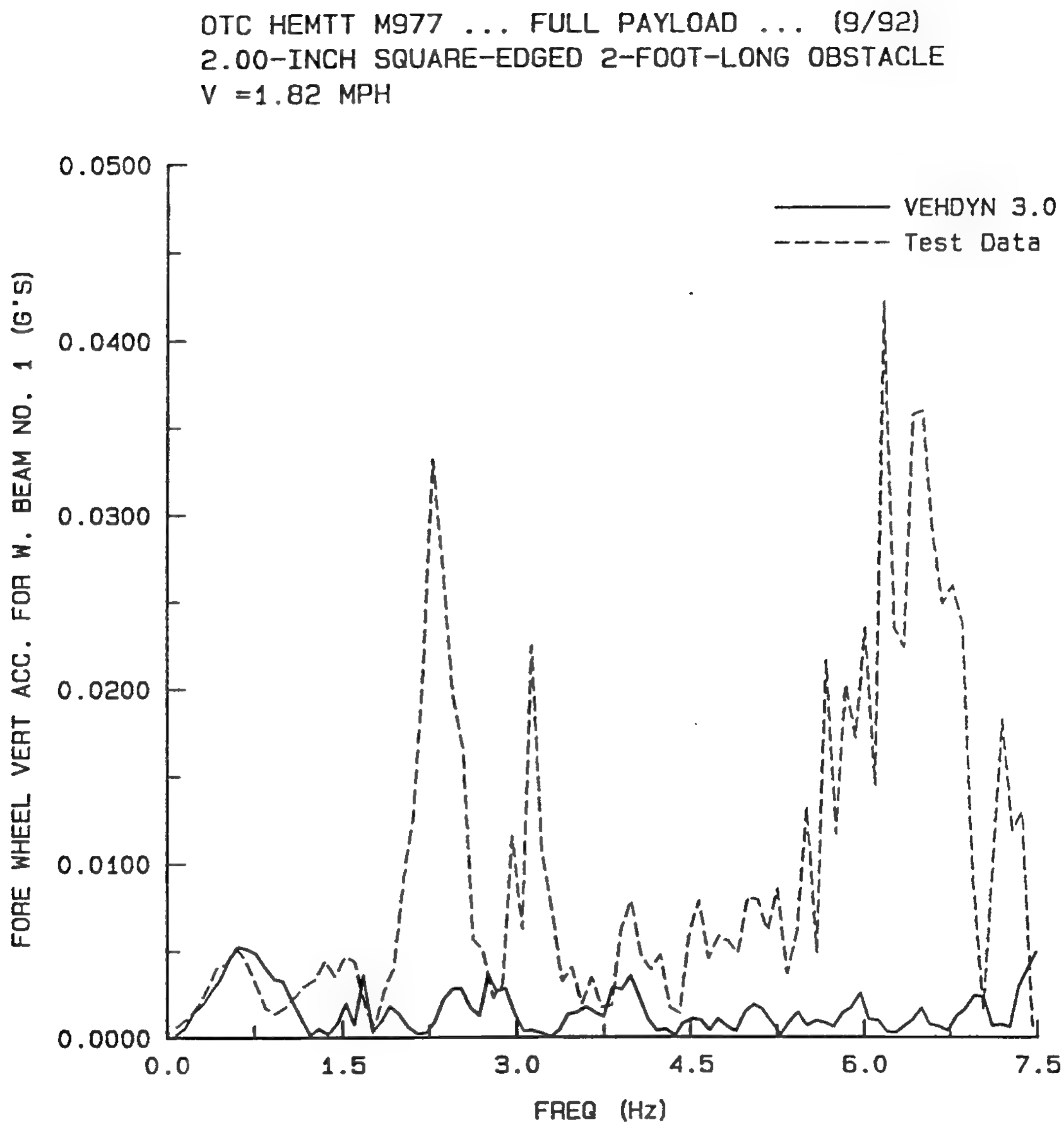

Figure A-56. Vertical acceleration frequency plot (frequency scale = 1.5 Hz/inch) of the forward-most axle for a fully loaded HEMTT traveling at 1.82 miles per hour encountering a 2.00-inch-high obstacle.

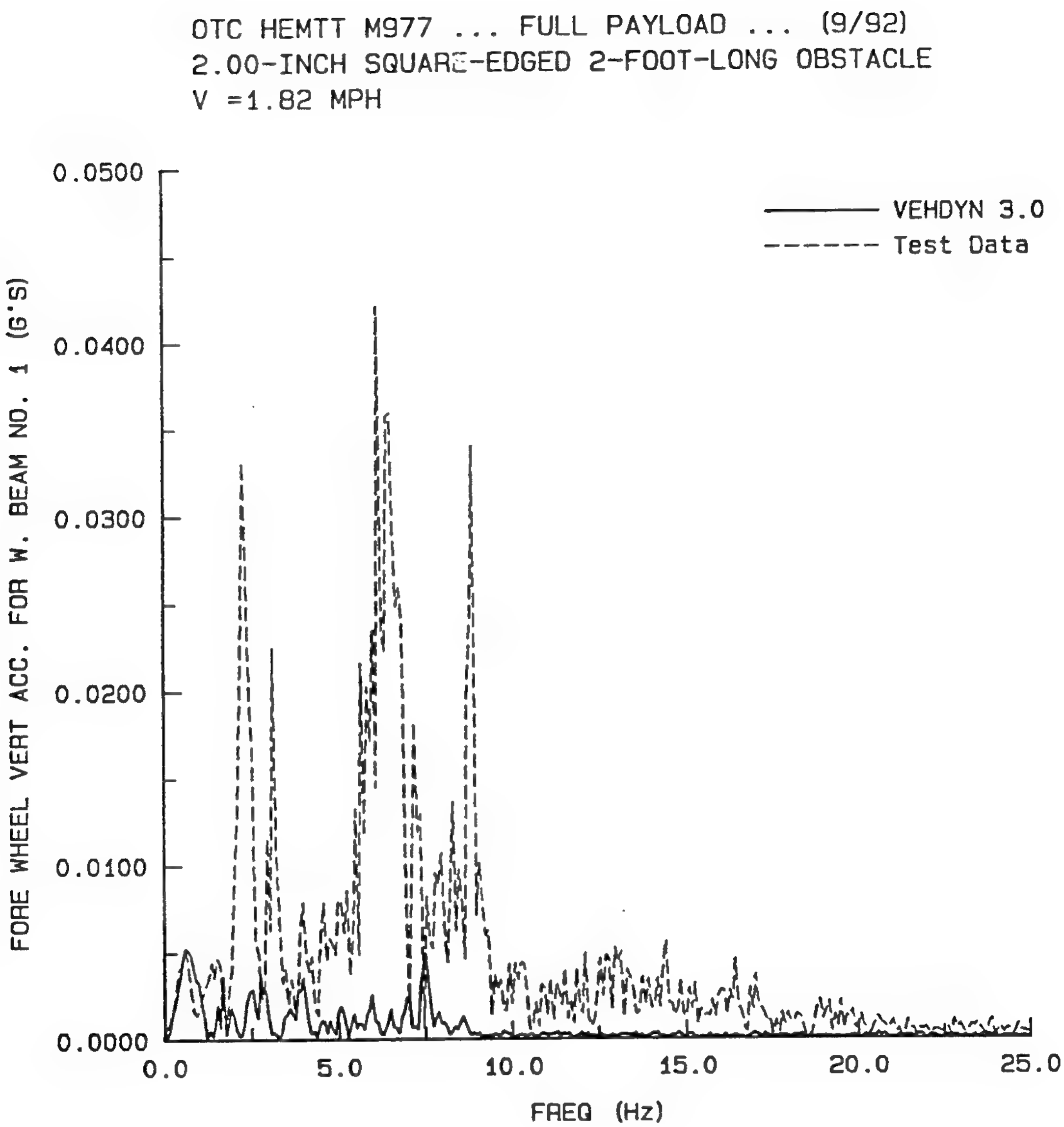

Figure A-57. Vertical acceleration frequency plot (frequency scale = 5.0 Hz/inch) of the forward-most axle for a fully loaded HEMTT traveling at 1.82 miles per hour encountering a 2.00-inch-high obstacle.

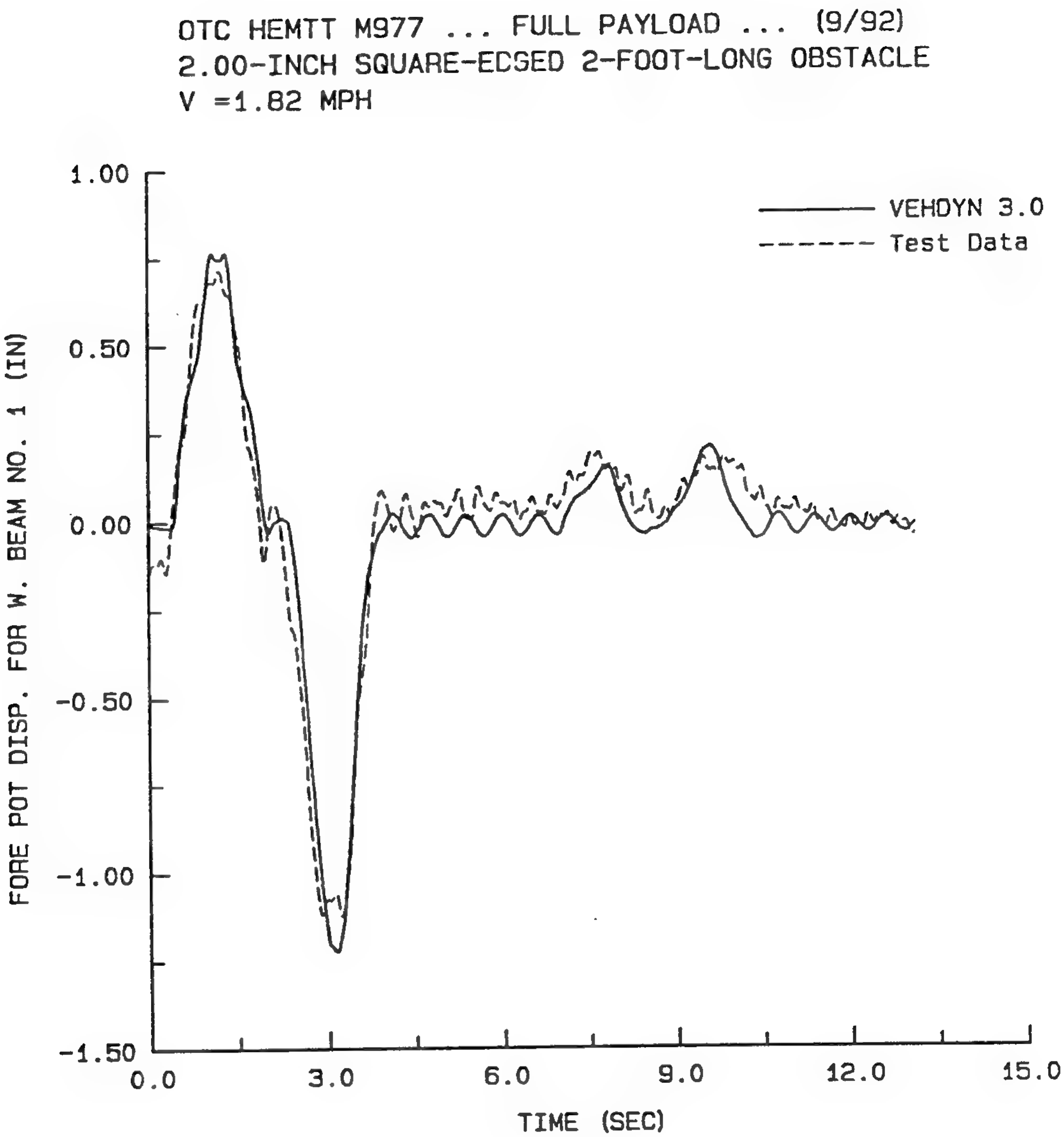

Figure A-58. Relative displacement time history of the forward-most axle with respect to the frame for a fully loaded HEMTT traveling at 1.82 miles per hour encountering a 2.00-inch-high obstacle.

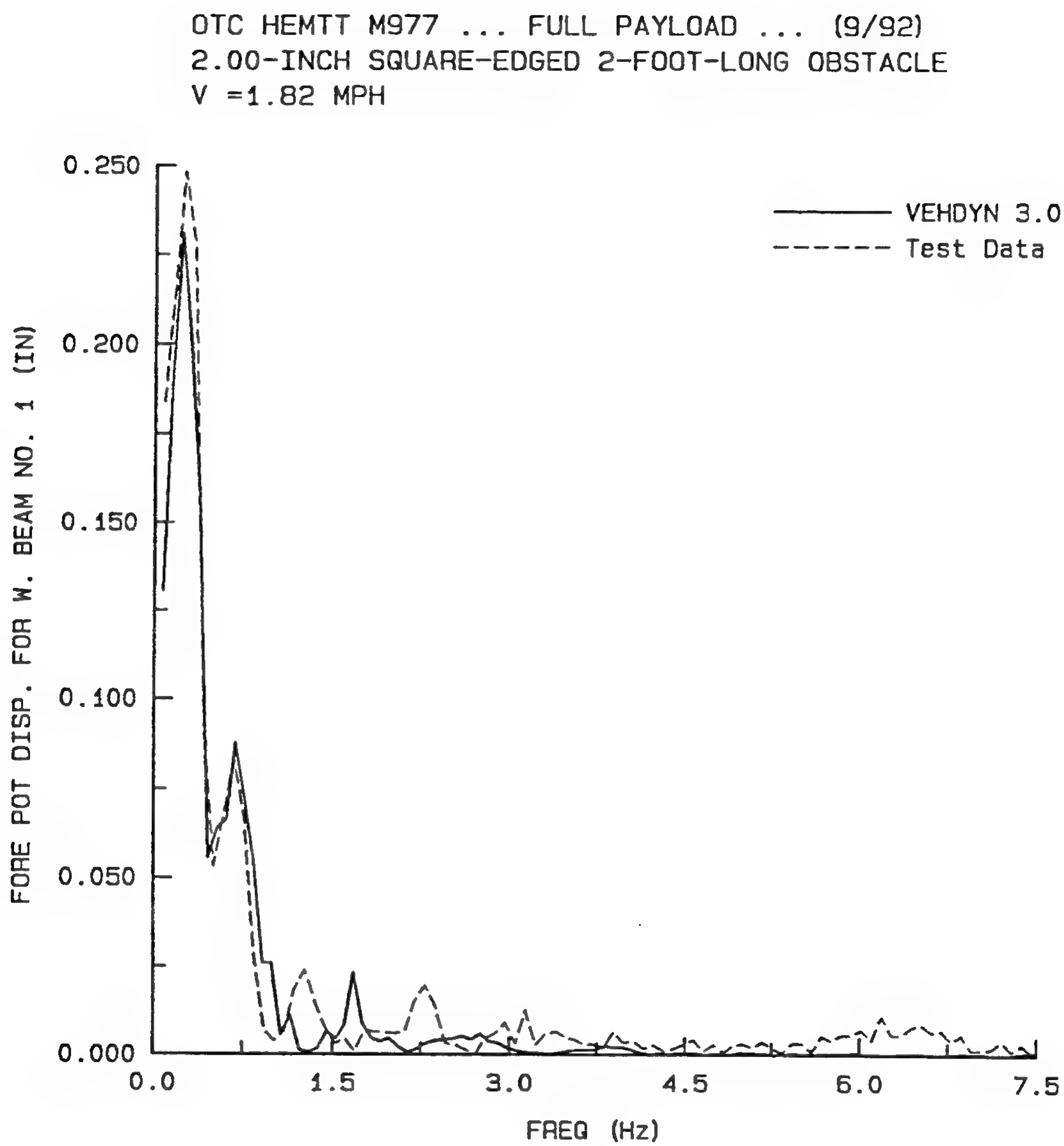

Figure A-59. Relative displacement frequency plot (frequency scale = 1.5 Hz/inch) of the forward-most axle with respect to the frame for a fully loaded HEMTT traveling at 1.82 miles per hour encountering a 2.00-inch-high obstacle.

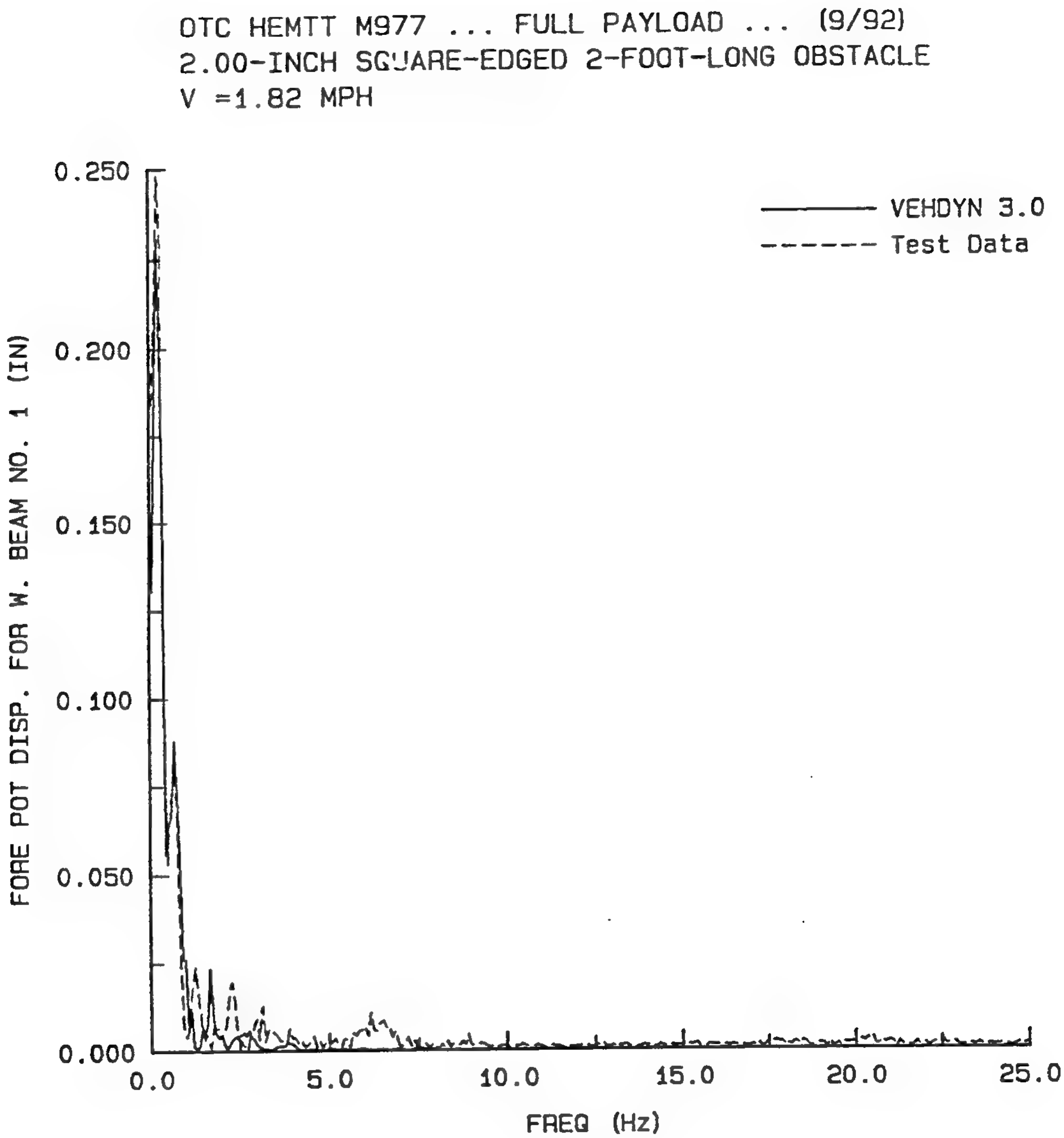

Figure A-60. Relative displacement frequency plot (frequency scale = 5.0 Hz/inch) of the forward-most axle with respect to the frame for a fully loaded HEMTT traveling at 1.82 miles per hour encountering a 2.00-inch-high obstacle.

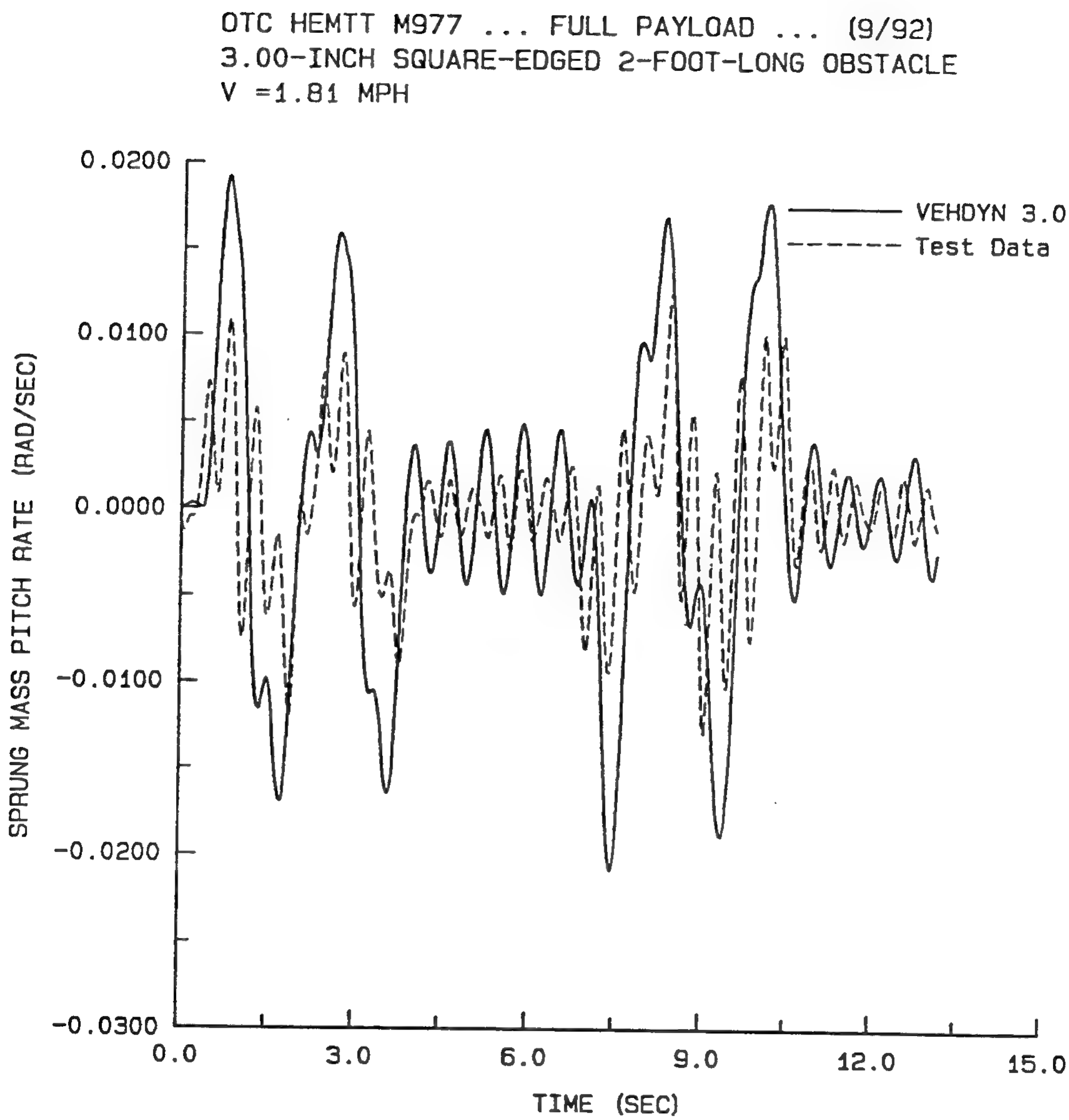

Figure A-61. Sprung mass pitch rate time history for a fully loaded HEMTT traveling at 1.81 miles per hour encountering a 3.00-inch-high obstacle.

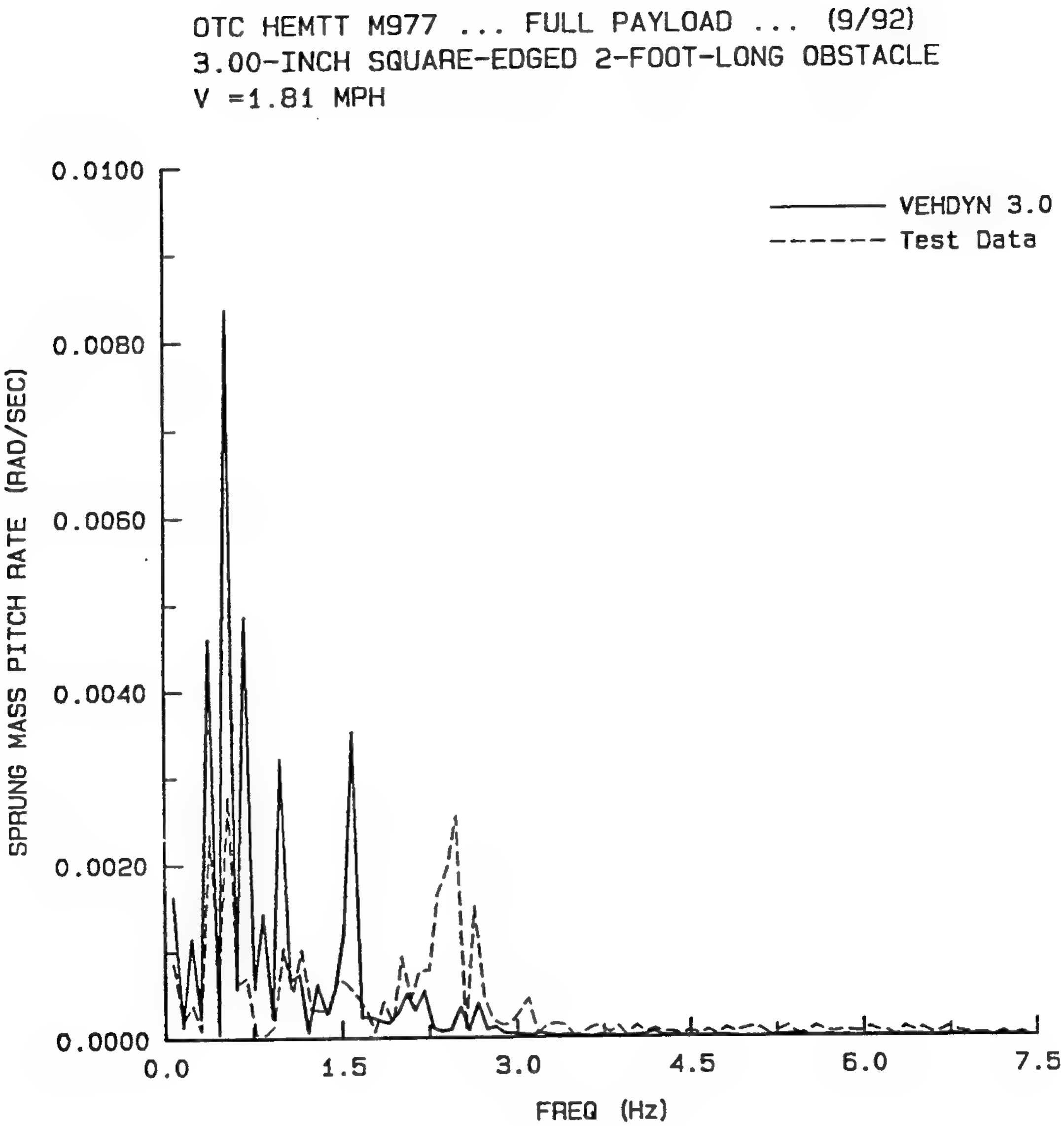

Figure A-62. Sprung mass pitch rate frequency plot for a fully loaded HEMTT traveling at 1.81 miles per hour encountering a 3.00-inch-high obstacle.

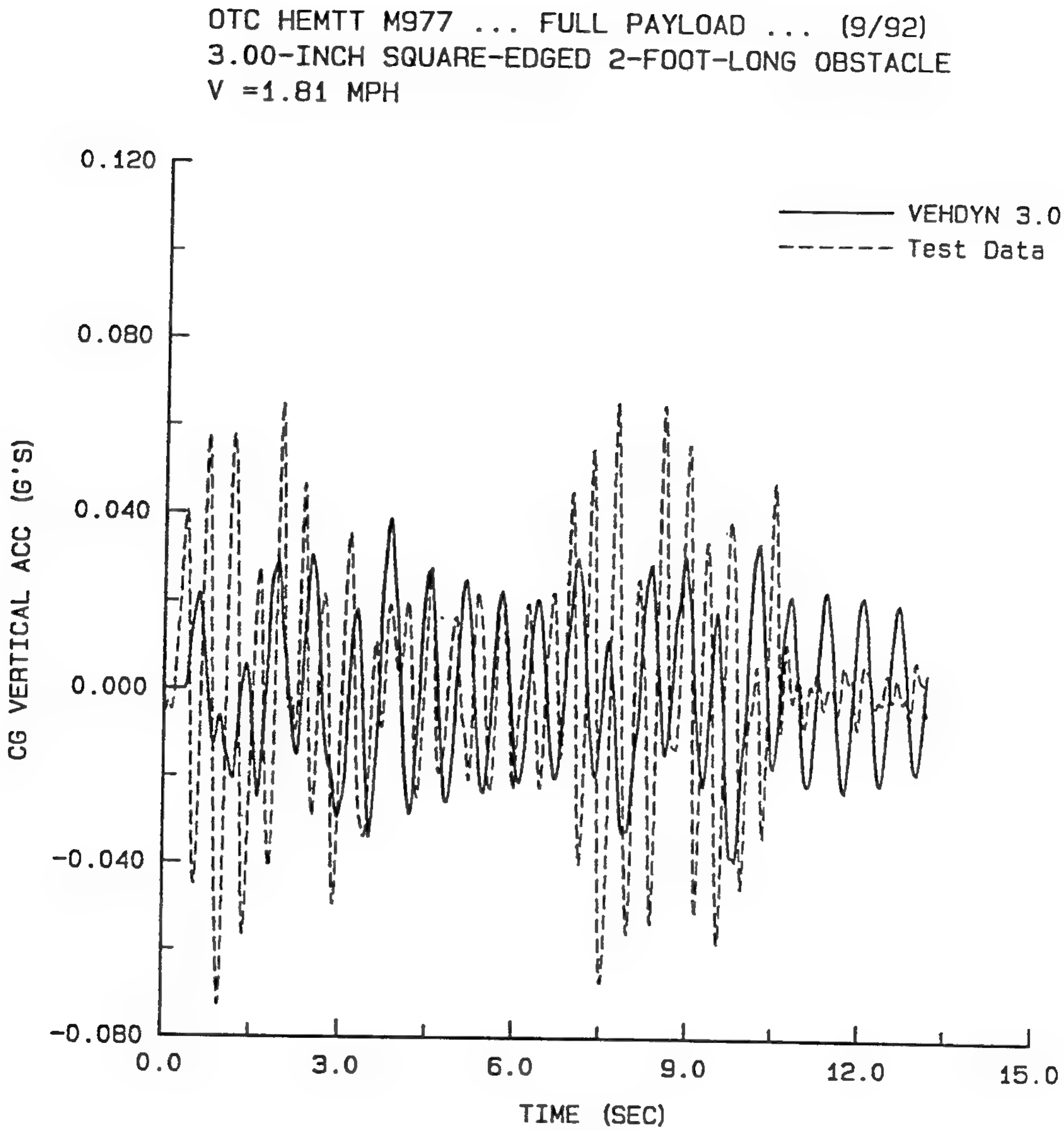

Figure A-63. CG vertical acceleration time history for a fully loaded HEMTT traveling at 1.81 miles per hour encountering a 3.00-inch-high obstacle.

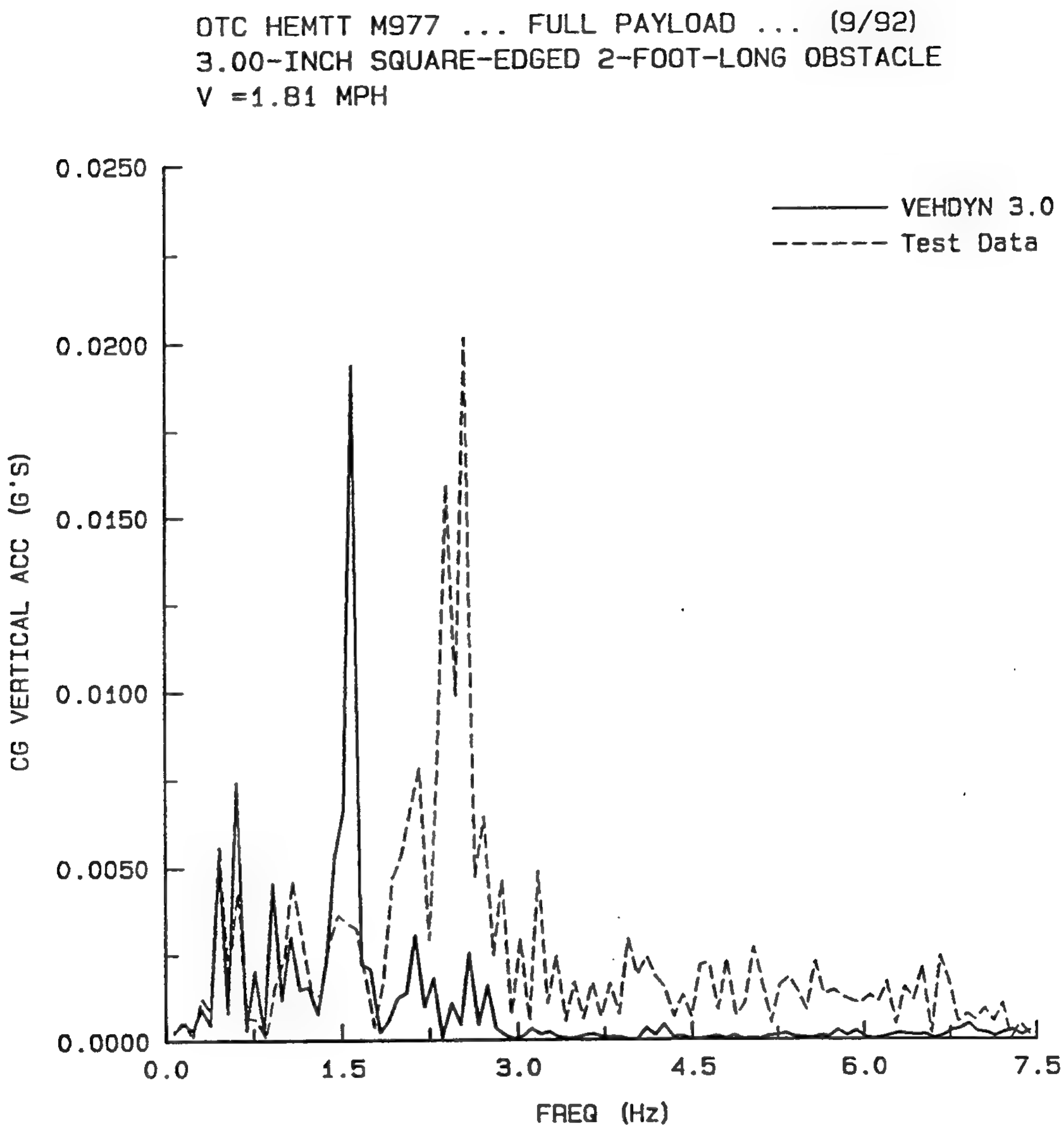

Figure A-64. CG vertical acceleration frequency plot (frequency scale = 1.5 Hz/inch) for a fully loaded HEMTT traveling at 1.81 miles per hour encountering a 3.00-inch-high obstacle.

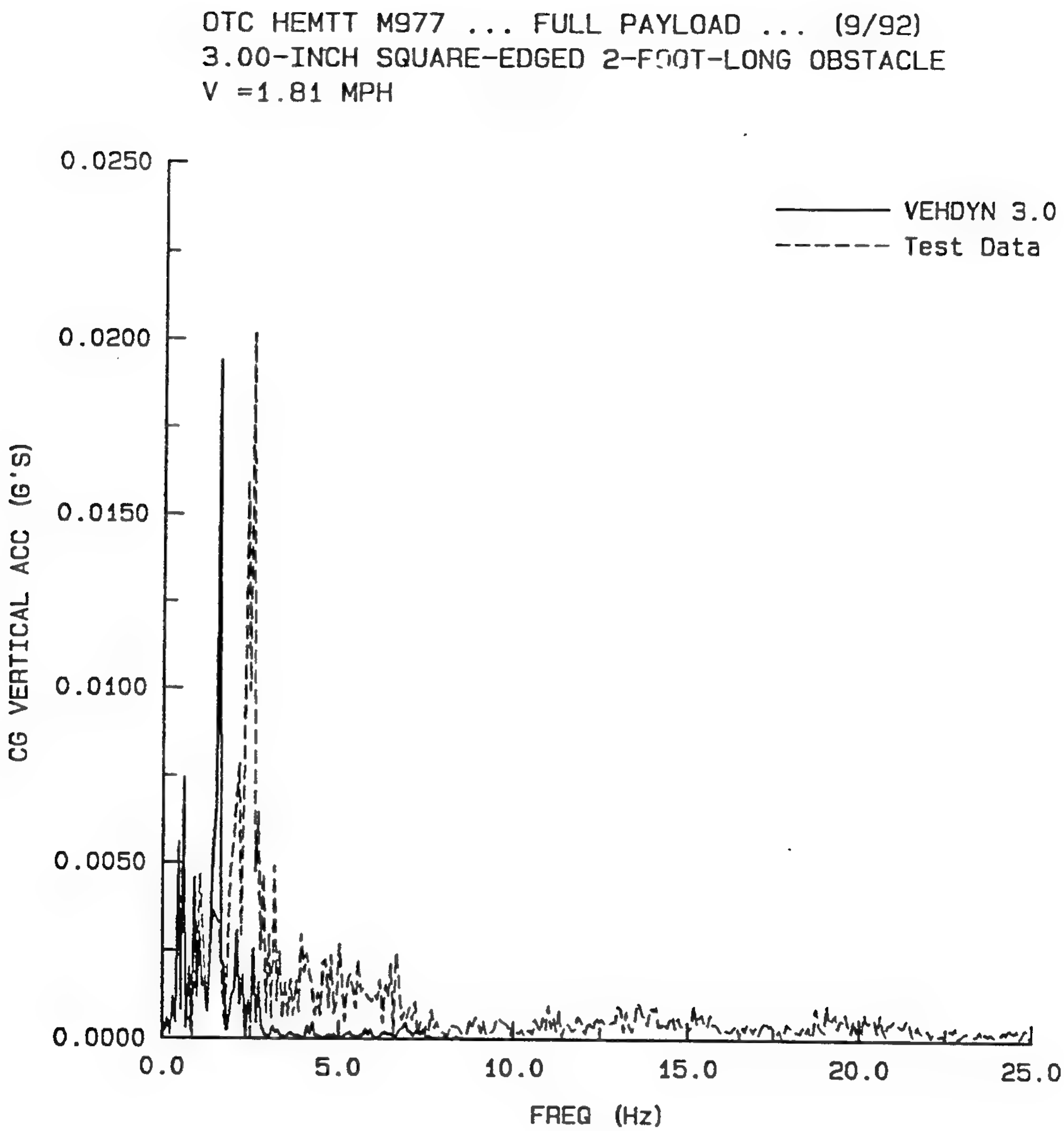

Figure A-65. CG vertical acceleration frequency plot (frequency scale = 5.0 Hz/inch) for a fully loaded HEMTT traveling at 1.81 miles per hour encountering a 3.00-inch-high obstacle.

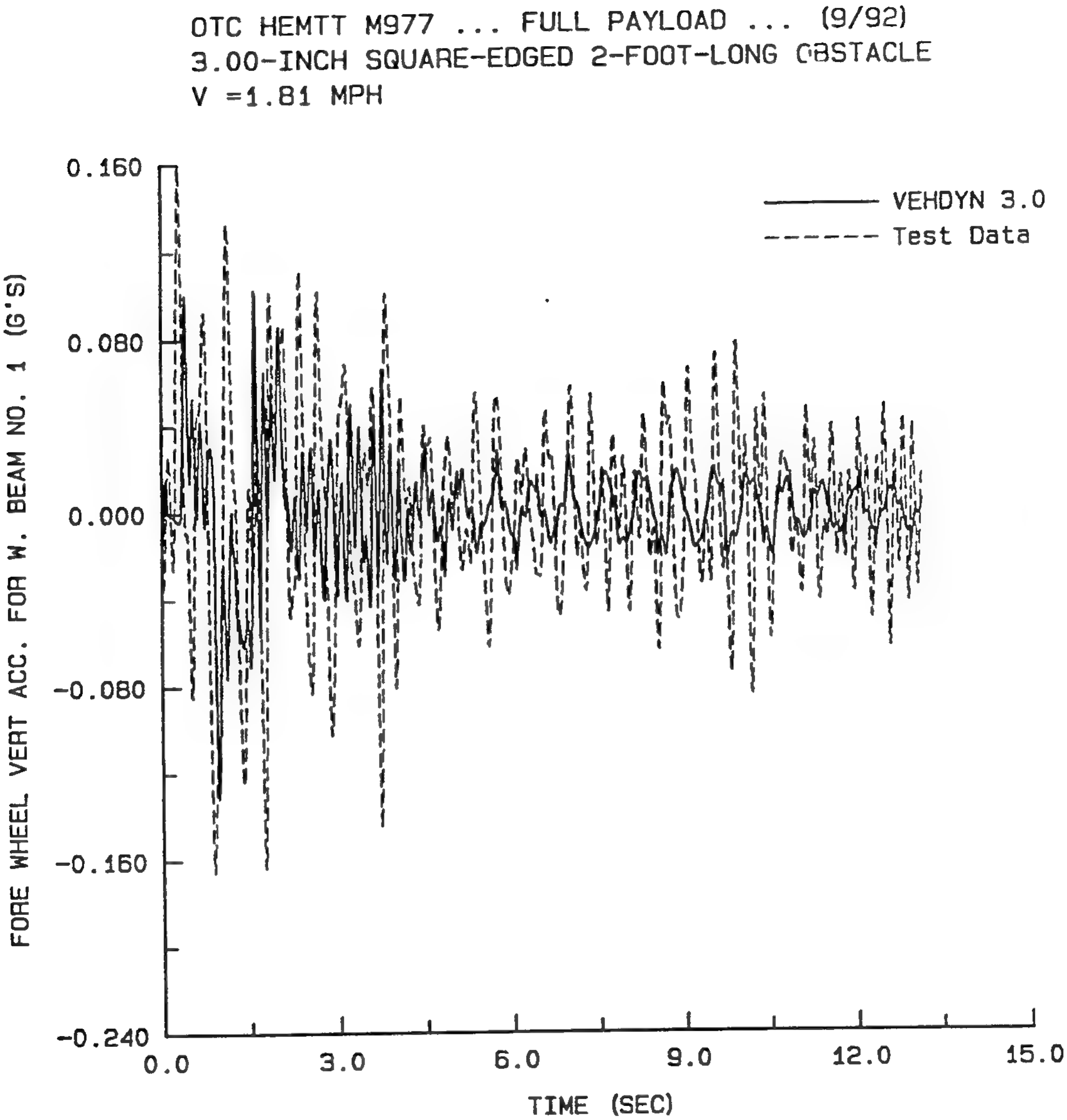

Figure A-66. Vertical acceleration time history of the forward-most axle for a fully loaded HEMTT traveling at 1.81 miles per hour encountering a 3.00-inch-high obstacle.

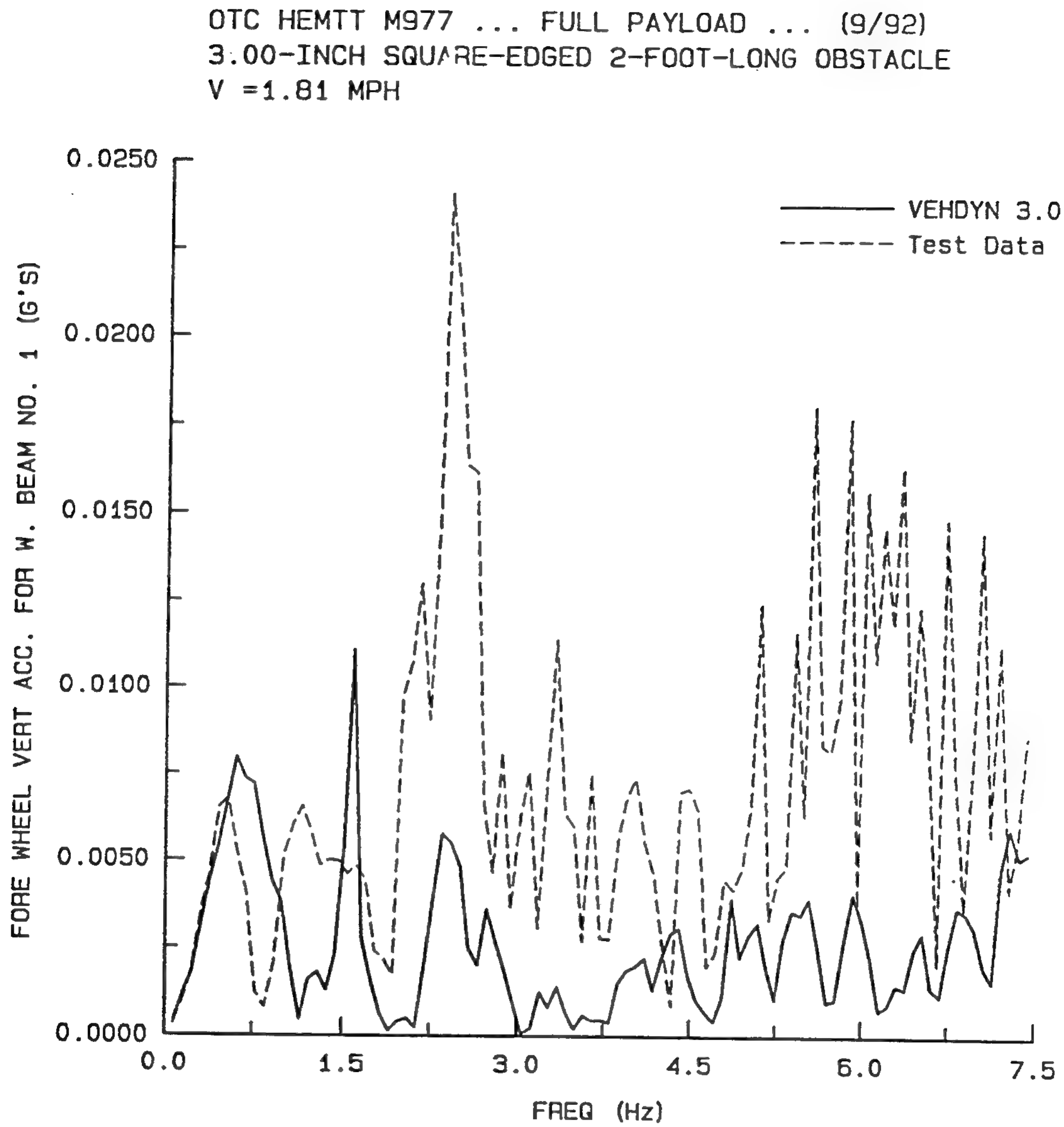

Figure A-67. Vertical acceleration frequency plot (frequency scale = 1.5 Hz/inch) of the forward-most axle for a fully loaded HEMTT traveling at 1.81 miles per hour encountering a 3.00-inch-high obstacle.

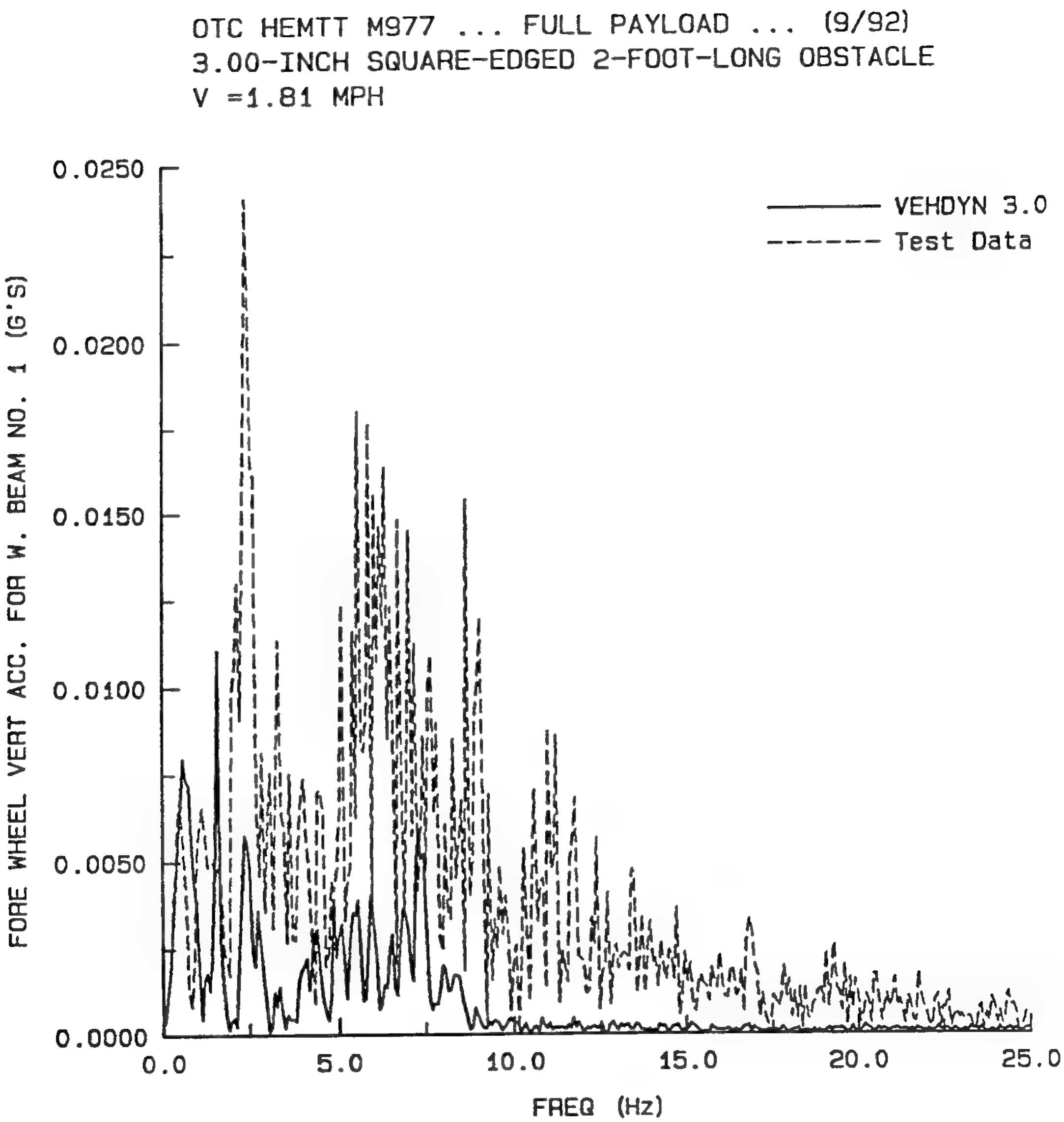

Figure A-68. Vertical acceleration frequency plot (frequency scale = 5.0 Hz/inch) of the forward-most axle for a fully loaded HEMTT traveling at 1.81 miles per hour encountering a 3.00-inch-high obstacle.

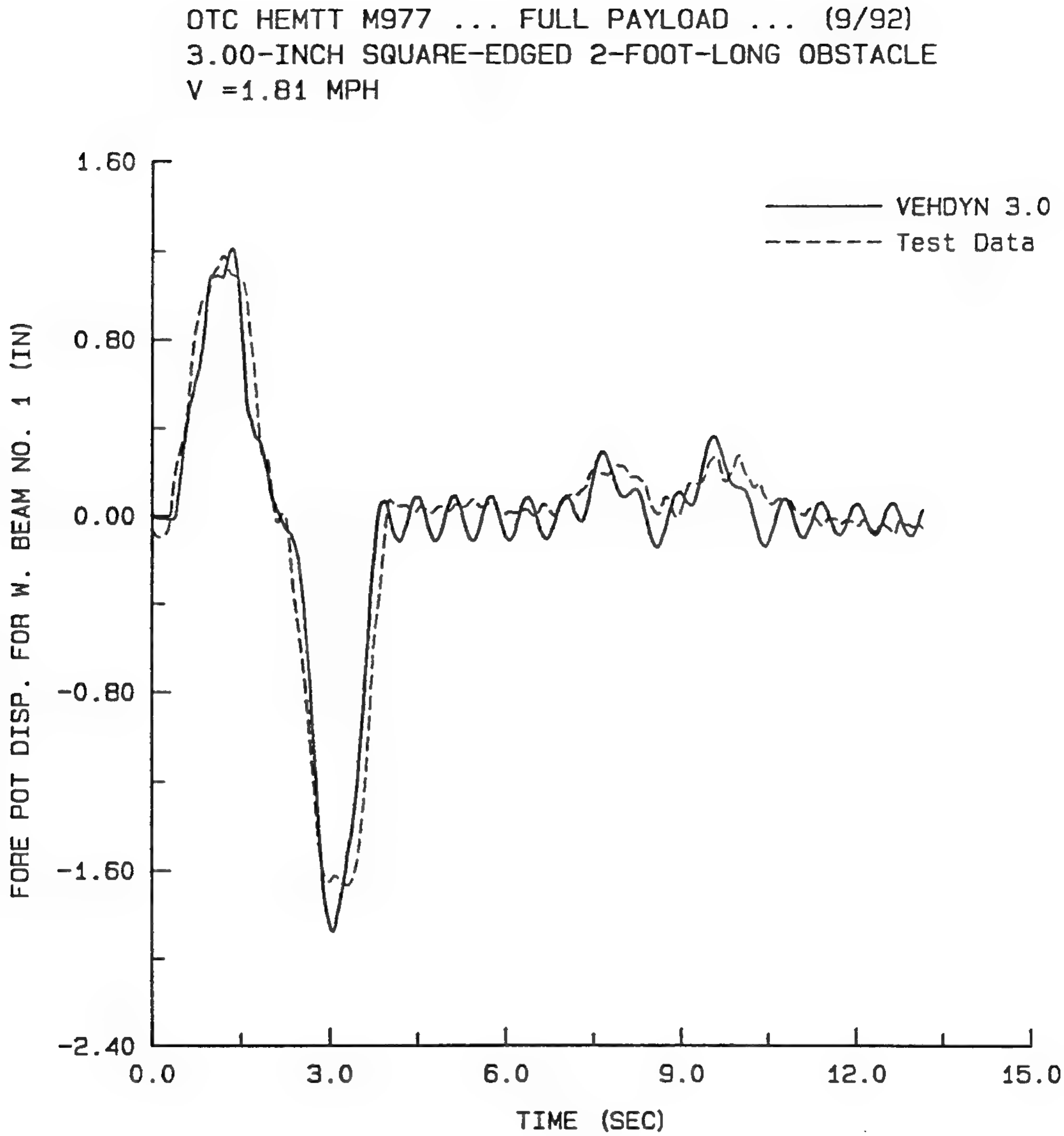

Figure A-69. Relative displacement time history of the forward-most axle with respect to the frame for a fully loaded HEMTT traveling at 1.81 miles per hour encountering a 3.00-inch-high obstacle.

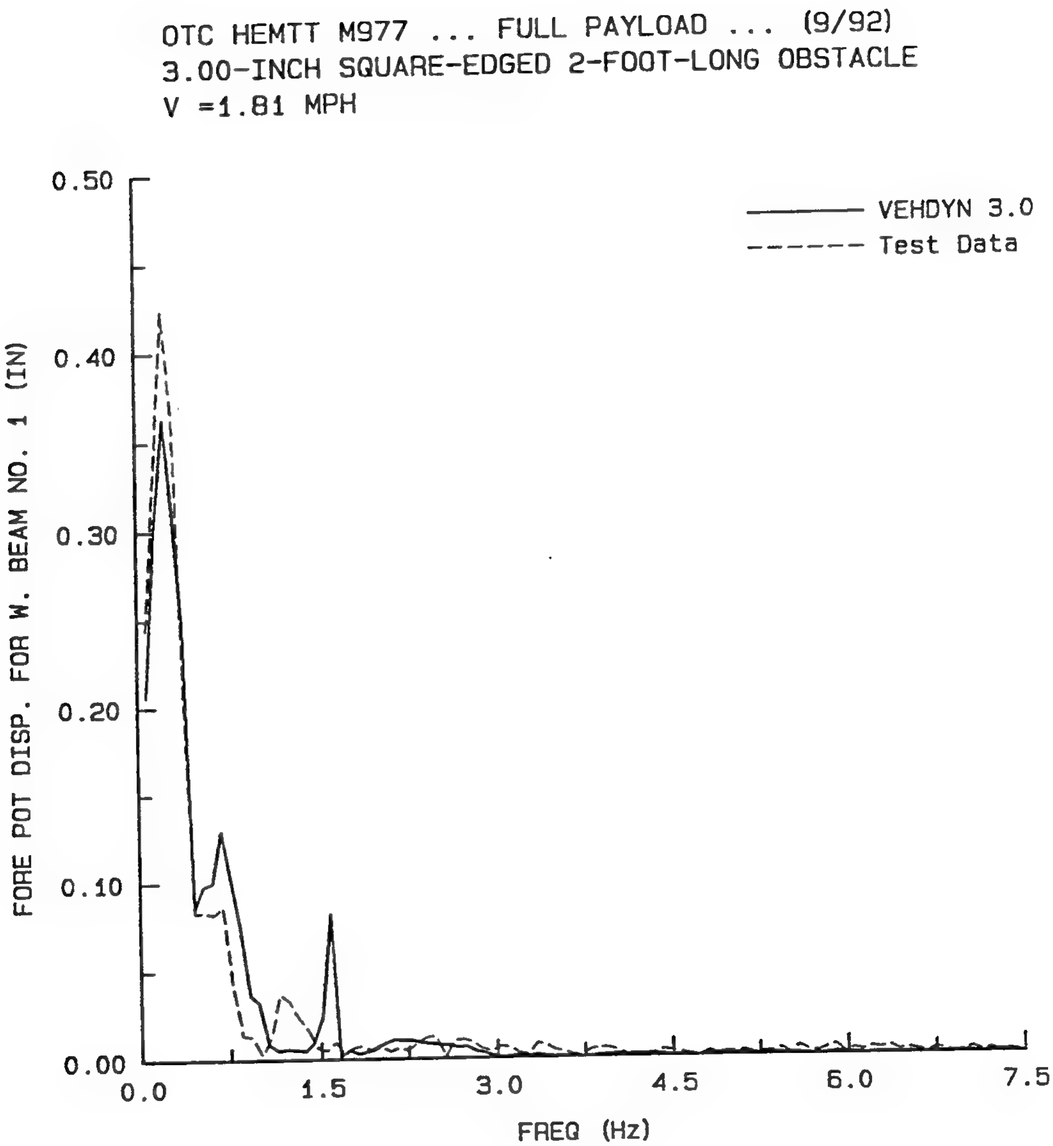

Figure A-70. Relative displacement frequency plot (frequency scale = 1.5 Hz/inch) of the forward-most axle with respect to the frame for a fully loaded HEMTT traveling at 1.81 miles per hour encountering a 3.00-inch-high obstacle.

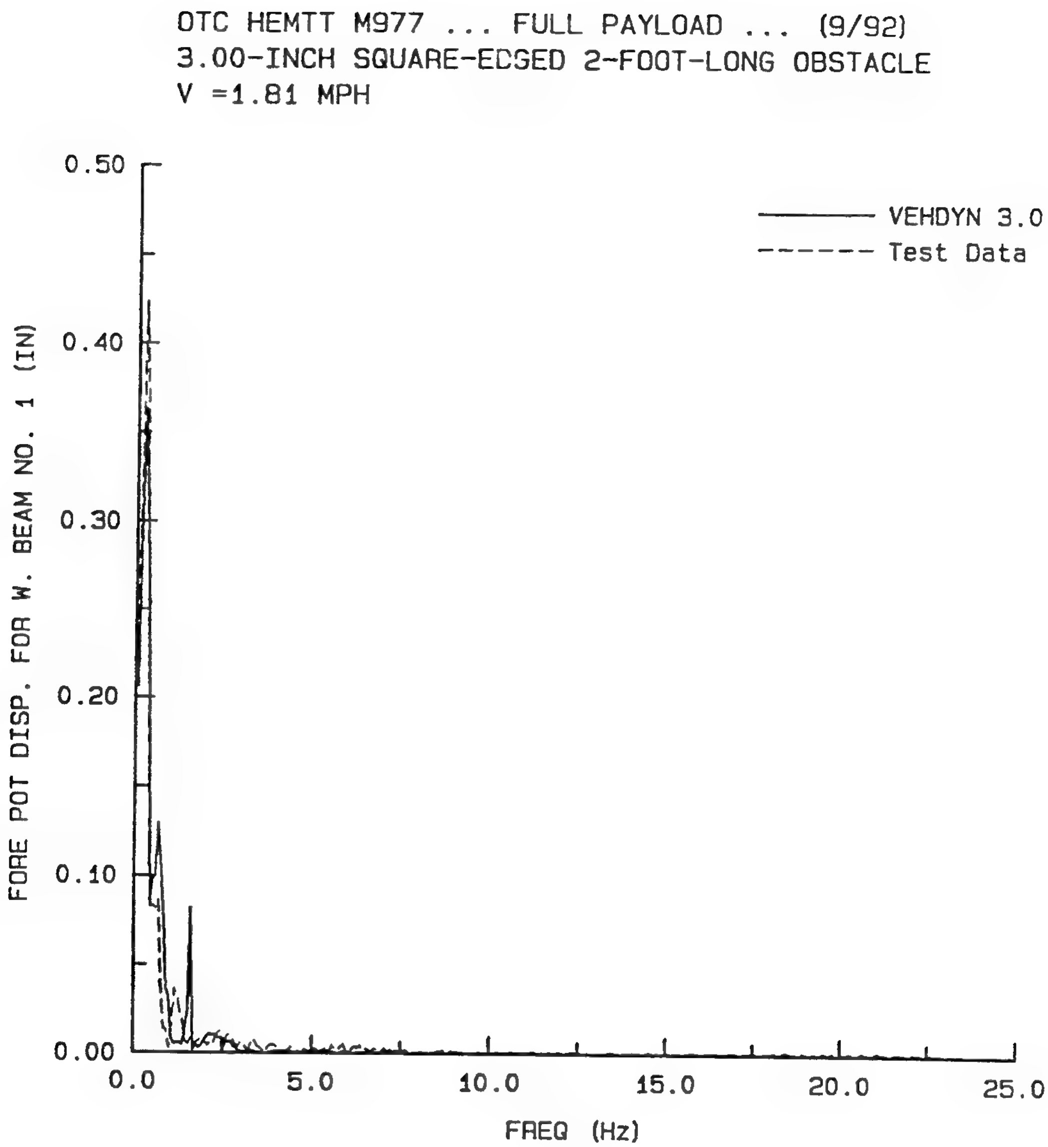

Figure A-71. Relative displacement frequency plot (frequency scale = 5.0 Hz/inch) of the forward-most axle with respect to the frame for a fully loaded HEMTT traveling at 1.81 miles per hour encountering a 3.00-inch-high obstacle.

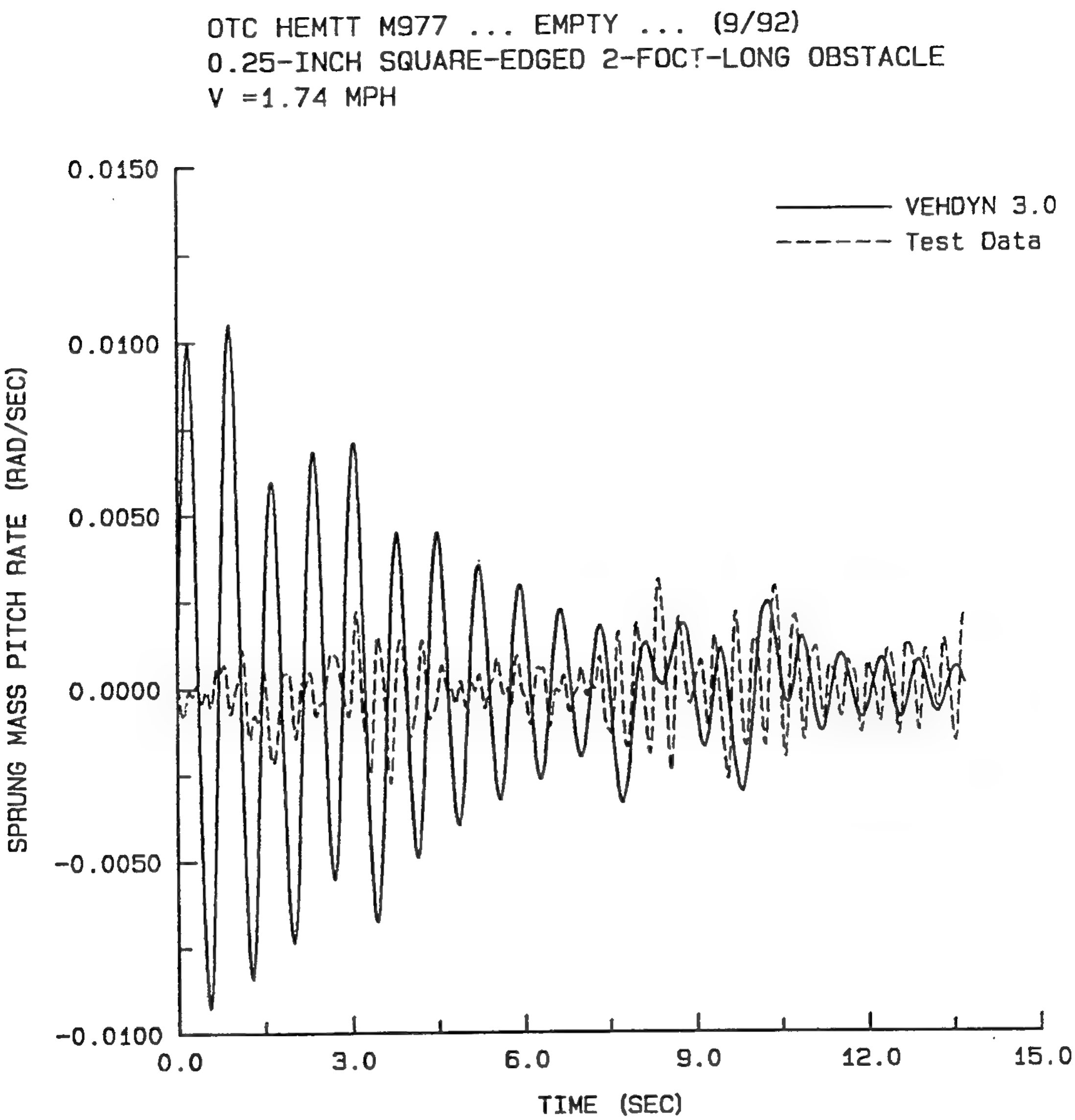

Figure A-72. Sprung mass pitch rate time history for an empty HEMTT traveling at 1.74 miles per hour encountering a 0.25-inch-high obstacle.

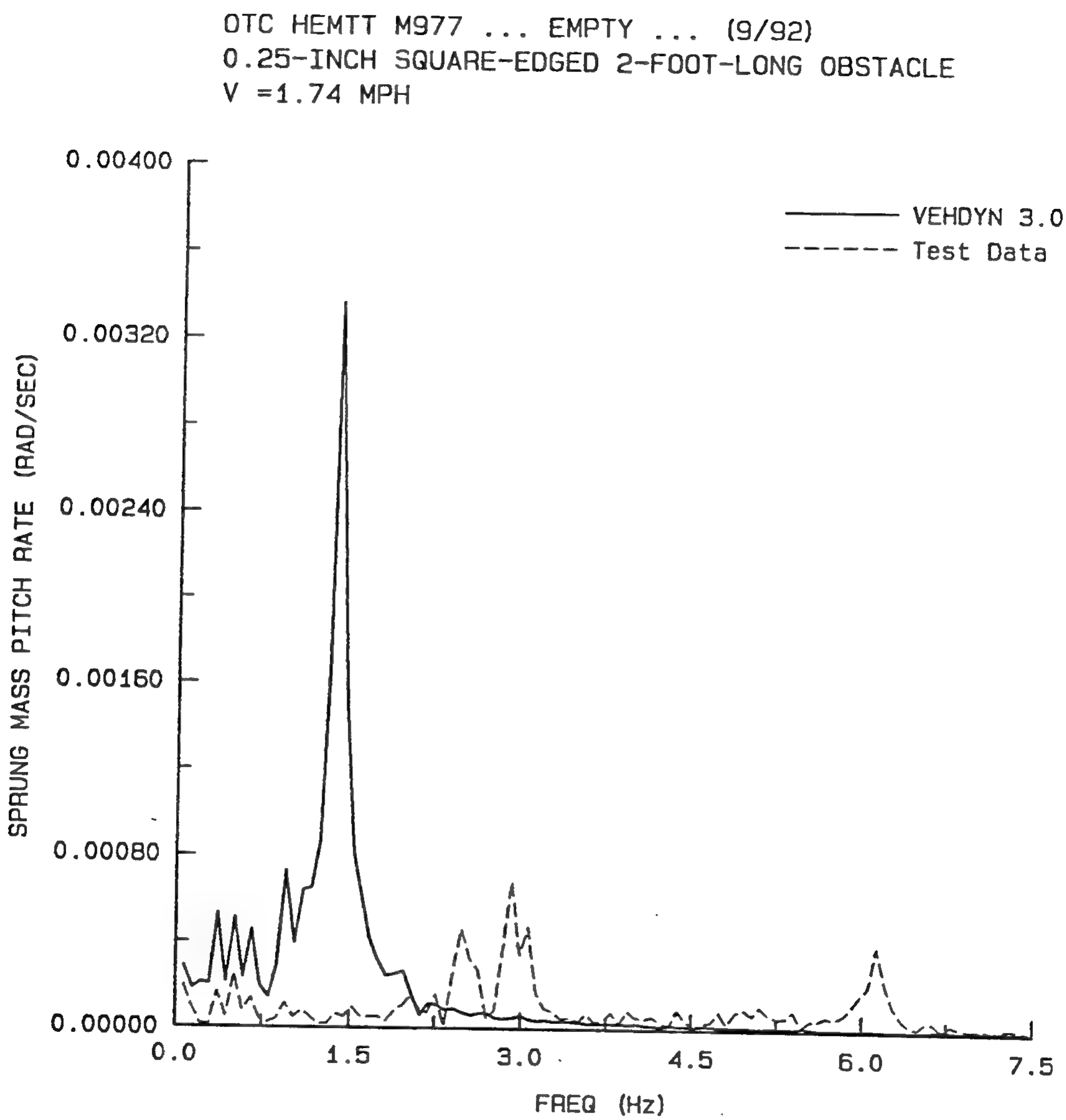

Figure A-73. Sprung mass pitch rate frequency plot for an empty HEMTT traveling at 1.74 miles per hour encountering a 0.25-inch-high obstacle.

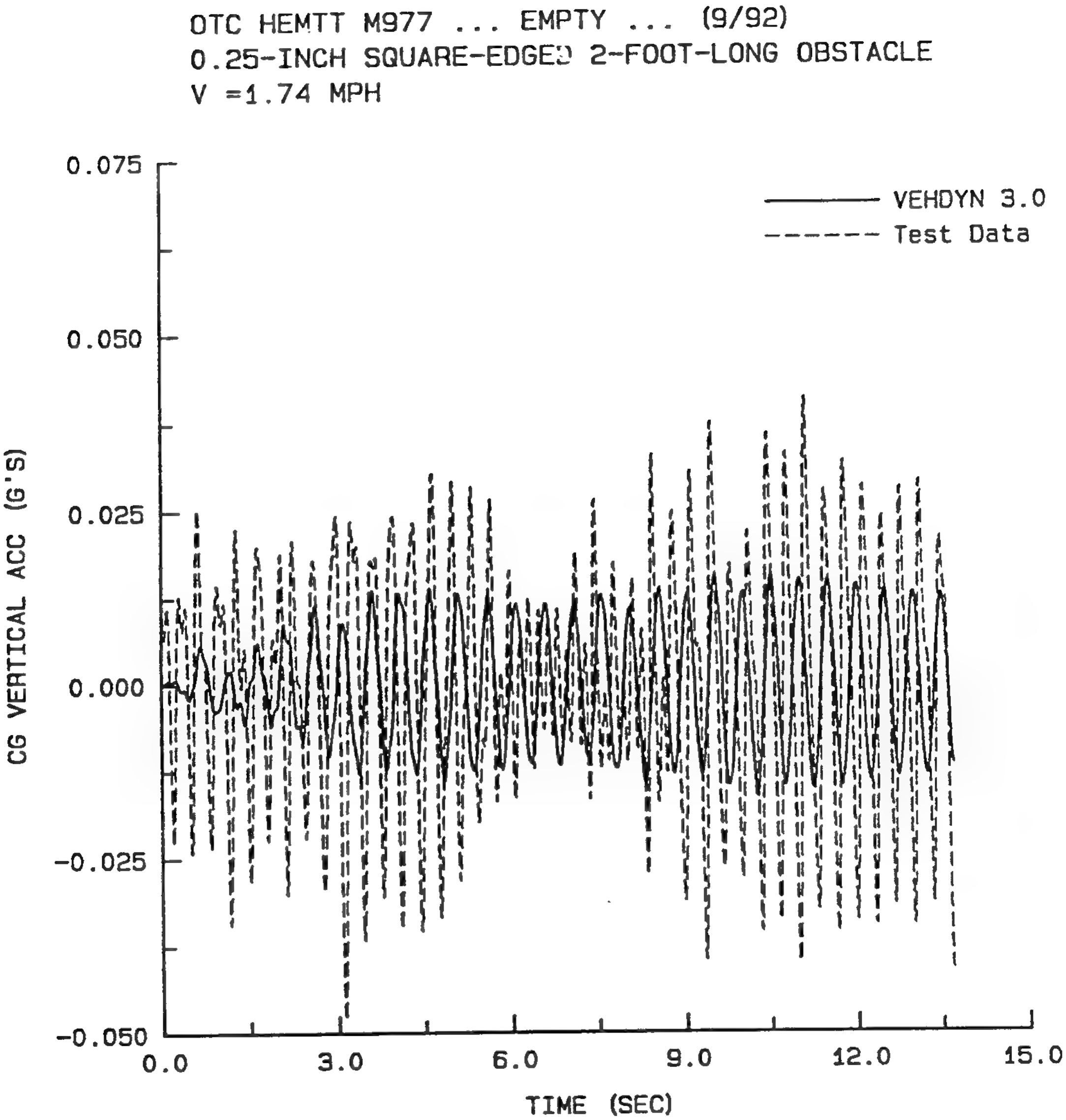

Figure A-74. CG vertical acceleration time history for an empty HEMTT traveling at 1.74 miles per hour encountering a 0.25-inch-high obstacle.

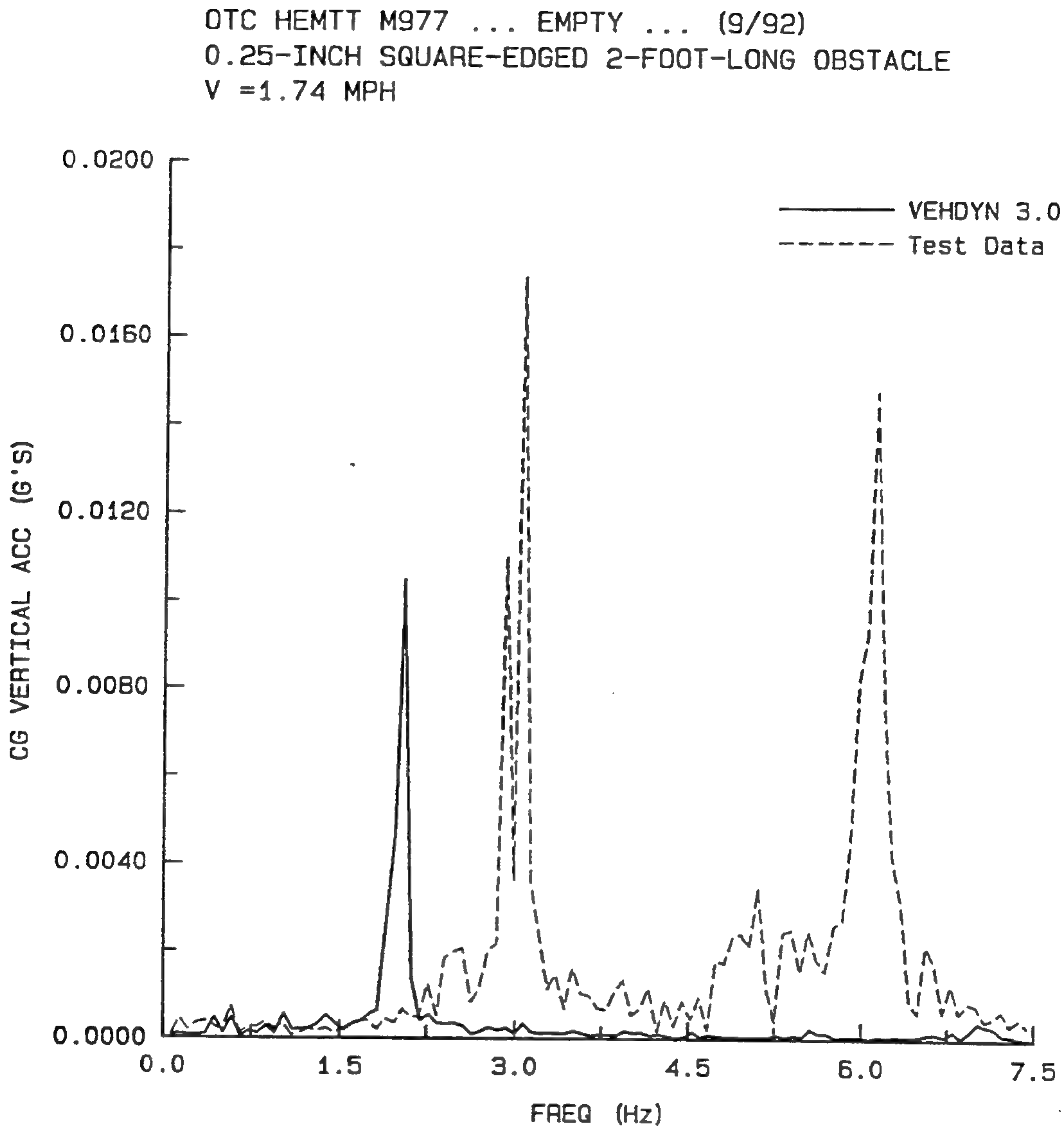

Figure A-75. CG vertical acceleration frequency plot (frequency scale = 1.5 Hz/inch) for an empty HEMTT traveling at 1.74 miles per hour encountering a 0.25-inch-high obstacle.

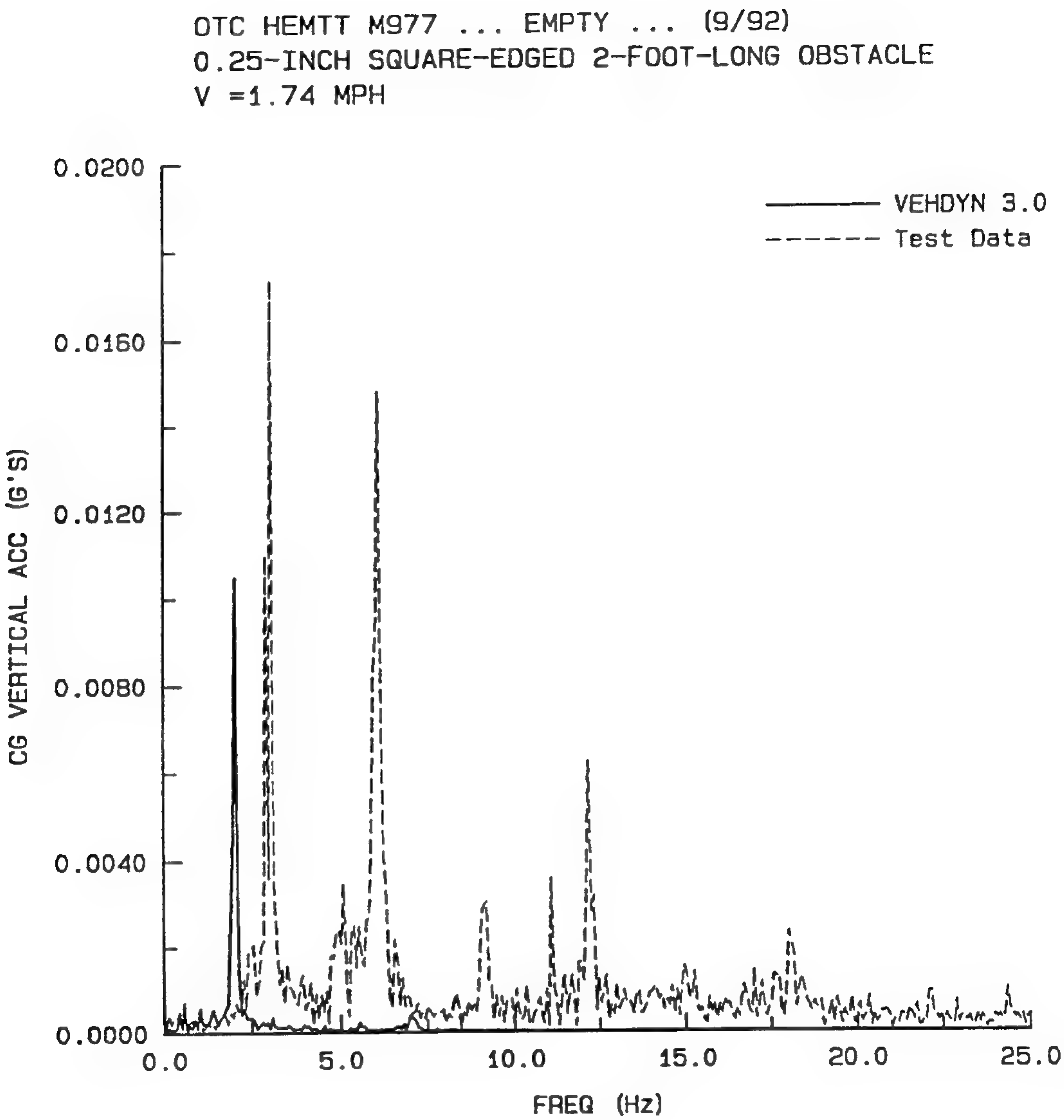

Figure A-76. CG vertical acceleration frequency plot (frequency scale = 5.0 Hz/inch) for an empty HEMTT traveling at 1.74 miles per hour encountering a 0.25-inch-high obstacle.

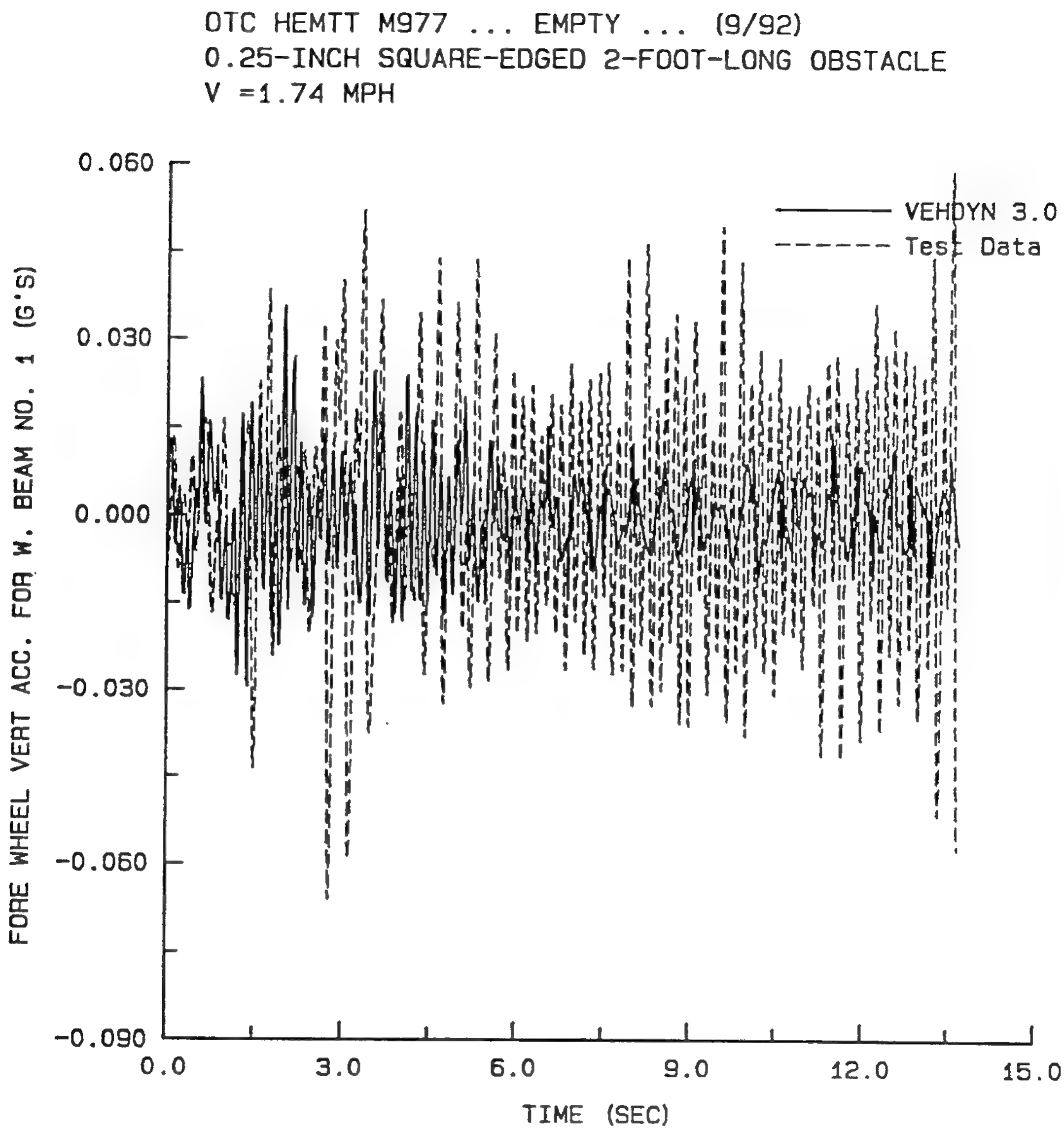

Figure A-77. Vertical acceleration time history of the forward-most axle for an empty HEMTT traveling at 1.74 miles per hour encountering a 0.25-inch-high obstacle.

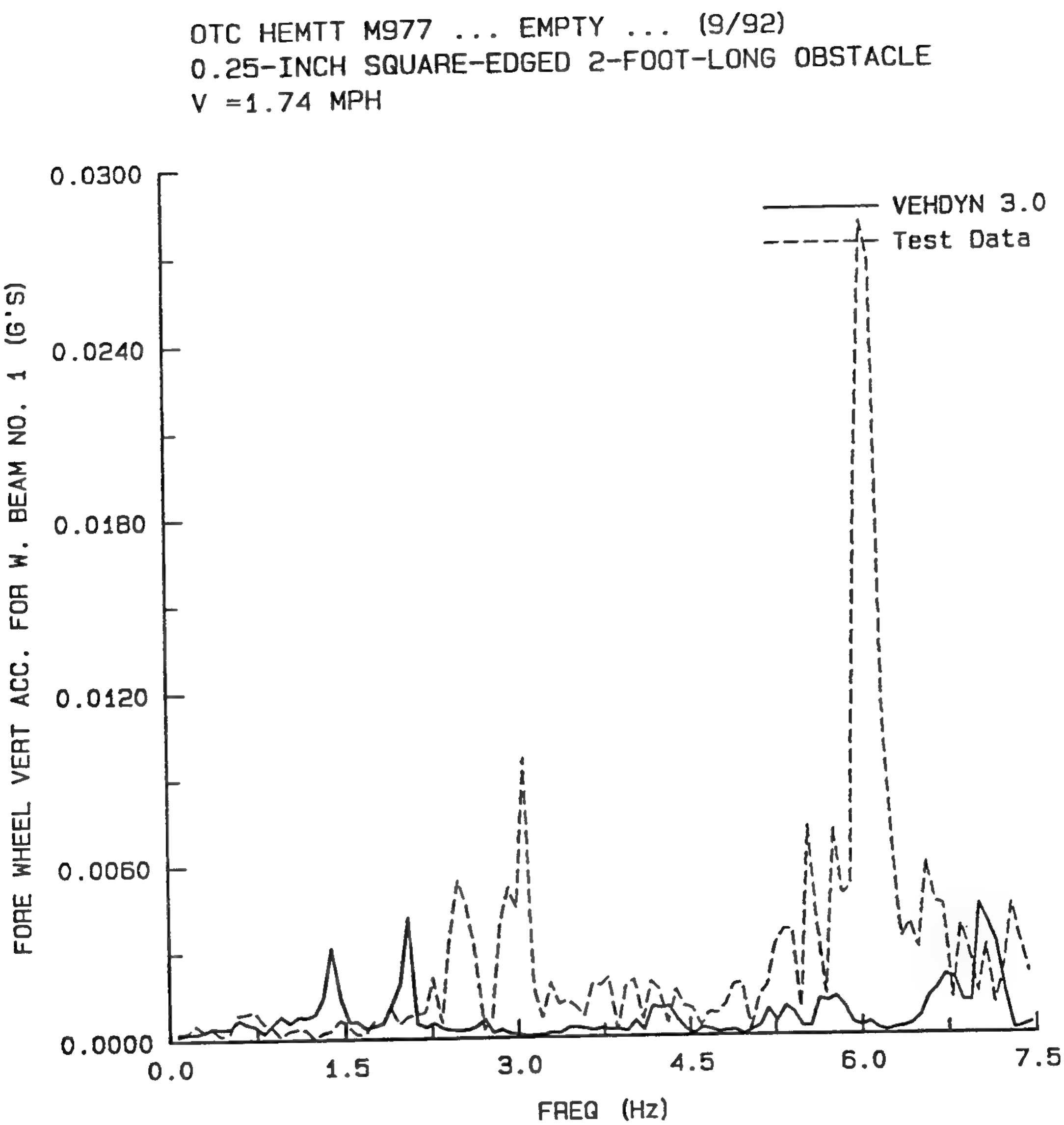

Figure A-78. Vertical acceleration frequency plot (frequency scale = 1.5 Hz/inch) of the forward-most axle for an empty HEMTT traveling at 1.74 miles per hour encountering a 0.25-inch-high obstacle.

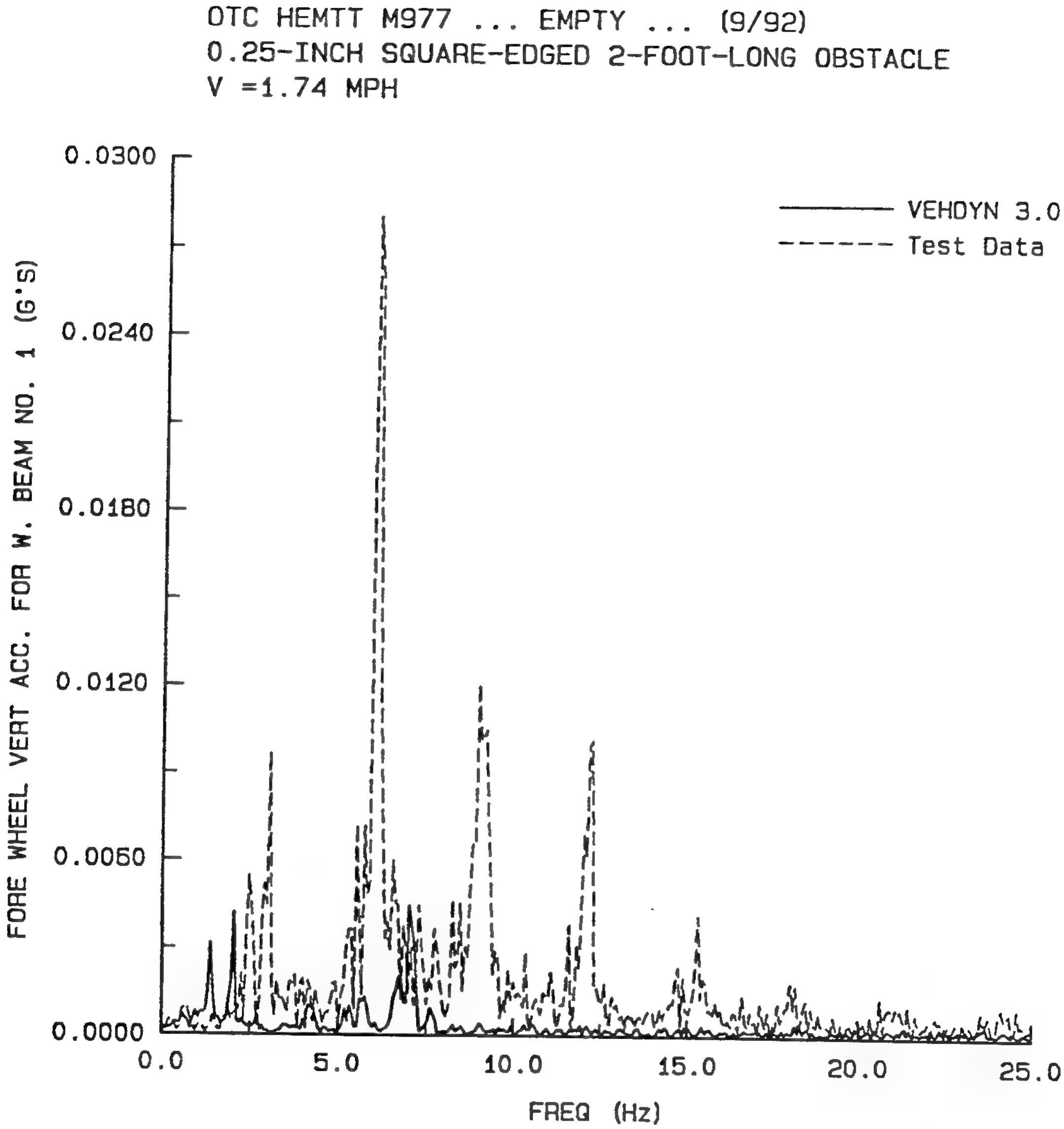

Figure A-79. Vertical acceleration frequency plot (frequency scale = 5.0 Hz/inch) of the forward-most axle for an empty HEMTT traveling at 1.74 miles per hour encountering a 0.25-inch-high obstacle.

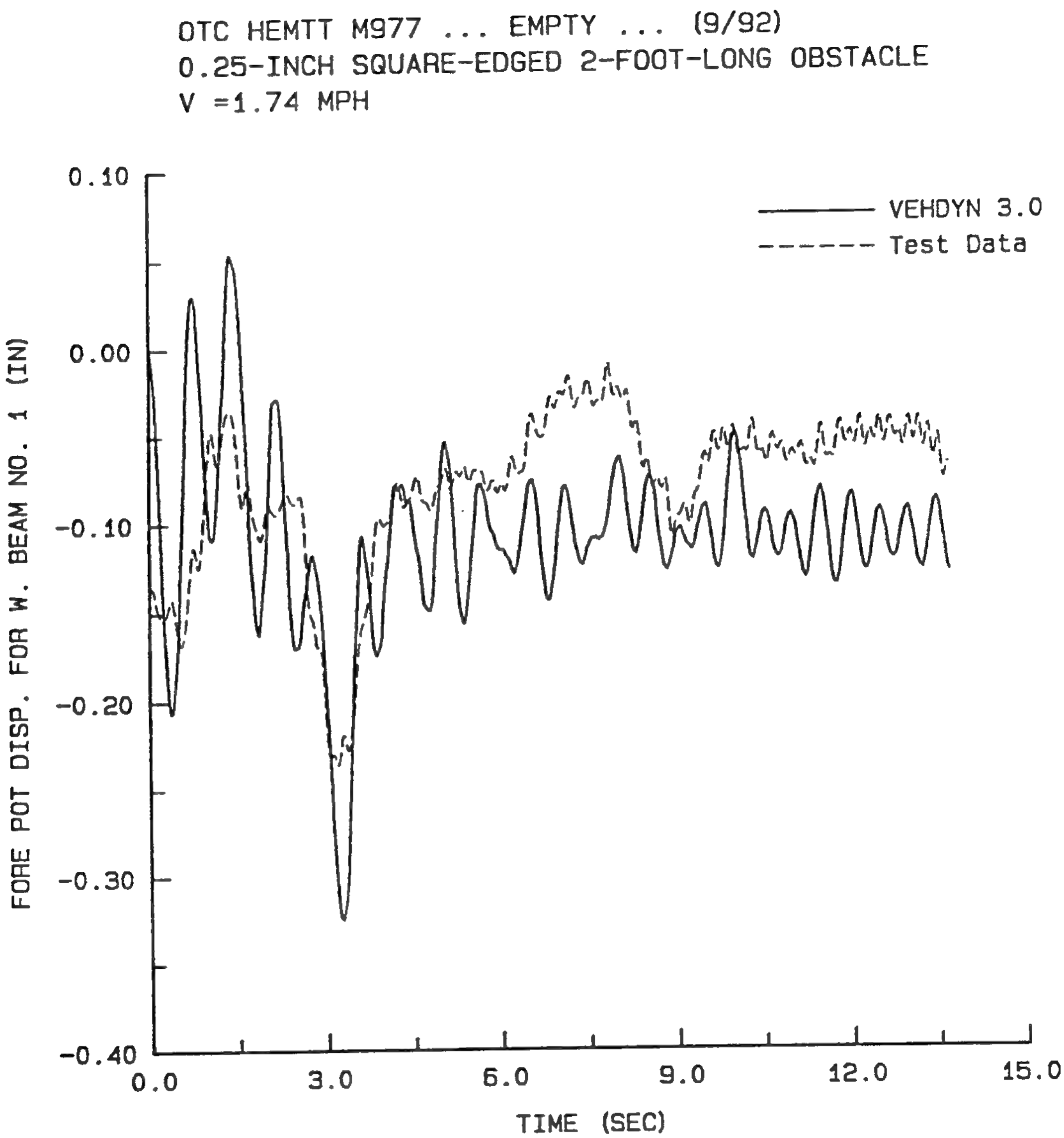

Figure A-80. Relative displacement time history of the forward-most axle with respect to the frame for an empty HEMTT traveling at 1.74 miles per hour encountering a 0.25-inch-high obstacle.

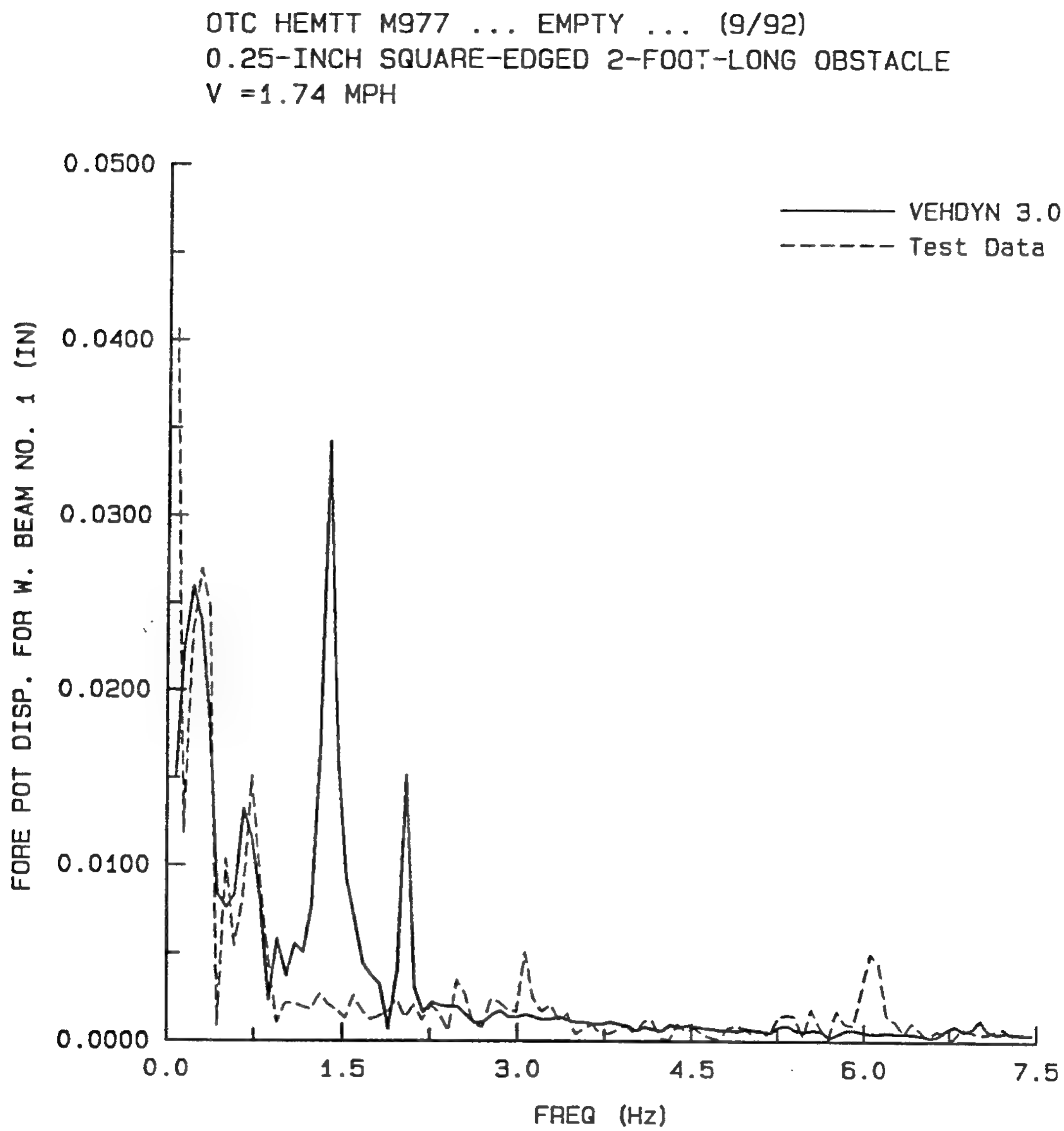

Figure A-81. Relative displacement frequency plot (frequency scale = 1.5 Hz/inch) of the forward-most axle with respect to the frame for an empty HEMTT traveling at 1.74 miles per hour encountering a 0.25-inch-high obstacle.

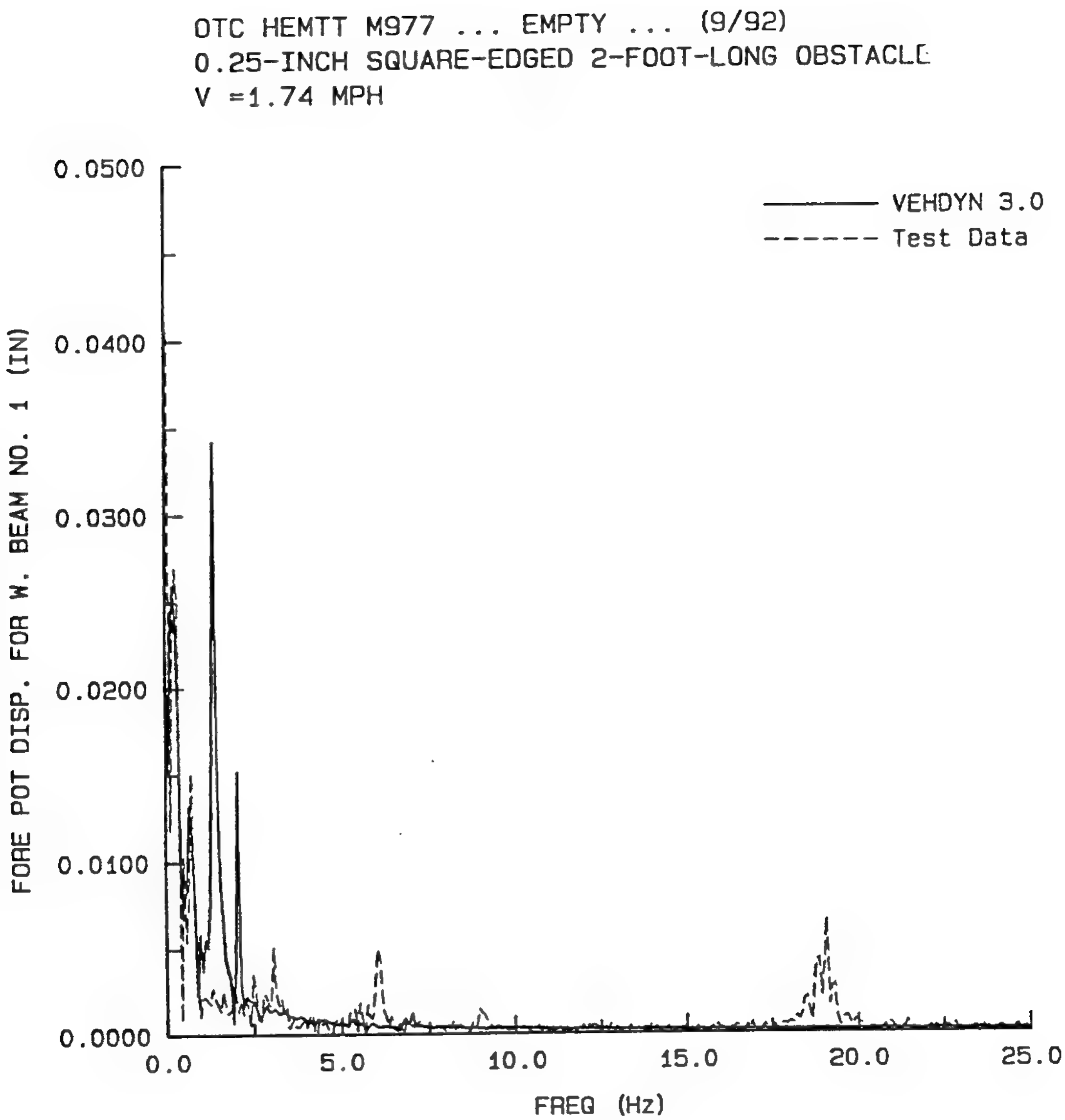

Figure A-82. Relative displacement frequency plot (frequency scale = 5.0 Hz/inch) of the forward-most axle with respect to the frame for an empty HEMTT traveling at 1.74 miles per hour encountering a 0.25-inch-high obstacle.

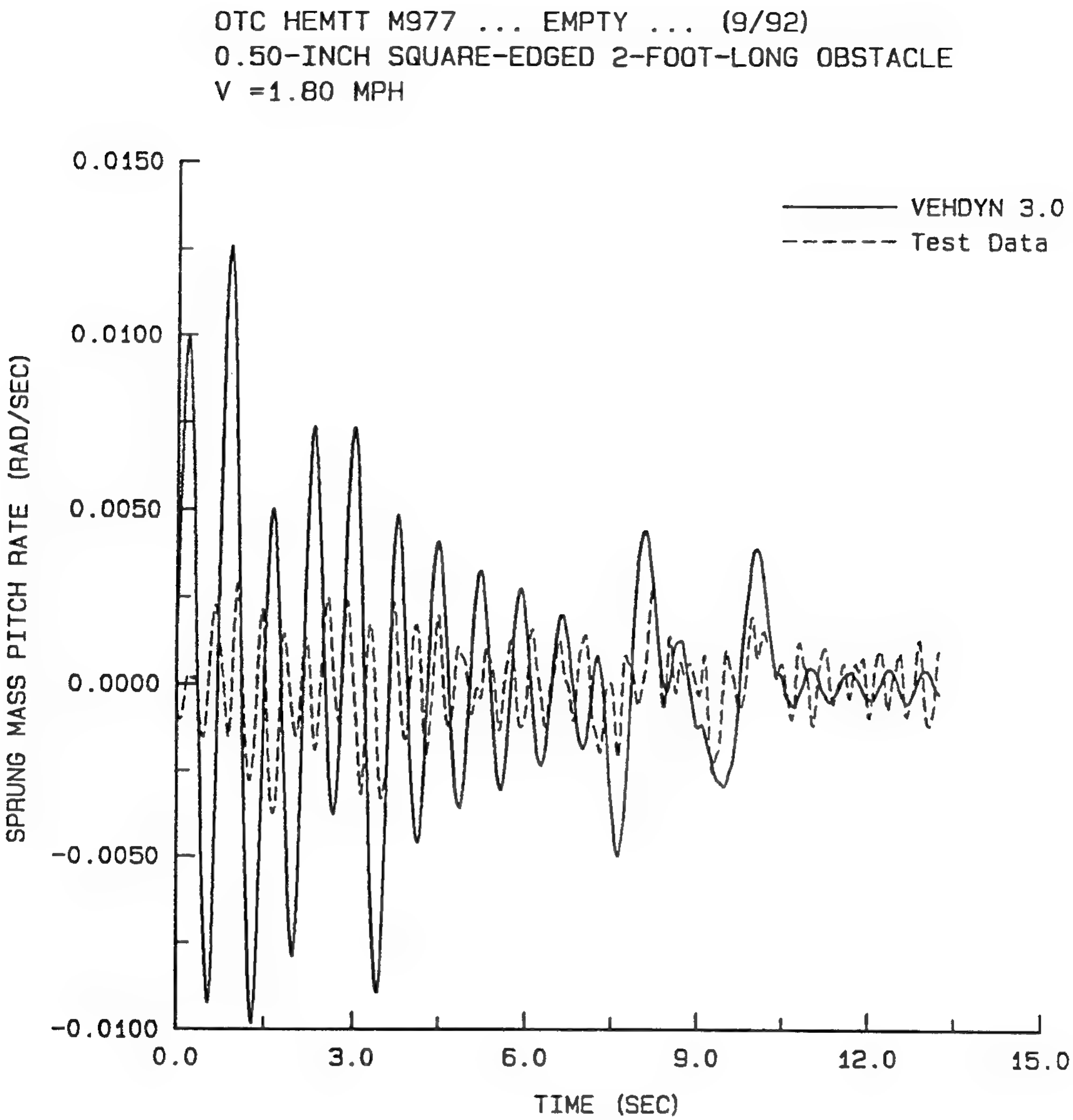

Figure A-83. Sprung mass pitch rate time history for an empty HEMTT traveling at 1.80 miles per hour encountering a 0.50-inch-high obstacle.

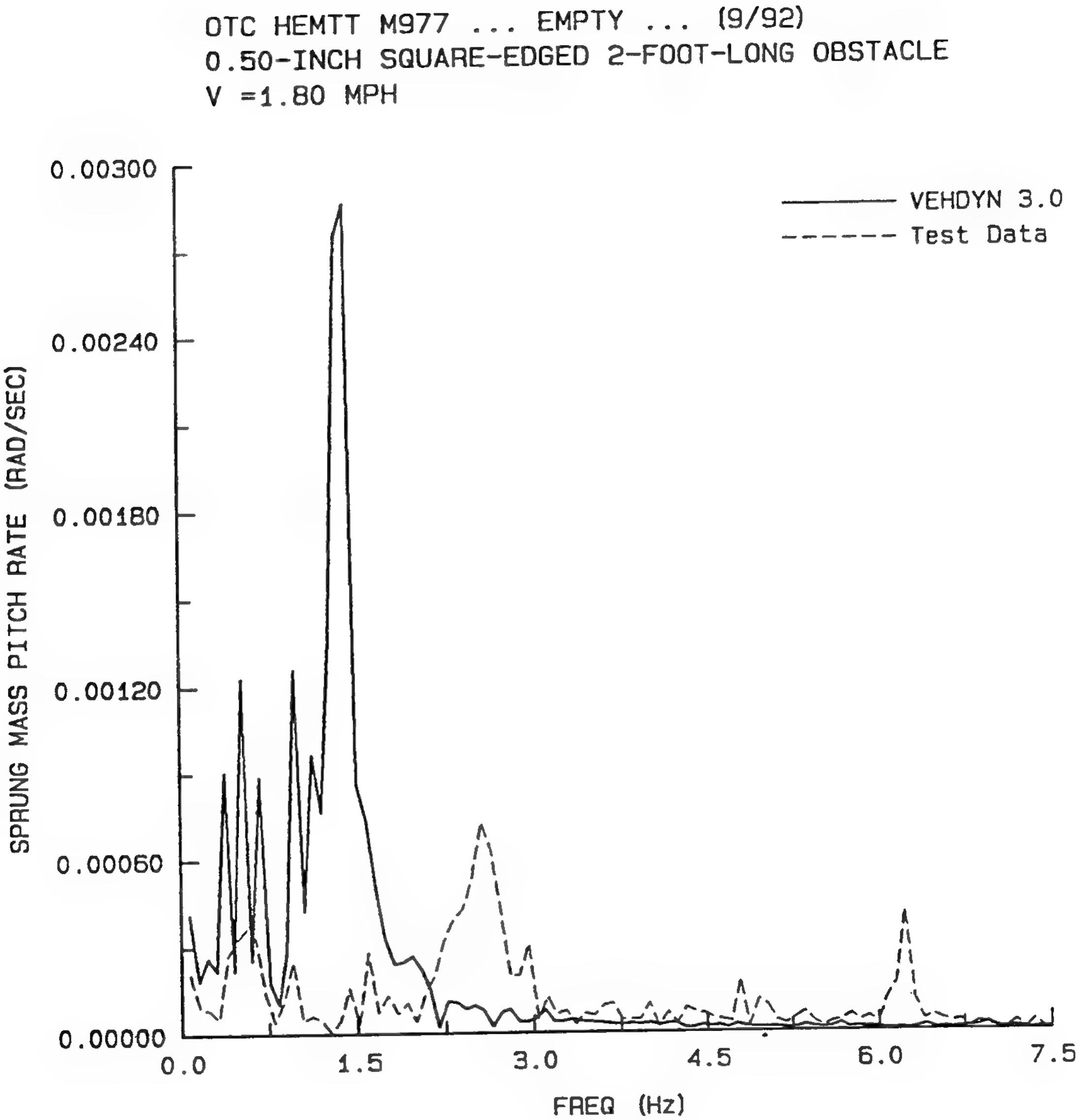

Figure A-84. Sprung mass pitch rate frequency plot for an empty HEMTT traveling at 1.80 miles per hour encountering a 0.50-inch-high obstacle.

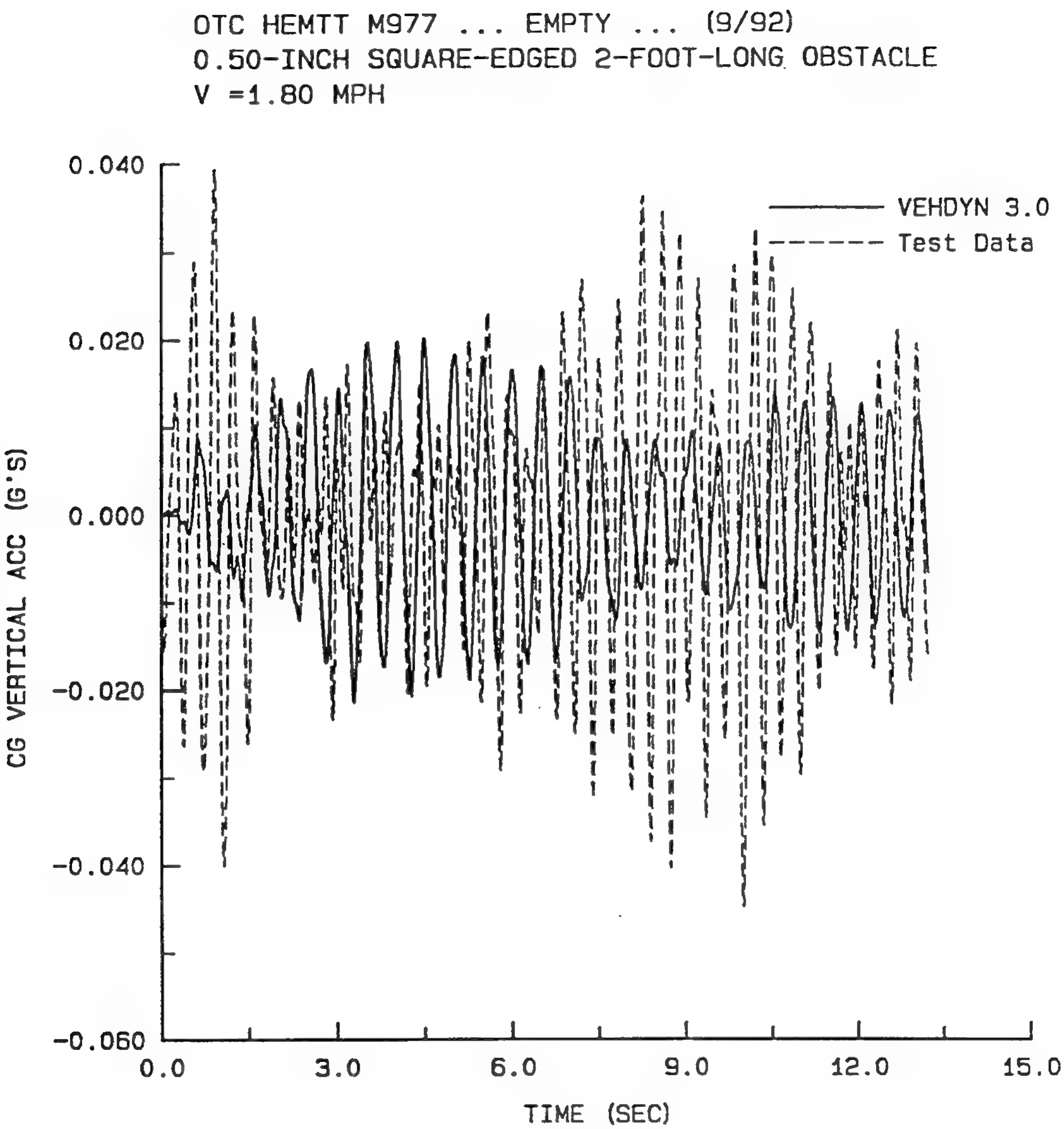

Figure A-85. CG vertical acceleration time history for an empty HEMTT traveling at 1.80 miles per hour encountering a 0.50-inch-high obstacle.

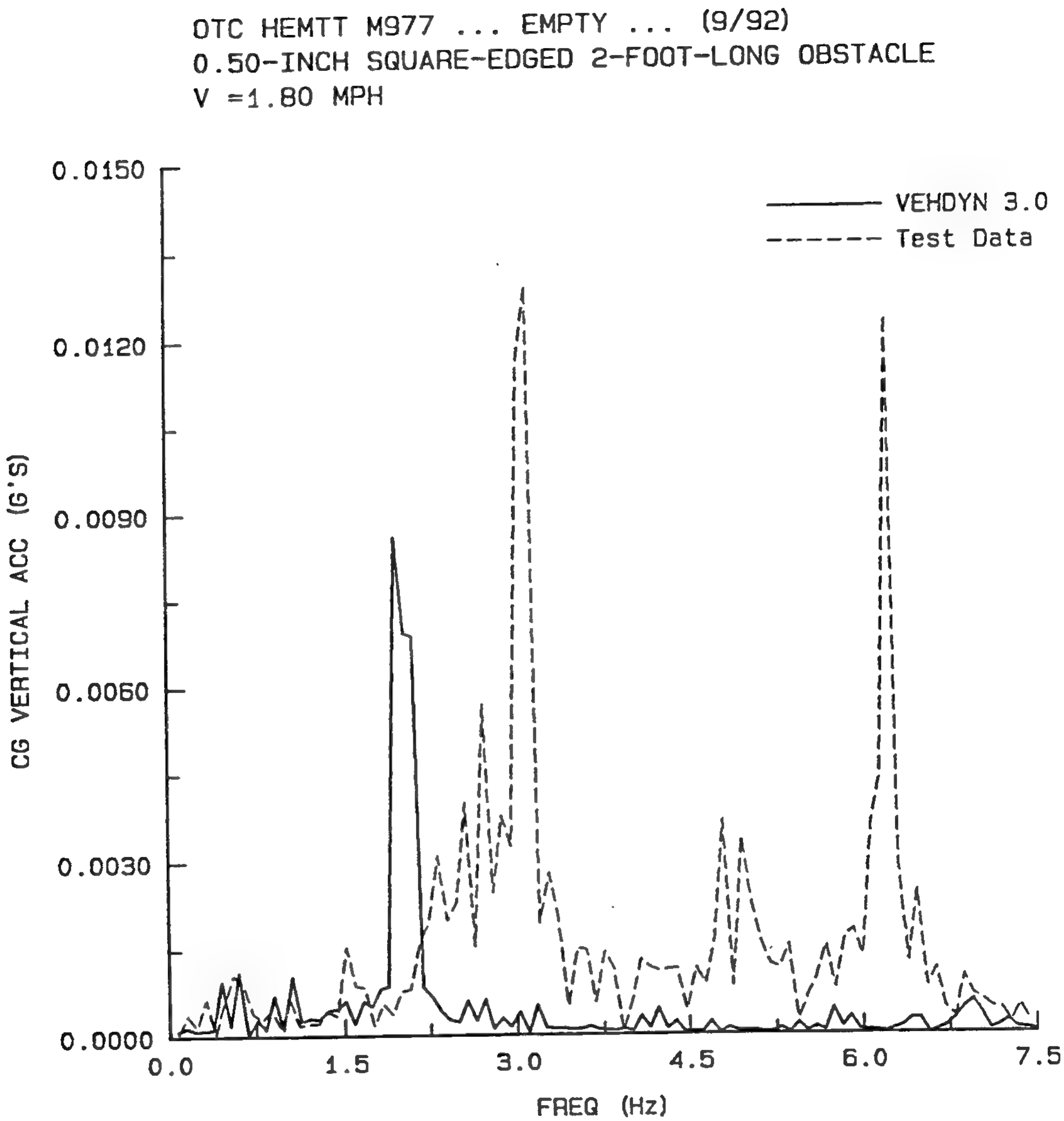

Figure A-86. CG vertical acceleration frequency plot (frequency scale = 1.5 Hz/inch) for an empty HEMTT traveling at 1.80 miles per hour encountering a 0.50-inch-high obstacle.

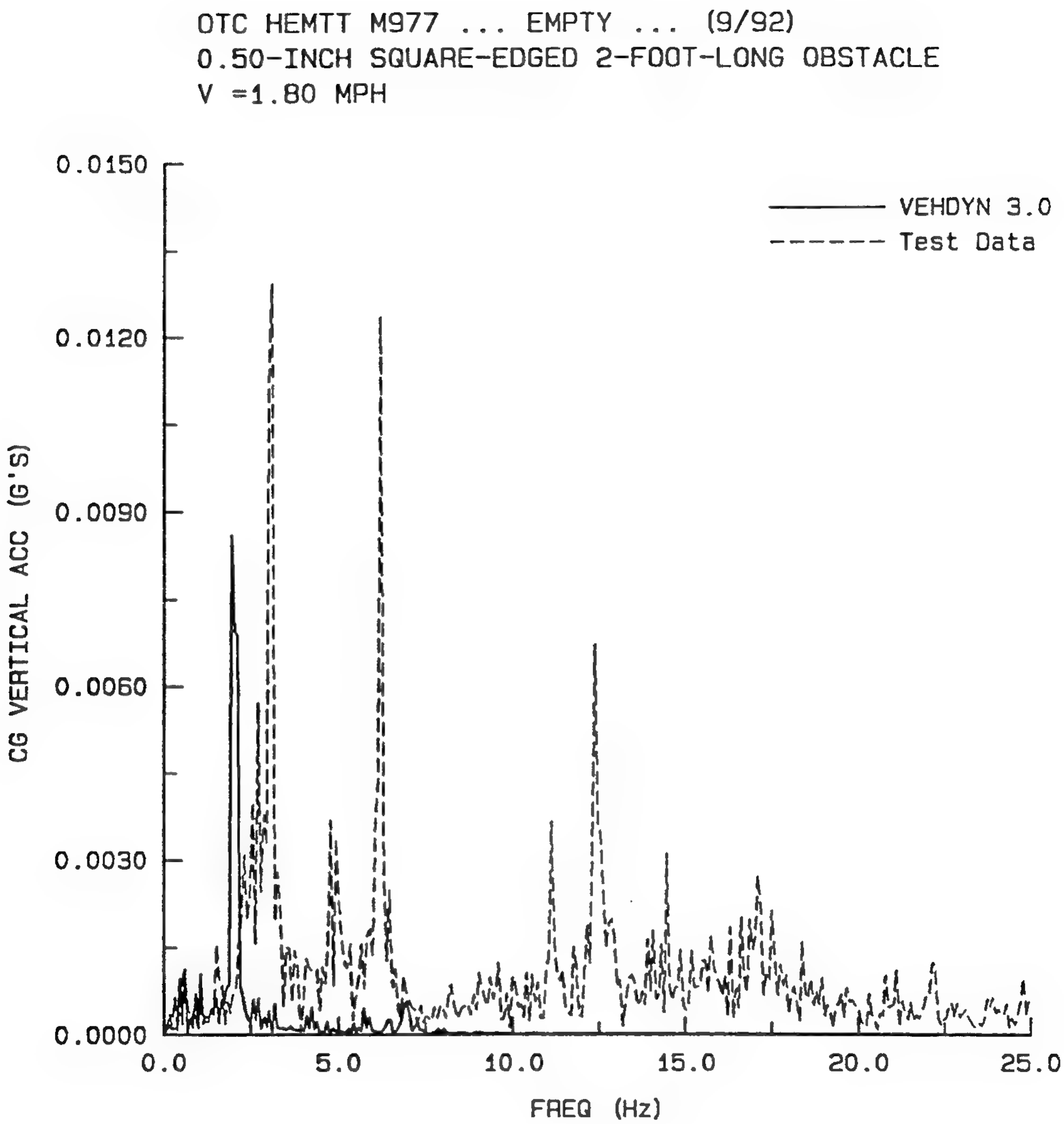

Figure A-87. CG vertical acceleration frequency plot (frequency scale = 5.0 Hz/inch) for an empty HEMTT traveling at 1.80 miles per hour encountering a 0.50-inch-high obstacle.

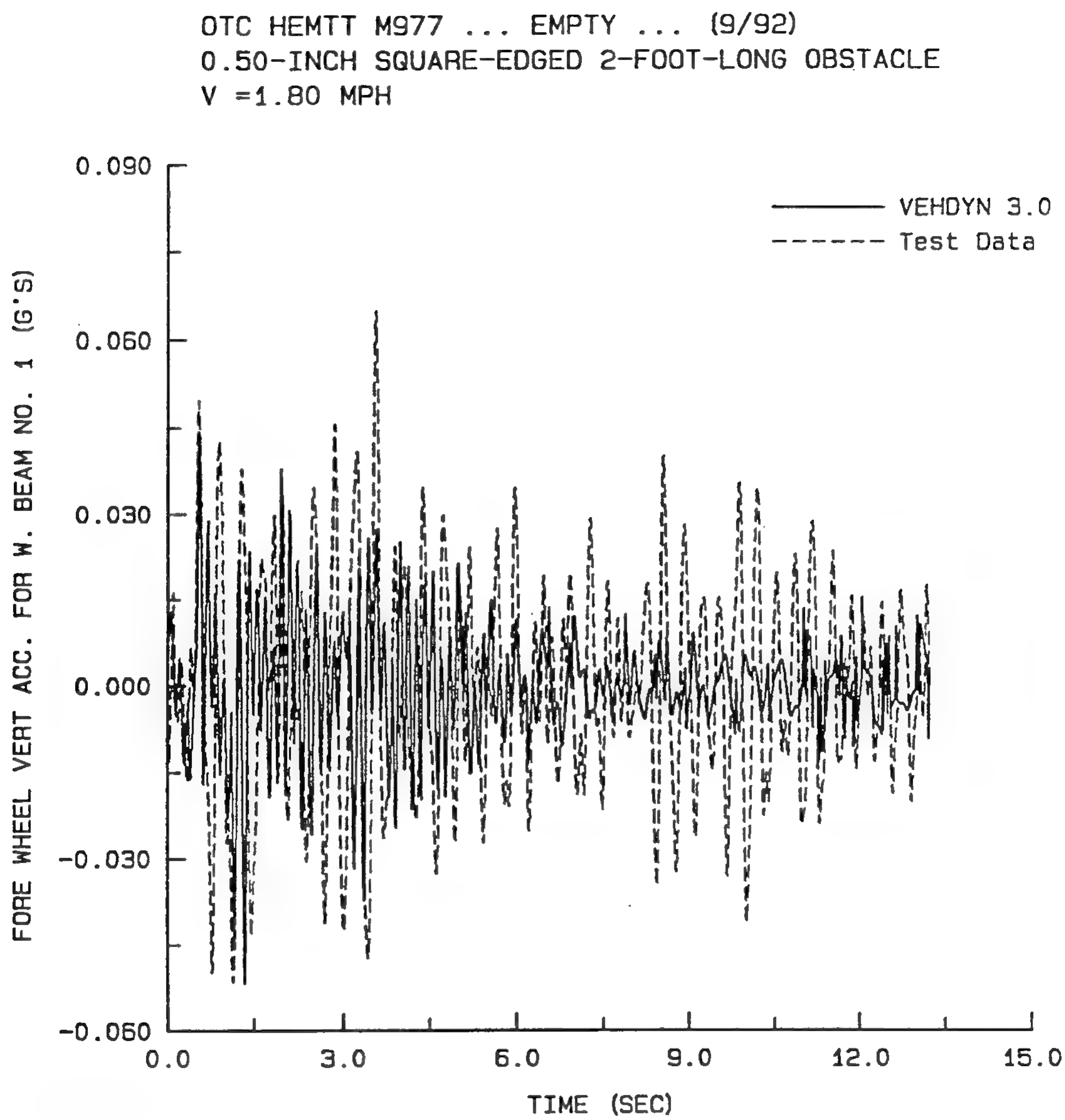

Figure A-88. Vertical acceleration time history of the forward-most axle for an empty HEMTT traveling at 1.80 miles per hour encountering a 0.50-inch-high obstacle.

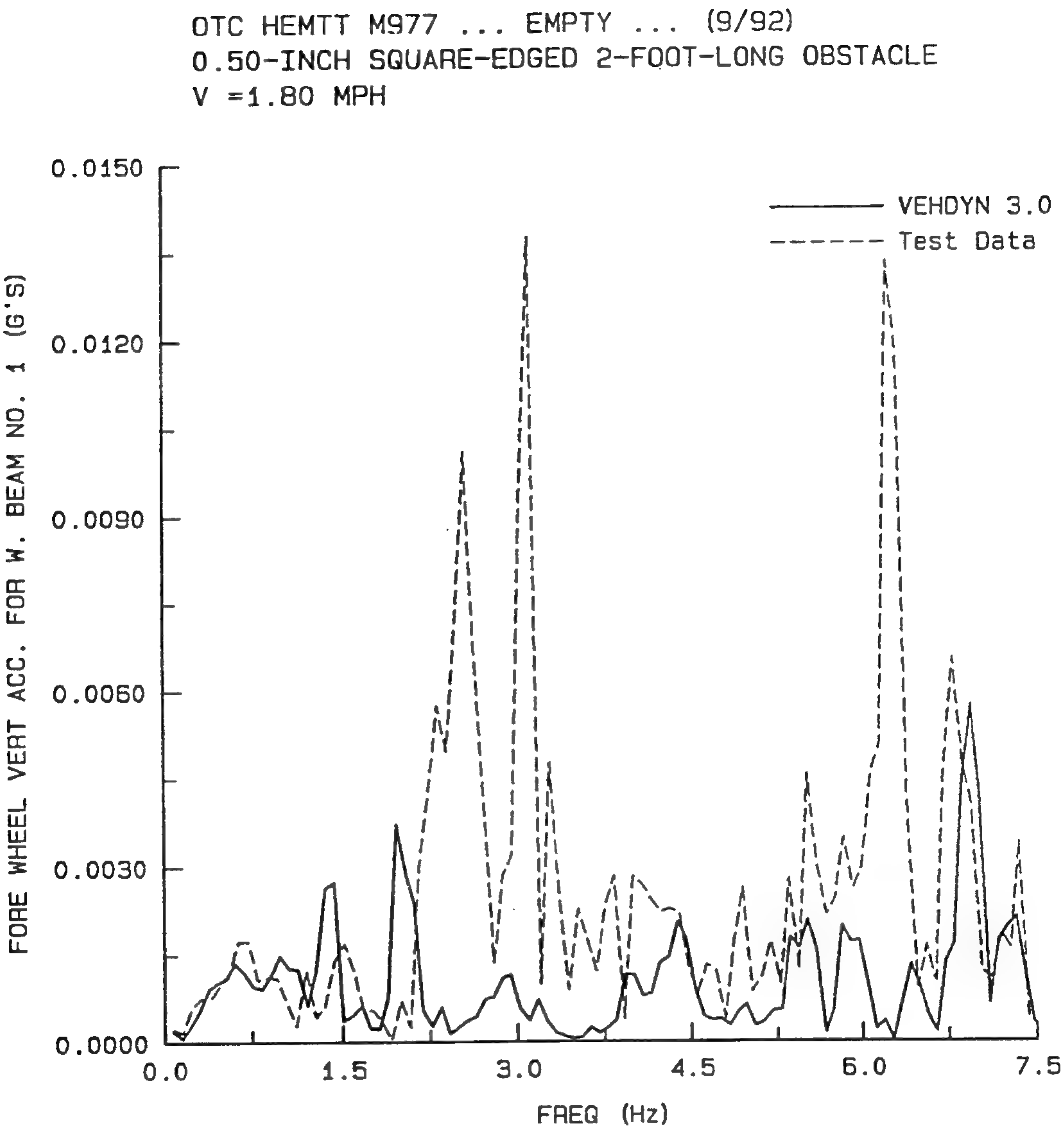

Figure A-89. Vertical acceleration frequency plot (frequency scale = 1.5 Hz/inch) of the forward-most axle for an empty HEMTT traveling at 1.80 miles per hour encountering a 0.50-inch-high obstacle.

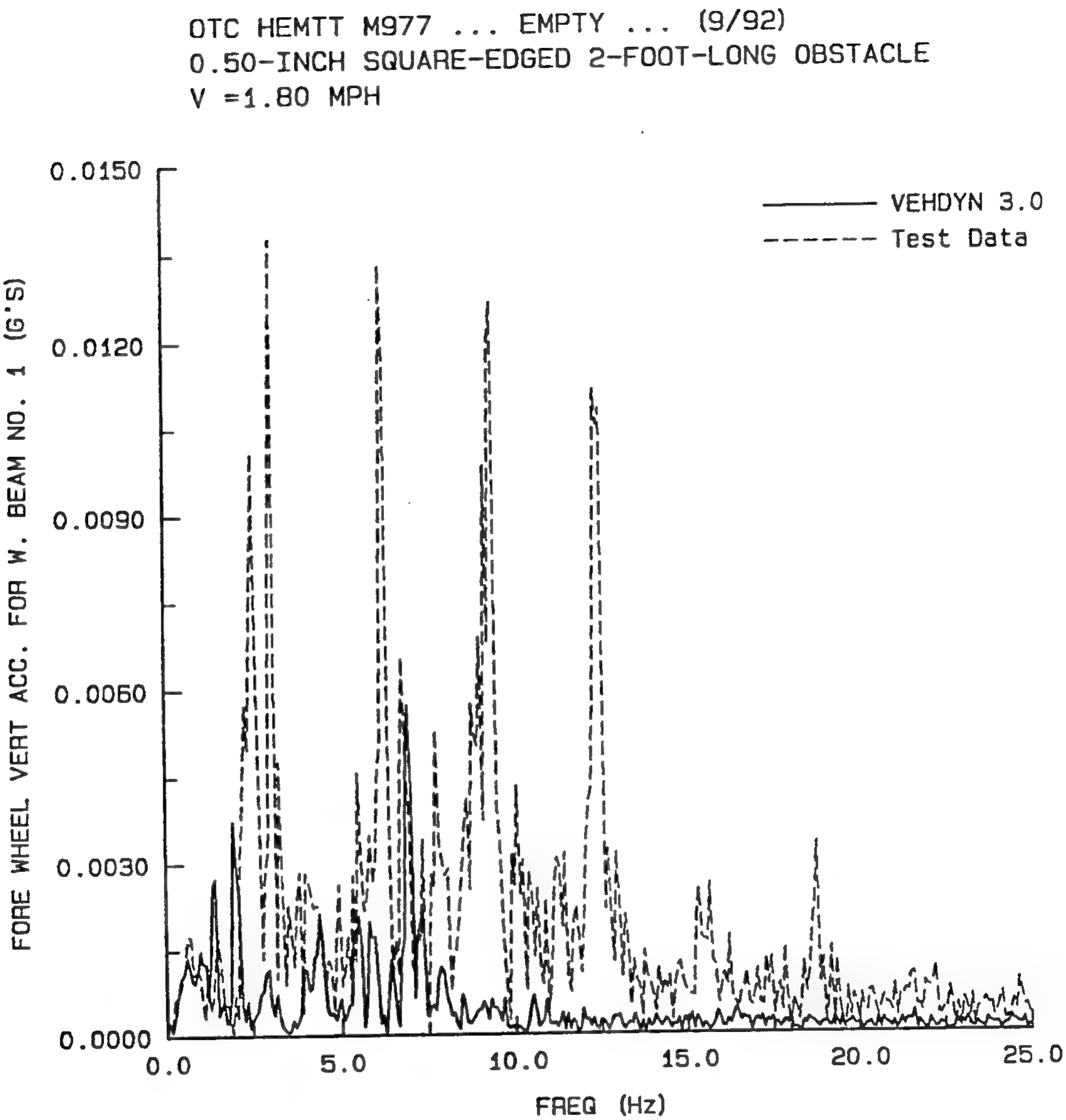

Figure A-90. Vertical acceleration frequency plot (frequency scale = 5.0 Hz/inch) of the forward-most axle for an empty HEMTT traveling at 1.80 miles per hour encountering a 0.50-inch-high obstacle.

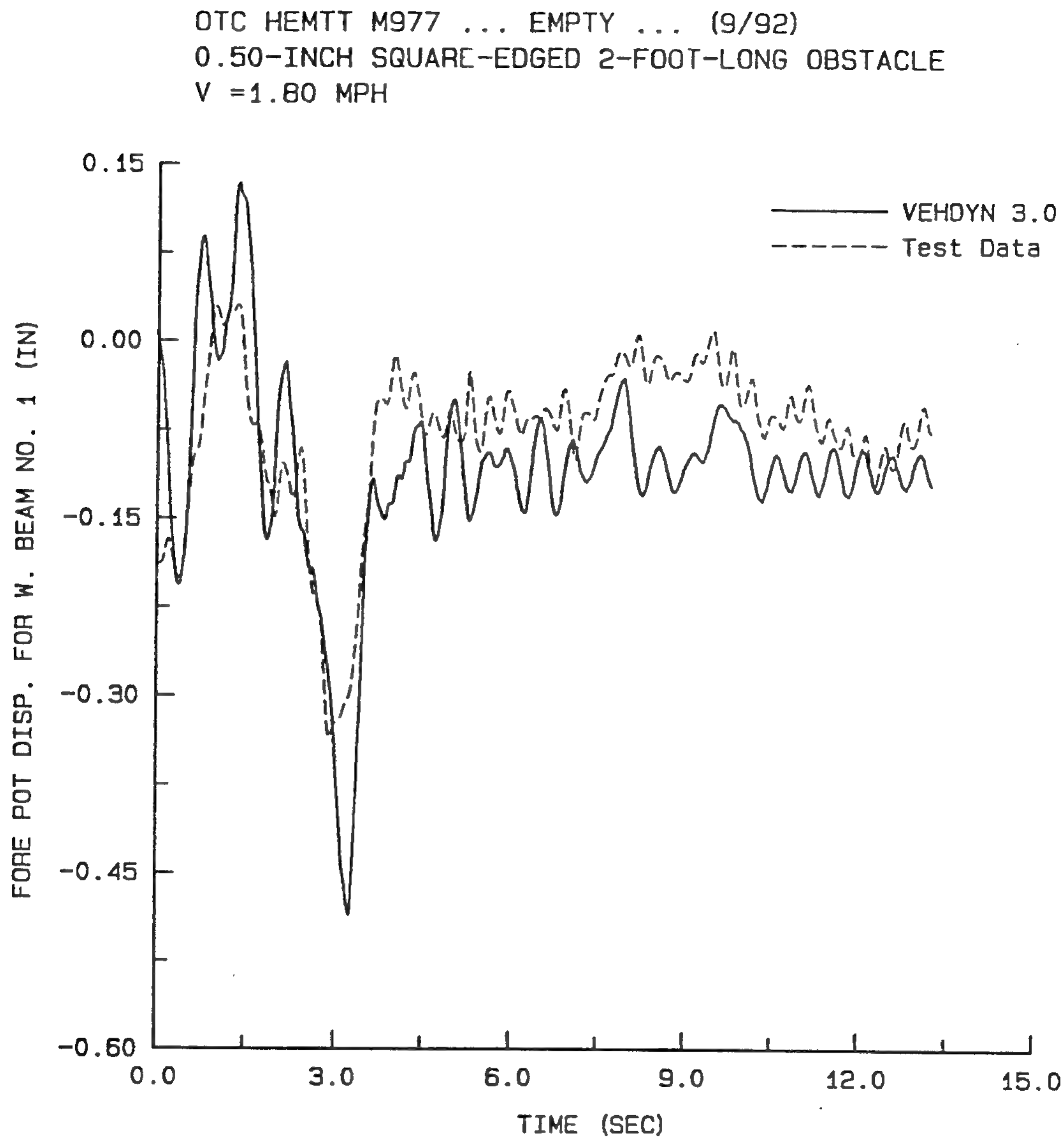

Figure A-91. Relative displacement time history of the forward-most axle with respect to the frame for an empty HEMTT traveling at 1.80 miles per hour encountering a 0.50-inch-high obstacle.

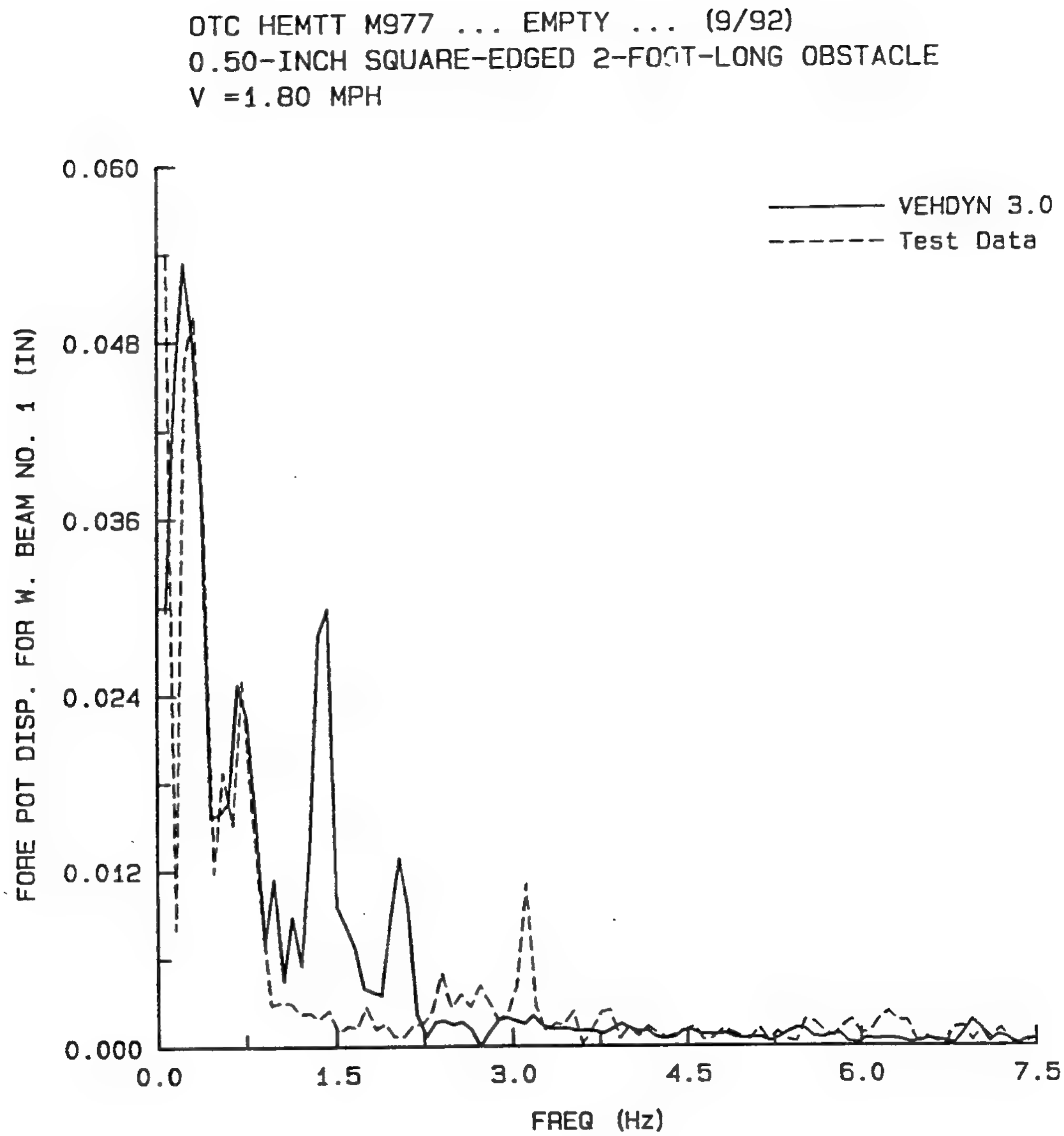

Figure A-92. Relative displacement frequency plot (frequency scale = 1.5 Hz/inch) of the forward-most axle with respect to the frame for an empty HEMTT traveling at 1.80 miles per hour encountering a 0.50-inch-high obstacle.

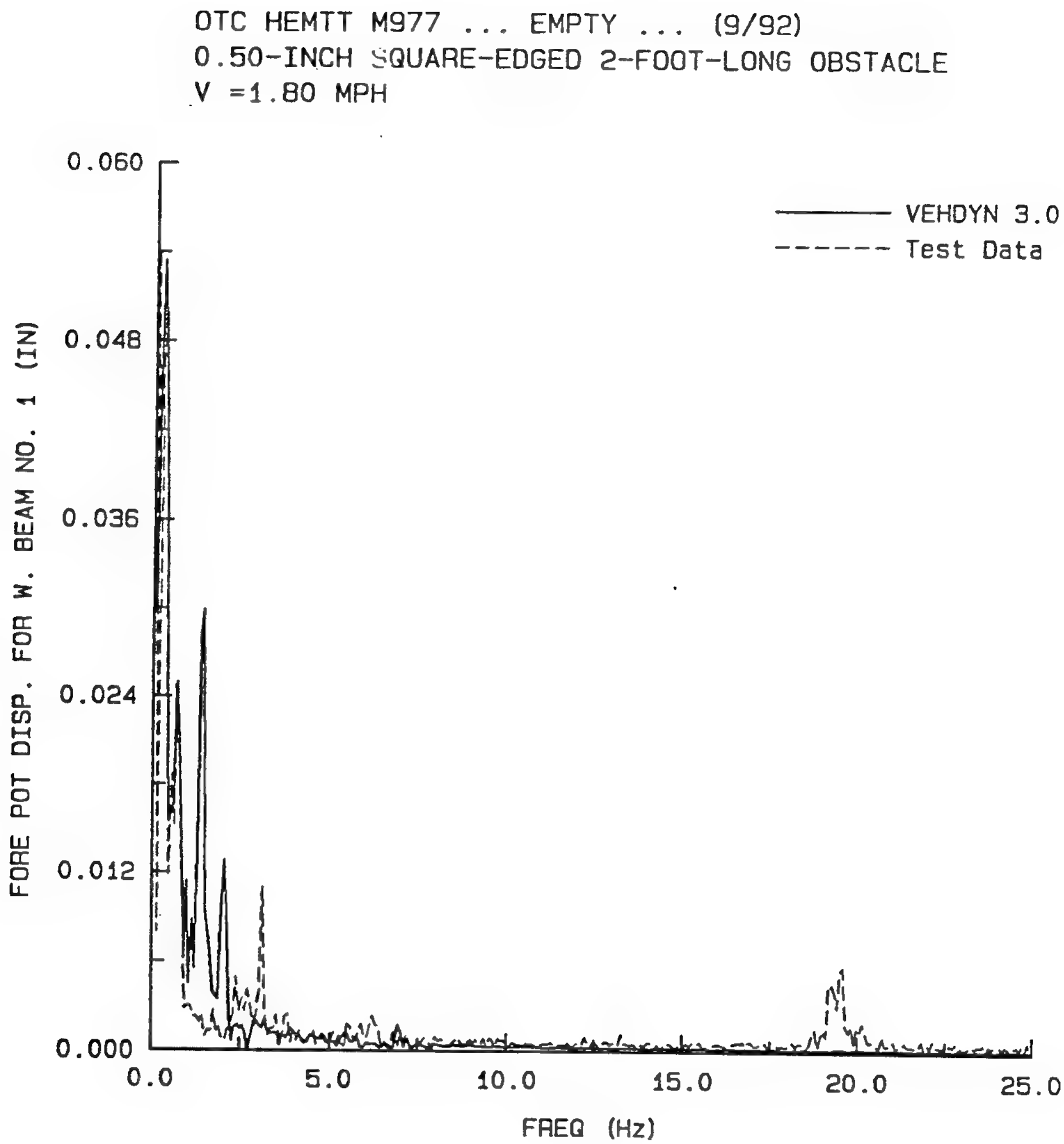

Figure A-93. Relative displacement frequency plot (frequency scale = 5.0 Hz/inch) of the forward-most axle with respect to the frame for an empty HEMTT traveling at 1.80 miles per hour encountering a 0.50-inch-high obstacle.

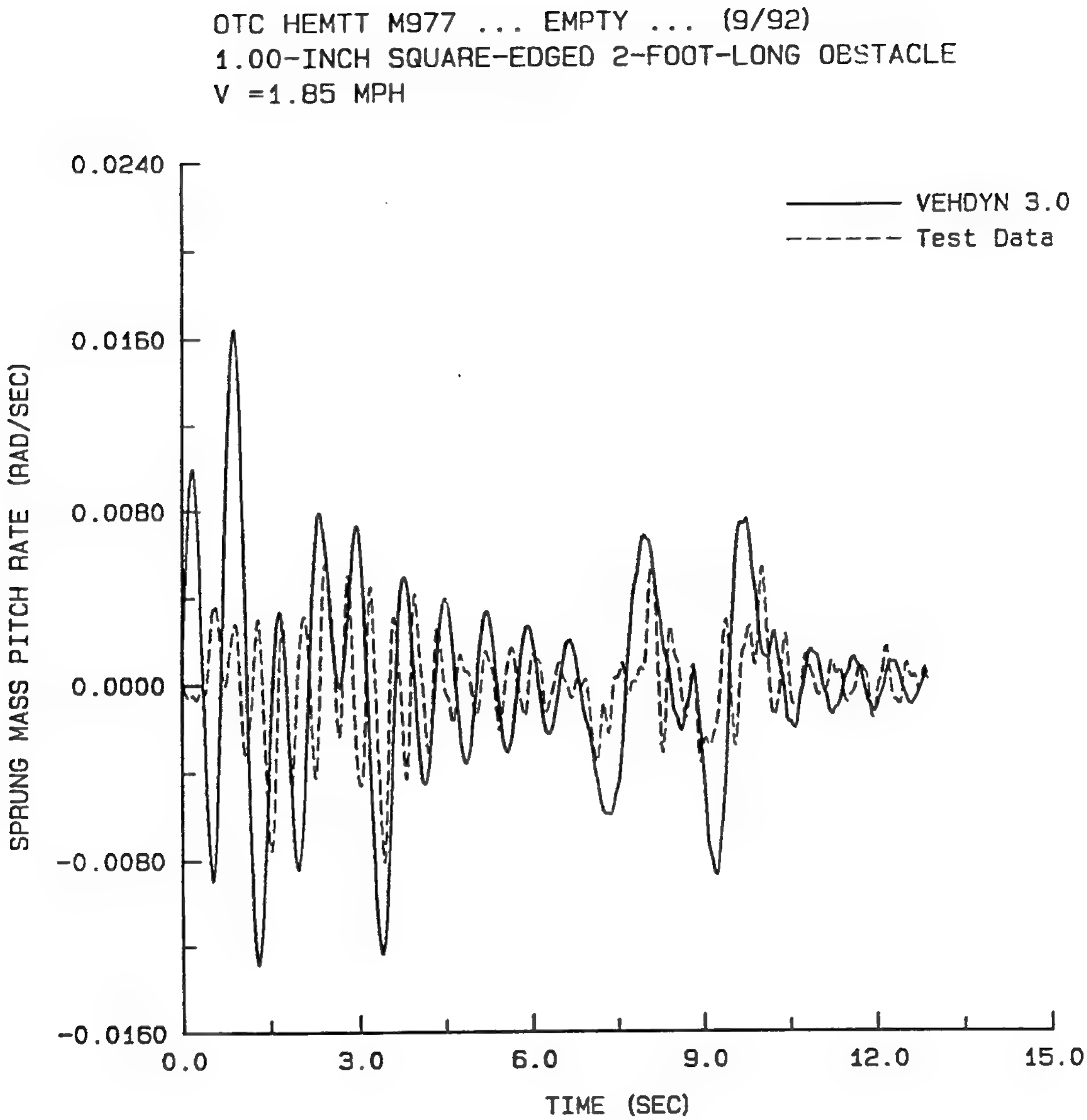

Figure A-94. Sprung mass pitch rate time history for an empty HEMTT traveling at 1.85 miles per hour encountering a 1.00-inch-high obstacle.

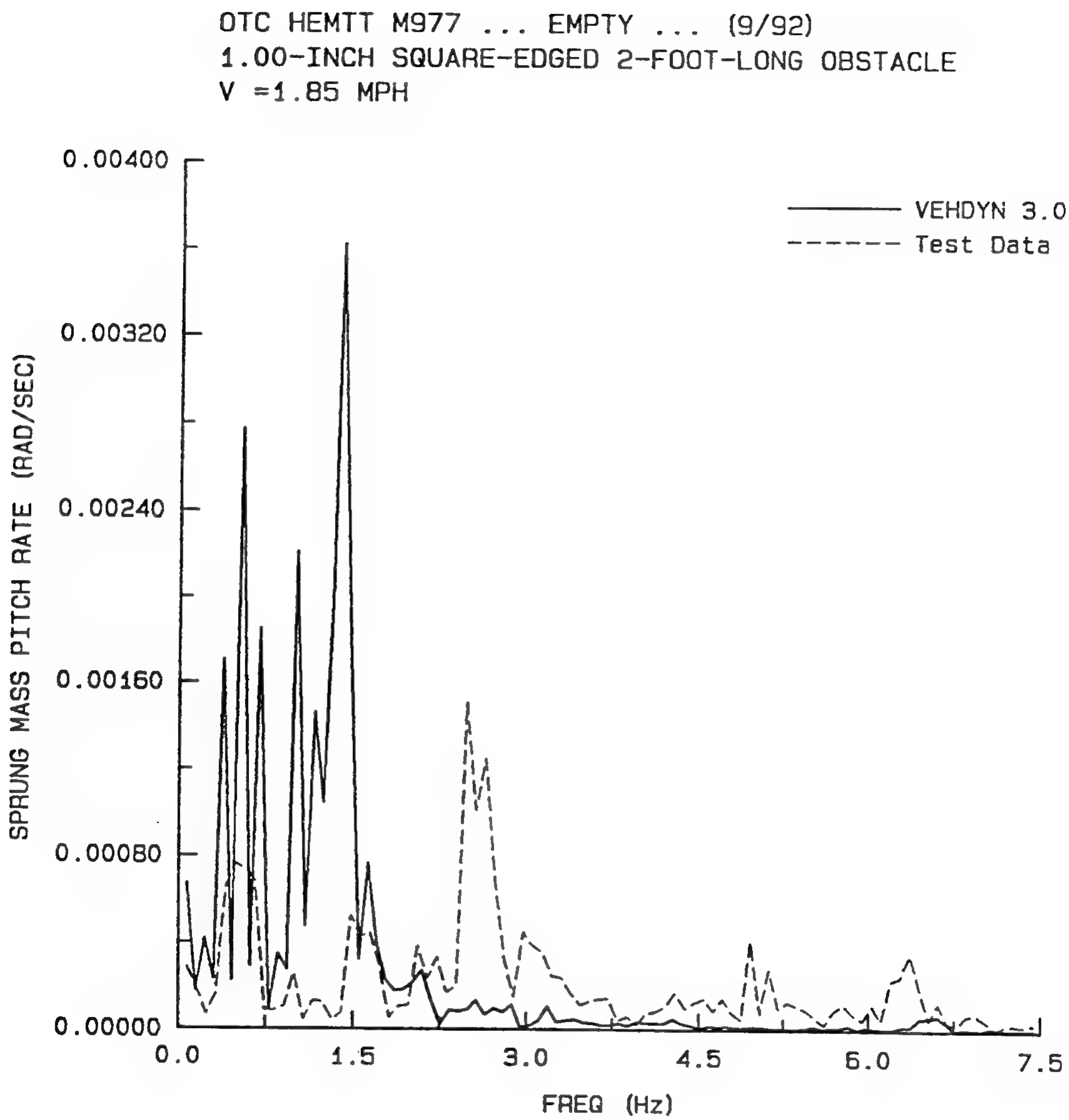

Figure A-95. Sprung mass pitch rate frequency plot for an empty HEMTT traveling at 1.85 miles per hour encountering a 1.00-inch-high obstacle.

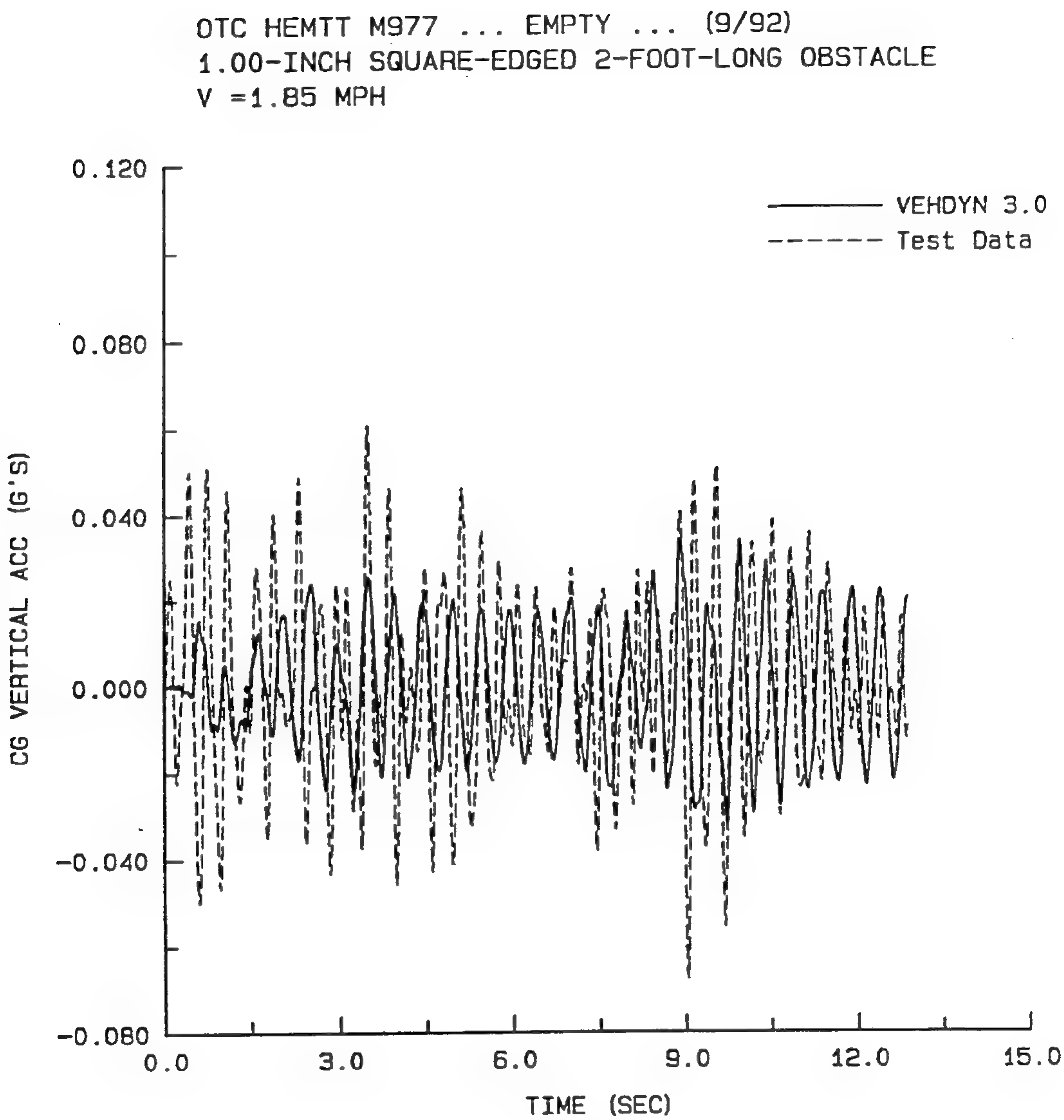

Figure A-96. CG vertical acceleration time history for an empty HEMTT traveling at 1.85 miles per hour encountering a 1.00-inch-high obstacle.

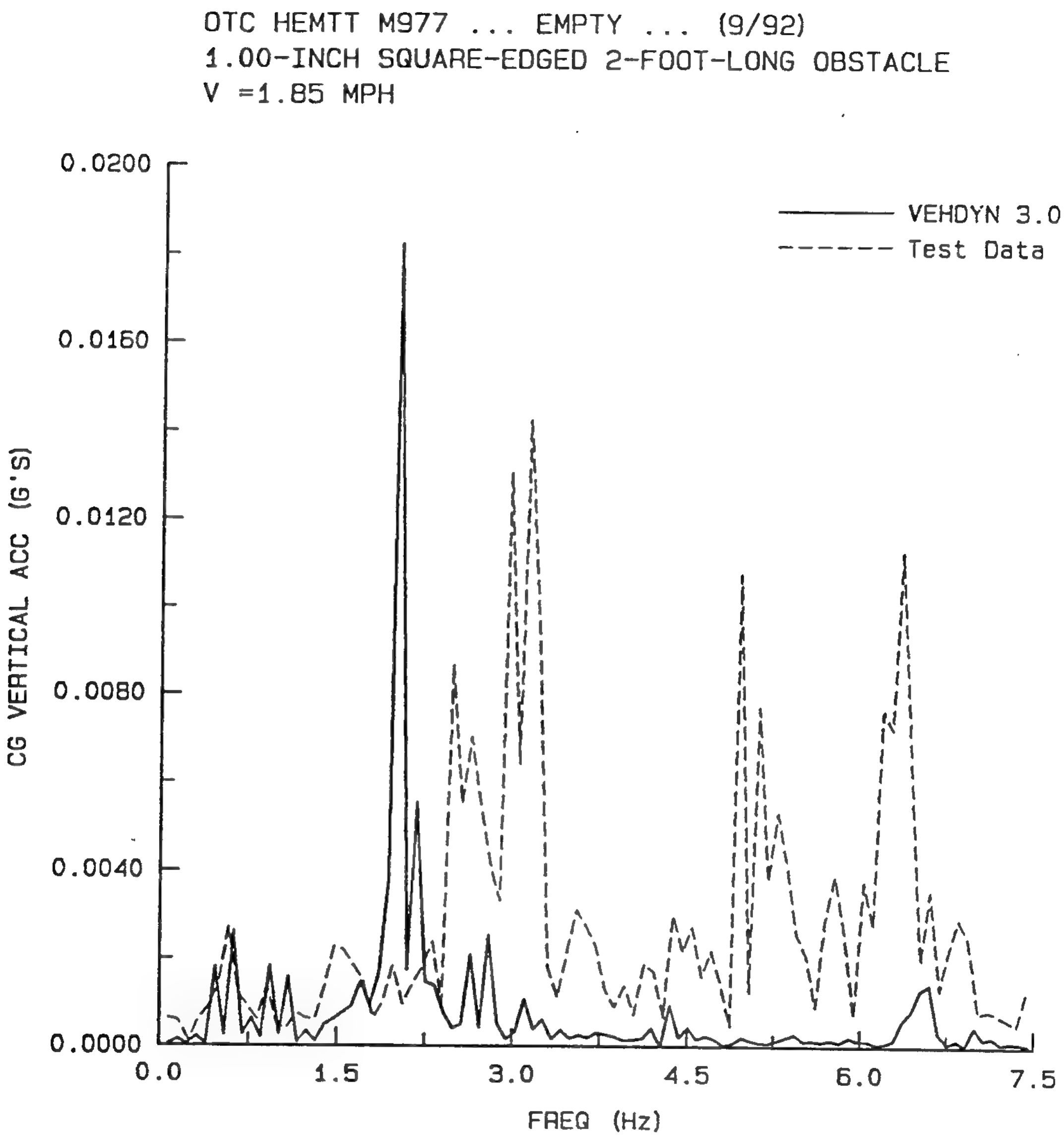

Figure A-97. CG vertical acceleration frequency plot (frequency scale = 1.5 Hz/inch) for an empty HEMTT traveling at 1.85 miles per hour encountering a 1.00-inch-high obstacle.

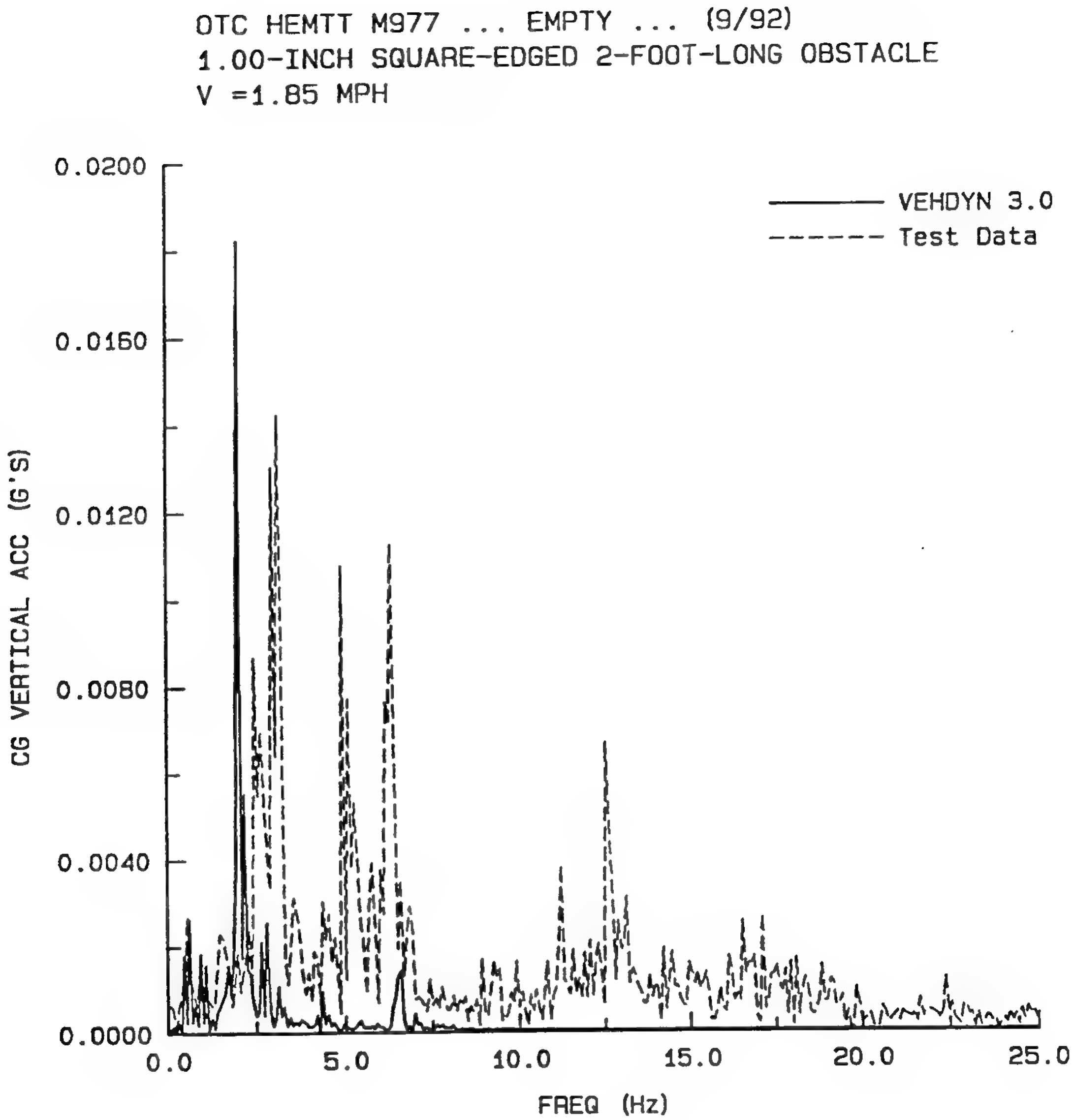

Figure A-98. CG vertical acceleration frequency plot (frequency scale = 5.0 Hz/inch) for an empty HEMTT traveling at 1.85 miles per hour encountering a 1.00-inch-high obstacle.

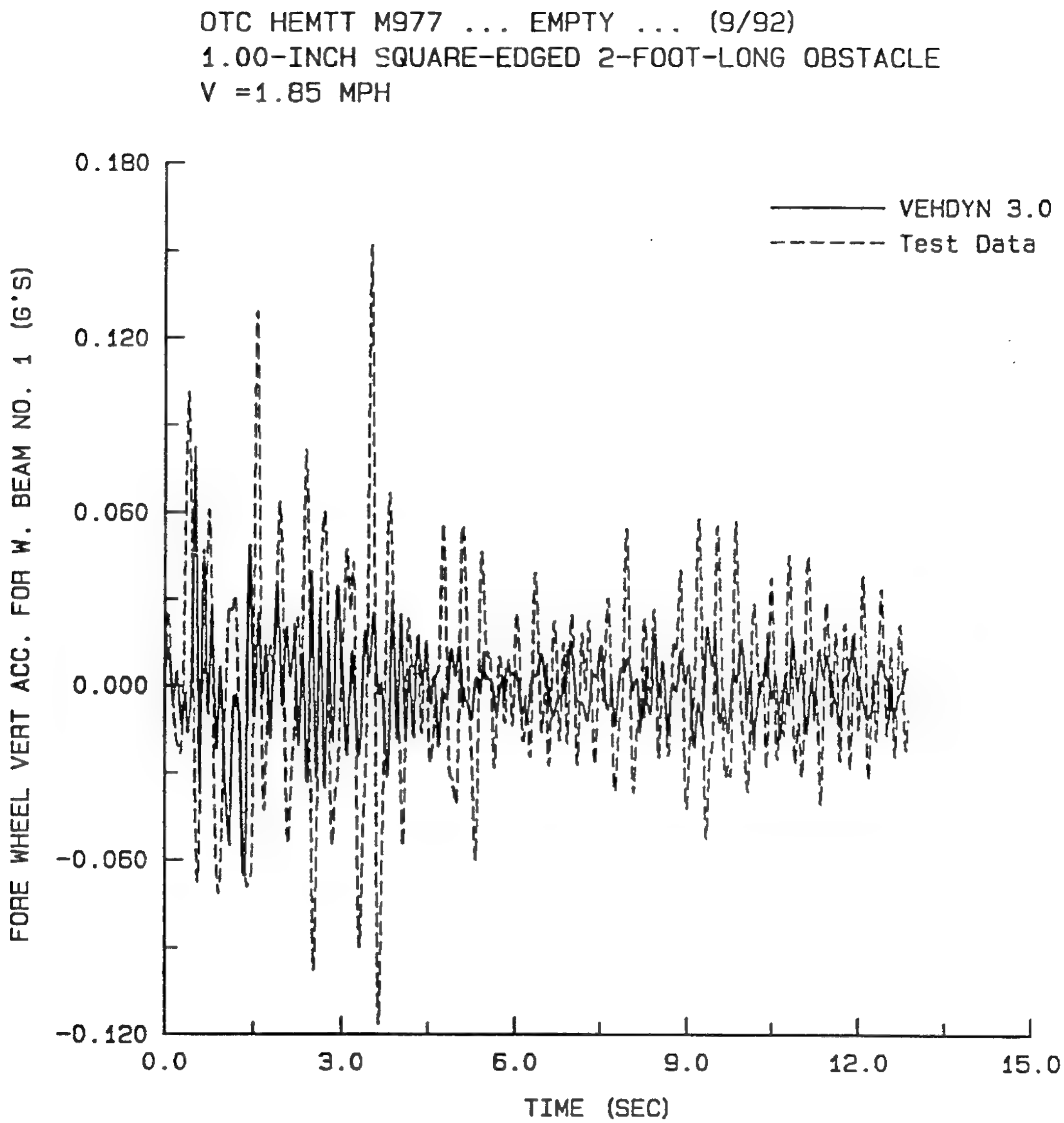

Figure A-99. Vertical acceleration time history of the forward-most axle for an empty HEMTT traveling at 1.85 miles per hour encountering a 1.00-inch-high obstacle.

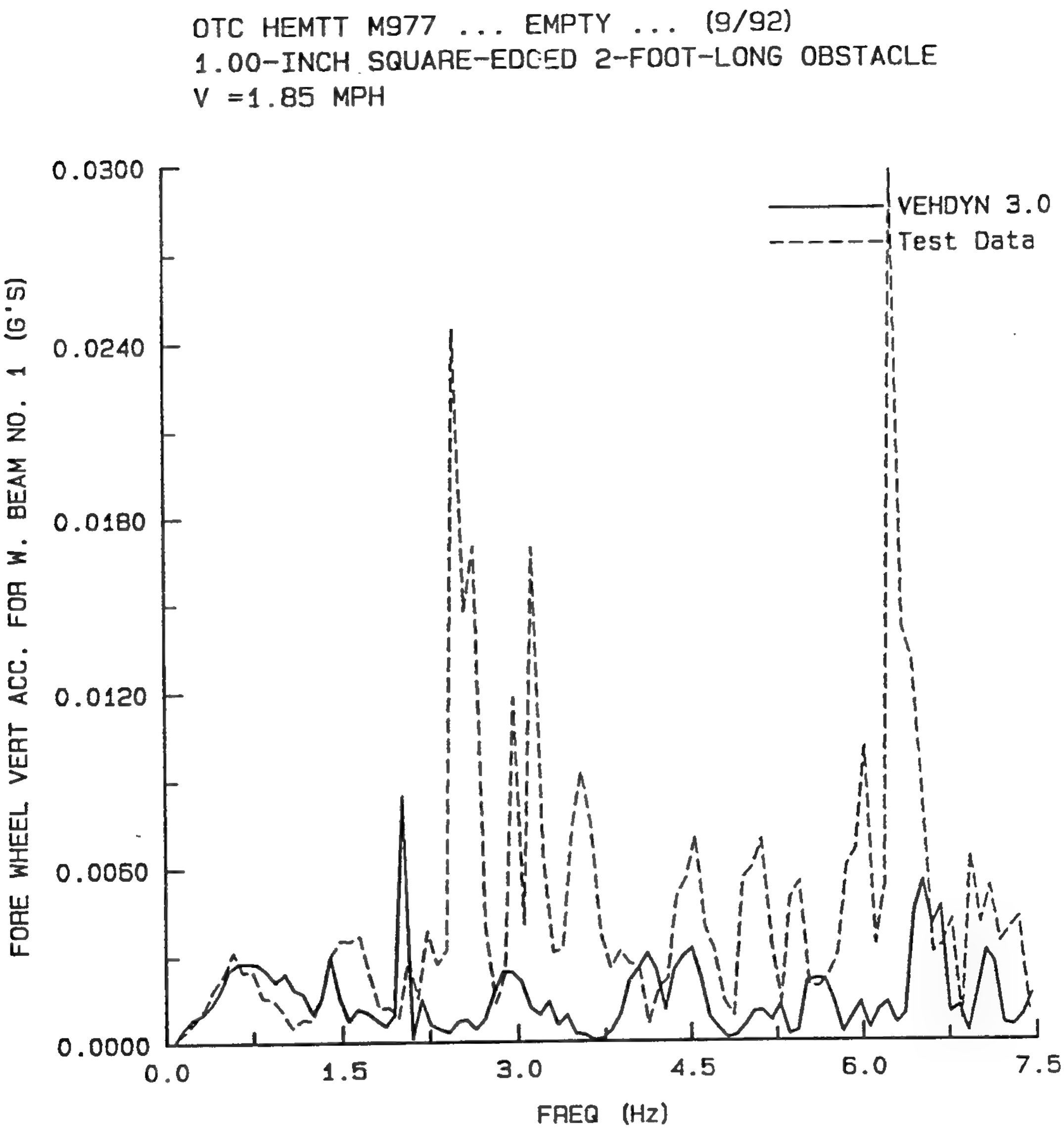

Figure A-100. Vertical acceleration frequency plot (frequency scale = 1.5 Hz/inch) of the forward-most axle for an empty HEMTT traveling at 1.85 miles per hour encountering a 1.00-inch-high obstacle.

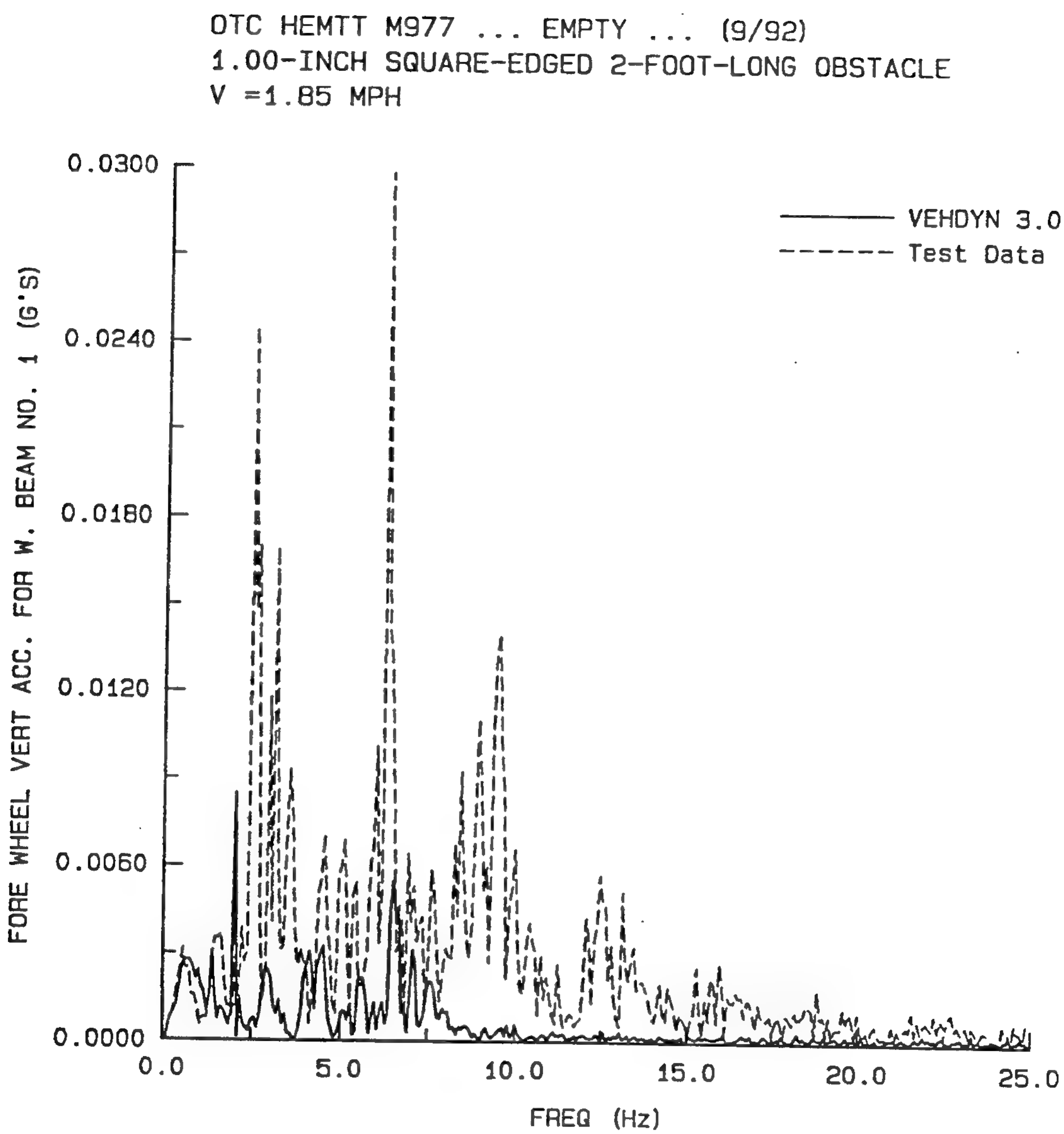

Figure A-101. Vertical acceleration frequency plot (frequency scale = 5.0 Hz/inch) of the forward-most axle for an empty HEMTT traveling at 1.85 miles per hour encountering a 1.00-inch-high obstacle.

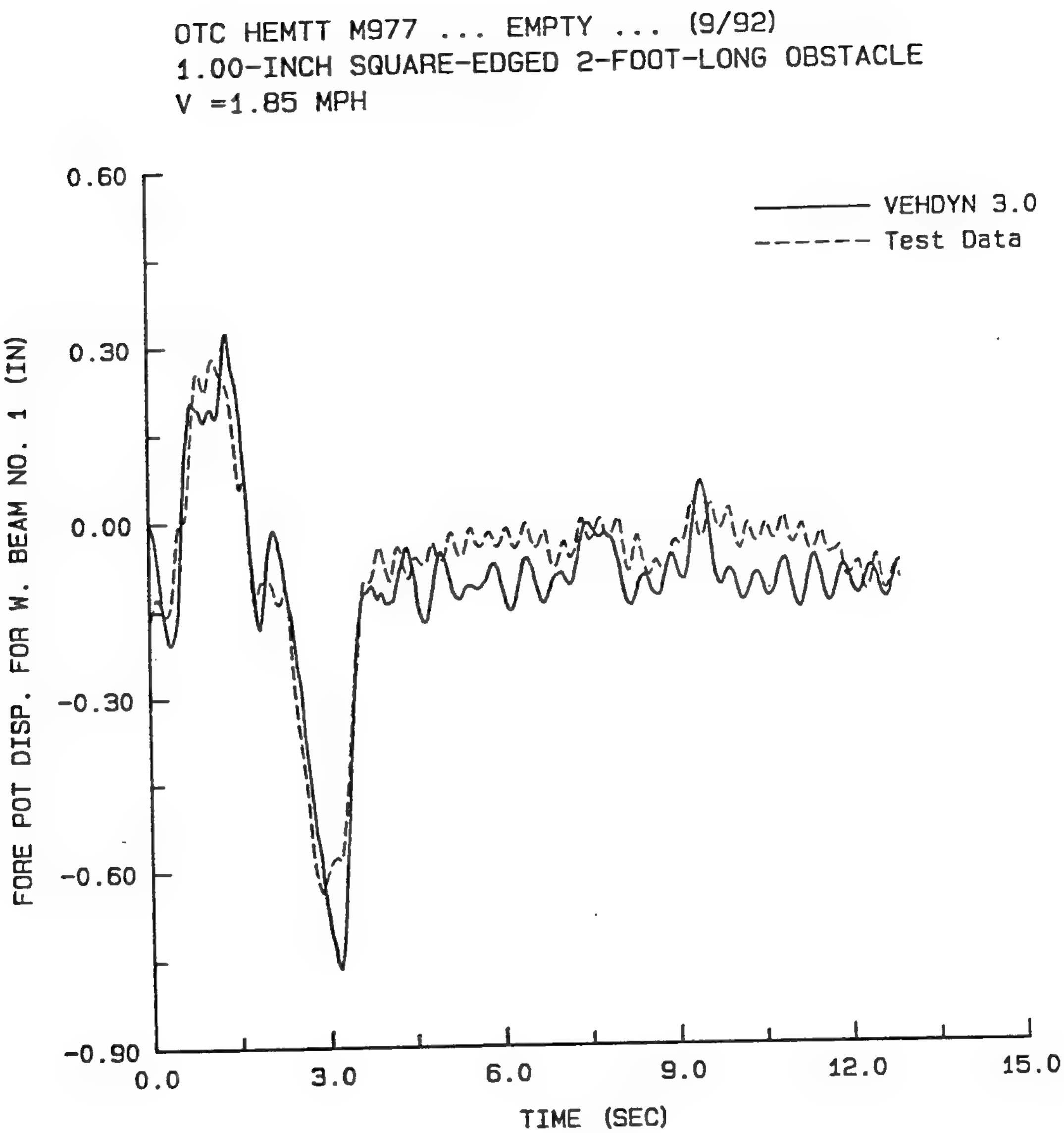

Figure A-102. Relative displacement time history of the forward-most axle with respect to the frame for an empty HEMTT traveling at 1.85 miles per hour encountering a 1.00-inch-high obstacle.

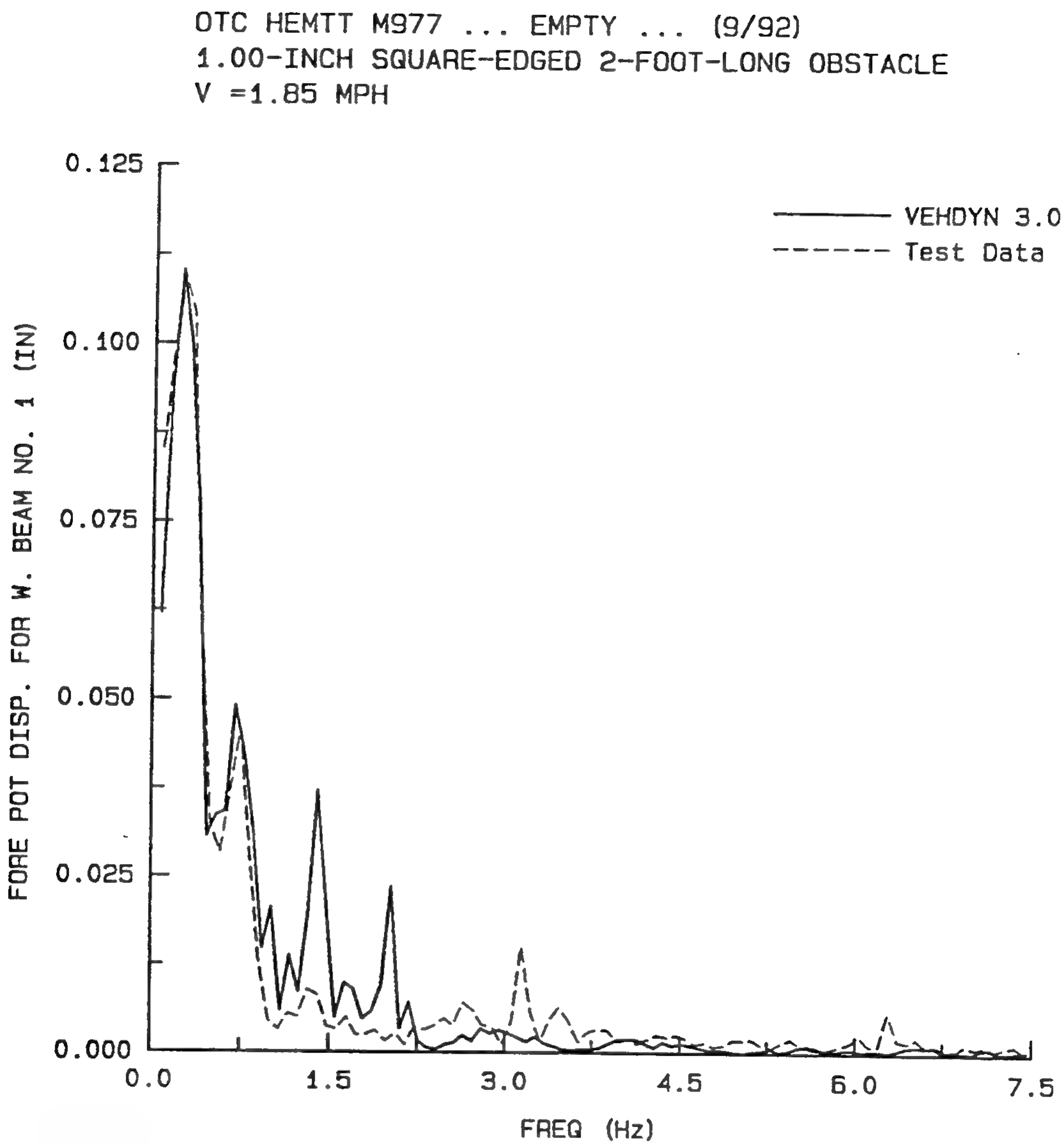

Figure A-103. Relative displacement frequency plot (frequency scale = 1.5 Hz/inch) of the forward-most axle with respect to the frame for an empty HEMTT traveling at 1.85 miles per hour encountering a 1.00-inch-high obstacle.

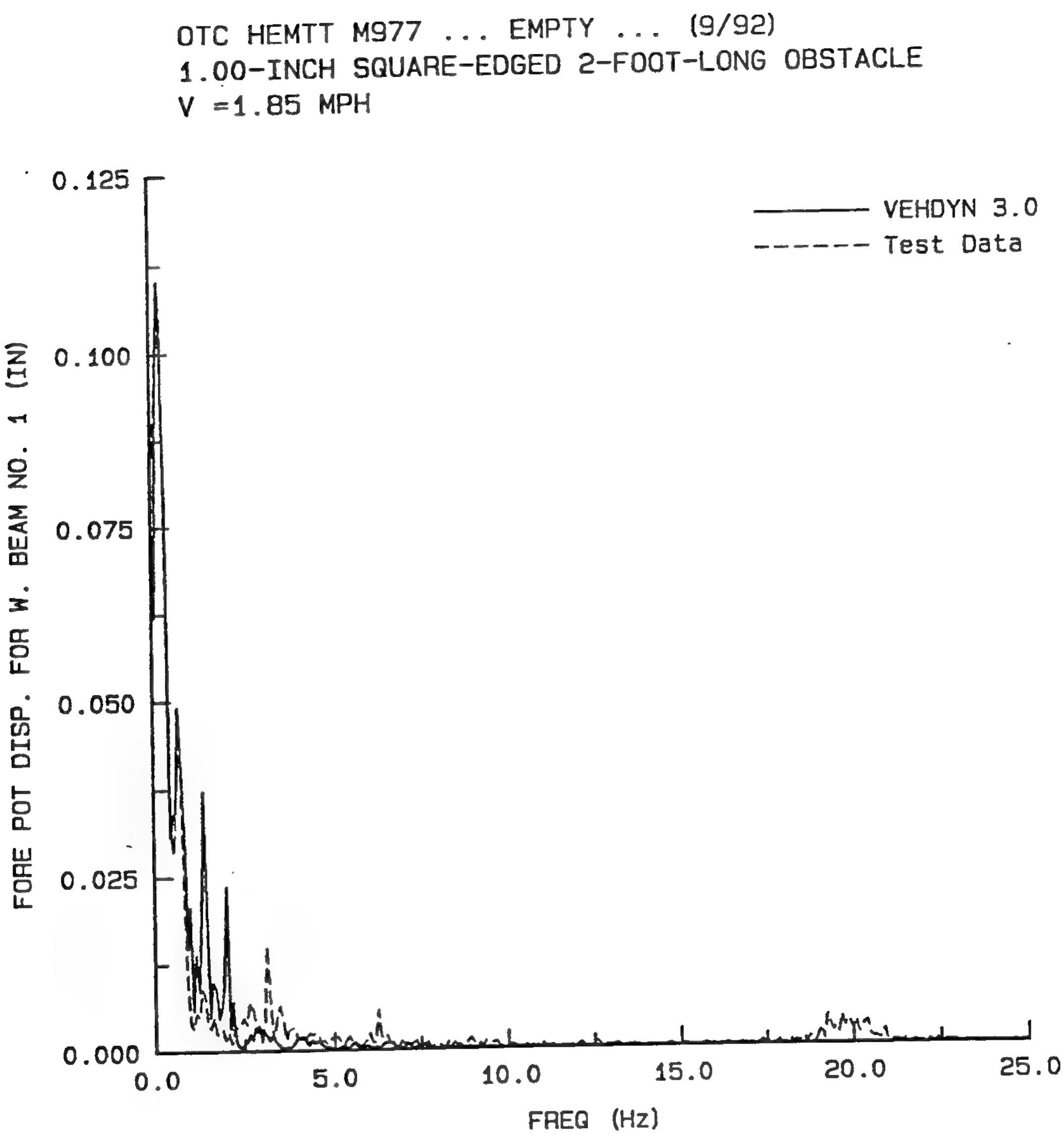

Figure A-104. Relative displacement frequency plot (frequency scale = 5.0 Hz/inch) of the forward-most axle with respect to the frame for an empty HEMTT traveling at 1.85 miles per hour encountering a 1.00-inch-high obstacle.

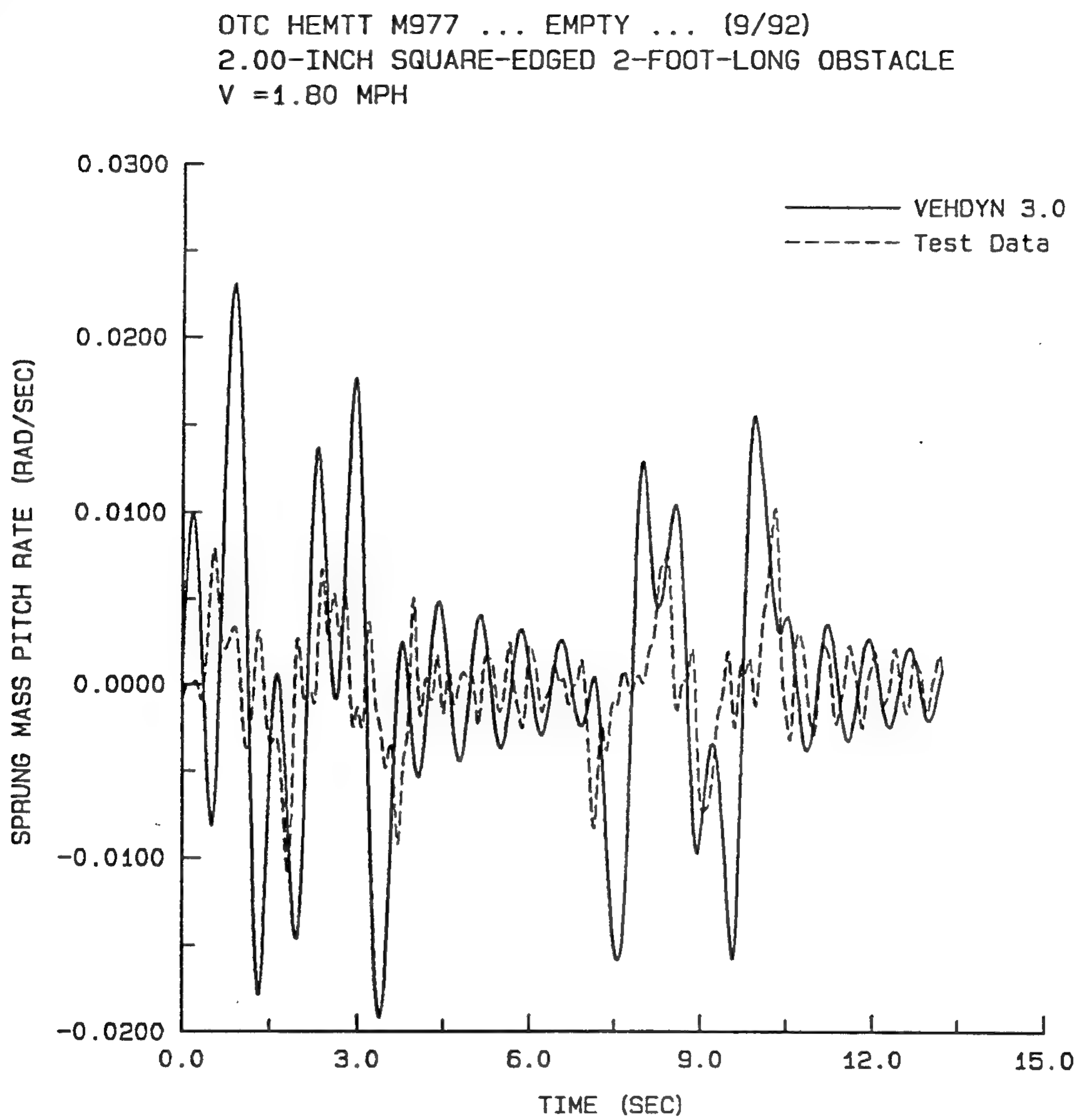

Figure A-105. Sprung mass pitch rate time history for an empty HEMTT traveling at 1.80 miles per hour encountering a 2.00-inch-high obstacle.

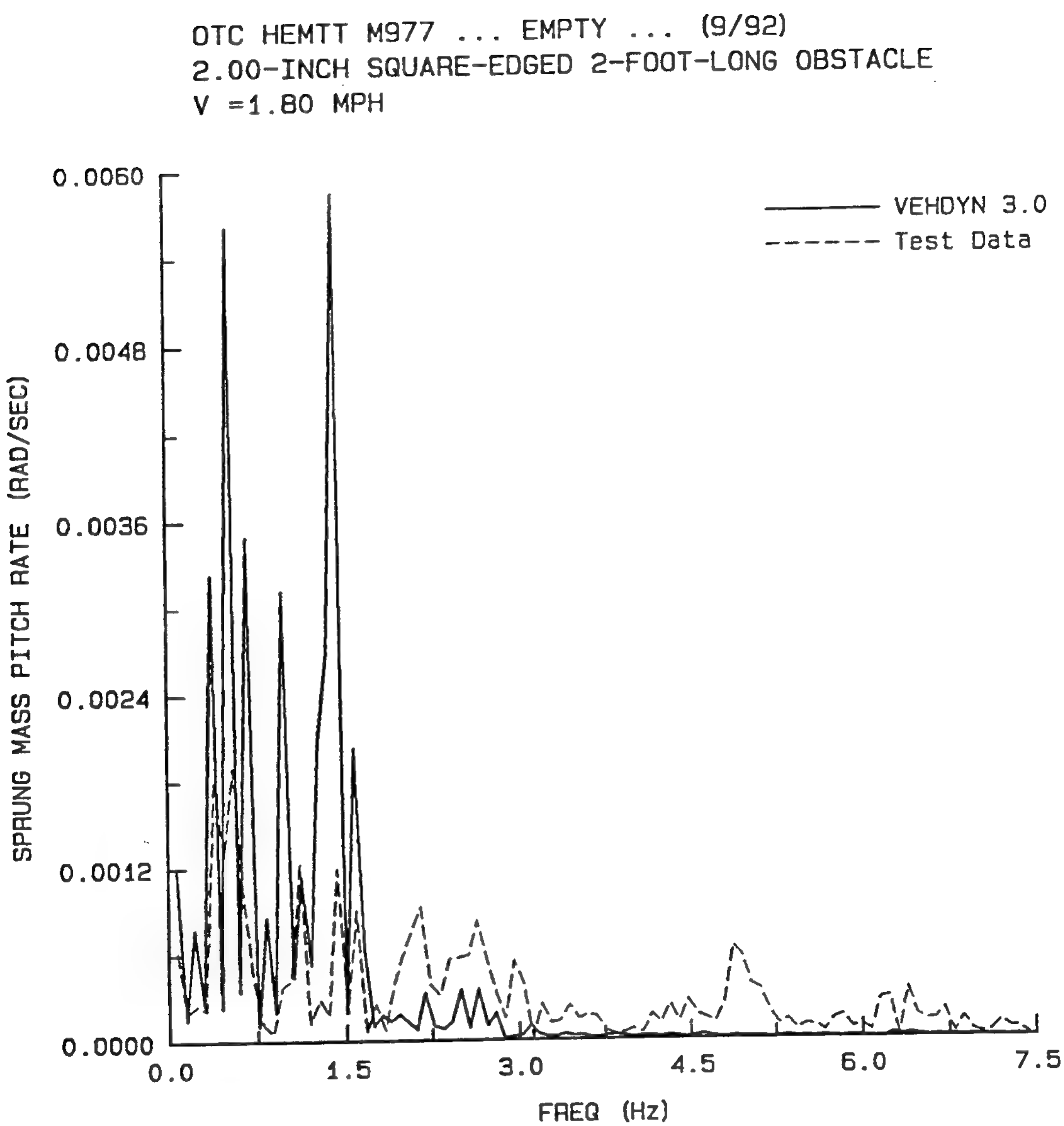

Figure A-106. Sprung mass pitch rate frequency plot for an empty HEMTT traveling at 1.80 miles per hour encountering a 2.00-inch-high obstacle.

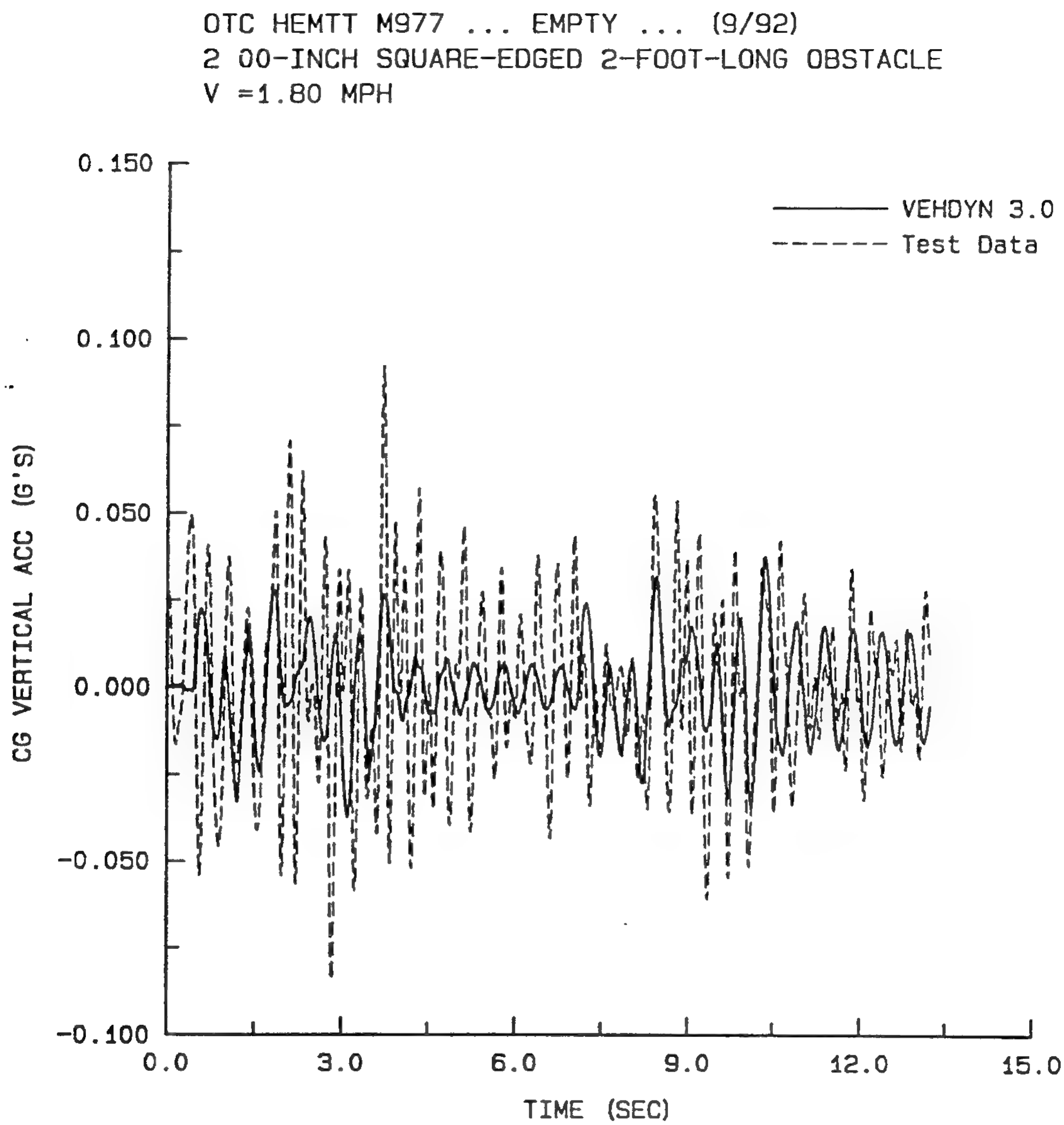

Figure A-107. CG vertical acceleration time history for an empty HEMTT traveling at 1.80 miles per hour encountering a 2.00-inch-high obstacle.

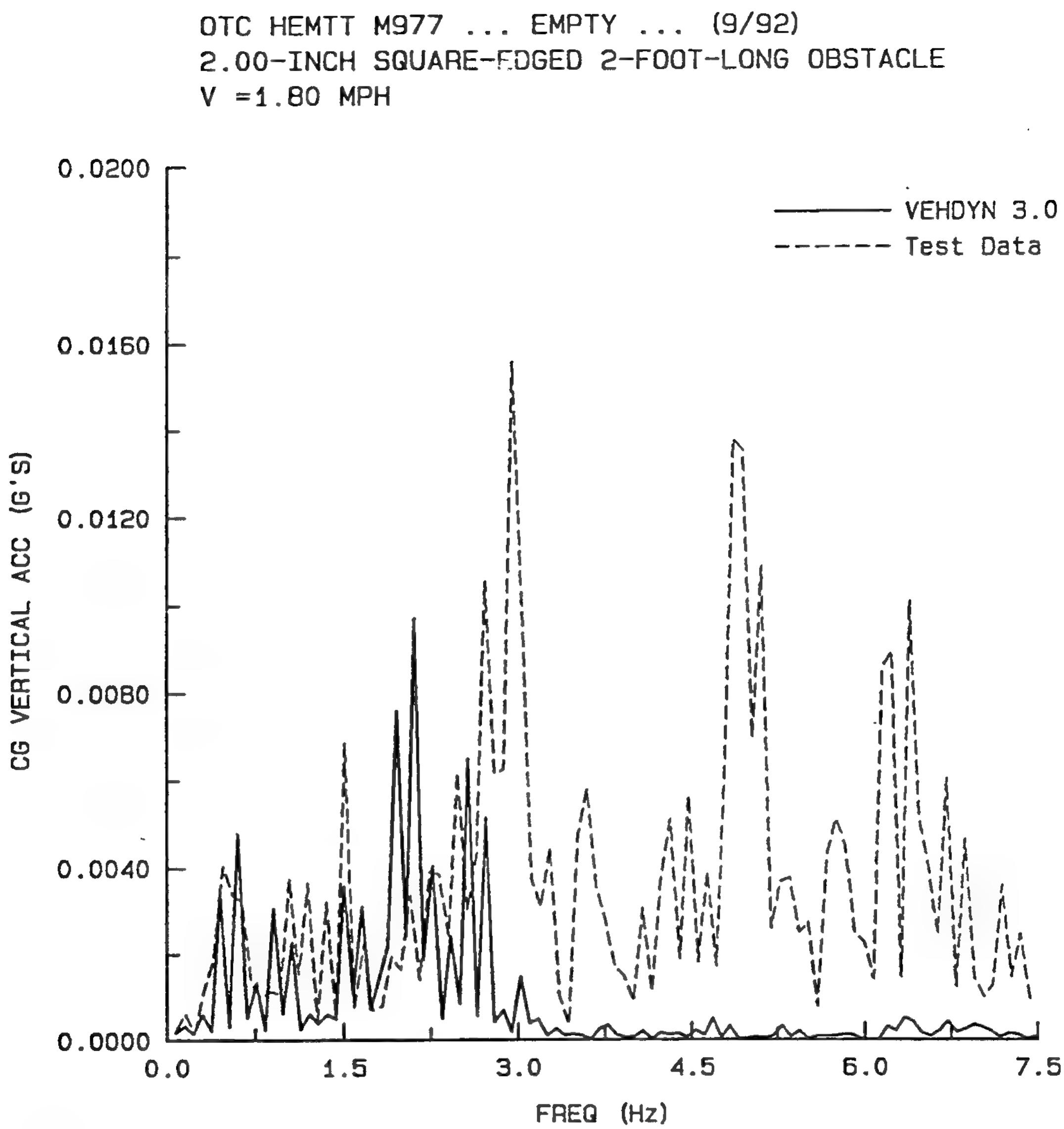

Figure A-108. CG vertical acceleration frequency plot (frequency scale = 1.5 Hz/inch) for an empty HEMTT traveling at 1.80 miles per hour encountering a 2.00-inch-high obstacle.

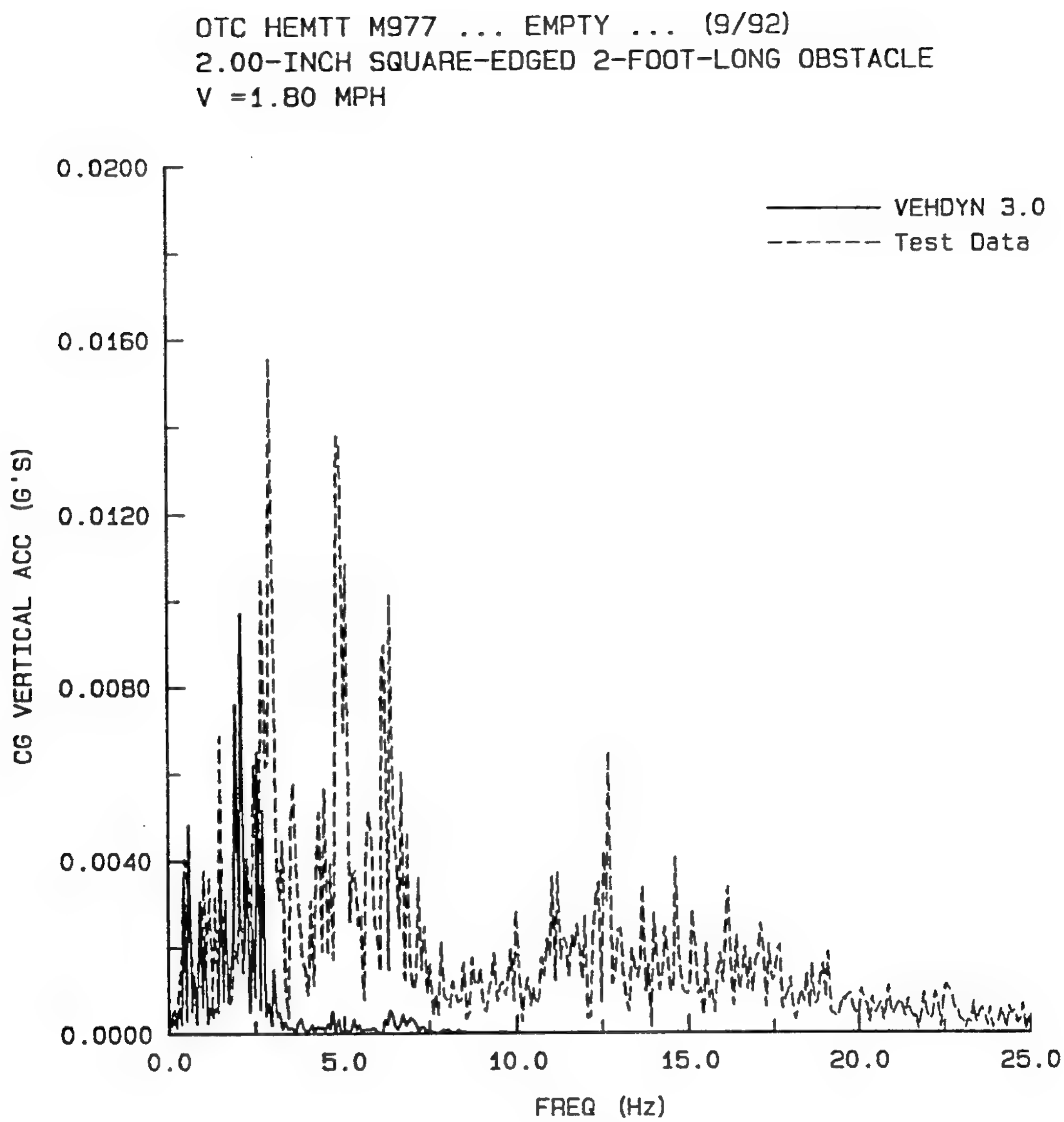

Figure A-109. CG vertical acceleration frequency plot (frequency scale = 5.0 Hz/inch) for an empty HEMTT traveling at 1.80 miles per hour encountering a 2.00-inch-high obstacle.

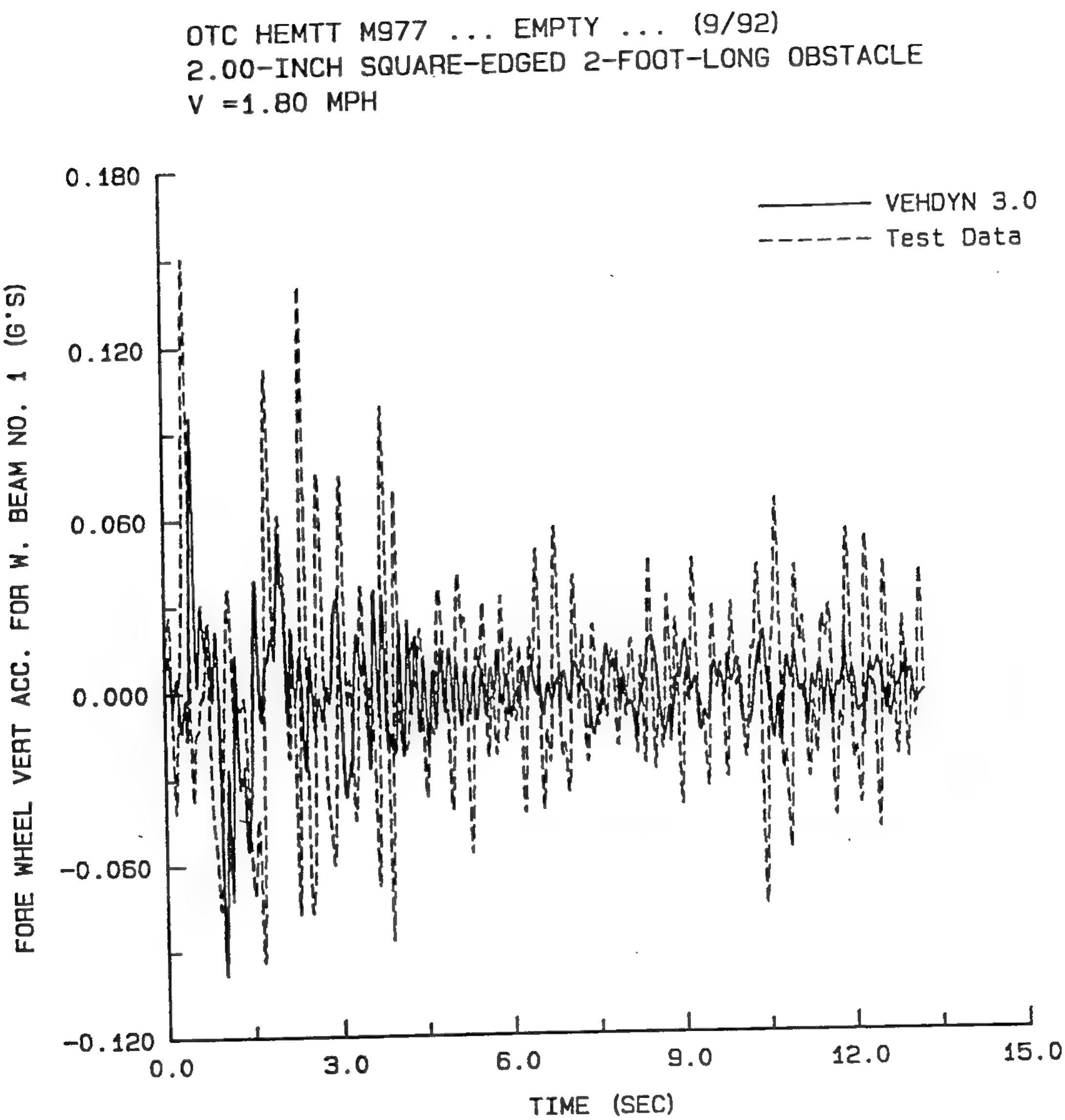

Figure A-110. Vertical acceleration time history of the forward-most axle for an empty HEMTT traveling at 1.80 miles per hour encountering a 2.00-inch-high obstacle.

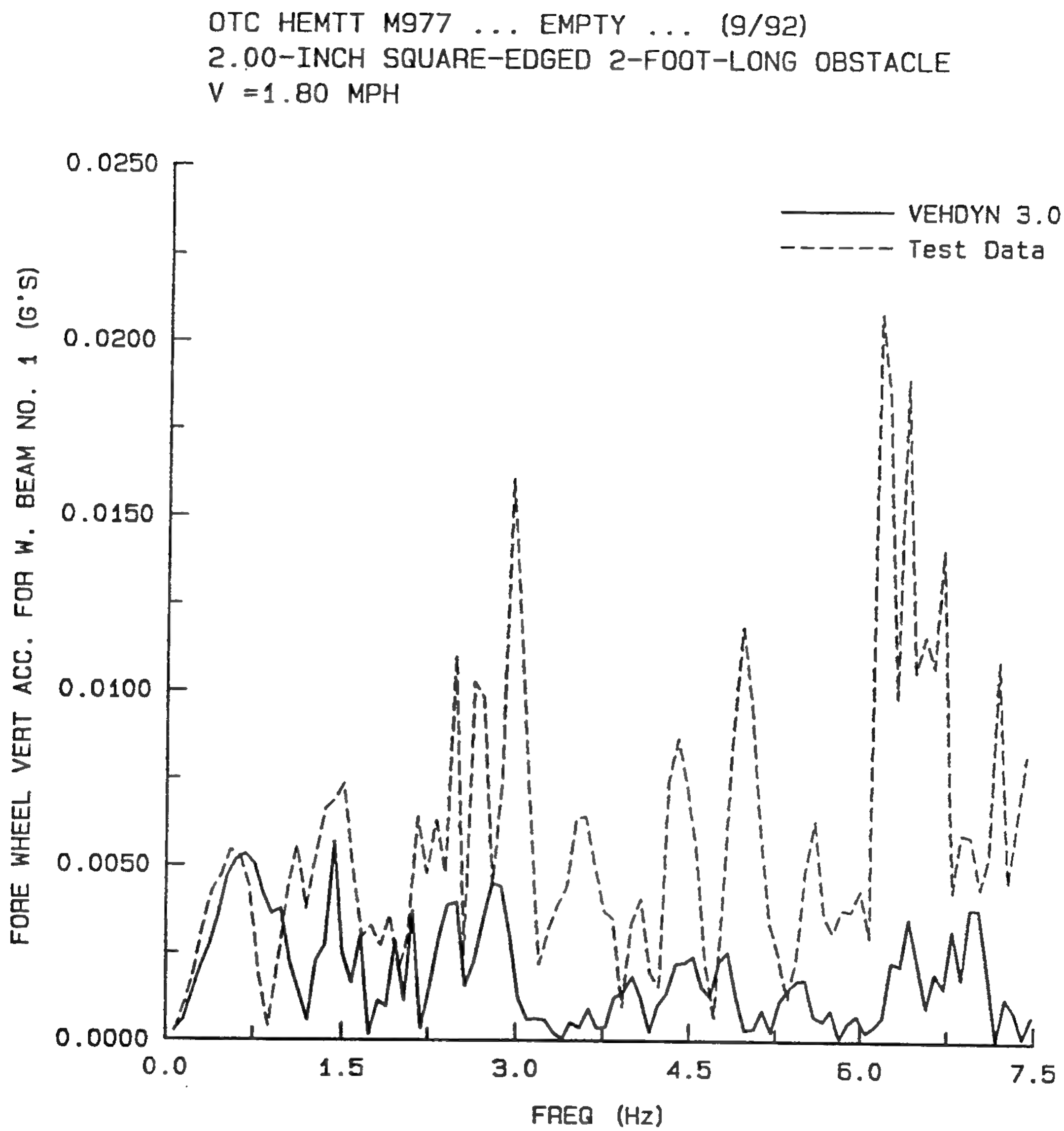

Figure A-111. Vertical acceleration frequency plot (frequency scale = 1.5 Hz/inch) of the forward-most axle for an empty HEMTT traveling at 1.80 miles per hour encountering a 2.00-inch-high obstacle.

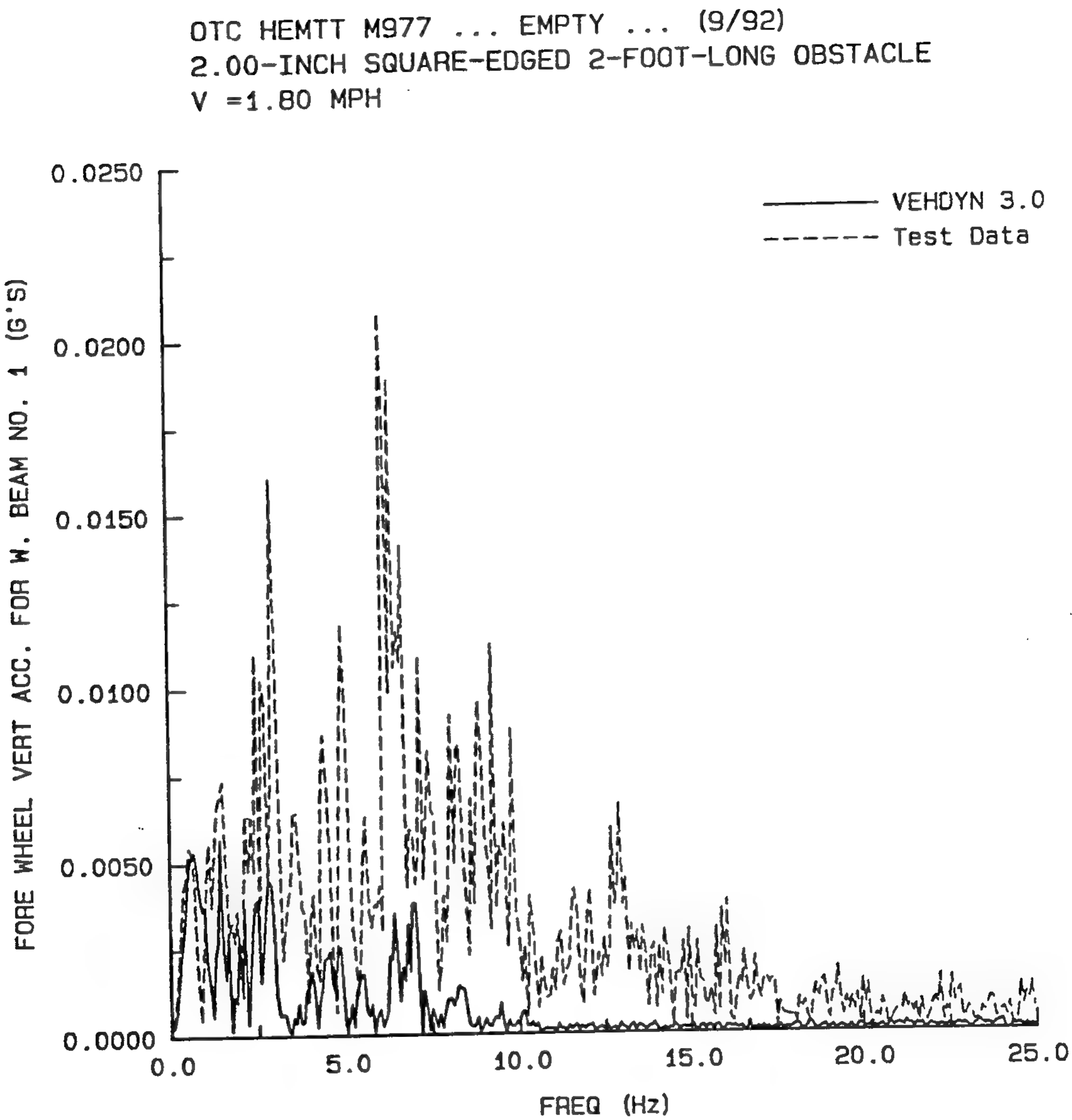

Figure A-112. Vertical acceleration frequency plot (frequency scale = 5.0 Hz/inch) of the forward-most axle for an empty HEMTT traveling at 1.80 miles per hour encountering a 2.00-inch-high obstacle.

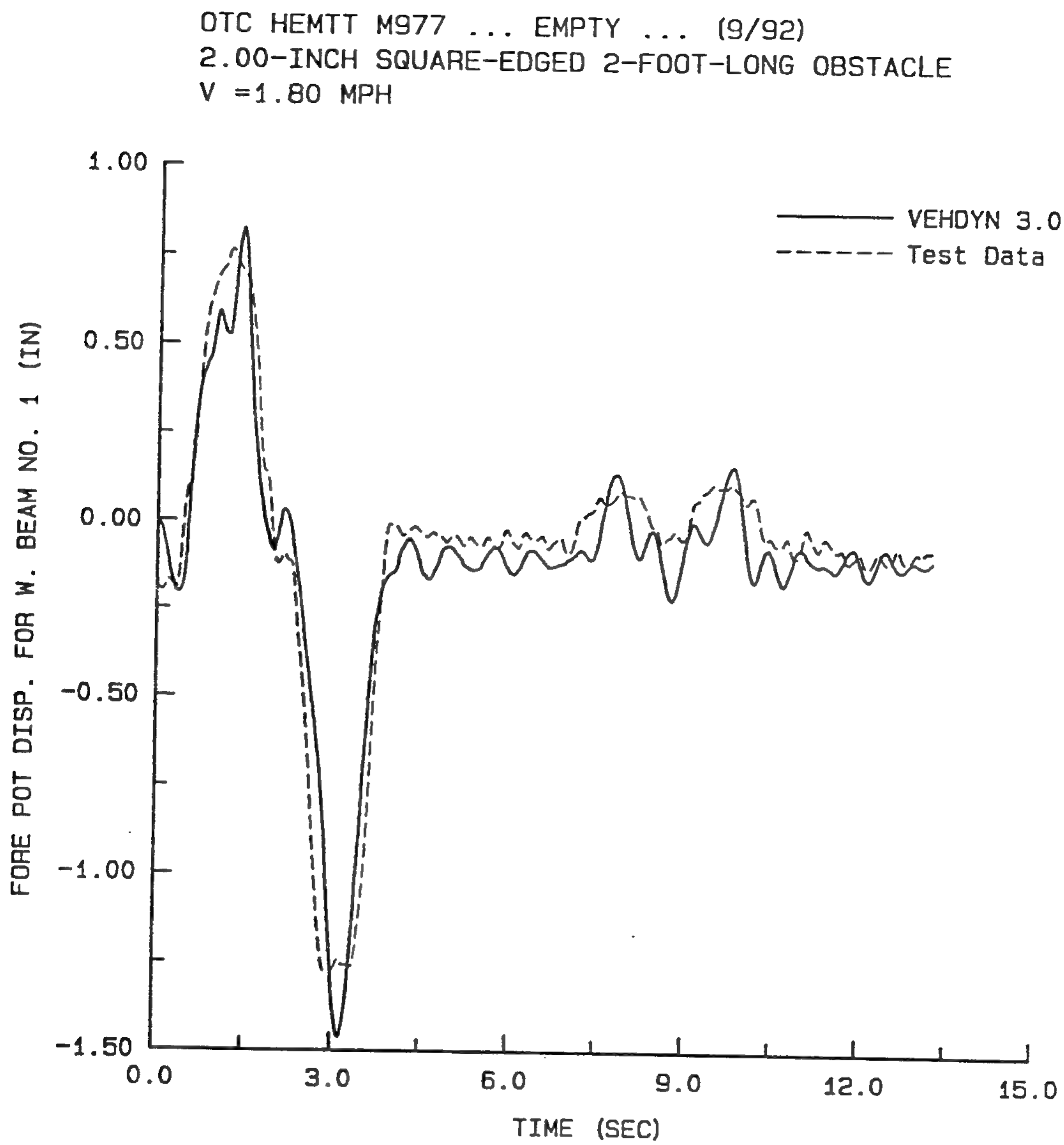

Figure A-113. Relative displacement time history of the forward-most axle with respect to the frame for an empty HEMTT traveling at 1.80 miles per hour encountering a 2.00-inch-high obstacle.

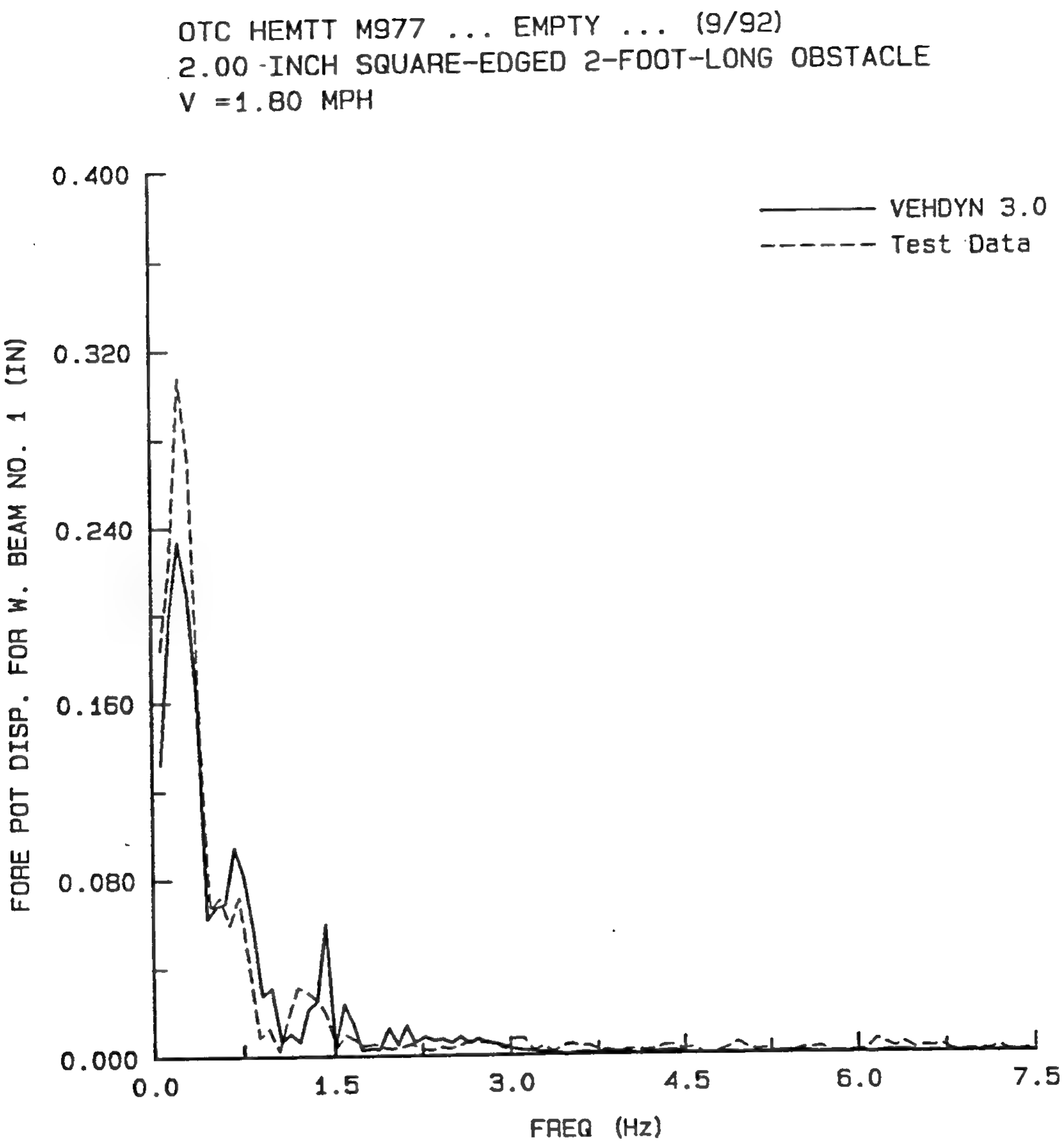

Figure A-114. Relative displacement frequency plot (frequency scale = 1.5 Hz/inch) of the forward-most axle with respect to the frame for an empty HEMTT traveling at 1.80 miles per hour encountering a 2.00-inch-high obstacle.

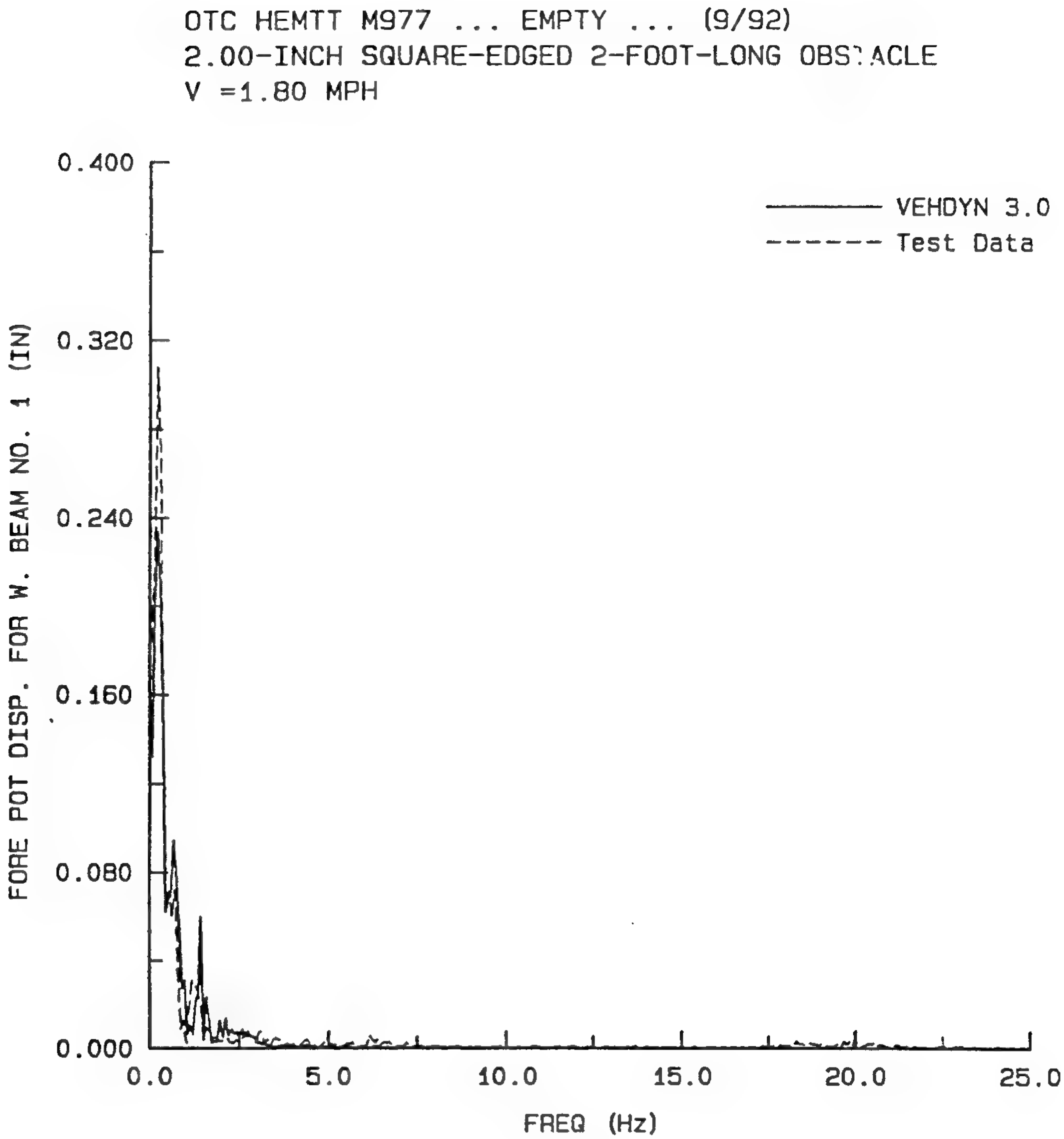

Figure A-115. Relative displacement frequency plot (frequency scale = 5.0 Hz/inch) of the forward-most axle with respect to the frame for an empty HEMTT traveling at 1.80 miles per hour encountering a 2.00-inch-high obstacle.

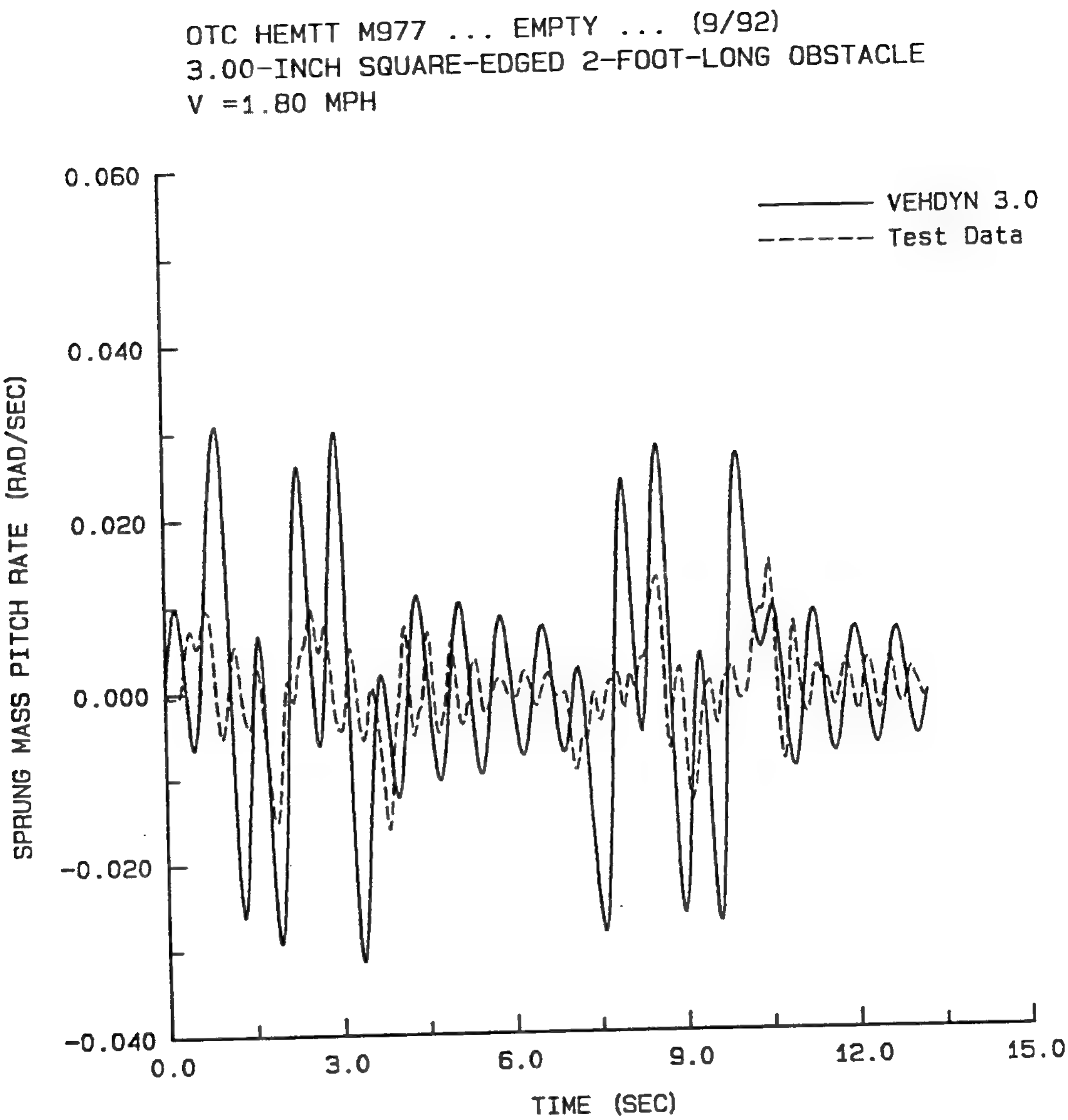

Figure A-116. Sprung mass pitch rate time history for an empty HEMTT traveling at 1.80 miles per hour encountering a 3.00-inch-high obstacle.

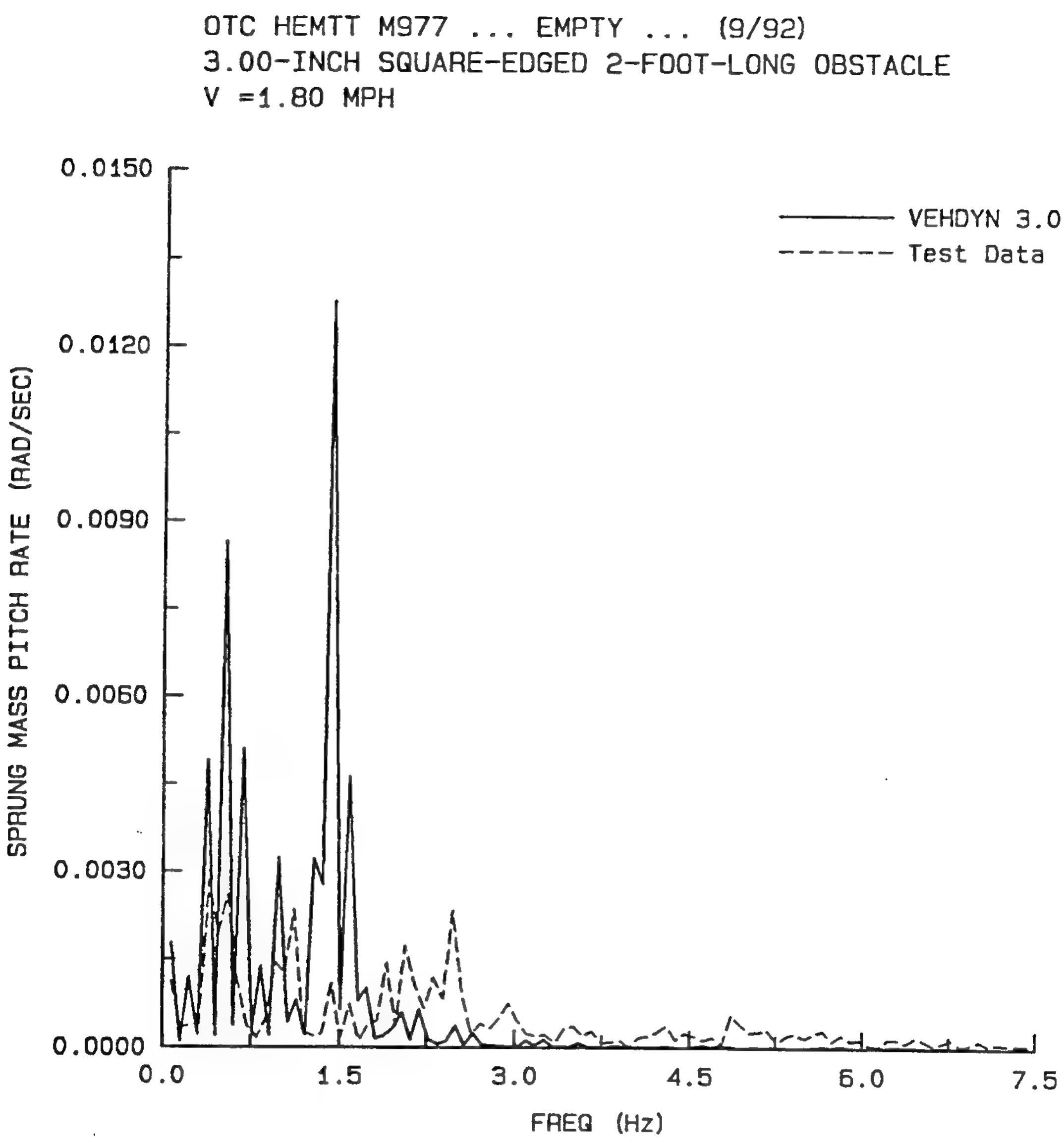

Figure A-117. Sprung mass pitch rate frequency plot for an empty HEMTT traveling at 1.80 miles per hour encountering a 3.00-inch-high obstacle.

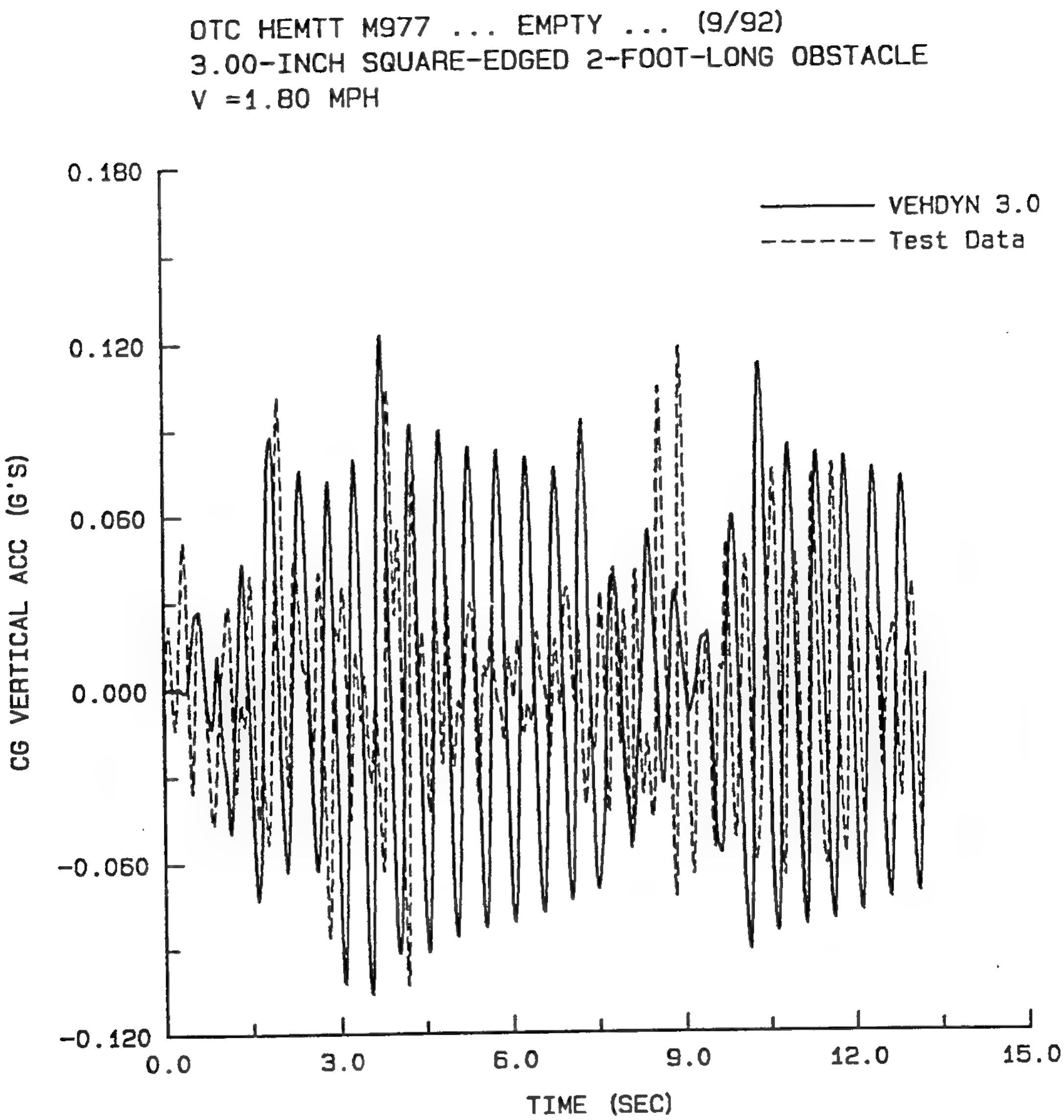

Figure A-118. CG vertical acceleration time history for an empty HEMTT traveling at 1.80 miles per hour encountering a 3.00-inch-high obstacle.

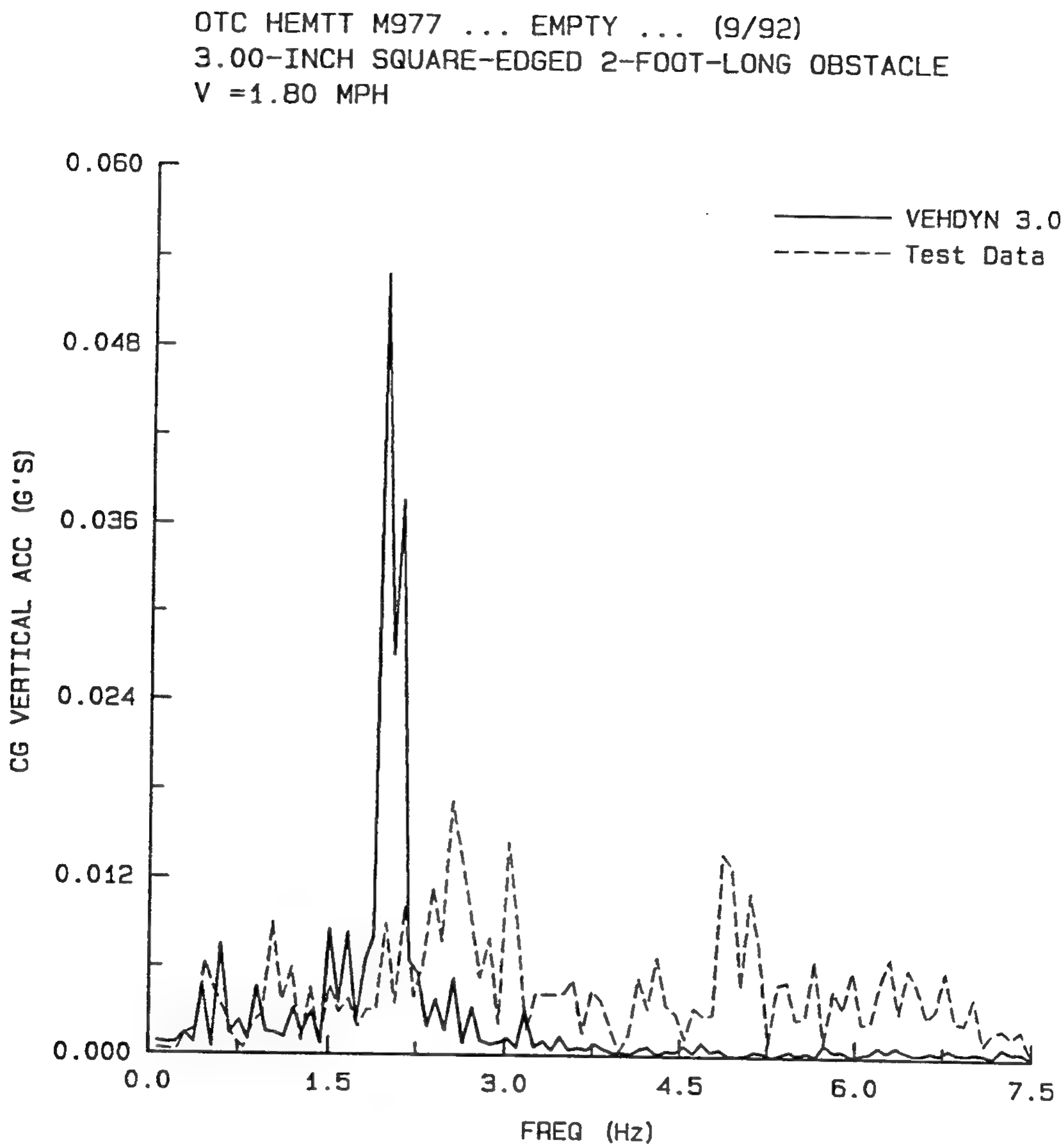

Figure A-119. CG vertical acceleration frequency plot (frequency scale = 1.5 Hz/inch) for an empty HEMTT traveling at 1.80 miles per hour encountering a 3.00-inch-high obstacle.

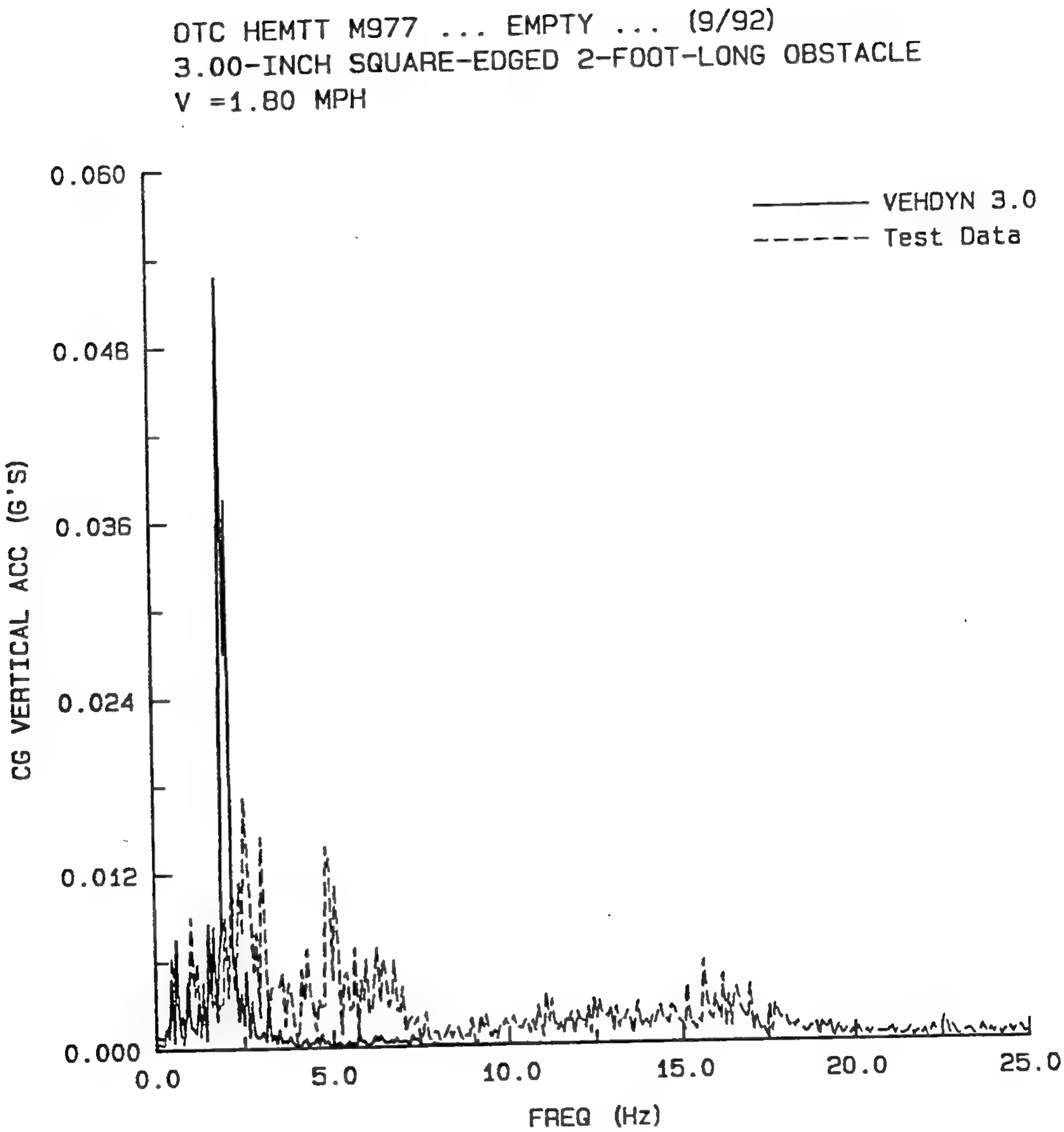

Figure A-120. CG vertical acceleration frequency plot (frequency scale = 5.0 Hz/inch) for an empty HEMTT traveling at 1.80 miles per hour encountering a 3.00-inch-high obstacle.

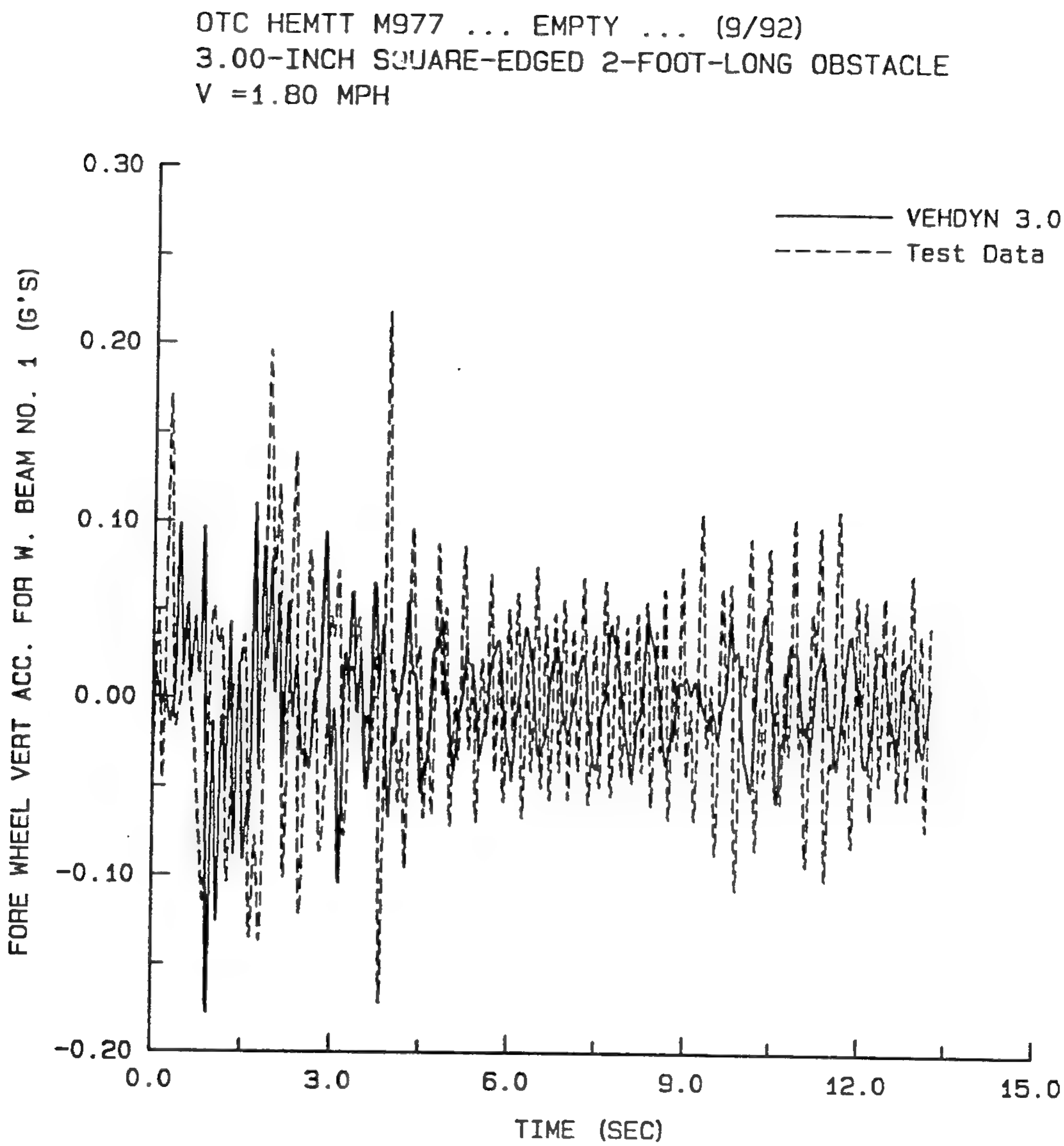

Figure A-121. Vertical acceleration time history of the forward-most axle for an empty HEMTT traveling at 1.80 miles per hour encountering a 3.00-inch-high obstacle.

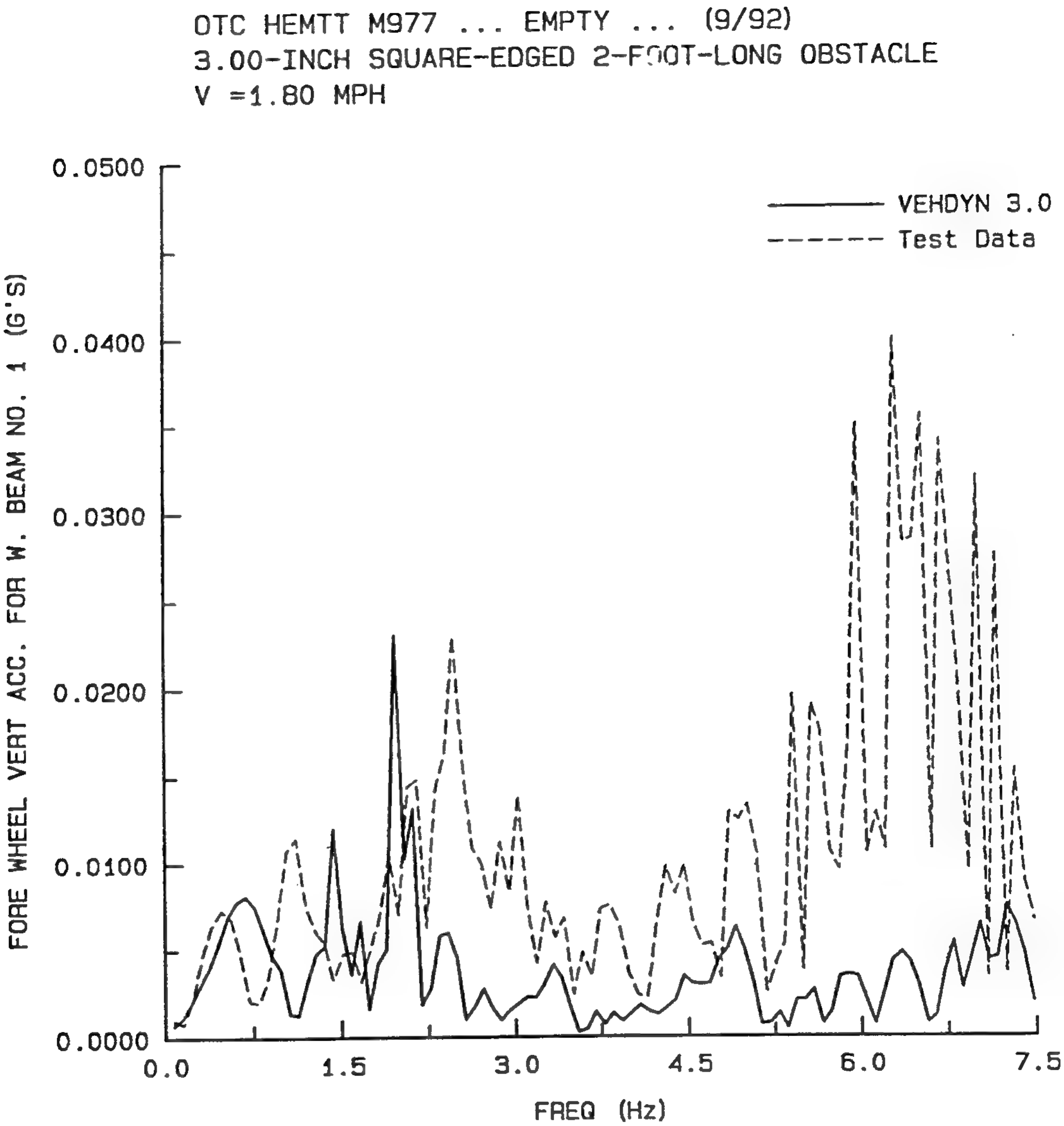

Figure A-122. Vertical acceleration frequency plot (frequency scale = 1.5 Hz/inch) of the forward-most axle for an empty HEMTT traveling at 1.80 miles per hour encountering a 3.00-inch-high obstacle.

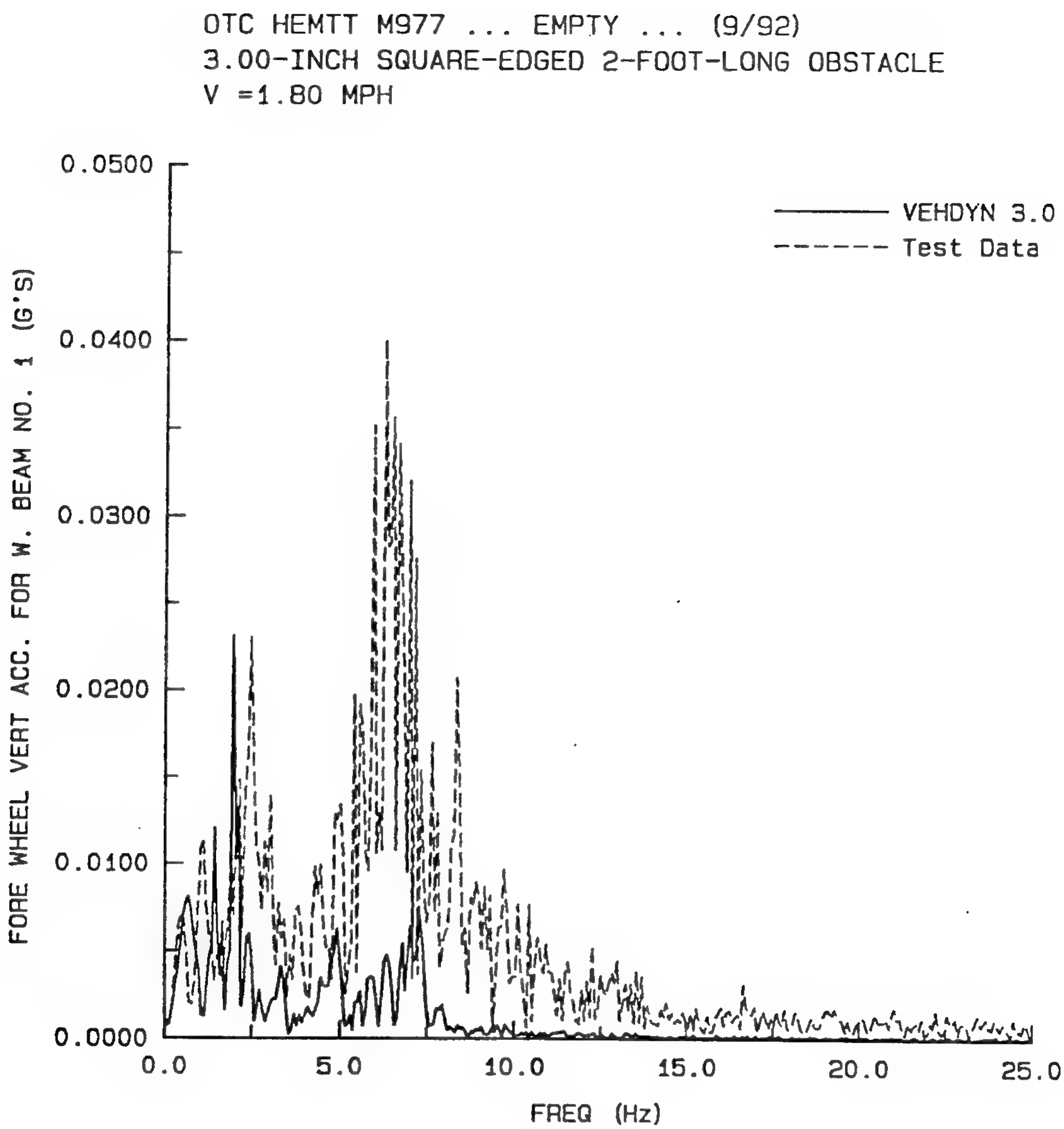

Figure A-123. Vertical acceleration frequency plot (frequency scale = 5.0 Hz/inch) of the forward-most axle for an empty HEMTT traveling at 1.80 miles per hour encountering a 3.00-inch-high obstacle.

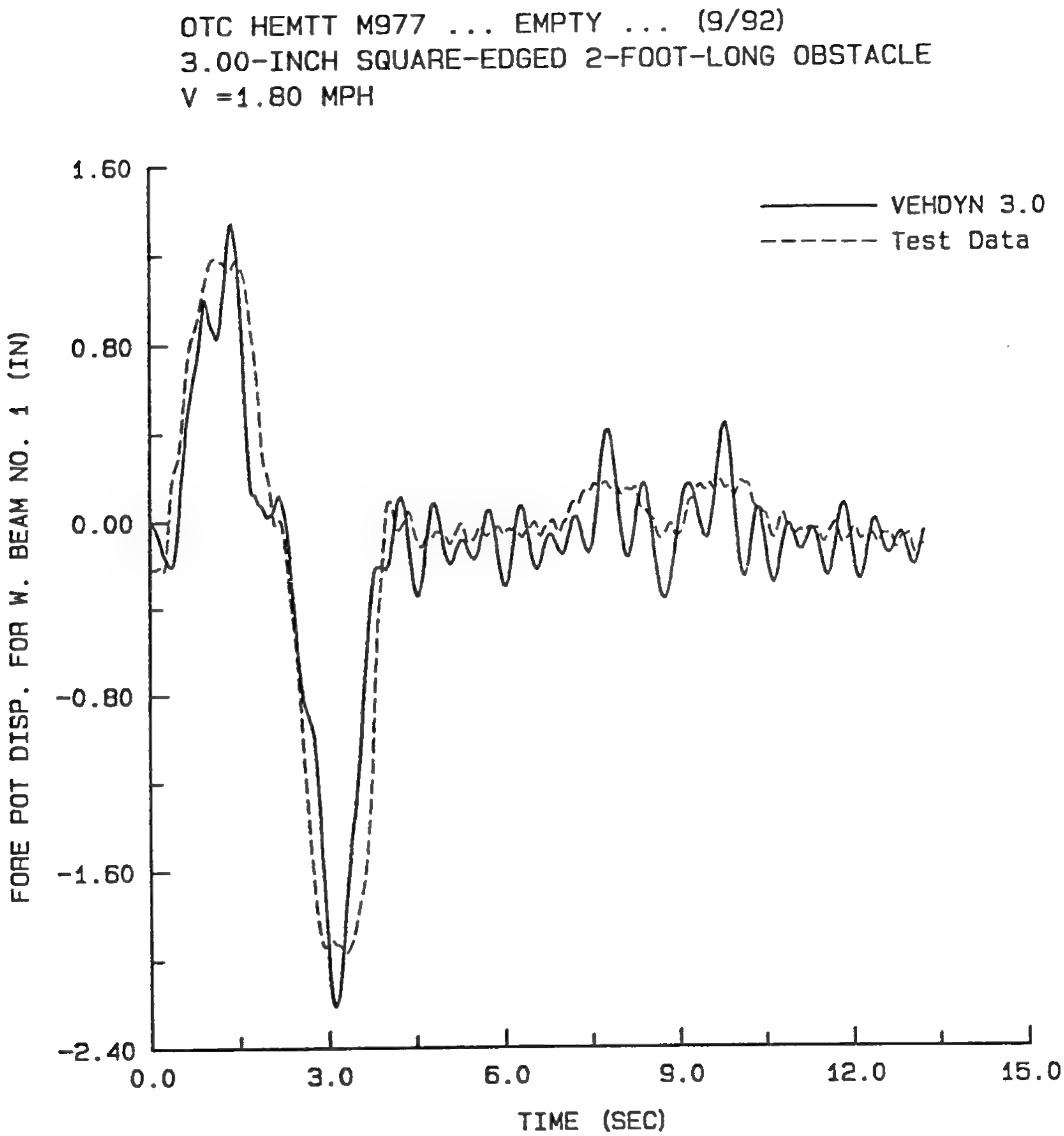

Figure A-124. Relative displacement time history of the forward-most axle with respect to the frame for an empty HEMTT traveling at 1.80 miles per hour encountering a 3.00-inch-high obstacle.

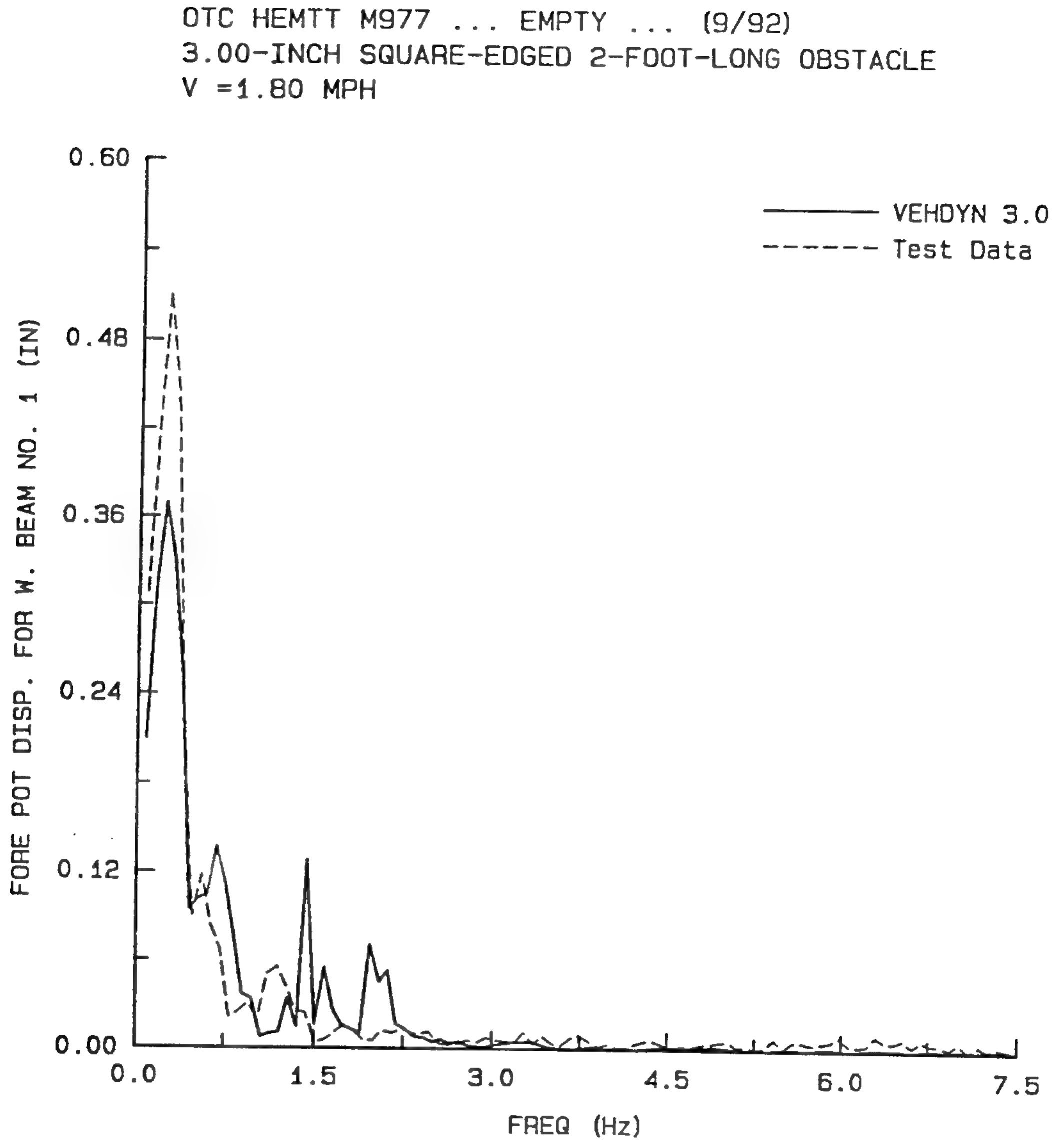

Figure A-125. Relative displacement frequency plot (frequency scale = 1.5 Hz/inch) of the forward-most axle with respect to the frame for an empty HEMTT traveling at 1.80 miles per hour encountering a 3.00-inch-high obstacle.

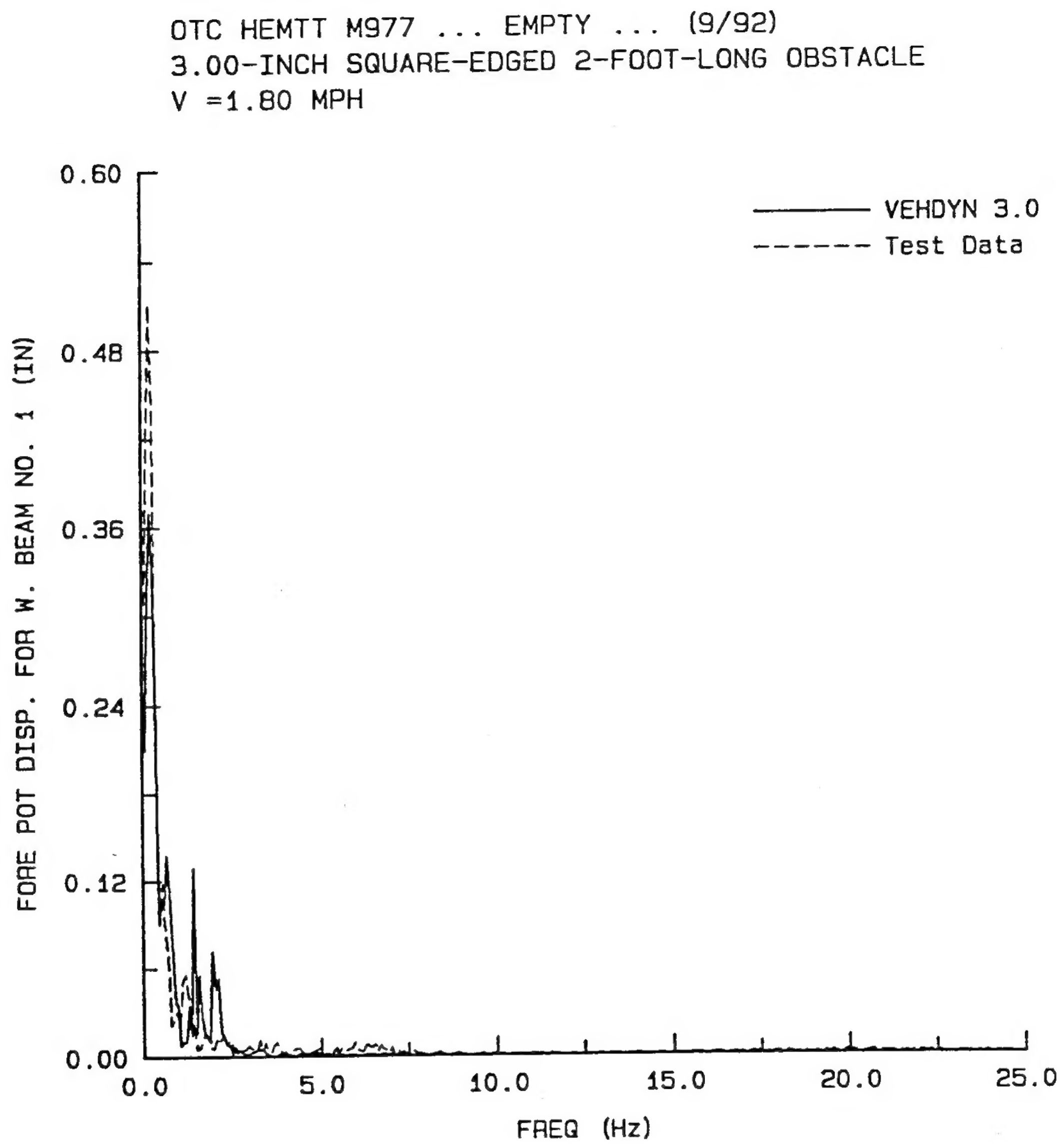

Figure A-126. Relative displacement frequency plot (frequency scale = 5.0 Hz/inch) of the forward-most axle with respect to the frame for an empty HEMTT traveling at 1.80 miles per hour encountering a 3.00-inch-high obstacle.

APPENDIX B

NOTATION

c	Linear damping coefficient, lb-sec/in
c_f	Linear damping coefficient for front portion of vehicle, lb-sec/in
c_r	Linear damping coefficient for rear portion of vehicle, lb-sec/in
f_d	Damped sinusoidal frequency, sec^{-1}
k	Linear spring constant, lb/in
k_f	Linear spring constant for front portion of vehicle, lb/in
k_r	Linear spring constant for rear portion of vehicle, lb/in
m	Mass, $lb\text{-}sec^2/in$
n	Number of cycles to be considered in the computation of log decrement in damper free oscillation theory
$t_0, \ldots, t_n$	Times associated with corresponding amplitudes $x_0, \ldots, x_n$, sec
w_f	Portion of sprung weight over front suspension system, lb
w_r	Portion of sprung weight over rear suspension system, lb
$x_0, \ldots, x_n$	Successive amplitudes of sinusoidal acceleration trace from vehicle drop test, g's
$\ddot{Z}_1$	Vertical acceleration of the forward-most vehicle axle, g's
$\ddot{Z}_{CG}$	Vertical acceleration of the CG of the sprung mass, g's
δ	Log decrement from damped free oscillation theory
δ_1	Displacement measured by the forward-most string pot, in
ζ	Damping factor from damped free oscillation theory
$\dot{\theta}$	Pitch rate of the sprung mass, rad/sec

REPORT DOCUMENTATION PAGE

Form Approved
OMB No. 0704-0188

Public reporting burden for this collection of information is estimated to average 1 hour per response, including the time for reviewing instructions, searching existing data sources, gathering and maintaining the data needed, and completing and reviewing the collection of information. Send comments regarding this burden estimate or any other aspect of this collection of information, including suggestions for reducing this burden, to Washington Headquarters Services, Directorate for Information Operations and Reports, 1215 Jefferson Davis Highway, Suite 1204, Arlington, VA 22202-4302, and to the Office of Management and Budget, Paperwork Reduction Project (0704-0188), Washington, DC 20503.

1. AGENCY USE ONLY *(Leave blank)*

2. REPORT DATE
February 1995

3. REPORT TYPE AND DATES COVERED
Report 2 of a series

4. TITLE AND SUBTITLE
HEMTT Dynamic Sensitivity to Small Obstacles at Low Velocities;
Report 2: Validation Study Using VEHDYN 3.0

5. FUNDING NUMBERS
C - DNA MIPR 92-681
PE - 4613
PR - AE
TA - CB
WU - DH926810

6. AUTHOR(S)
Daniel C. Creighton, Randolph A. Jones

7. PERFORMING ORGANIZATION NAME(S) AND ADDRESS(ES)
U.S. Army Engineer Waterways Experiment Station
3909 Halls Ferry Road
Vicksburg, MS 39180-6199

8. PERFORMING ORGANIZATION REPORT NUMBER
Technical Report
GL-95-2

9. SPONSORING/MONITORING AGENCY NAME(S) AND ADDRESS(ES)
Defense Nuclear Agency
6801 Telegraph Road
Alexandria, VA 22310-3398

10. SPONSORING/MONITORING AGENCY REPORT NUMBER

11. SUPPLEMENTARY NOTES
Available from the National Technical Information Service, 5285 Port Royal Road, Springfield, VA 22161.

12a. DISTRIBUTION/AVAILABILITY STATEMENT
Approved for public release; distribution is unlimited.

12b. DISTRIBUTION CODE

13. ABSTRACT *(Maximum 200 words)*

The Vehicle Dynamic Model (VEHDYN) 3.0, developed at the U.S. Army Engineer Waterways Experiment Station, was used to compare selected displacements, velocities, and accelerations with field-measured quantities for both an empty and a fully loaded M977 HEMTT truck. Test conditions (detailed in Report 1 of this series) included having the HEMTT negotiate small square-edged obstacles (0.25 - 3.00 inches high) at low velocities (1.80 ± 0.06 mph). Time history and Fast Fourier Transform comparisons are provided.

The VEHDYN 3.0 model did a reasonable job at predicting the motion, especially the action of the HEMTT walking beam suspensions and overall low-frequency response.

A procedure was demonstrated that takes acceleration data from low-amplitude front and rear drop tests and develops linear spring and damper response relationships for the HEMTT.

14. SUBJECT TERMS
See reverse.

15. NUMBER OF PAGES
166

16. PRICE CODE

17. SECURITY CLASSIFICATION OF REPORT	18. SECURITY CLASSIFICATION OF THIS PAGE	19. SECURITY CLASSIFICATION OF ABSTRACT	20. LIMITATION OF ABSTRACT
UNCLASSIFIED	UNCLASSIFIED		SAR

NSN 7540-01-280-5500

Standard Form 298 (Rev. 2-89)
Prescribed by ANSI Std Z39-18
298-102

14. Concluded.

Computer simulation	VEHDYN 3.0
Low velocity	Vehicle dynamics
Validation	Weighing-in-motion